The University of Hull

Asymmetric Hydrogenation Catalysed by Platinum and Iridium

being a Thesis submitted for the Degree of Doctor of Philosophy

in the University of Hull

by

Keith Edward Simons B.Sc. (Hull), M.Sc. (Liverpool)

June 1994

Acknowledgements

I would like to express my sincere thanks to all those who supported me through my thesis, especially:

Professor Peter B. Wells, my academic supervisor for his guidance, support and confidence in me, both before and during my Ph.D.

Dr Arthur Ibbotson, my industrial supervisor for his support and advice. The SERC and Zeneca Fine Chemical Manufacturing Organisation who financed my studies.

Professor Dennis Dowden for agreeing to examine this thesis.

Ken Griffin and Ivor Dodgson of Johnson Matthey for catalysts, discussions and driving me to Poitiers!

Dr Peter Johnston, Dr Gary Bond and Dr. Richard Moyes for their valuable discussions and even more valuable friendship.

The technical services of School of Chemistry, especially Alan Roberts and Dr. David Ewing.

.....and finally to

Steve, Wim, Simon, Chris, Heike, Ian, Nia and Angela who helped make the years truly wonderful.

For my Mother and Father

Summary

The enantioselective hydrogenation of α-ketoesters over supported platinum metal catalysts which have been modified by chiral molecules has been studied. The aim of this thesis was (a) to gain a greater understanding of the kinetics of asymmetric hydrogenation of methyl pyruvate (MeCOCOOMe) to methyl lactate (MeCH(OH)COOMe) over cinchonidine modified EUROPT-1, (b) to diversify the reaction, by variation of the metal, modifier and reactant and (c) to test and develop a mechanism to explain the reaction by both mathematical and molecular modelling.

It was found that only very small quantities of cinchonidine modifier were required to render EUROPT-1, a 6.3 % Pt/silica catalyst, suitable for asymmetric hydrogenation of methyl pyruvate. The plots of the variation of with reaction rate and of optical yield with modifier loadings reached plateau values at a loading of ca. 0.8 mg cinchonidine per 100 mg EUROPT-1. The shape of the curves has been fitted to a mathematical model which gives evidence that the mechanism is a result of a 1:1 interaction between modifier and reactant.

Modification of catalyst by mixtures of cinchonidine and cinchonine, or of quinine and quinidine has been performed and results obtained as to the effect on reaction rate and optical yield. The variation of the latter with the mole fraction of modifier has been fitted to a mathematical model which supports the view that the mechanism is a result of a 1:1 interaction.

It has been discovered that Iridium, especially when supported on calcium carbonate, is an effective catalyst for both racemic and enantioselective hydrogenation of methyl pyruvate. When $Ir/CaCO_3$ was reduced and modified by cinchonidine, hydrogenation of methyl pyruvate at 273 K and 10 bar in ethanol resulted in an optical yield of 39 %. The reaction is approximately zero order in reactant and first order in hydrogen, being first order overall. The apparent activation energy was 22 ± 2 kJ mol-1.

The unmodified reaction proceeded at a very fast rate with an apparent activation energy of 11 ± 2 kJ mol-1. The enhanced rate was explained in terms of stabilisation of the half-hydrogenated state by the carbonate support. Rhodium, Osmium and Rhenium were found not to be effective for asymmetric hydrogenation, which in the case of rhodium is contrary to the literature.

Diversification of the modifier was found to be possible, the best alternative being by the use of 10,11-dihydroquinine 4-methyl-2-quinoyl ether which gave an optical yield of 22 %. The amino acids tryptophan and histidine were found to give poor but reproducible enantiomeric excesses. Ephedrines and benzyl pyrrolidine methanol were found not to be effective modifiers which is contrary to the literature.

A molecular modelling study resulted in a new proposal for the asymmetric hydrogenation site which explained the mechanism in terms of a 1:1 interaction between modifier and reactant at the catalyst surface. The proposal successfully accounts for the observed enantioselectivity in terms of steric hindrance to the unwanted product. The proposed mechanism is in agreement with experimental data in the literature.

Chapter 1

Introduction

1.1 Chirality

1.1.1 History

The origin of the study of chirality dates back to 1815 when Jean-Baptiste Biot discovered that certain substances were able to rotate polarised light[1]. Thirty three years later, Louis Pasteur (a former student of Biot) made the significant proposal that optical activity was the result of molecular asymmetry[2]. This achievement came through a study of the crystals from argol, formed on the side of wine-vessels. The major component, (+)-tartaric acid rotated plane-polarised light in a clockwise direction, the minor component showed no optical activity as it was the racemic mixture. However, the sodium-ammonium double salt of this mixture produced crystals of mirror images to each other. When these were separated (by hand), Pasteur discovered that the different crystals, (which otherwise had identical chemical properties) rotated plane polarised light in equal, but opposite directions.

The precise definition of molecular asymmetry was proposed by van't Hoff[3] and Le Bel.[4] The former recognised that a tetravalent carbon (as had been recently proposed to exist by Kekulé) having bonds directed to the four corners of a tetrahedron, could (when each of the bonds was to a different group) generate two molecules, each being the mirror-image of the other. Le Bel in his paper, concentrated not on an asymmetric carbon atom, but on the asymmetry of the entire molecule, as a molecule can be chiral even though it contains no chiral carbon atom. Thus the modern-day principles of stereochemistry were born.

1.1.2 Concepts

A molecule is chiral if its mirror image is not superimposable on itself. Chirality is therefore a geometrical attribute of the entire molecule. The two stereoisomers or enantiomers, have identical physical properties, with the exception of their ability to

rotate plane-polarised light in opposite directions. This phenomenon is the result of the interaction of the electric and magnetic field of the plane polarised light with the molecules which it encounters. In a racemic mixture, the plane of the light will be rotated clockwise and counter-clockwise in equal proportions so the net result is zero rotation. When there is an enantiomeric excess of one enantiomer over the other, this cancelling out effect does not occur and rotation results, the degree of which is dependent on the concentration, enantiomeric excess, temperature, wavelength of light, solvent and length of the polarimeter tube.

The chemical nomenclature, used to distinguish between different stereoisomers is based on the 'Cahn-Ingold-Prelog convention'[5] which, except for its application to amino acids, has been widely accepted. The convention uses a series of sequential rules to assign an order of priority to the four substituents of any stereogenic centre. Using the rules, a configuration can be assigned as being R or S (from the Latin for right and left, *rectus* and *sinister*, respectively).

The vast majority of chiral molecules contain stereogenic carbon atoms, where the interchange of two of the groups will form the stereoisomer. However, other molecules without this condition can still be chiral, in molecules where rotation about a single bond is highly hindered, asymmetry of the molecule can result. Such an example is 1,1'-bi -2-naphthol (see figure 1.1).

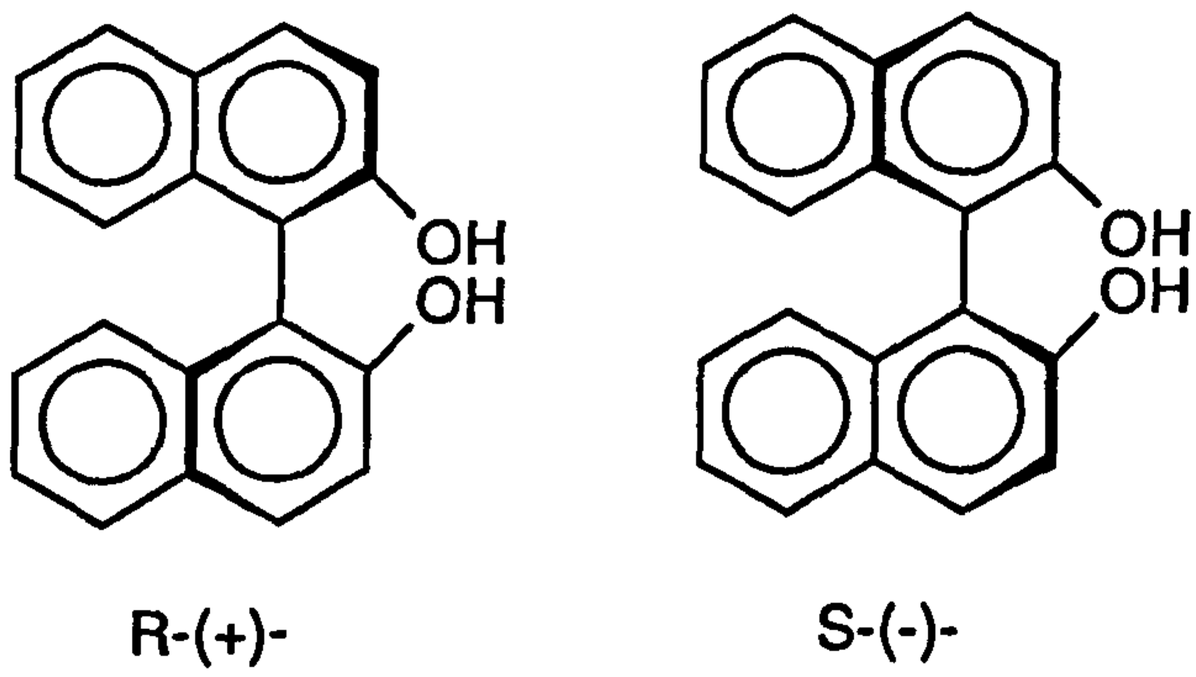

R-(+)- S-(-)-

Figure 1.1

The two atropisomers of 1,1'-Bi -2-naphthol

In addition to carbon, phosphorus and sulphur can also be stereogenic centres, an example of the former being the pesticide, cyanofenfos (figure 1.2).

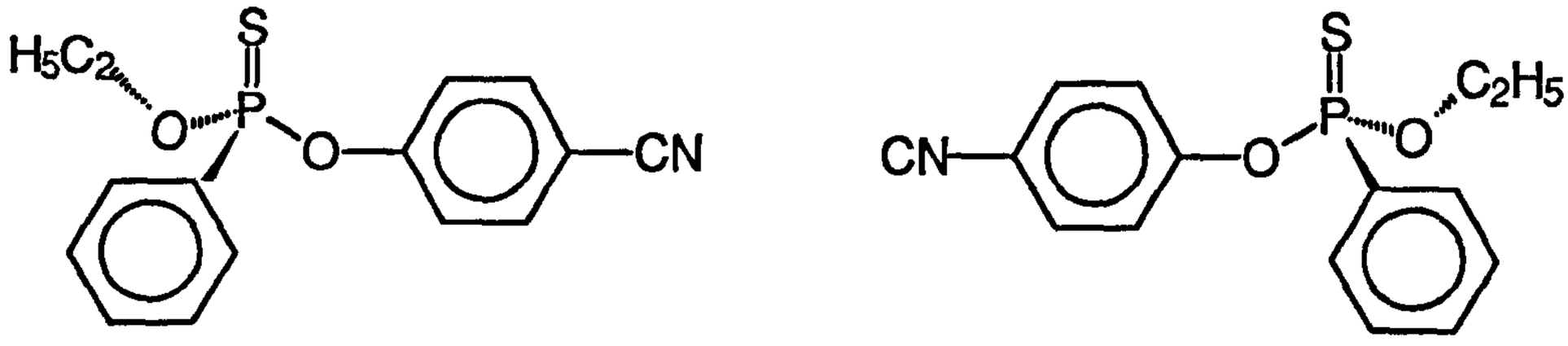

S-cyanofenfos R-cyanofenfos

Figure 1.2

The two enantiomers of Cyanofenfos

1.1.3 Chirality and Bioactivity

Chirality is not a prerequisite for a molecule to have biological activity as a pharmaceutical, pesticide, herbicide or fragrance, but in those cases in which the bioactive molecule contains one or more stereogenic centres, the desired biological activity often resides solely with one enantiomer, the *eutomer*. The other enantiomer, or *distomer* may be ballast and at worst can have undesired (perhaps unknown) side effects.

Examples of pharmaceuticals where both enantiomers have desirable properties include the anti-inflammatory agent ibuprofen - figure 1.3 (although the S-enantiomer is active the R-enantiomer undergoes a unidirectional metabolic inversion of configuration[6]) and the hypoprothrombinaemic agent Warfarin - figure 1.3 (although the S-enantiomer is 5-6 times more powerful than the R form). Cases where the different isomers have different pharmacological properties include the near-enantiomers quinine and quinidine. The former is an antimalarial drug, the latter an antiarrhythmic. A tragic case where it was thought that one of the enantiomers was inert is thalidomide which was sold as the racemate (figure 1.3). The R-enantiomer was the effective sedative in the

treatment of pregnant women, whereas the S-enantiomer underwent metabolic conversion into an embryotoxin[7,8].

Chirality is also of importance in the agrochemical, fragrance and flavouring industries. Alkyl (R)-α-aryloxypropionate and Pyrethrin are a herbicide and pesticide, respectively (see figure 1.3). S-Limonene smells of lemons whereas the R-enantiomer smells of oranges (figure 1.3). Finally the artificial sweetener Aspartame (figure 1.3) is only active in the (S,S) form, its mirror-image being bitter tasting.

Recently the United States Food and Drug Administration (FDA) announced that in the future its policy will be only to approve the sale of a racemic compound when the bioactivity of both of the enantiomers is known[9]. Currently, regulations for Canada, the E.U. and Japan are being formulated[10]. In practice this will encourage a company to produce pure enantiomers, rather than go to the expense of conducting a study on the unwanted enantiomer. The ramifications of the decision of the FDA to the pharmaceutical industry have been discussed by Deutsch[11], and the ironies highlighted of a company going to great expense to produce a racemic mixture, half of which it cannot charge for and has no therapeutic value to the patient.

1.2 Heterogeneous Enantioselective Catalysis

The earliest reported heterogeneous enantioselective reaction was in 1932 when Schwab *et al.* achieved dehydrogenation of racemic 2-butanol on quartz supported Pt, Pd, Ni and Cu catalysts[12,13]. In this case the chiral environment was generated by the quartz which is available as both enantiomorphs. However, only low enantiomeric excesses of 1% were achieved. A further example of using this approach, but generating higher optical yields came in 1958 when Pd/silk fibroin was used as a hydrogenation catalyst[14].

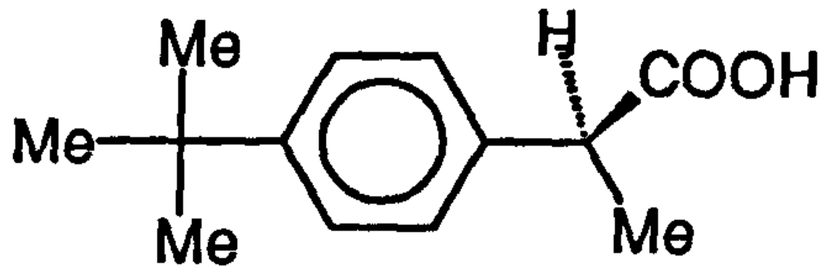

S-Ibuprofen

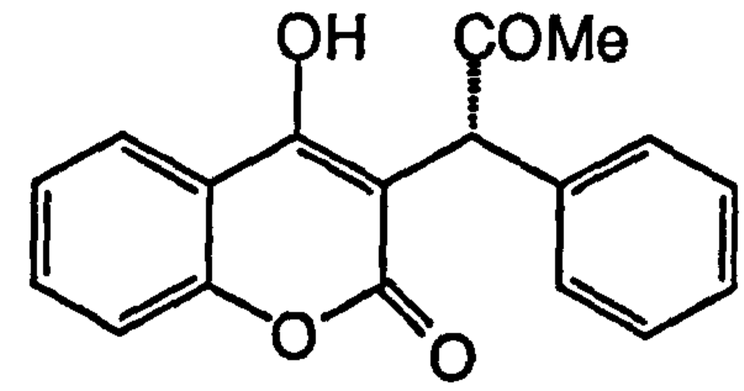

S-Warfarin

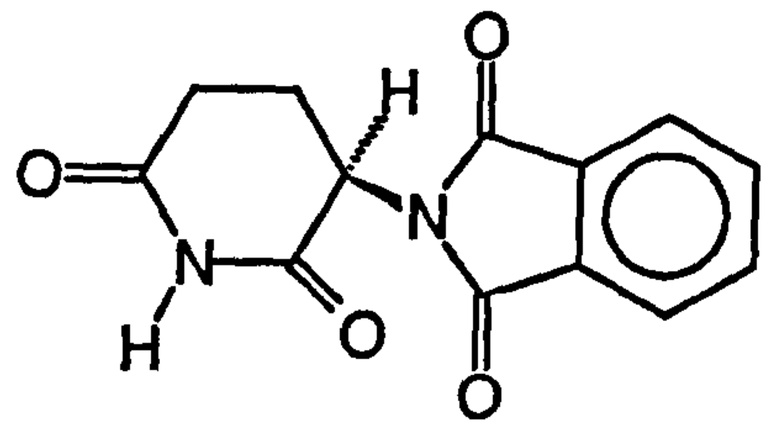

R-Thalidomide

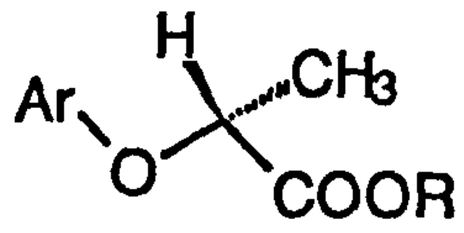

Alkyl (R)-α-aryloxypropionate

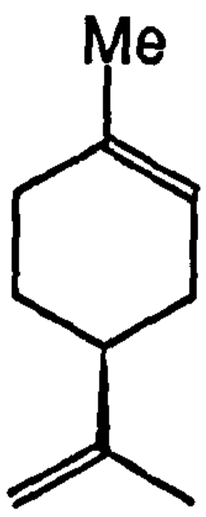

S-Limonene

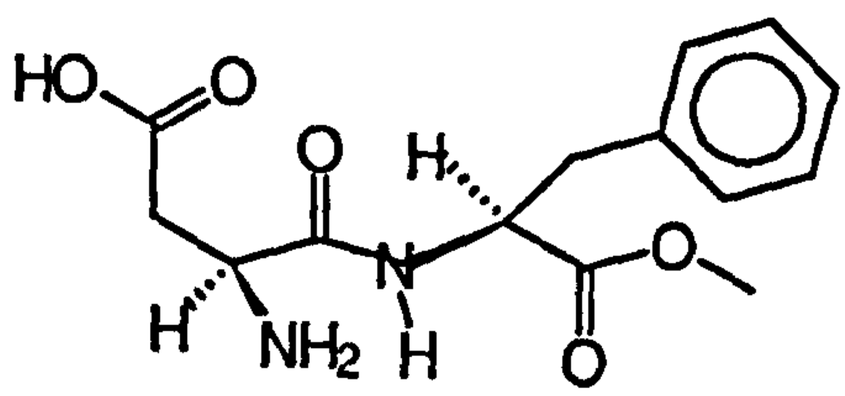

(S,S) Aspartame

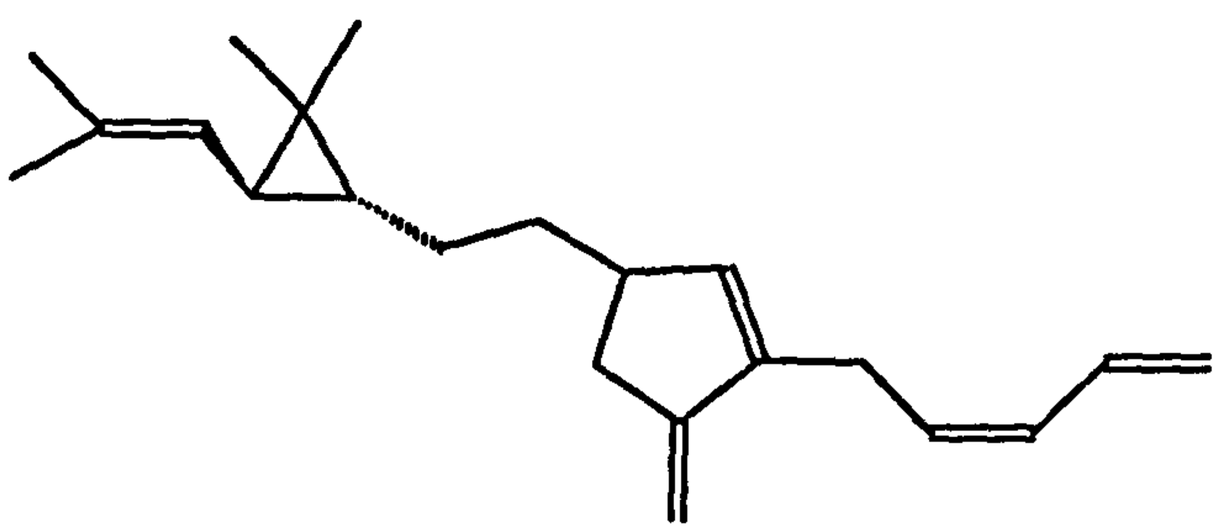

Pyrethrin I

Figure 1.3

Important Chiral Molecules

A different approach was taken by Lipkin and Stewart who generated a chiral environment on a PtO_2 catalyst by adding hydrocinchonine. This is the first such example of adding a chiral substance, generally termed a *modifier* to a heterogeneous catalyst. This approach was also used to develop one of the most studied enantioselective heterogeneous reactions, namely the use of Ni-tartrate-NaBr catalysts to hydrogenate β-ketoesters in high enantiomeric excess. This topic has recently been reviewed[15].

Other systems which give high enantiomeric excesses have recently been reported and include diethyltartrate modified Ti-pillared montmorillonite for chiral epoxidation,[16] the best reported enantiomeric excess being 98 % (see scheme I). Further work by the same authors extended the system to include the asymmetric oxidation of prochiral sulphides to sulphoxides (see scheme II)[17]. Corma *et al.* also recently reported that they had managed to immobilise Rh and Ni complexes containing L-proline ligands in the wide pored zeolite-Y. They were then able to hydrogenate N-acyldehydrophenylalanine derivatives with enantioselectivities greater than 95 %[18] (see scheme III).

The only remaining system where high enantioselectivities can be easily achieved is the Orito reaction, which has been studied in this thesis and is described in section 1.4.

1.3 Relative Merits of Heterogeneous and Homogeneous Enantioselective Catalysis

There are distinct advantages in developing heterogeneous enantioselective catalysis from both a financial and a process engineering point of view. One of the major problems of homogeneous enantioselective catalysis, from an economic point of view, is catalyst recovery. Virtually all of the very expensive soluble chiral catalyst may require recovery for the process to be economically viable. This is both a difficult and expensive process in itself, which can result in destruction of the catalyst and loss of the chiral ligands[19] (it is the latter, and the catalyst synthesis that accounts for most of the cost, the price of the precious metal being small in comparison). With a solid catalyst, simple filtration will recover most of the precious metal catalyst, though the chiral modifier will

probably require replacement. Since synthesis of the catalyst is not required, the process should be much more economical.

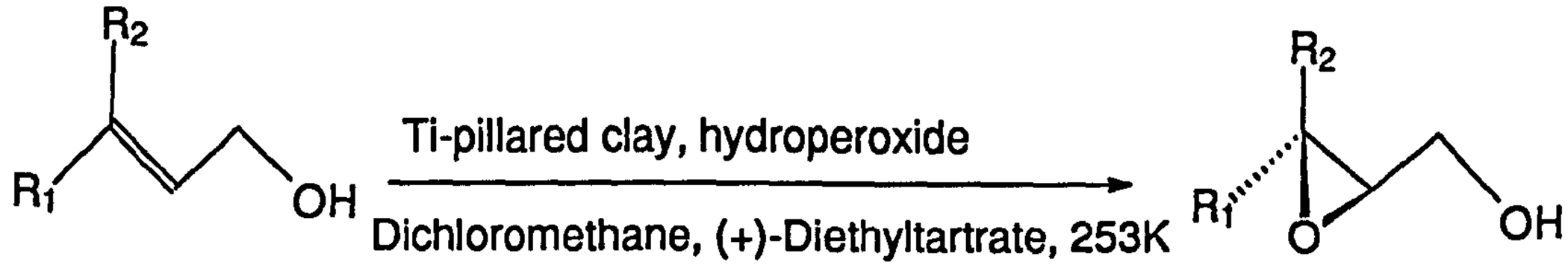

Scheme I
Asymmetric epoxidation of olefins

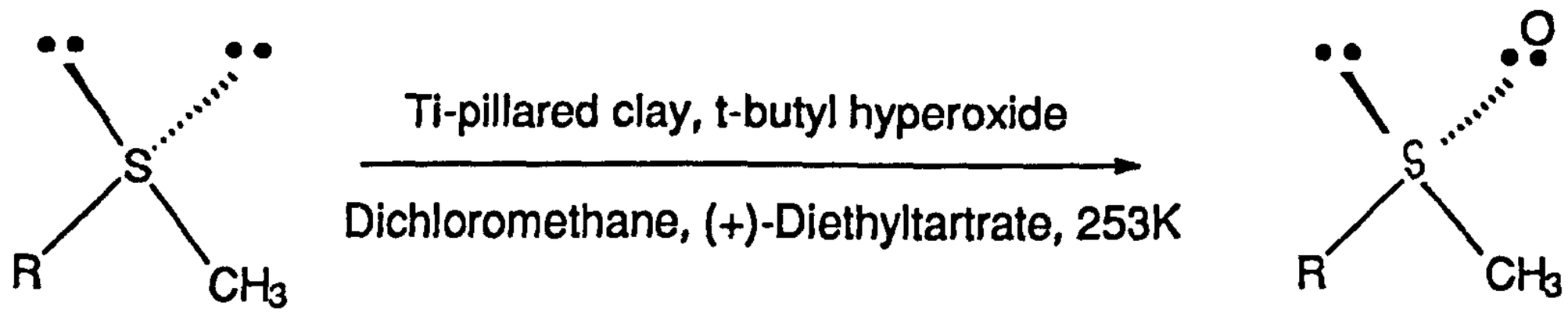

Scheme II
Asymmetric oxidation of prochiral sulphides to sulphoxides

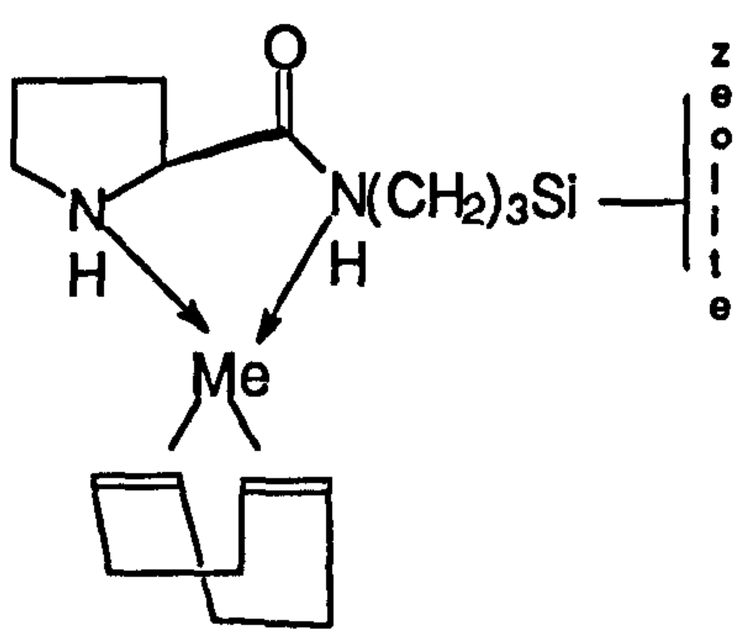

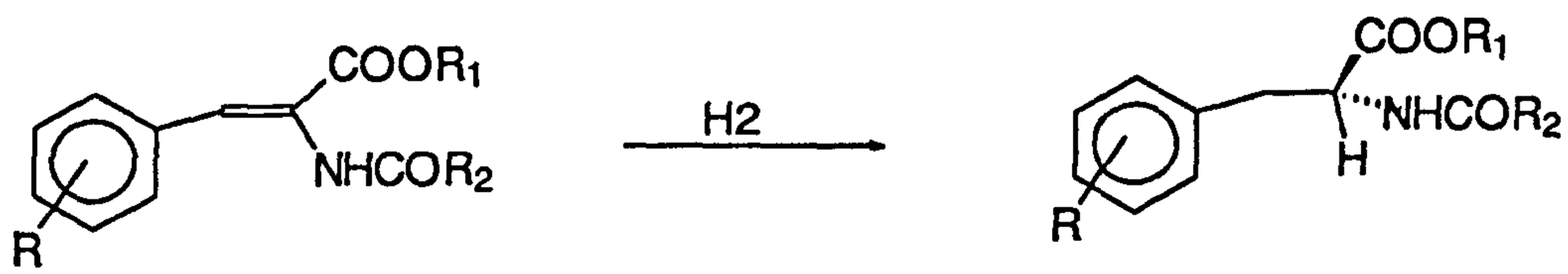

Scheme III
Hydrogenation of N-acyldehydrophenylalanine derivatives

Although high enantioselectivities can be achieved in heterogeneous catalysis (up to 95 %)[20,21,22] only a few distinct systems are known, as opposed to the many commercial systems known in homogeneous catalysis[23,24,25,26] which can have nearly 100 % enantioselectivity. Ciba-Geigy operated a 10-200 kg scale production of a benazapril intermediate using a dihydrocinchonidine modified Pt/alumina catalyst, but this has now finished.[27]

The productivity of the heterogeneous reaction can also be higher than that of its homogenous counterpart. Taking the asymmetric reduction of β-ketoesters as an example, it has been estimated that the productivity of the tartaric acid-NaBr modified Ni catalyst at ca. 40 g^{-1} l^{-1} h^{-1} is four times greater than that of the homogeneous reduction which uses a Ru-BINAP as catalyst[28].

1.4 The Orito Reaction

1.4.1 Original Findings

Enantioselective hydrogenation of α-ketoesters by cinchona alkaloid modified supported platinum catalysts was reported by Orito and co-workers in a series of papers from 1979-1982.[29,30,31,32] In addition a patent was issued[33]. They found that if a 5 % Pt/carbon catalyst was stirred for 20 h in a 1% solution of either cinchonidine or quinine it was an effective catalyst for the asymmetric hydrogenation of methyl pyruvate or methyl benzoyl formate to R-(+)-methyl lactate or R-(-)-methyl mandelate respectively (see scheme IV). The enantioselectivity could be directed in the opposite direction by use of either cinchonine or quinidine. (The structure of the alkaloids can be found in figure 2.1).

$$MeCOCOOMe + H_2 \rightarrow MeCH(OH)COOMe$$

$$C_6H_5COCOOMe + H_2 \rightarrow C_6H_5CH(OH)COOMe$$

Scheme IV

They also studied the effect of using various solvents and various pre-treatment methods of the catalyst. The optical yield observed was dependent on the choice of solvent. They tested a variety of esters, alcohols and aromatic solvents and found the highest optical yield to be 81.9 % when methyl benzoyl formate was hydrogenated to R-(-)-methyl mandelate in methyl propionate. For the same reaction, the lowest optical yield of 61.5 % was obtained when methyl acetate was used as solvent. The reduction temperature of the catalyst was found to be important in obtaining good optical yields, with an optimum temperature being about 573 K.

Orito *et al.* also observed that the choice of catalyst preparation method and carbon support caused a variation in the optical yield. They attributed this variation to the different catalyst morphology, specifically the particle size and distribution. They also observed that under certain conditions, the addition of bases such as triethylamine could enhance the optical yield.

In a separate study using Pt/Al_2O_3 as catalyst they found similar effects for heat treatment and additives, however they managed to obtain an optical yield of 86.8 % for methyl pyruvate conversion to R-(+)-methyl lactate in a hydrogenation conducted in benzene, with quinine as both modifier and additive. An optical yield of 83.9 % was obtained for R-(-)-ethyl mandelate when the catalyst was modified by cinchonidine in benzene or diethyl ether.

1.4.2 Findings of Others

No further studies were reported by the Japanese workers, and research appeared to have halted until H.U. Blaser of the Swiss company, Ciba Geigy, Basel took interest in the Orito reaction. This led to collaboration with A. Baiker at the *Eidgenössische Technische Hochschule.* The field of study was then joined by P.B Wells of the University of Hull. The early work of these workers was reproduction of Orito's findings, but going into greater detail, followed by optimisation and diversification of the reaction.

The observation by Orito that the degree of enantioselectivity was sensitive to the catalyst morphology and preparation method was one of the first areas examined. Blaser, Baiker, Wells and their co-workers all found Pt particle size to be an important factor. The Swiss researchers recommended particles of 3-4 nm in size with a dispersion of not greater than 0.1 - 0.2 to attain high enantioselectivity (up to 90 %). They also found that the best catalysts resulted from the use of 5 % H_2PtCl_6 as pre-cursor on an alumina support with reduction by aqueous solutions of Na(HCOO), CH_2O or K(HCOO).[34,35,36] Wells *et al.* however chose to perform the majority of their studies with a 6.3 % Pt/silica, EUROPT-1 which had a mean metal particle size of 2 nm and a dispersion of 60 %,[37] their highest reported optical yield was 77 %. Their use of catalysts with smaller Pt particles resulted in diminished enantioselectivity[38].

The effect of pre-heating the catalyst prior to modification was studied further by these workers. Blaser *et al.* found that heat treatment of Pt/alumina catalysts at 673 K could raise optical yields by 15-20 %.[39] Sutherland *et al.* also noticed an increased optical yield by thermal treatment, their best result of 77 % enantiomeric excess coming when hydrogen was desorbed at 673 K, prior to the introduction of the modifier[38].

The metal of choice has been reported to be almost exclusively restricted to Pt. Although slight optical yields have been reported for Rh and Pd (the latter giving S-(-)-lactate in enantiomeric excess when cinchonidine was used as modifier), no enantiomeric excess was observed for Ni or Ru[34].

The choice of solvent is a major influence on the optical yield and rate of reaction. A general trend was observed that solvents with a dielectric constant between 2 and 8 gave the best optical yields[40]. However exceptions did exist, as acidic solvents gave higher, and basic solvents gave lower enantioselectivities than would be expected from their dielectric constant. The use of acetic acid as solvent led to one of the highest reported optical yields for a heterogeneous enantioselective reaction.

Several attempts have been made to optimise optical yields by variation of the modifier structure. The use of 10,11-dihydrocinchonidine was found to improve optical yields[34,41]. The replacement of the hydroxyl group in cinchonidine with a methoxyl group had little effect, whereas replacement by a hydrogen, chlorine or acetate group reduced the optical yield. Alkylation of the quinuclidine nitrogen resulted in zero enantiomeric excess.[42] From these studies it was concluded that the quinuclidine nitrogen plays a major role, whereas the substituent at C9 does not.

The examination of the reaction kinetics have been performed by both the Swiss and the British researchers[34,37,41,43]. All agree that the reaction is best performed at pressures greater than 10 bar and at temperatures less than 313 K. They all observed that the reaction was zero order in pyruvate and approximately first order in hydrogen for pressures less than or equal to 10 bar. However, Blaser reported that at pressures above 20 bar the reaction was 0-0.5 order in pyruvate. Where the 10,11-dihydrocinchonidine modified reaction obeys the Arhenius equation, Blaser *et al.* found the activation energy to be 29 ± 4 kJ mol-1 and Meheux *et al.* 33 ± 4 kJ mol^{-1} The optical yield was moderately influenced by the reaction pressure having a slight maximum at 50-70 bar.

The majority of the research has involved the study of α-ketoester hydrogenation, although a few other reactions have been found to be achievable. The first reported variations of the reaction was by Blaser who was able to perform hydrodehalogenation of dichlorobenzazepinone (figure 1.4) using cinchonine modified $Pd/BaSO_4$ in tetrahydrofuran solvent with tert-butylamine additive, achieving an optical yield of 50 %.[20] Blaser *et al.* also reported the ability of cinchona alkaloid modified Pt metal catalysts to catalyse the asymmetric hydrogenation of α-ketoacids[44]. These particularly focused on the use of 4-phenyl-2-oxobutyric acid, the hydrogenation of which could be utilised in the production of the angiotensin-converting enzyme inhibitor Benzepril. The highest optical yield attained was 85 % with the combination of a 5 % Pt/Al_2O_3 with O-methyl-dihydrocinchonidine in 10 % H_2O/EtOH. One of the most surprising results of the study was that the use of N-benzyl cinchonidine chloride led to

an 33 % enantiomeric excess of (S)-4-phenyl-2-hydroxybutyric acid. This result contrasts to that observed for α-ketoester hydrogenation with this modifier, where no reaction is observed[42].

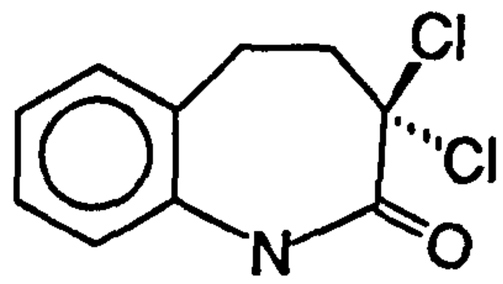

Figure 1.4

Dichlorobenzazepinone

Vermeer *et al.* also recently reported success in the asymmetric hydrogenation of the conjugated diketones, butane-2,3-dione and hexane-3,4-dione over cinchonidine modified EUROPT-1 to give enantioselectivities of 38 and 33 % respectively in favour of the R-(+)-hydroxyketone[45]. The best results were obtained when dichloromethane was used as solvent.

1.4.3 Mechanism

Since the reaction is reasonably reproducible, there is no controversy over any of the findings mentioned above. Where the great debate is focused is on the mechanism of the reaction. This is mainly as a result of the proposal of the so-called 'Template Theory'[37] which gave a molecular view of the mechanism. Although no formal mechanism was proposed at the time, an alternative explanation suggested a simple 1:1 interaction between the alkaloid and the pyruvate at the Pt surface,[35,42] although the interactions existing in solution were also considered to be crucial[46,47].

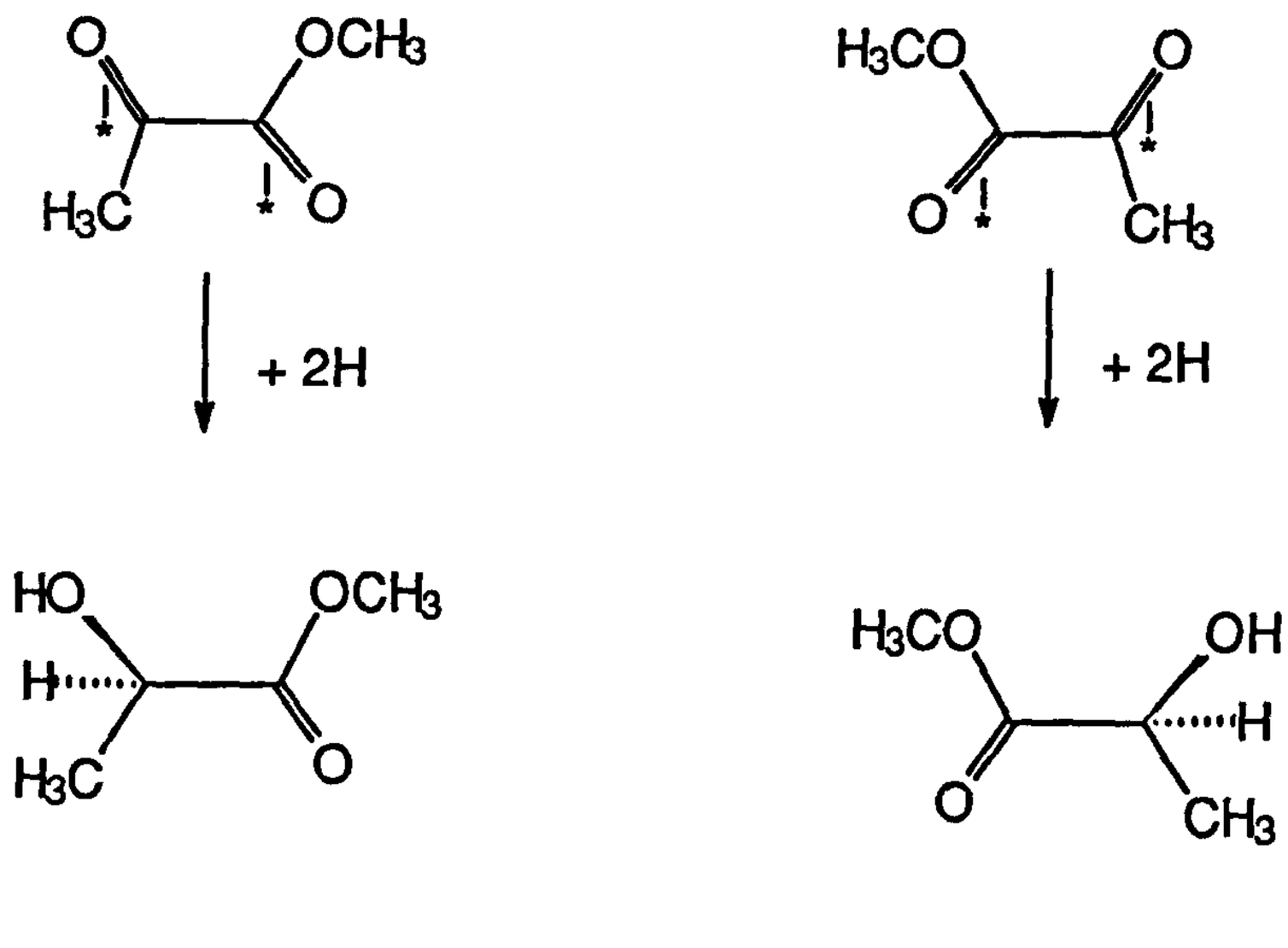

(R)-(+)-Methyl Lactate (S)-(-)-Methyl Lacate

Figure 1.5

The two enantiofaces of methyl pyruvate that can approach a catalyst surface

Before an explanation of the former mechanism is presented, it is convenient to consider the way in which the reactant can be assumed to approach the catalyst surface. Pyruvate can adsorb on a Pt catalyst, presenting one of its two enantiofaces to the surface. Based on the assumption that the pyruvate molecule is in the trans conformation, pyruvate can adsorb with its carbonyl groups, *top-left*, *bottom-right*, relative to the central C-C bond, or conversely *top-right*, *bottom-left*. The former case results in R-(+)-lactate formation, the latter S(-)-lactate. This is depicted in figure 1.5, and depends on the assumption that the addition of hydrogen atoms is below the plane of adsorption. The adsorption is assumed to occur on two adjacent Pt atoms, in an analogous manner to that described for alka-1,3dienes[48]. On an unmodified surface adsorption of both of the enantiofaces would be equally likely to occur, and so racemic product would result. It was proposed that the cinchonidine molecules would adsorb by the quinoline ring in an ordered non-close-packed manner. This ordered array of molecules left exposed shaped ensembles of Pt atoms (supposedly in a (100) configuration) into which pyruvate molecules could only conveniently adsorb onto the modified surface to give R-(+)-lactate on hydrogenation. The same arguments were proposed to be valid for S-(-)-lactate

formation when cinchonine was used as modifier. Although this argument accounted for enantio-differentiation, the carbonyl group to be hydrogenated was far from the quinuclidine nitrogen which, as mentioned above is a crucial component of the modifier.

In the light of this finding, and the scepticism declared by the author, the template theory (which was proposed solely to interpret the sense of the enantioselectivity) was revised[15], placing the carbonyl group to be hydrogenated in the vicinity of the quinuclidine nitrogen. This took into account the proposal that the quinuclidine-N was responsible for stabilising the half-hydrogenated state of the reactant by hydrogen bonding to the hydroxyl group[49] (see figure 1.6), thus leading to an enhanced rate of reaction. Two active sites were proposed and enantioselectivity was again explained in terms of steric hindrance, accommodating the pyruvate differently, but retaining the ordered array of alkaloid. The pyruvate molecule could easily adsorb in a planar fashion to produce R-(+)-lactate on hydrogenation (as depicted in figure 1.7), but adsorption of the alternative enantioface of the pyruvate was hindered by a second alkaloid molecule, arbitrarily placed adjacent to the first. The second type of active site for enantioselective hydrogenation occurred at the edge of the Pt crystallite, where adsorption of a pyruvate molecule adjacent to *one* alkaloid was only possible in a manner which produced R-(+)-lactate on hydrogenation.

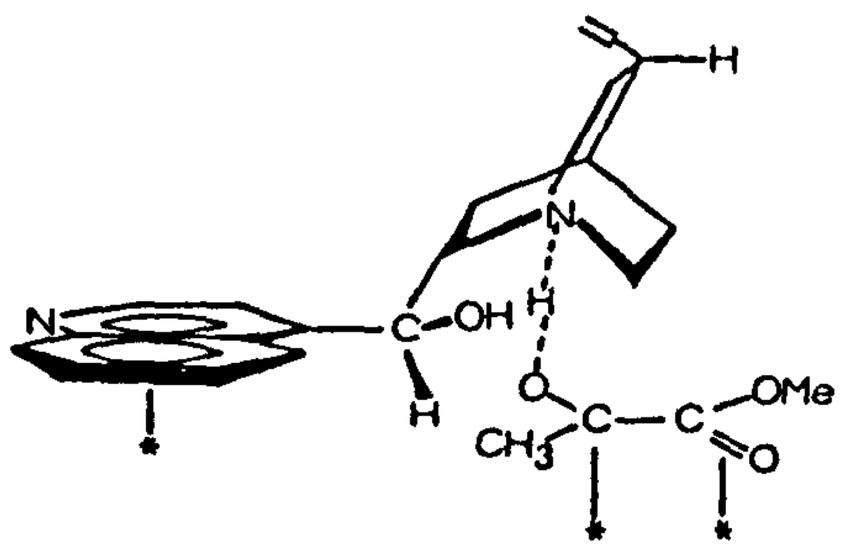

Figure 1.6

Stabilisation of hhs by hydrogen bonding to quinuclidine-N (reproduced from reference 49)

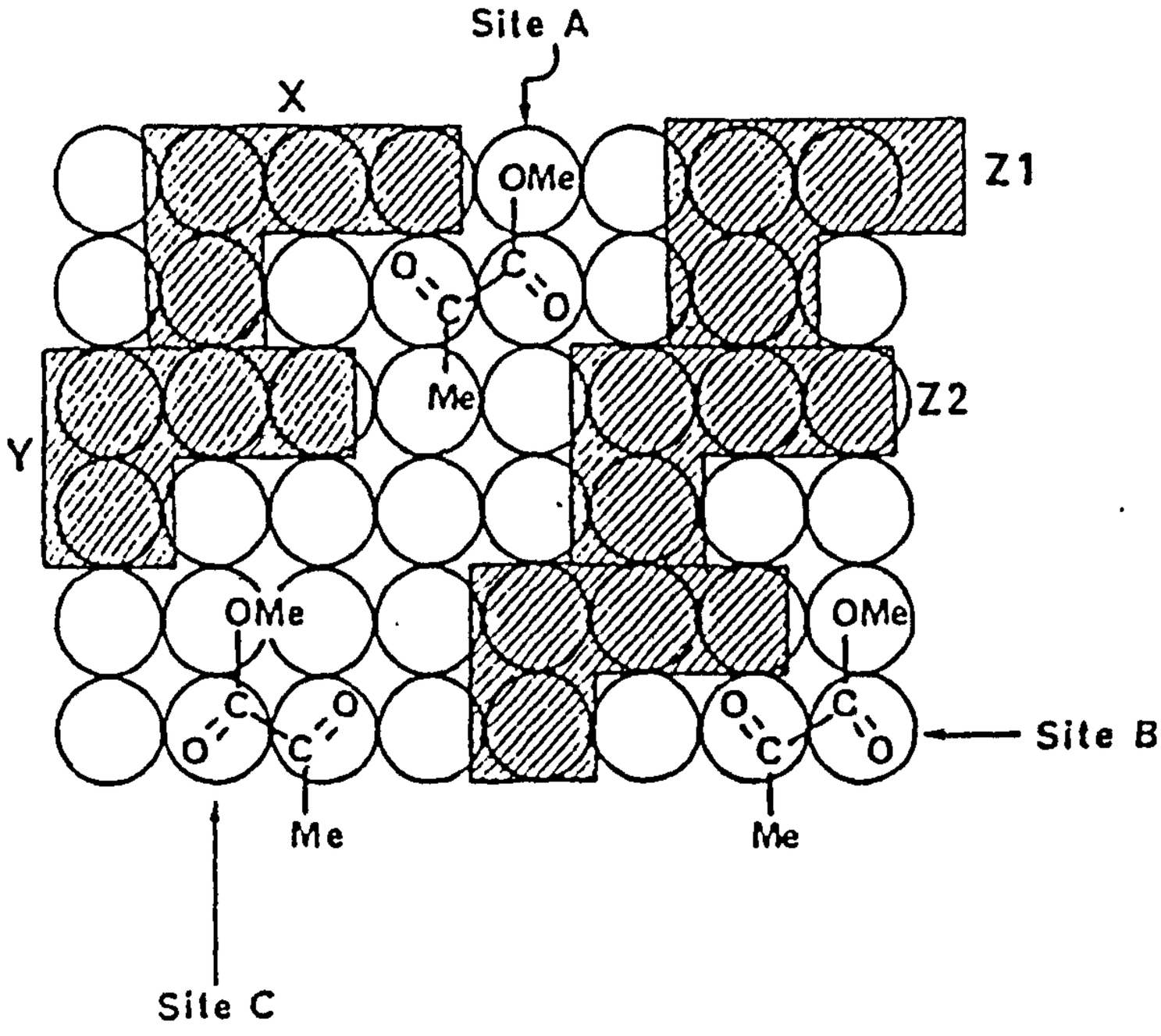

Figure 1.7

The Revised Template Theory showing Cinchonidine Molecules Adsorbed on a Pt (100) surface leaving shaped ensembles such that only one enantioface of methyl pyruvate can adsorb (reproduced from reference 15)

---

[1]J.B. Biot, Bull. Soc. Philomath., Paris 190 (1815).

[2]L. Pasteur, C.R. Acad.Sci., 26, (1848) 535.

[3]J.H. van't Hoff, Arch. Neerl. Sci. Exacts Nat. 9 (1874) 445.

[4]J.A. Le Bel, Bull. Soc. Chim. Fr., 22 (1874) 337.

[5]R.S. Cahn, C.K. Ingold and V. Prelog, Agnew. Chem. Int. Ed. Engl., 5 (1966) 385.

[6]R.D. Knihinicki, R.O. Day, G.G. Graham and K.M. Williams, Chirality, 2 (1990) 134.

[7]G.W. Mellin and M. Katzenstein, New. Engl. J. Med., 267 (1962) 1184.

[8]G. von Blaschke, H.P. Kraft, K. Finkenstcher and F.Köhler, Arzneim.-Forsch./Drug Res., 29 (1979) 1640.

[9]FDA Policy Statement, Chirality, 4 (1992) 338.

[10]A.G. Rauws and K. Groen, Chirality 6 (1994) 72.

[11]D.H. Deutsch, CHEMTECH, March 1991 157.

[12]G.M. Schwab and L. Rudolph, Naturwiss., 20 (1932) 362.

[13]G.M. Schwab, F. Rost and L. Rudolph, Kolloid-Zeitschrift, 68 (1934)157.

[14]T. Isoda, A. Ichikawa and T. Shimamoto, Rikagaku Kenkyusho Hokuku, 34 (1958) 134.

[15]G. Webb and P.B. Wells, Catal. Today, 12 (1992) 319.

[16]B.M. Choudary, V.L.K. Valli and A. Durga Prasad, J. Chem. Soc., Chem. Commun., (1990) 1186.

[17]B.M. Choudary, S. Shobha Rani and Y.V. Subba Rao, (L. Guczi, F. Solymosi and P. Tétényi, Eds.) in New Frontiers in Catalysis, 1993 Elsevier.

[18]A. Corma, M. Iglesias, C. Del Pino and F. Sanchez, J. Chem. Soc., Chem. Commun., (1991) 1253 .

[19]J.K. Stille, J. Macromol. Sci-Chem, A21 (1984) 1689.

[20]H.U. Blaser, Tetrahedron:Asymmetry 2 (1991) 843.

[21]H.U. Blaser and M. Müller, Stud. Surf. Sci. Catal., 59 (1991) 73.

[22]H.U. Blaser, Chem. Rev. 92 (1992) 935.

[23]G. W. Parshall and W.A. Nugent, CHEMTECH, March 1988, 184.

[24]G. W. Parshall and W.A. Nugent, CHEMTECH, May 1988, 314.

[25]G. W. Parshall and W.A. Nugent, CHEMTECH, June 1988, 376.

[26]Chirality in Industry, (Eds. A.N. Collins, G.N. Sheldrake and J. Crosby), J. Wiley and Sons, 1992.

[27]H.U. Blaser, personal communication.

[28]R.A. Sheldon, in "Chirotechnology", Dekker Inc, New York 1993.

[29]Y. Orito, S. Imai and S. Niwa, Nippon Kagaku Kaishi, (1979) 1118.

[30]Y. Orito, S. Imai and S. Niwa and G-H. Nguyen, Yuki Gosei Kagaku-shi, 37 (1979) 173.

[31]Y. Orito, S. Imai and S. Niwa, Nippon Kagaku Kaishi, (1980) 670.

[32]S. Niwa, S. Imai and Y. Orito, Nippon Kagaku Kaishi, (1982) 137.

[33]Y. Orito, S.Imai and S. Niwa, USP 4,329,487.

[34]H.U. Blaser, H.P. Jalett, D.M. Monti, J.F. Reber, and J.T. Wehrli, Stud. Surf. Sci Catal., 41 (1988) 153.

[35]J.T. Wehrli, A. Baiker, D.M. Monti and H.U. Blaser, J. Mol. Catal, 49 (1989) 195.

[36]J.T. Wehrli, A.Baiker, D.M. Monti and H.U. Blaser, J. Mol. Catal., 61 (1990) 207.

[37]I.M. Sutherland, A.Ibbotson, R.B. Moyes and P.B. Wells, J.Catal 125 (1990) 77.

[38]S.D. Jackson, M.B.T. Keegan, G.D. McLellan, P.A. Meheux, R.B. Moyes, G. Webb, P.B. Wells, R. Whyman and J. Willis, Preparation of Catalysts V, (G. Poncelet, P.A. Jacobs, P. Grange and B. Delmon (Eds)), pp 135-144, Elsevier, Amsterdam, 1991.

[39]H.U. Blaser, H.P. Jalett, D.M. Monti and J.T. Wehrli, Appl. Catal. 52 (1989) 19.

[40]H.U. Blaser, H.P. Jalett and J. Wiehl, J. Mol. Catal., 68 (1991) 215.

[41]P.A. Meheux, A. Ibbotson and P.B. Wells, J. Catal, 128 (1991) 387.

[42]H.U. Blaser, H.P. Jalett, D.M. Monti, A. Baiker and J.T. Wehrli, Structure-Activity and Selectivity Relationships in Heterogeneous Catalysis, (R.K. Grasselli and A.W. Sleight (Eds.)), 1991, Elsevier, Amsterdam.

[43]H.U. Blaser, p. 317 "Advances in Catalyst Design", (M.Grazini and C.N. Rao (Eds.)) World Scientific, Trieste, 1991.

[44]H.U. Blaser and H.P. Jalett, (M. Guisnet *et al.* Eds.) Stud. Surf. Sci. Catal. 78 (1993) 139.

[45]W.A.H. Vermeer, A. Fulford, P. Johnston and P.B. Wells, J. Chem. Soc., Chem. Commun., (1993) 1053.

[46]J.L. Margitfalvi, P. Marti, A. Baiker, L. Botz and O. Sticher, Catal. Letts. 6 (1990) 281.

[47]J.L. Margitfalvi, B. Minder, E. Tálas, L. Botz and A. Baiker, p 2471 (L. Guzi et al, eds.), in New Frontiers in Catalysis, 1993, Elsevier.

[48]A. J. Bates, Z.K. Leszczynski, J.J. Phillipson, P.B. Wells and G.R. Wilson, J. Chem. Soc. A 507 (1970).

[49]G. Bond, P.A. Meheux, A. Ibbotson and P.B. Wells, Catal. Today, 10 (1991) 371.

Chapter 2

Experimental

2.1 Materials

2.1.1 EUROPT-1

The standard reference catalyst, EUROPT-1 was used extensively in this study. The catalyst was manufactured by Johnson Matthey for the Research Group on Catalysis of the Council of Europe (later EUROCAT). Their purpose was to achieve the extensive characterisation of a Pt catalyst and thereby to make available a standard reference material that would be made available for calibration purposes to workers in both universities and industry.

EUROPT-1 is a 6.3 % Pt/silica catalyst, prepared by impregnation of $Pt(NH_3)_4Cl_2$ onto silica by ion exchange, followed by reduction in hydrogen at 673 K. The as received catalyst is substantially oxidised. The total surface area of the catalyst is 185 ± 5 m^2g^{-1}, the size distribution of the visible Pt particles in the as received state ranges from 0.9 to 3.5 nm, 75 % of these particles being ≥ 2.0 nm[1,2,3,4,5] in diameter. The dispersion of the Pt is about 60 %.

EXAFS spectroscopy suggests that an average metal particle consists of 55 Pt atoms arranged as a 7 x 7 raft-like array of platinum atoms in a (111) configuration, with a further 8 atoms on top of the 'raft'[6]. However, XRD measurements taken by other members of the EUROCAT group suggest a 55 atom cubo-octahedral structure[7,8,9].

Reduction of the catalyst in hydrogen commences at 200 K, reaching a maximum at 330 K and is complete at 423 K. Bulk reoxidation does not occur immediately on exposure to air at 298 K but slowly over a number of days[10].

2.1.2 Ir/calcium carbonate

Two commercial 5 % Ir/calcium carbonate catalysts were supplied by Johnson Matthey. These catalysts[11] were prepared from H_2IrCl_6 and have metal surface areas of 4.5 m^2g^{-1} (measured by CO chemisorption and assuming the linear bonding mode). The support has a surface area in the range of 2 - 10 m^2g^{-1}. Two different batches were supplied which are designated Ir/$CaCO_3$-1 and Ir/$CaCO_3$-2. The former was reduced by the manufacturer, but the latter was not.

2.1.3 Other Catalysts

Other catalysts or catalyst pre-cursors used are summarised in table 2.1. Unless otherwise stated they were used as received. The GHI catalyst was prepared at Billingham during a collaborative study between Glasgow University, Hull University and ICI Chemicals and Polymers. The preparation, characterisation and reactivity of this catalyst have been reported[12,13,14].

10 % and 20 % Ir/silica samples were prepared at Hull by J. Martos in the late 1970's. Silica was impregnated with an aqueous solution of H_2IrCl_6 and was then reduced in flowing hydrogen at 673 K for 6 h. Electron microscopy showed a particle size distribution extending from 2.0 to 10.0 nm. The distribution had a maximum at 4.0 nm for 20 % Ir/silica and at 2.5 nm for 10 % Ir/silica[15]. Only very small quantities of these materials were available for study (ca. 0.1 g).

Ir/alumina was a research catalyst manufactured by Johnson Matthey. The metal surface area (measured by CO chemisorption and assuming the linear bonding mode) was 14.4 m^2g^{-1}. The total surface area of the catalyst, as measured by nitrogen BET was 120 m^2g^{-1}. Measurement of pore size distribution by nitrogen BET and Hg porosimetry suggested a mean pore radius of 75 Å and the mean particle size measured by use of a Coulter counter was 12.1 μm[16].

Table 2.1

Other Catalysts used in Studies

Catalyst	Source
5 % Ir/alumina	Johnson Matthey[a]
10 % Ir/silica	Hull[b]
20 % Ir/silica	Hull[b]
5 % Pt/calcium carbonate	Aldrich
3 % Os/alumina	Hull[b]
20 % Re_2O_3/alumina	Hull[b]
5 % Rh/alumina	Johnson Matthey

[a] Research sample
[b] Catalysts prepared by previous workers

2.1.4 Cinchona Alkaloids

Cinchona alkaloids are naturally occurring substances first discovered by Pellettier and Caventou in 1820 in the bark, branches and roots of trees belonging to the cinchona species of the *Rubiaceae* family found in South America. Their name derives from the fact that they were amongst the first discovered examples of basic nitrogenous carbon-containing compounds and being 'alkali-like' they were named alkaloids. The principle cinchona alkaloids are cinchonidine, cinchonine, quinine and quinidine (figure 2.1); the former and latter pairs are near-enantiomers. The principle difference in each pair is the configuration at the C8 and C9 positions, the minor difference being the position of the vinyl group attachment on the quinuclidine moiety. It is this minor difference that prevents each pair of alkaloids being enantiomers.

Hydrogenation of the naturally occurring alkaloid at 5 bar in ethanol solvent over a Pd/C catalyst results in hydrogen addition across the vinyl group at the C10 and C11 positions[17]. The 10,11-dihydrocinchonidine (DHC) prepared by P. Meheux using this

method was used in parts of this study. The alkaloids and the source of supply are summarised in table 2.2.

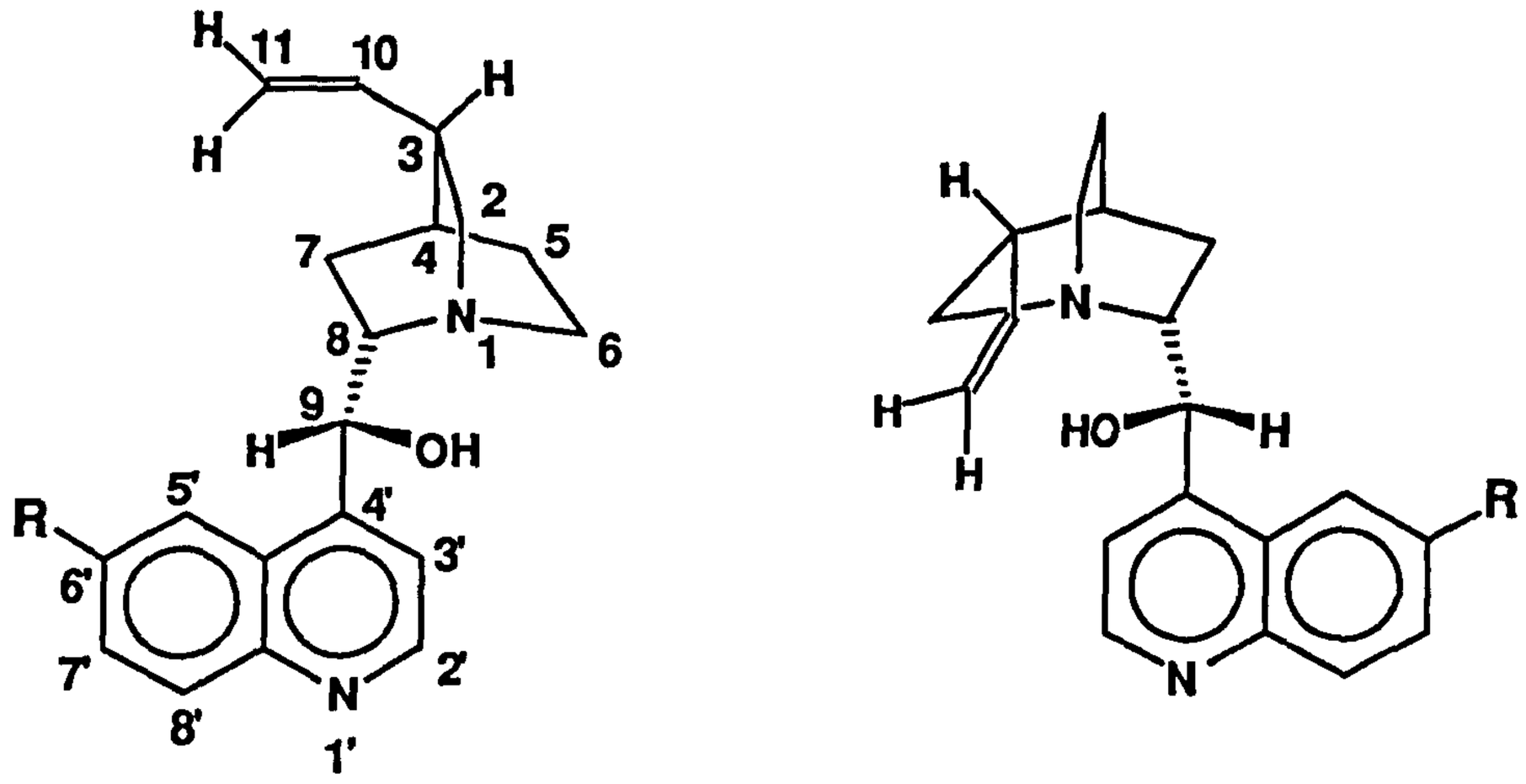

R = H	Cinchonidine	Cinchonine
R=OMe	Quinine	Quinidine

Atom	C_3	C_4	C_8	C_9
Configuration	R	S	S	R

C_3	C_4	C_8	C_9
R	S	R	S

Figure 2.1

Structure of the principal alkaloids

Table 2.2

Source of Principle Alkaloids

Alkaloid	Supplier
Cinchonidine	Aldrich
Cinchonine	Hopkin & Williams
Quinidine	B.D.H
Quinine	Ventron
DHC	Prepared in Hull

2.1.5 Cinchona Alkaloid Derivatives

Various derivatives of the cinchona alkaloids are available or may be synthesised. Four such derivatives that have recently become commercially available from Aldrich are 10,11-dihydroquinine 4-methyl-2-quinoyl ether, 10,11-dihydroquinine 9-phenanthryl ether and also the 10,11-dihydroquinidine analogues. The structures for the former two compounds, showing the large bulky substituents at the C9 position are shown in figures 2.2 and 2.3.

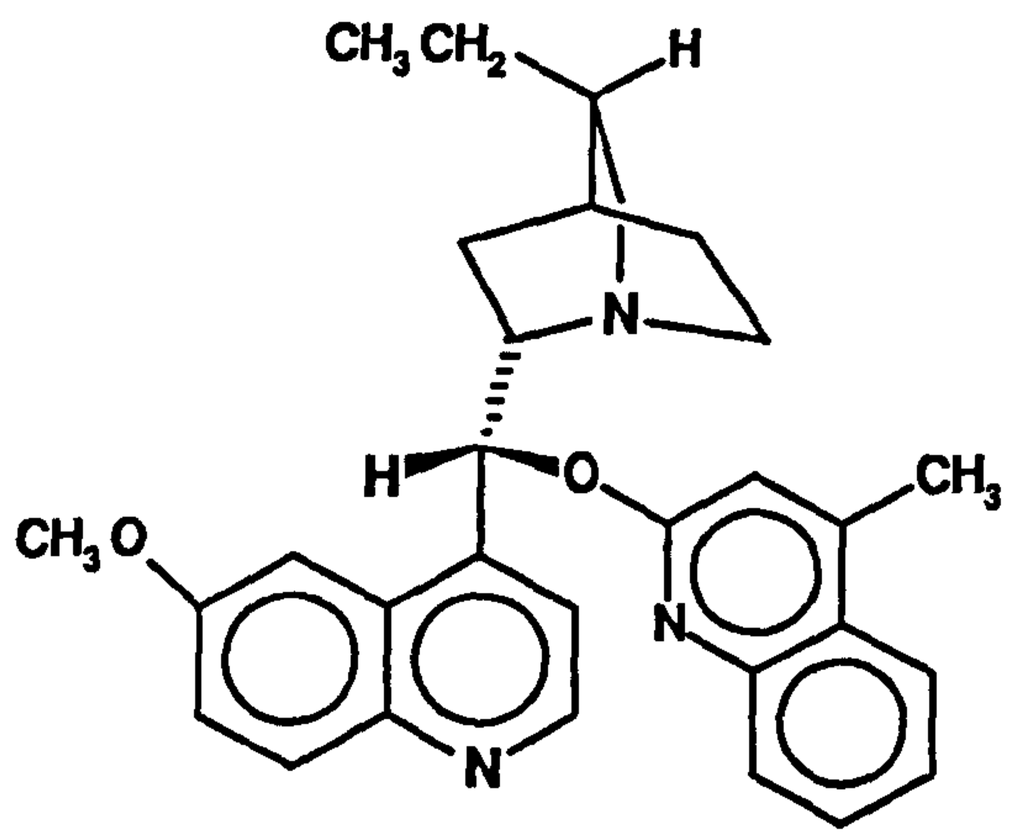

Figure 2.2.

Structure of 10,11-dihydroquinine 4-methyl-2-quinoyl ether

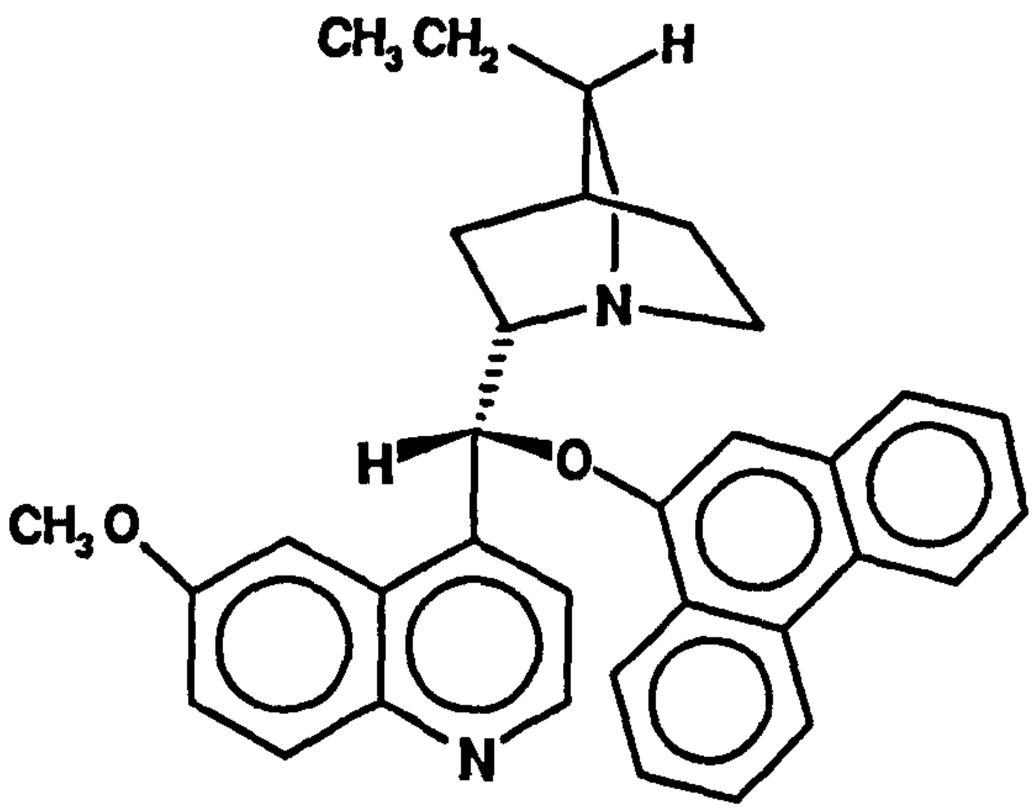

Figure 2.3

Structure of 10,11-dihydroquinine 9-phenanthryl ether

2.1.6 Ephedrine Derivatives

Ephedrine contains chiral centres at the C1 and C2 positions and is available in all four stereoisomers. The structure of one enantiomer is given in figure 2.4. Also available was the analogue deoxyephedrine (or methylated amphetamine) shown in figure 2.5. All the ephedrine derivatives used were supplied by Sigma.

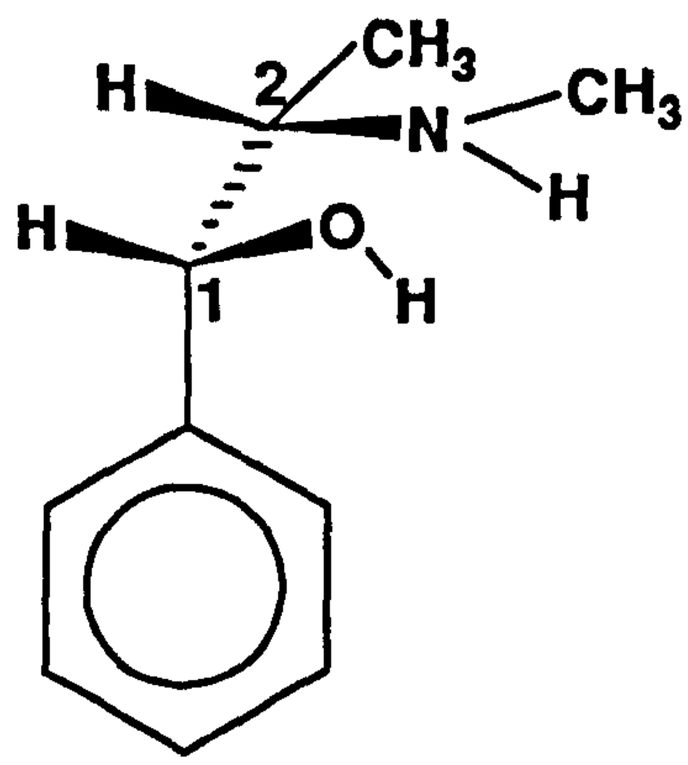

Figure 2.4

Structure of 1R,2S-Ephedrine

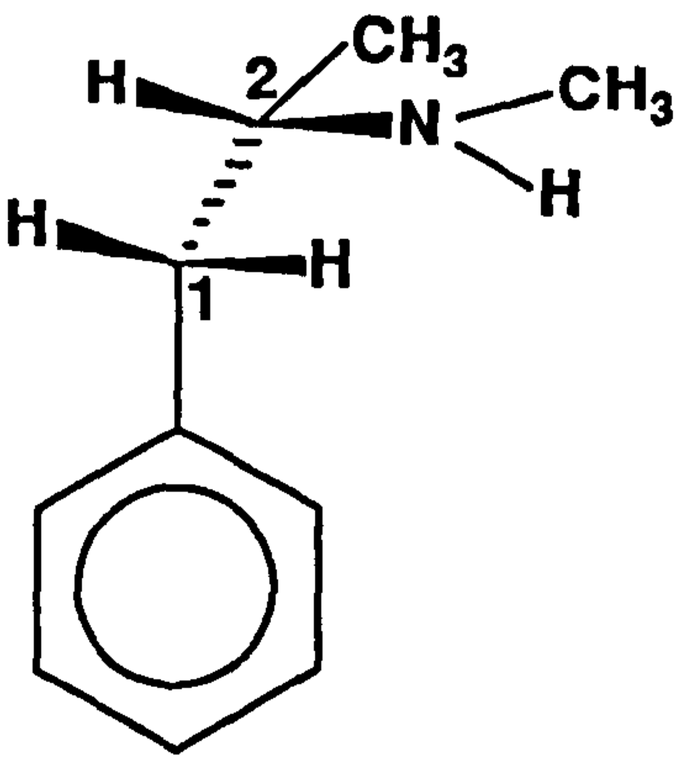

Figure 2.5

Structure of (-)-Deoxyephedrine

2.1.7 Non-Alkaloid Modifiers

The α-amino acids tryptophan and histidine, which only posses one chiral centre, were used as modifiers. They are analogous to the cinchona alkaloids in that they contain an N-C-C-O sequence of atoms, an aromatic ring and are 'L-shaped' in nature. These amino acids, purchased from Sigma were L- and D-histidine, L- and D-tryptophan and L- and D-tryptophan methyl ester. The structures of L-histidine and L-tryptophan given in figures 2.6 and 2.7.

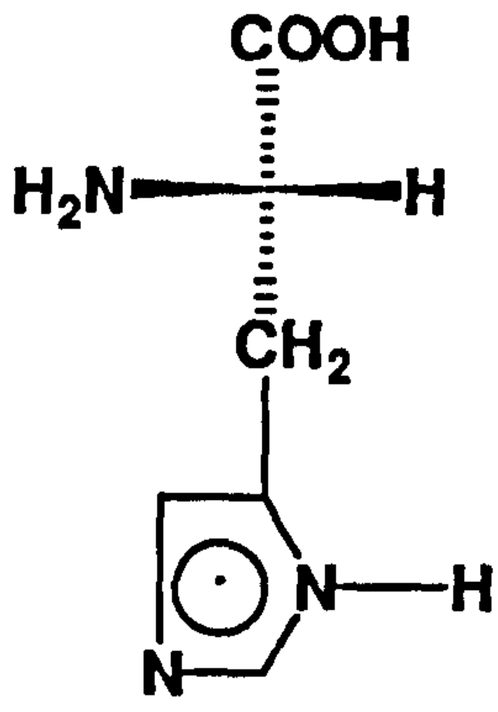

Figure 2.6

Structure of L-Histidine

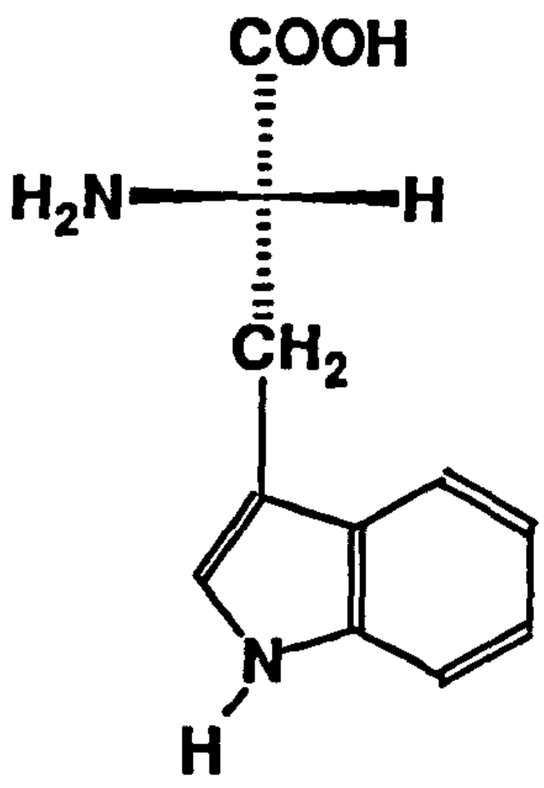

Figure 2.7

Structure of L-Tryptophan

S-(-)-1-benzyl-2-pyrrolidine methanol, which also contains one chiral centre, an aromatic ring and a N-C-C-O sequence, was used as a modifier. Its structure is given in figure 2.8. The material was supplied by Aldrich.

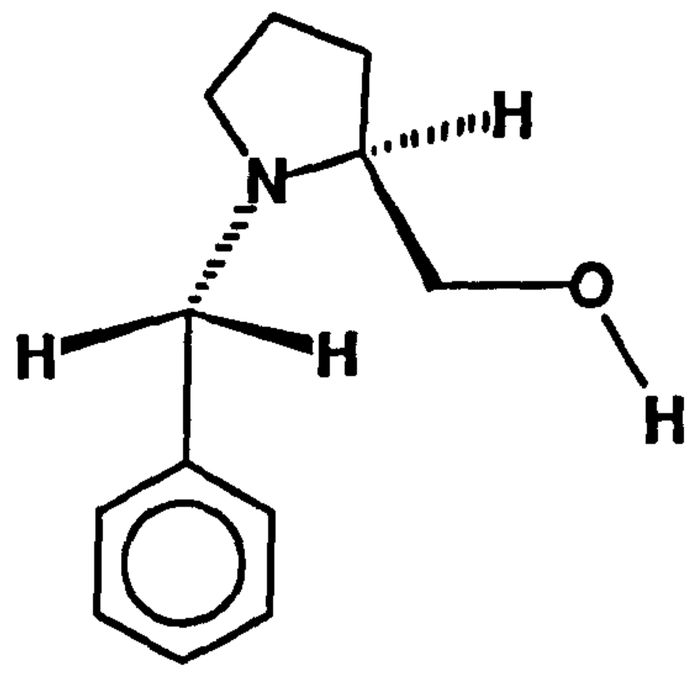

Figure 2.8

Structure of S-(-)-1-benzyl-2-pyrrolidine methanol

2.1.8 Other Materials

Other materials were used as-received and are listed, with the supplier in table 2.3.

2.2 Apparatus

2.2.1 Vacuum Apparatus

A general purpose glass vacuum apparatus equipped with greaseless Young's Taps and Springham ground glass taps was used for catalyst activation. Vacuum was achieved by use of a two-stage Edwards Speedivac oil rotary pump in conjunction with an Edwards oil diffusion pump. Pressure inside the apparatus could be measured using a mercury manometer, or at higher vacuum by a Heraeus Autovac control unit with a Pirani-type LBK pressure sensor.

Table 2.3

Additional materials used in studies

Material	Supplier
Methyl pyruvate	Fluka
Benzil	BDH
Quinuclidinol	Aldrich
Dichloromethane	Fisons
Dodecanol	BDH
Ethanol	BDH
Methylacetoacetate	Aldrich
1,2-Dichloroethane	BDH
Toluene	AnalaR
Hydrogen	Energas
Deuterium	BOC
Nitrogen	BOC
5% Hydrogen/Argon	ECM
Carbon Dioxide	G&E

2.2.2 Static Reduction

Static reduction of the catalyst was performed in 17 or 20 ml glass vessels equipped with a Young's tap and Suba-Seal No. 17 as shown in figures 2.9 and 2.10, respectively. The reduction vessel was sealed using a Viton 'O' ring on a B19 cone to the glass vacuum apparatus described in section 2.2.1. The reduction vessel was heated using an Amalgams Tubular furnace powered by a 0-240 V Variac. The temperature was monitored by a Kane-May 450 digital thermometer with chromel-alumel thermocouple probe.

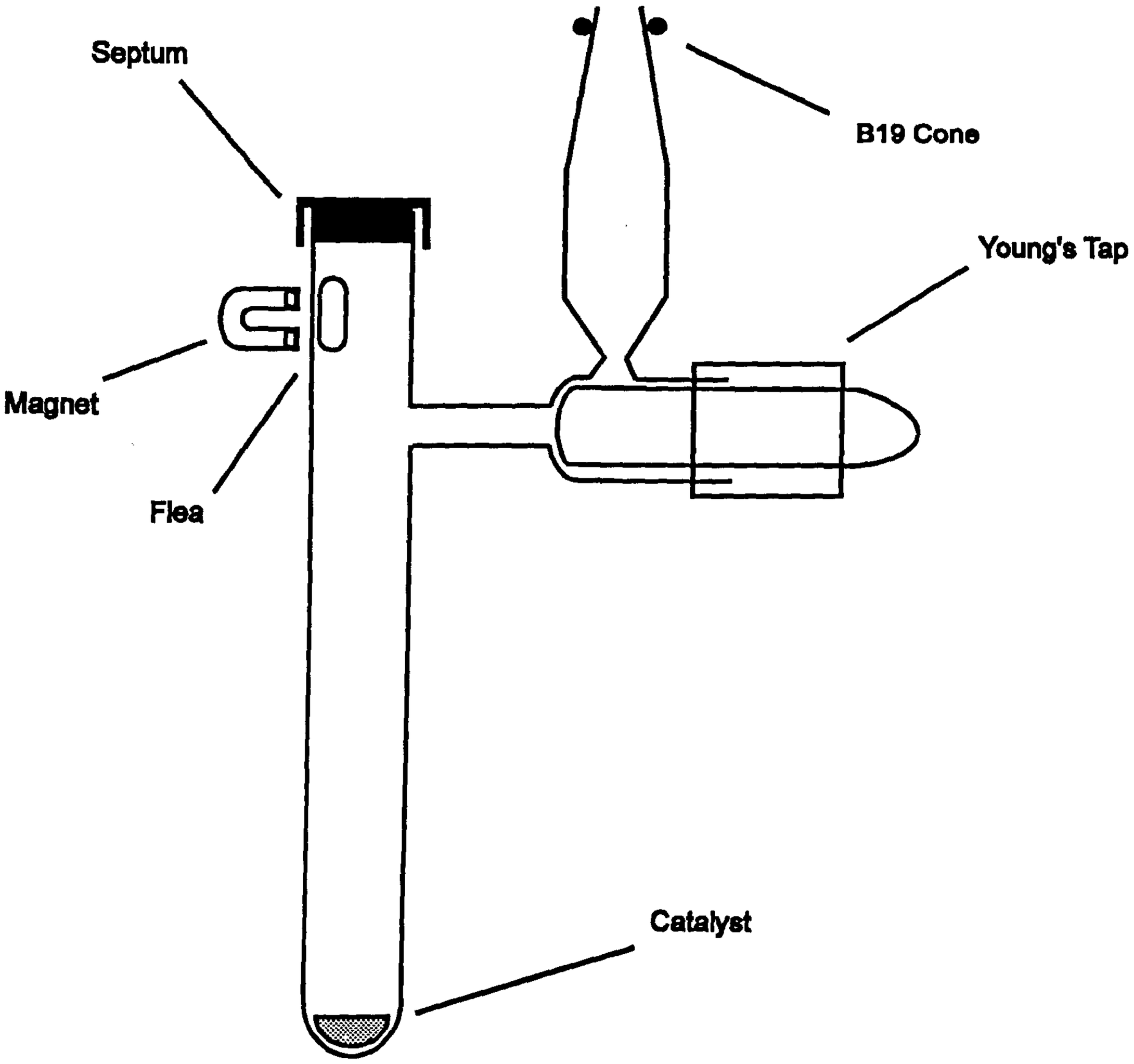

Figure 2.9

17 ml Static Reduction Vessel

If the catalyst was subsequently to be used for a deuterium tracer study a 1/2 " teflon coated magnetic stirrer bar or 'flea' was held in the upper part of the side-arm of the static reduction vessel by a small removable magnet secured by an elastic band. After catalyst reduction the 'flea' would fall onto the catalyst upon removal of the magnet. The contents of the reduction vessel could be stirred by a Gallenkamp magnetic stirrer.

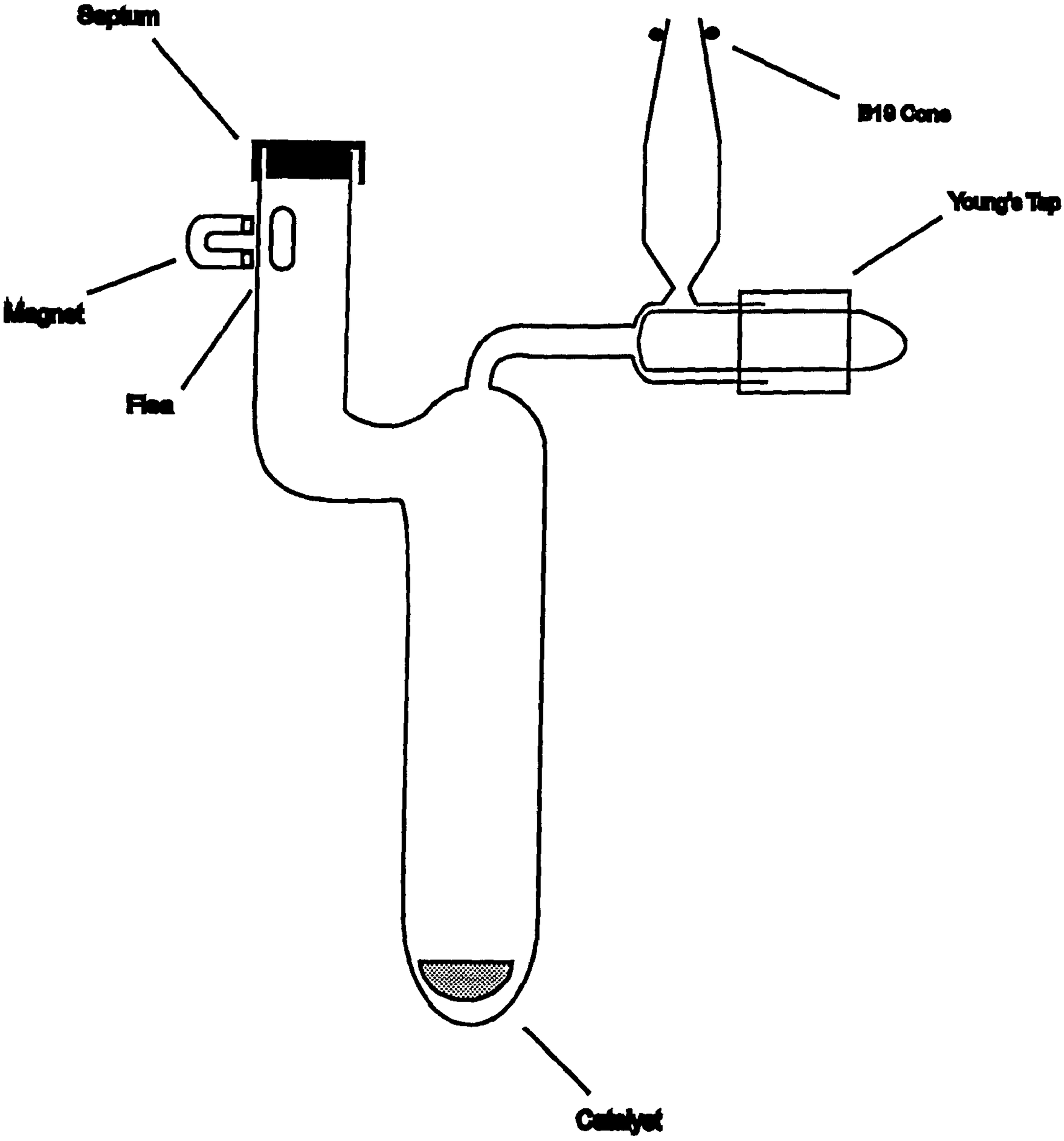

Figure 2.10

20 ml Static Reduction Vessel

2.2.3 Flow reduction

Flow reduction of the catalyst was performed in the glass vessel depicted in figure 2.11. The catalyst was placed onto a porous glass frit and the vessel secured to a B19 socket on the vacuum apparatus (see section 2.2.1) using a Viton 'O' ring on a glass B19 cone. A glass to metal seal onto a 1/4 " Wade coupling allowed connection to a

flexible teflon tube through which the exhaust gas was vented to the fume cupboard. A Perkin-Elmer F11 gas chromatograph oven with a small hole cut into the insulation was raised around the reduction vessel and used as a furnace. The temperature was controlled by a Perkin-Elmer linear temperature programmer and monitored by a Kane-May 450 digital thermometer with chromel-alumel thermocouple probe. Gas flow could be switched by use of a selector valve between 5% H_2/Ar and CO_2 and the rate of flow controlled and measured by a GEC-Marconi Series 100 flow meter at a pressure measured by a Budenburg 0 - 30 psi gauge.

2.2.4 Catalyst Modification

Modifier solution was injected into the static reduction vessel described above using a 20 ml pyrex syringe and 2" metal needle. This was replaced at a later time by 10 ml plastic disposable syringes and 1" needles (to decrease the opportunity for contamination). Modification itself occurred in a 100 ml glass beaker which was placed on a Gallenkamp magnetic stirrer, and the contents agitated by a 1" teflon coated stirrer bar.

2.2.5 Modifier Recovery

Modifier solution was placed in open sample bottle and subjected to a gentle flow of air. The apparatus is depicted in figure 2.12.

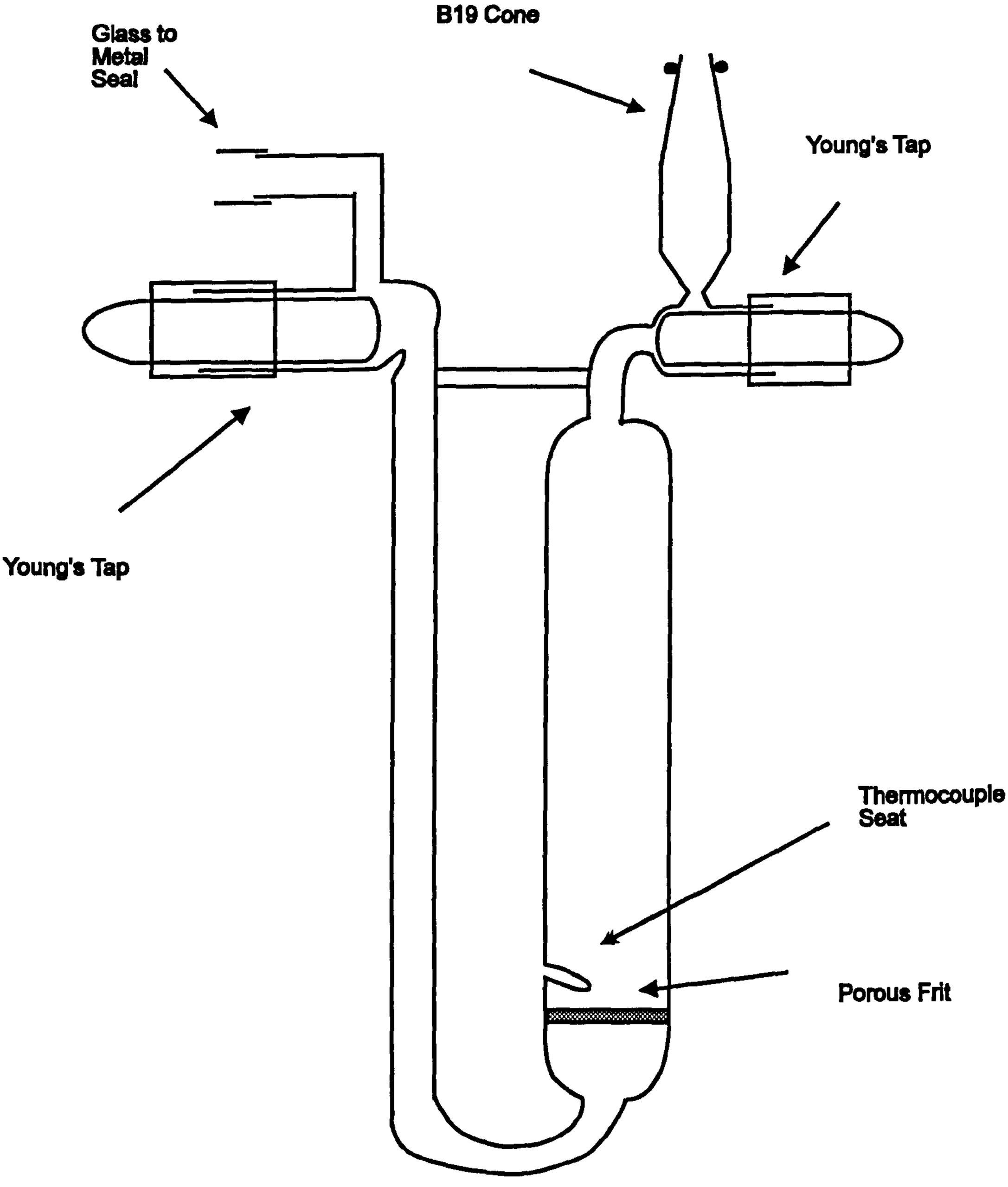

Figure 2.11
Flow reduction Vessel

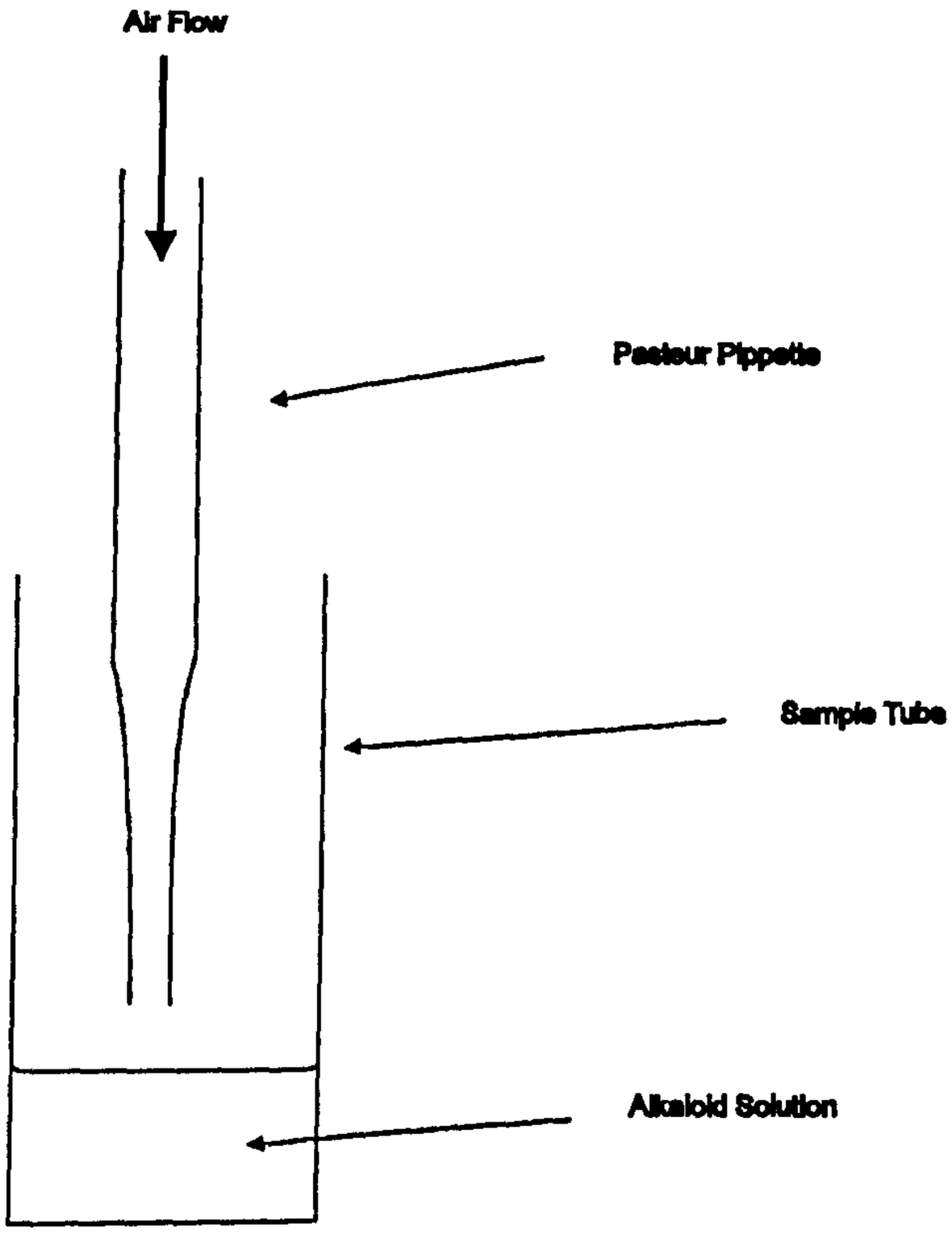

Figure 2.12

Apparatus for Modifier Recovery

2.2.6 Catalyst Sintering

In order to sinter the catalyst, high temperatures were required. This was achieved in Hull by replacing the flow reduction vessel described in figure 2.11 with a simple silica tube into which porcelain boats were placed. The tube was placed horizontally into an unbranded tubular furnace and closed at each end with ground glass seals to which were attached flexible plastic tubes. The ends of the furnace were then sealed by silica wool insulation. The rest of the equipment was as described in section 2.2.3.

Sintering of the Ir/alumina catalyst at very high temperatures was performed at the Leverhulme Centre for Innovative Catalysis, Liverpool University in a Carbolite tubular furnace in the same vessel as described above. The flow of gas could be split

between hydrogen and carbon dioxide using a 3-way valve, controlled using a Brooks flow controller and measured with a bubble-meter.

2.2.7 Fischer-Porter Autoclave

Hydrogenation at medium pressure was performed in a Fischer-Porter reaction system as shown in figure 2.13. The apparatus contained two reactors, only one of which was used at a time. Each reactor was a 200 ml round bottomed glass vessel able to withstand 12 bar pressure. The glass vessel was sealed, using a viton 'O' ring and washer to a metal mount and secured by two metal collars the lower of which had a teflon liner. When the two metal collars were screwed into each other, the teflon liner pressed the glass reactor into the seal, so ensuring the pressure integrity of the reactor. The reactor mount contained a tube through which reactant gas could flow into the reaction vessel. A thermocouple probe placed in the hollow metal dip-tube, sealed at the bottom enabled the temperature of the reactor to be measured by a Kane-May 450 digital thermometer. The 1" teflon-coated magnetic stirrer bar with teflon collar was stirred with a Gallenkamp magnetic stirrer to agitate the reactor contents. A metallic wire mesh was placed around the pressure vessel as a safety precaution against flying glass in the event of failure of the pressurised vessel. The temperature of the reaction was maintained by placing a water bath around the reactor vessel. The temperature could be lowered below ambient by using an acetone/$CO_{2\ (s)}$ mixture in place of the water bath.

On one reactor mount was a Nupro 2-way valve, the end of which housed a septum. When the valve was opened liquid could be injected through the septum into the reactor vessel. This option was only possible if the reactor pressure was at atmospheric pressure or lower. During hydrogenation the valve would remain closed.

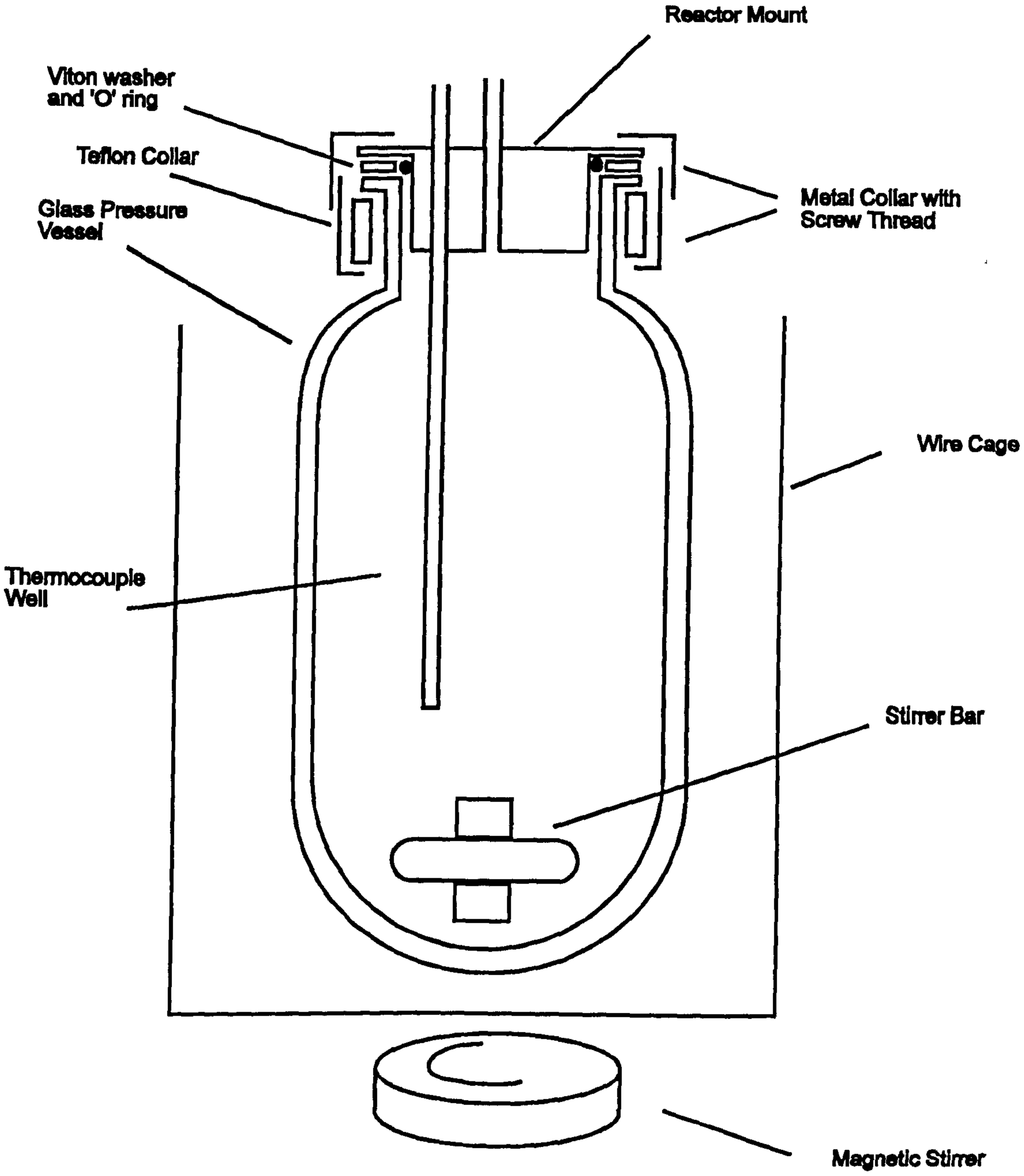

Figure 2.13

Fischer-Porter Reaction Vessel

The remainder of the reactor system, made up from 1/4" stainless steel tubing, consisted of a WIKA 0 - 200 psi pressure gauge, a HOKE pressure relief valve set at 220 psi, a line in from the hydrogen dosing system and a vent line to the fume cupboard to which could also be attached a two-stage Speedi-Vac oil rotary pump. The Hone needle valves were later replaced for Nupro 2-way valves during the period of study. The vent

line was also changed to consist of a Nupro 2-way valve in series with a Whitey needle valve. A polycarbonate blast screen, surrounding the reaction system, could be lowered into place before operation of the autoclave.

The hydrogen dosing system was designed and built in Hull by Dr. I.M. Sutherland and is represented in figure 2.14. Hydrogen and nitrogen gas could be admitted into the system via Nupro two-way valves in series with Nupro non-return valves at a pressure controlled by a BOC 0-16 bar regulator. As a safety precaution hydrogen gas was supplied via an intermediate lecture bottle reservoir at 20 bar pressure. From time to time this would be completely emptied and flushed with hydrogen.

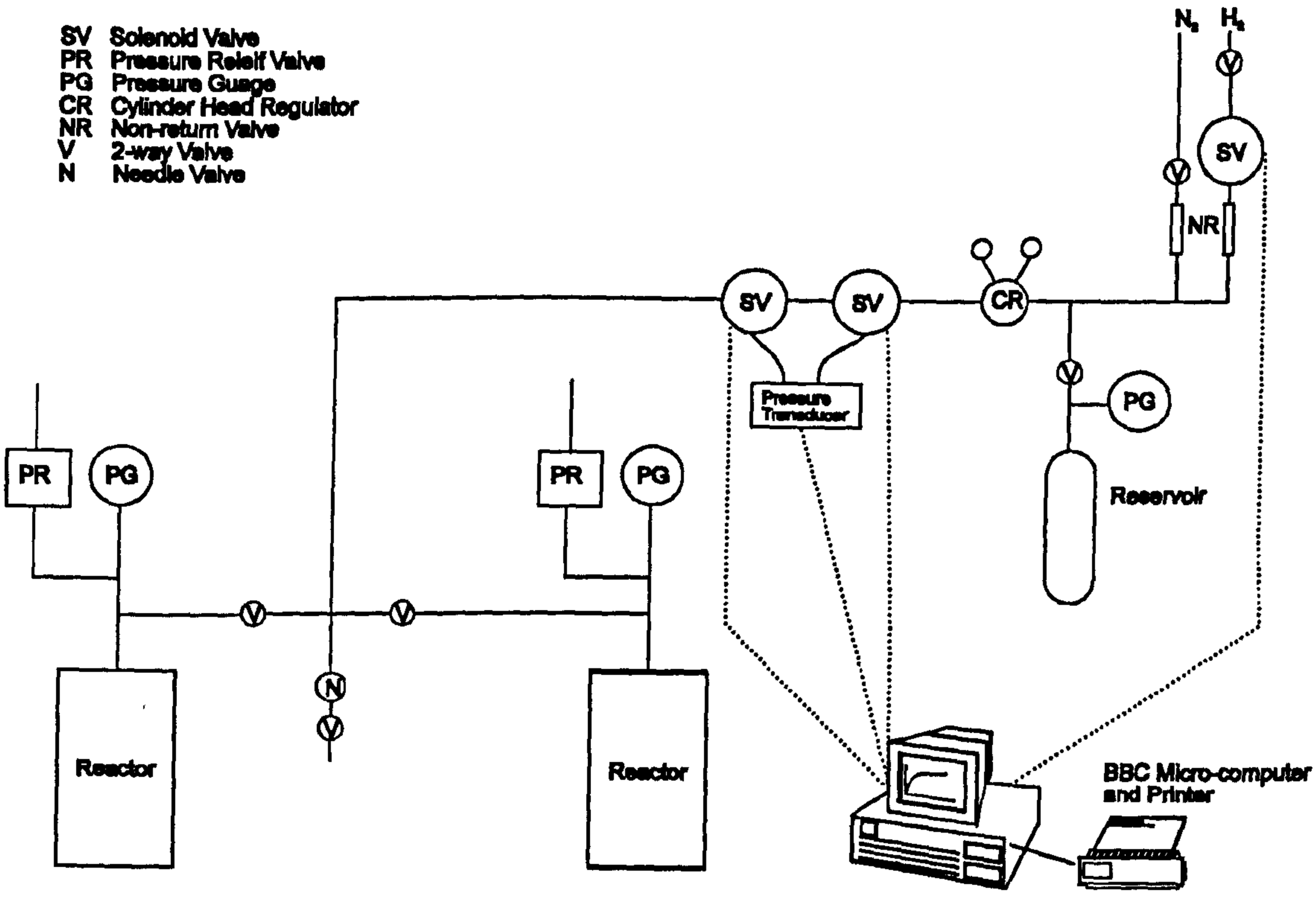

Figure 2.14

Hydrogen Dosing System

The difference between the reference hydrogen pressure and the reactor pressure was detected using a South East Labs pressure transducer supplied with a constant 24 V

input by a Farnell stabilised power supply unit. Between the regulator and the reactor were two R.S. solenoid valves, *between which* was a constant volume of ca. 15 ml (later in the work this was replaced by a constant volume of ca. 8.6 ml). When the transducer detected an increase in the differential pressure of 20 torr (i.e. hydrogen consumption in the reactor) R.S. relays would activate the solenoid valves in a sequence which (a) dosed the known volume at known pressure into the reactor and (b) recharged the constant volume to the reference pressure. Pressure was therefore maintained constant (± 0.03 bar).

The hydrogen metering system was controlled by a program running on a BBC Model B micro-computer. The differential pressure from the transducer was measured as a voltage, into the computer's on-board Analogue to Digital converter (a voltage limiter was incorporated into the circuit to protect the computer). The relays operating the solenoid valves were controlled using the computer's 'User-Port'. Hydrogen consumption was displayed on the monitor as a function of time and results were saved to disk.

2.2.8 Büchi Autoclave

Hydrogenation at medium pressures could also be achieved in the Büchi autoclave, pressure tested to 12 bar at 473 K and represented in figure 2.15. The 250 ml round bottomed glass reactor vessel was housed in a further 1000 ml glass jacket. The glass vessel was secured to a viton seal on the metallic reactor mount by eight bolts. Agitation of the reactor contents was achieved by a metal impeller secured to a metal stirrer shaft. The stirrer shaft was magnetically coupled to a drum that was rotated using a drive belt to a Planetrol motor capable of variable speeds up to 2200 r.p.m. To ensure adequate mixing and operation outside diffusion control limitations the reactor had a baffle that prevented any vortex in the reactor. A metal dip-tube sealed at the end housed a thermocouple probe. Pressure inside the reactor could be partially or fully released by use of an Autoclave Engineers Needle Valve. All the metal parts in the reactor were

chrome plated. The pressure vessel was housed behind removable polycarbonate blast shielding.

Temperature control of the reactor was achieved by pumping cryogenic liquid through the space between the reactor and glass jacket. Heating of the reactor to temperatures up to 523 K was achieved by a Julabo HC8 heating unit. The unit consisted of heating elements submerged in a large reservoir of dimethyl polysiloxane (flash point 533 K). A recirculator would pump the liquid through the reactor. The unit monitored the temperature of the reaction mixture by use of a PT100 sensor, the feedback from which determined the amount of heating supplied to the liquid. When the desired operating temperature was between 293 K and 313 K, the silicone oil was cooled by flowing water through internal coils in the reservoir. This was necessary counteract the heating effect from the recirculator pump.

For operation of the reactor at sub-ambient conditions a Churchill refrigeration unit was used. The unit was capable of maintaining a constant temperature in the range of ca. 268 - 318 K. A mixture of 25 % v/v ethylene glycol in water was pumped through the reactor lining via a large reservoir. Temperature control was maintained by the Churchill unit by internal measurement. The temperature in the reactor was measured using a Kane-May 450 digital thermometer and chromel-alumel thermocouple probe housed in a dip-tube.

The hydrogen dosing system used on the Büchi autoclave was similar to the one described in section 2.2.7 with the exceptions that: a R.S. adjustable voltage power supply was used; the hydrogen pressure in the lecture bottle reservoir was 10.4 bar; and the South East Labs. pressure transducer was twice as sensitive as the model on the Fischer-Porter reactor.

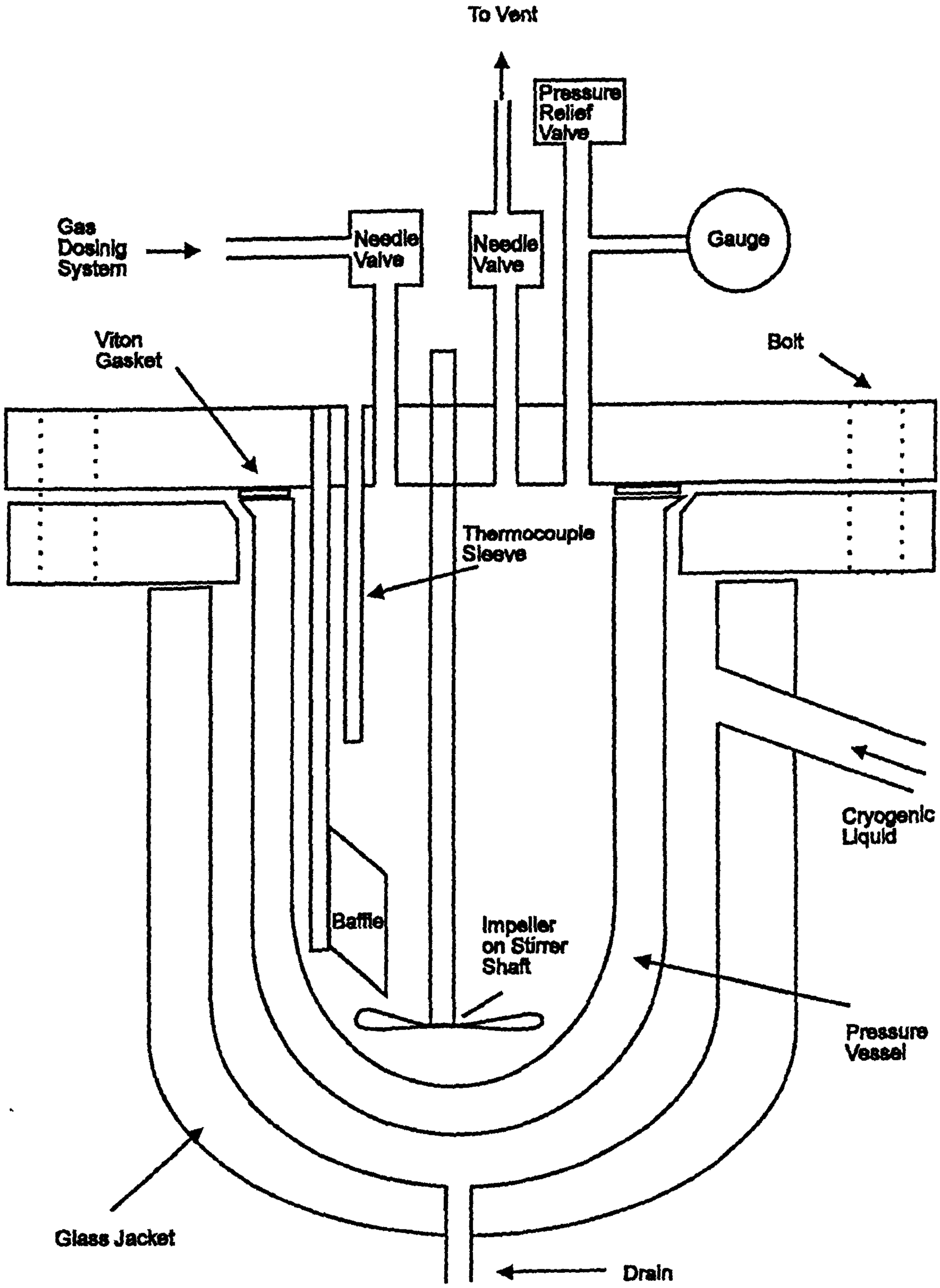

Figure 2.15

Büchi Autoclave

2.2.9 Product Separation

Products and reactants were separated from the catalyst by vacuum filtration using a Pyrex Porosity No. 4 sintered funnel in a conical flask. The alkaloid residues and excess solvent were separated from the products and reactants using a Büchi Rotorvapour-R at water vacuum.

2.2.10 Conventional Gas-Liquid Chromatography

Conversion of methyl pyruvate to methyl lactate was determined by gas-liquid chromatography. Separation of reactants and products was achieved in a 1m by 7 mm. (internal diameter) copper column packed with 10% Carbowax 20 M on 40/60 Chromasorb in a Perkin-Elmer 8500 gas chromatograph. The signal from the flame ionisation detector was measured by the internal integrator and the results displayed to the monitor and output to the Perkin-Elmer GP100 printer.

2.2.11 Polarimetry

The optical rotation of the products was measured by use of an automatic Optical Activity AA-10 polarimeter. The sample cell had a path length of 2 dm and its temperature was maintained at 298 K by use of a Grant Instruments thermostat-pump and water bath. Rotation was measured at the sodium D-line to an accuracy of $\pm 0.005^{\circ}$.

2.2.12 Chiral Gas-Liquid Chromatography

At a late stage in the work, product analysis using chiral chromatography became available. Product separation was achieved by injecting the sample through a split capillary injector onto a 50 m, Cydex B capillary column from SGE Ltd. on the same Perkin-Elmer 8500 gas chromatograph as described in section 2.2.10.

2.2.13 Ultra-Violet Spectroscopy

Spectroscopy was performed on a Phillips PU 8720 scanning UV-VIS spectrophotometer operating in absorption mode. The machine was micro-processor controlled and could scan wavelengths between 190 and 900 nm in 0.1 nm steps, automatically subtracting the background solvent spectrum from the sample spectra. Hardcopy output was available from an attached graphics printer.

2.2.14 NMR and Mass Spectrometry

The structures of alkaloid samples were determined using both a Finnigan Mat. 1020 automated mass spectrometer and a JEOL 270 MHz FT-NMR spectrometer.

2.2.15 Electron Microscopy

Catalyst morphology was examined using a JEOL JEM 100C electron microscope operating in transmission mode at 100 KeV.

2.2.16 Molecular Modelling

A variety of systems were used for molecular modelling and computational chemistry. The majority of the work was carried out using the package "HyperChem 2 for Windows" (AutoDesk), running under Windows 3.1 on a 50 MHz 486DX with 8 Mbytes of memory (Atomstyle). The spreadsheet package Microsoft Excel 4 for Windows was used interactively with HyperChem. Colour hard copy output was achieved using the Hewlett-Packard DeskJet 500C printer.

The package CHEM-X from Molecular Design was used on a DEC VAX/VMS mainframe computer at the University of London Computer Centre over a JANET link and at the Johnson-Matthey Technology Centre at Royston. Operation of the former

system was on a TEKTRONIX graphics terminal and for the latter a SIGMA graphic terminal and plotter was used.

Early work was also performed on the packages ALCHEMY II from TRIPOS Associates and Desk-Top Molecular Modeller from Oxford Electronic Publishing. Both these packages ran on IBM-PC compatible machines.

2.3 Procedures

2.3.1 Static reduction of EUROPT-1

Activation of the catalyst at Hull was achieved using the procedures developed by Sutherland[18] and Meheux[17] using the apparatus described in section 2.2.2. 0.1 g (± 10 mg) samples of as received EUROPT-1 were placed in a reduction vessel and evacuated for 0.5 h at 10^{-4} torr. The reduction vessel was then sealed and secured to the glass vacuum apparatus which was subsequently flushed with hydrogen several times to ensure complete purging of air from the system. The vacuum apparatus was then filled with hydrogen, the tap on the reduction vessel opened and the catalyst exposed to 760 torr (± 30 torr) hydrogen pressure at 298 K (± 5 K). The reduction vessel was again sealed from the vacuum apparatus and the catalyst reduced at 393 K (± 10 K) for 0.5 h. The reduction vessel was then allowed to cool to room temperature. It should be noted that no attempt was made to remove the water formed upon completion of reduction of the catalyst.

2.3.2 Static Reduction of other Catalysts

Static reductions of other supported metal catalysts studied were usually performed using a similar procedure as described for EUROPT-1 in section 2.3.1. If the quantity of available catalyst was low, a reduced sample weight would be used for

experimentation. Activation temperatures given in table 2.4 were used to ensure complete reduction.

Table 2.4

Activation Temperatures for Other Catalysts

Catalyst	Reduction Temperature / K
20% Re_2O_3/alumina	723
3 % Os/alumina	653
Pt/calcium carbonate	673
Ir/calcium carbonate	593
Pd/calcium carbonate	673
5 % Rh/alumina	493
5 % Ir/alumina	443
Pt/silica (GHI)	573

2.3.3 Flow Reduction of GHI H_2PtCl_6/silica Catalyst

It was necessary to subject the GHI H_2PtCl_6/silica catalyst pre-cursor to a flow reduction in order to activate the catalyst. The procedure adopted by Meheux[17] was followed with the exception that the pre-cursor was first dried at 383 K for 18 h.

Using the apparatus described in section 2.2.3, 1.5 g samples of the dried catalyst pre-cursor were placed in the flow reduction vessel and subjected to a flow 5% H_2 /Ar mixture at 25 ml min^{-1} for 1h at 298 K. The temperature was then raised to 573 K (± 10 K) which was held constant for 1 h before the catalyst was allowed to cool to room temperature. Gas flow was then switched to CO_2 at 40 ml min^{-1} at 298 K for 0.5 h to passivate the catalyst. The catalyst was then removed from the flow reduction vessel in the open laboratory and stored for later use whereby the catalyst was re-reduced following the method described above for EUROPT-1.

2.3.4 Sintering of 5% Rh/alumina

The melting point of Rh is 2239 K, hence at 823 K it would be expected that supported Rh particles would sinter in flowing hydrogen. Therefore, using the equipment described in section 2.2.6, 0.5 g samples of as-received 5% Rh/alumina in porcelain boats were placed in a silica reduction tube and subjected to a flowing 5 % H_2/Ar gas mixture at 25 ml min^{-1} and 298 K for 0.5 h. The temperature was then raised to 823 K and held constant for 1 h. The reduction vessel was allowed to cool for 3 h. Gas flow was then switched to 25 ml min^{-1} CO_2 for 0.5 h at 343 K before the reduction tube was removed from the furnace by opening to atmosphere using the post-catalyst joint, and the catalyst allowed to cool to 298 K under flowing CO_2.

2.3.5 Sintering of Ir/alumina

The melting point of iridium is 2683 K, thus requiring a substantial temperature to sinter the metal particles on a supported catalyst. A similar method as described above for sintering the Rh/alumina catalyst was followed using the equipment described in section 2.2.6. 0.5 g samples of as received Ir/alumina catalyst in porcelain boats was placed in a silica reduction tube and hydrogen gas flowed over the catalyst for 1h at 80 ml min^{-1} and 298 K before the temperature was raised to 1223 K and held constant for 4 h. The vessel was then allowed to cool to 298 K and gas flow switched to flowing CO_2 for 0.5 h. The vessel was then opened to atmosphere and the catalyst stored for later use.

2.3.6 *In situ* Reduction of EUROPT-1

A series of experiments was performed whereby no pre-treatment of EUROPT-1 was performed. The procedure followed was to place as received 0.1 g (± 10 mg) samples of EUROPT-1 directly into the Fischer-Porter reaction vessel, reactants were then added (see later) and the reactor purged several times with low pressures of N_2 and then H_2. Reduction of the catalyst then occurred in the Fischer-Porter reactor *in situ* on

stirring the reactor contents under H_2 at 10 bar pressure. Such reductions therefore took place in ethanol solution in the presence of methyl pyruvate and cinchonidine.

2.3.7 Standard Modification

The preparation of a catalyst surface capable of achieving enantioselective hydrogenation is achieved by the process of 'modification' by which a chiral substance is adsorbed onto the catalyst surface from solution at ambient temperature.

The general procedure for the modification of the catalyst was to (i) prepare a fresh 1% wt/wt solution of alkaloid by dissolving 0.2g (± 10 mg) of alkaloid in 40 ml of solvent, (ii) inject a 5 ml aliquot onto the catalyst, through the suba-seal into the reduction vessel, (iii) to shake the mixture thoroughly to ensure a fully wetted catalyst before washing the contents of the reduction vessel into a 100 ml beaker with the remaining 35 ml of modifier solution and (iv) to stir the solution and catalyst in air for 1h at 298K (± 5K). The excess solution was then either decanted off (EUROPT-1) or if the catalyst was too fine to allow this, the solid was separated from the solution using a centrifuge (carbonate- and alumina-supported catalysts).

2.3.8 Modification with Mixtures of Alkaloid Modifier

The effect of using a mixture of cinchonidine and cinchonine as modifiers, which individually induce selectivity in favour of R-(+)- and S-(-)-methyl lactate respectively was studied. The purpose of this was to examine the effect on the asymmetric hydrogenation site of having two modifiers of inverse geometry in the system. The weight percent of cinchonidine in cinchonine solution was varied between 0 and 100% for samples containing 0.2 g of alkaloid in total, dissolved in 40 ml ethanol. This solution was then used for modification in the normal manner, as described in section 2.3.10. The same experimental procedure was repeated with the exception that the weight percent of *quinine* in *quinidine* was varied between 0 and 100% in the modifier solution.

2.3.9 Modification at Low Concentrations

In order to study the kinetics of the hydrogenation of methyl pyruvate with respect to cinchonidine, exact quantities ranging from 0.004 to 1 mg of modifier in 20 ml solvent were used for modification of the catalyst. This method was as opposed to using a large amount of alkaloid dissolved in solvent and decanting off the excess solution after the mixture had been stirred in air as explained in section 2.3.10 as a standard modification. In all cases the alkaloid used was cinchonidine. The effect of the pre-treatment process on the rate of reaction and optical yield was studied by omitting one or both of the pre-treatment steps.

Six series of experiments were performed, as summarised in table 2.5. Where the EUROPT-1 catalyst was reduced the method described in section 2.3.1 was followed. The GHI Pt/silica catalyst was reduced using the procedure explained in section 2.3.3. Fresh modifier solutions of varied concentrations were made up volumetrically and aliquots injected into the reduction vessel. The vessel was then shaken to ensure the catalyst was thoroughly wetted. The reduction vessel was then opened to air and the contents washed into the reaction vessel. The volume was then made up to 20 ml solvent. Where the catalysts were used as received, the cinchonidine solution was added directly to the catalyst in the reaction vessel. Where a modification time of 1 h is indicated the mixture was stirred in air using the reactor's teflon coated magnetic stirrer bar prior to hydrogenation.

Two experiments were performed in which the catalyst samples, having had a series II manner modification had the excess ethanolic solution of the modifier decanted off. The catalyst, containing only modifier that had adsorbed from solution was then washed into the reaction vessel with 20 ml ethanol. (A small amount of residual modifier from the beaker walls was probably transferred also).

Table 2.5

Pre-treatment Conditions of Catalysts used with Low Concentrations of Modifier

Series	Solvent	Modification Time / h	Catalyst	Catalyst State
I	Ethanol	1	(GHI) Pt/SiO_2	Reduced
II	Ethanol	1	EUROPT-1	Reduced
III	Ethanol	0	EUROPT-1	Reduced
IV	Ethanol	1	EUROPT-1	As Received
V	Ethanol	0	EUROPT-1	As Received
VI	Toluene	1	EUROPT-1	Reduced

2.3.9a Anaerobic Modification

One experiment was performed in which a 1 h modification took place under 4 bar N_2. The procedure followed was similar to that explained in section 2.3.12 for a series V experiment, whereby once the catalyst was wetted with modifier solution, the mixture was transferred directly to the reactor vessel. However, once the reaction vessel had been purged of air by nitrogen, the pressure was raised to 4 bar nitrogen and the mixture stirred for 1 h prior to the hydrogenation. It was hoped that this procedure would displace the small quantities of dissolved oxygen in solution. The nitrogen was then vented and 10 ml of methyl pyruvate injected into the reactor vessel through a septum before the hydrogenation was performed as described below.

2.3.10 Tryptophan, Histidine and Derivatives

The effectiveness of various amino acids as catalyst modifiers for the enantioselective hydrogenation of methyl pyruvate was examined. L- and D-histidine, L- and D-histidine methyl ester and L- and D-tryptophan methyl ester were used as

modifiers. The same procedure as explained in section 2.3.7 was followed. Great care was taken to ensure that all of the apparatus was scrupulously clean.

Bond *et al.* had found that various bases will enhance the rate of reaction[19]. During one such experiment they found quinuclidinol (which is non-chiral) would not only enhance the rate of reaction but also give R-(+)-methyl lactate in enantiomeric excess. This was later found to be due to trace quantities of cinchonidine being present in the reactor from previous experiments. One experiment was therefore performed whereby a modifier solution was prepared containing 0.1g quinuclidinol and 0.1g L-histidine methyl ester. The purpose of this being to ascertain whether this combination of modifiers, one with the property of enhancing the rate, the other with the property of inducing enantioselectivity would give higher optical yields.

2.3.11 Ephedrine Derivatives

The stereo-chemistry of the two chiral centres at the C8 and C9 positions of the cinchona alkaloid direct the enantioselectivity of the product of methyl pyruvate hydrogenation. The relationship is such that: C8 = S and C9 = R gives the (R)-(+)-product; C8 = R and C9 = S gives (S)-(-)- product; and C8 = R and C9 = R gives racemic product[17]. Ephedrine which had been found to be a modifier capable of producing modest optical yields[20] was available with analogous stereochemistry at the C1 and C2 chiral centres, including the C1 = S and C2 = S enantiomer, the analogue not being available for cinchonidine. Hence the importance of the stereochemistry could be confirmed.

Reduced EUROPT-1 was modified by various ephedrine derivatives in ethanol solvent. For the solids, 0.2 g of alkaloid was used in the same manner as that explained for the general procedure. For the modification by deoxyephedrine, 0.4 ml was dissolved in 40 ml ethanol, and the general procedure then followed normally. Due to the risk of

contamination by cinchonidine from previous experiments resulting in 'fake' optical yields, extreme care was taken that the apparatus was thoroughly clean.

2.3.12 Benzyl Pyrrolidine Methanol

Meheux had found that benzyl pyrrolidine methanol could be used as a modifier to effect enantioselective hydrogenation of methyl pyruvate[17]. Experiments were performed to confirm the reaction and to study whether the reaction could be applied to other metals.

Reduced EUROPT-1 and Ir/CaCO3 were modified by the non-alkaloid benzyl pyrrolidine methanol. 0.2 ml samples of modifier in 40 ml ethanol were used in the same manner as described for deoxyephedrine in section 2.3.11.

2.3.13 Absence of Modifier

In order to compare results between reactions carried out in the presence and absence of added modifier, experiments were performed whereby only the solvent was injected into the reduction vessel and the catalyst wetted. The catalyst and solvent were then transferred directly to the reactor. A great deal of care was required to ensure that all the apparatus was scrupulously clean.

Not only were these experiments carried out to discover the racemic rates of reaction, but also to confirm that the apparatus was free from trace quantities of alkaloids before studies of new candidate modifiers.

2.3.14 Hydrogenation

One of two different autoclaves was used from time to time throughout the work. The choice being dictated by availability and suitability for the desired experiment. In

each case the general procedure followed was similar, though minor alterations to operation was necessary.

2.3.15 Fischer-Porter

The standard procedure was to charge the reactor vessel with modified catalyst in 20 ml solvent and then to add 10 ml (113 mmol) of methyl pyruvate; the vessel was then sealed into place and submerged in a water bath at the desired temperature. The solenoid valves were opened and the system was purged several times with nitrogen (3 bar), followed by purging with hydrogen (3 bar). The vessel was then pressurised to 10.8 bar with hydrogen. The solenoid valves would then be closed and the pressure of the reactor reduced to 10.0 bar.

The date, experiment number and ambient temperature would be entered into the computer which would then measure the difference between the regulator and reactor pressure and perform an internal calibration so that it could accurately determine the dosing volume.

The contents of the reactor were then stirred at a speed setting of 5 on the Gallenkamp Hot plate stirrer and the hydrogen dosing system activated to keep the pressure constant and record the hydrogen content as a function of time. The reaction was allowed to progress to the desired conversion.

2.3.16 Büchi Autoclave

For experiments conducted in the Büchi autoclave a similar procedure was followed as explained for the Fischer Porter autoclave above, but with the following exceptions. Due to the reactor vessel being larger, 50 ml of solvent was required to ensure optimum mixing conditions[21]. Temperature control was achieved using either a

Julabo heating unit for experiments performed above ambient temperature or by a Churchill cooling unit for those performed below ambient.

Due to the increased sensitivity of the pressure transducer on the hydrogen dosing system attached to the Büchi autoclave the reactor was charged to 10.4 bar, the solenoid valves closed and the reactor pressure reduced to 10.1 bar. The contents of the reactor were then stirred at a speed of 1200 r.p.m. unless otherwise stated.

2.3.17 Product Separation and Analysis

The catalyst was filtered from the reaction mixture and the alkaloid separated using a rotary evaporator, with the reactants heated at 388 K. Excess solvent was removed by use of the rotary evaporator at 298K and the optical rotation found by polarimetry at 298 K. A solution was then prepared containing 50 µl of sample, 25 µl of methyl acetoacetate and 1.0 ml 1,2-dichloroethane. 1µl of the solution sample injected into the glc column. The nitrogen carrier gas flow rate was 45 ml min^{-1}. The initial temperature of the oven was 332 K and after 4 min. the temperature was ramped at 30 K min^{-1} to 383 K and kept constant for 15 min. The conversion to methyl lactate was found by peak integration, using the calibrated values of Meheux[17]. Optical yield was found, according to the equation:

$$\text{Optical Yield} = \frac{[\alpha]_D^T}{[\alpha]_o^T} = \frac{100\alpha}{[\alpha]_o^T lc}$$

measured at the sodium D-line, where $[\alpha]_o^T$ is the specific rotation of the pure enantiomer under the same conditions (8.25º for R-(+)-methyl lactate), α is the measured optical rotation, l is the path length of the cell (2 dm), and c is the solute concentration.

Product analysis by chiral gas liquid chromatography was performed by injecting 0.3 µl samples of the reaction mixture after the catalyst had been removed by filtration. Conversion and enantiomeric excess was determined by peak integration.

2.3.18 Variation of Reaction Conversion

The majority of reactions were allowed to proceed until completion, before being stopped and the catalyst separated and all reactants and products used for the analysis as described in section 2.3.17. To study the reaction as conversion is varied one or both of two different procedures were followed.

One procedure used was to monitor the reaction and stop the reaction at varied quantities of hydrogen consumption as measured by the micro-computer. Using this procedure several runs, each requiring pre-treatment and modification of the catalyst as explained in sections 2.3.2 and 2.3.7 were required.

The alternative to this was to pre-treat and modify the catalyst and then proceed with the reaction to a low conversion. The reaction would then be stopped and a 1 ml sample withdrawn from reaction mixture. The reactor was then re-pressurised quickly, and the reaction re-commenced. The study would therefore generate several data points at different conversions per experimental run. This technique was however only practical when product analysis was performed by chiral chromatography as the conventioal product analysis method described in section 2.3.17 required far more sample. In practice both methods were employed.

2.3.19 Variation of Reactant Concentration for $Ir/CaCO_3$

The Fischer Porter reactor and the Büchi reactor required different volumes of reactants to function at optimum conditions, outside of diffusion control limitations. Though it was known that EUROPT-1 had zero-order kinetics in methyl pyruvate concentration, it was not known whether the same case applied to $Ir/CaCO_3$. Therefore in order to ensure that comparison of the results from both reactors could be drawn, and to compare the kinetics of methyl pyruvate concentration for $Ir/CaCO_3$ against

EUROPT-1, the amount of ethanol solvent was varied from 20 ml to 150 ml for 10 ml methyl pyruvate and the reaction allowed to proceed to the desired conversion.

2.3.20 Variation in Hydrogen Pressure

For the study of the order of reaction with respect to hydrogen concentration for the $Ir/CaCO_3$, the pressure of the reactor was varied from 4.1 to 10.1 bar. For reactions occurring at 10.1 bar or below the Fischer-Porter and Büchi autoclaves were operated as described in section 2.3.15 and 2.3.16, though pressurising the reactor to varied pressures.

2.3.21 Ultra-Violet Spectroscopy

The study of the kinetics of methyl pyruvate hydrogenation at low concentration required knowledge of the amount of cinchonidine in solution and the amount that is adsorbed on EUROPT-1.

100 mg samples were of EUROPT-1 catalyst were reduced as described in section 2.3.1. 20 ml of modifier solution containing 0.5 mg of cinchonidine was then injected through the septum into the reduction vessel and the catalyst fully wetted. The mixtures were then stirred and the absorption of cinchonidine in solution was examined by UV spectroscopy over the wavelength range 190 to 350 nm using the equipment described in section 2.2.13. It was necessary to filter the solutions to reduce the amount of fine particulate catalyst that would affect the absorption spectra. The experiments were repeated using as received EUROPT-1 in order to distinguish physisorption on the silica from chemisorption on the metal.

For the experiments conducted in ethanol with reduced catalyst, changes in the absorption spectra with modification time were examined. For the experiments

conducted in toluene, the solutions were only stirred for three minutes and the adsorption spectra examined.

For the study in ethanol solution a calibration graph was produced to ensure that absorption versus concentration obeyed the Beer-Lambert law over the concentrations under study. This involved taking spectra for known concentrations of cinchonidine in 20 ml ethanol and measuring absorption at the frequencies of major absorption.

2.3.22 Benzil Hydrogenation

In an attempt to diversify the reaction away from α-keto esters the reactant was changed to a diketone (figure 2.16). A standard catalyst pretreatment procedure was followed and then the reactor was charged with 2 g of reactant in 20 ml ethanol and the reaction commenced in the normal manner. Upon the completion of the reaction, the solid product was separated from the catalyst as described in section 2.3.17 with the exception that a 'hot-filtration' involving warm ethanol was required to dissolve the benzoin product. The product was then washed with cold ethanol to remove any traces of alkaloid. The product was characterised by melting point determination and any optical activity examined by dissolving a small quantity in ethanol and analysing by polarimetry.

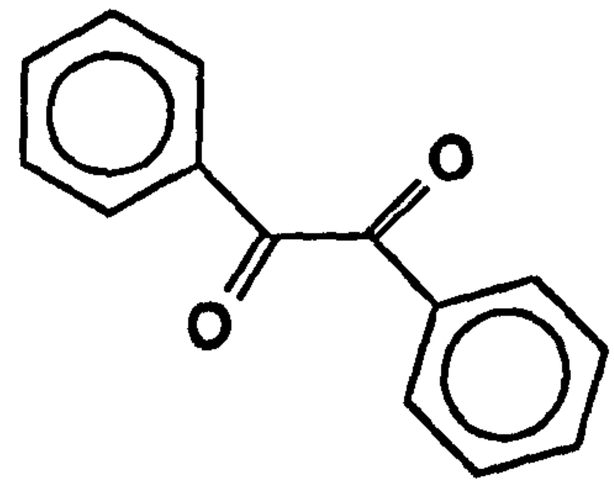

Figure 2.16

Structure of Benzil

2.3.23 Deuterium Tracer Study

The mode of the adsorption of the alkaloid on the $Ir/CaCO_3$ catalyst was examined by deuterium exchange investigation. 10,11-dihydrocinchonidine (dhc) was used in preference to cinchonidine as any effect of adsorption or deutrogenation of the vinyl group in cinchonidine would be avoided. The catalyst pre-treatment was identical to that stated in section 2.3.2 for $Ir/CaCO_3$ with the exception that deuterium gas was used (without further purification) for reducing the catalyst.

A mixture of 0.1 g dhc in 10 ml deutero-ethanol was prepared in a dry nitrogen environment provided by a glove box and the solution injected into the reduction vessel, through the septum at 298 K, wetting the catalyst. The contents were then stirred under the deuterium atmosphere of the reduction vessel for 18 h at 298K.

The dhc was then recovered by filtration as described for post-reactor hydrogenation products in section 2.3.17, followed by evaporation of the deutero-ethanol solvent under flowing air using the apparatus described in section 2.2.5. The recovered dhc was then analysed by NMR and mass spectrometry.

The above experiment was repeated on a further time, but on this occasion the mixture was stirred in the reduction vessel for 9 days.

2.3.24 Molecular Modelling

The structure of the alkaloid had been examined before at Hull[18,21] by use of the molecular modelling packages DTMM and Alchemy. Though these packages are effective for visualisation of the alkaloid molecules, the algorithms to discover the minimum energy conformations are not efficient. The packages tend to discover local, as opposed to global energy minima which produce misleading results.

Using the package HyperChem II the minimum energy conformations of the alkaloid were elucidated. The procedure followed was to create the structure using default values for bond lengths and angles and after ensuring that the chiral centres of the alkaloid were as desired, the structure was optimised with the MM+ forcefield calculations (a variation on MM2[22]) using the Polak-Ribiere algorithm[23]. The global energy minimum was confirmed using molecular dynamics to perform a 'soft-anneal'. This involves 'heating' the molecule from 0 K to 473 K in 0.1 K steps and then slowly 'cooling' the molecule back down to 0 K. This procedure has the effect of giving each atom of the molecule finite amounts of velocity at each step, thus allowing any energy barriers from local minima to be breached, thus resulting in a global energy minimum conformation. Default values were used for all the parameters involved in calculation.

Assuming that the quinoline and the quinuclidine ring system of the alkaloid are in an optimised form, there are four bonds about which there can be envisaged a degree of freedom for rotation. Referring to figure 2.1 they are: the bond C9-O, resulting in rotation of the hydroxyl group; the bond C3-C10, resulting in rotation of the vinyl group; the bond C9-C4' resulting in rotation of the quinoline ring; and the bond C9-C8 resulting in rotation of the quinuclidine ring.

Plots of energy versus rotation for each of these individual bonds were produced by rotating the bonds in 1 ° steps and finding energy of the molecule by molecular mechanics calculation. This was achieved by driving the HyperChem II program from EXCEL 4 using Dynamic Data Exchange. For these calculations the other bond angles were kept at the values determined by the previous molecular dynamics calculations.

This process was then repeated with the variation that both of the bonds responsible for rotation of the quinoline and quinuclidine ring were varied at the same time to produce a 3-dimensional view of energy versus torsion angles. In practice, it was not possible to achieve 1° steps as the computation time and memory requirements were too great. It was therefore necessary to perform energy calculations at 5° intervals.

In order to examine the variation of the energy of interaction between the alkaloid molecule and approaching reactant the two molecules were brought up to each other in various orientations 'by hand' and the total molecular mechanical energy of the system calculated. During this process a Pt(111) surface was used purely as a 'backdrop' to guide the choices of positions available; its exact location relative to the adsorbates being based on the empirical arguments presented in the text.. As no paramaterisation of the interaction between Pt and adsorbed molecules is available this 'backdrop' was removed before calculation.

For comparison, a brief study on the package CHEMX was made, repeating the above calculations. A major difference however was that it was possible to measure only the inter-molecular forces between the alkaloid molecule and methyl pyruvate when the two species were brought into proximity to each other. Default values were again used in calculation, these being not necessarily the same as used in calculations performed with HyperChem II.

---

[1]G.C. Bond and P.B. Wells, Appl. Catal., 18 (1985) 225.

[2]J.W. Geus and P.B. Wells, Appl. Catal., 18 (1985) 231.

[3]A. Frennet and P.B. Wells, Appl. Catal., 18 (1985) 243.

[4]P.B. Wells, Appl. Catal., 18 (1985) 259.

[5]R.W. Joyner, Chem. Soc. Faraday Trans., I 76 (1980) 357.

[6]S.D. Jackson, M.B.T. Keegan, G.D. McLellan, P.A. Meheux, R.B. Moyes, G. Webb, P.B. Wells, R. Whyman, and J. Willis, Preparation of Catalysts V (G. Poncelet, P.A. Jacobs, P. Grange and B. Delmon, Eds., Elsevier, Amsterdam, 1991).

[7]V. Gnutzman and W. Vogel, J. Phys. Chem., 94 (1990) 4991.

[8]Z. Paál, H. Groenewg and J. Paál-Lukács, J. Chem. Soc. Faraday Trans. 86 (1990) 3159.

[9]E. Fülöp, V. Gnutzmann, Z. Paál and W. Vogel, Appl. Catal., 66 (1990) 319.

[10]G.C. Bond and M. Gelsthorpe, Appl. Catal., 35 (1987) 169.

[11]I.L. Dodgson, personal communication.

[12]S.D. Jackson, B.M. Glanville, J. Willis, G.D. McLellan, G. Webb, M.B.T. Keegan R.B. Moyes, S. Simpson, P.B. Wells and R. Whyman, J. Catal. 139 1 (1993) 191.

[13]S.D. Jackson, B.M. Glanville, J. Willis, G.D. McLellan, G. Webb, R.B. Moyes, S. Simpson, P.B. Wells and R. Whyman, J. Catal. 139 1 (1993) 207.

[14]S.D. Jackson, B.M. Glanville, J. Willis, G.D. McLellan, G. Webb, R.B. Moyes, S. Simpson, P.B. Wells and R. Whyman, J. Catal. 139 1 (1993) 221

[15]A.G. Burden, J.Grant, J. Martos, R.B. Moyes, and P.B. Wells, Faraday Discuss. Chem. Soc. 72 (1981) 95.

[16]K. Griffin, personal communication.

[17]P. A. Meheux, Ph. D. Thesis, University of Hull, 1991.

[18]I.M. Sutherland, Ph.D. Thesis, University of Hull, 1989.

[19]G. Bond, P.A. Meheux, A. Ibbotson and P.B. Wells, Catal. Today, 10 (1991) 371.

[20]H.U. Blaser, H.P. Jallet, D.M. Monti, J.F. Reber and J.T. Wehrli, Stud, Surf. Sci. 41 (1988) 153.

[21]G. Bond, personal communication.

[22]N.L. Alinger, J. Am. Chem. Soc., 99 (1977) 8127 .

[23]Fletcher, R. in Practical Methods of Optimization, J. Wiley& Sons, New York, 1981.

Chapter 3

Results

3.1 Normal Modification

The hydrogen uptake curve for the racemic hydrogenation of methyl pyruvate at 10 bar H_2 and 298 K over unmodified EUROPT-1 is shown in figure 3.1 (represented by green squares). The inset of figure 3.1 shows the initial 3 mmols of reaction in greater detail. There are two regions in the hydrogen uptake curve for racemic reaction. The majority of the reaction occurs at a slow constant rate of ca. 50 mmols h^{-1} (g cat.)$^{-1}$ but the first few percent of reaction occurs at a rate 2-4 times faster. The convention adopted by workers in this laboratory in the past has been to quote the former value.

When EUROPT-1 was modified by cinchonidine using the procedure outlined in section 2.3.7 and subsequently used for the hydrogenation of methyl pyruvate at 10 bar H_2 and 298 K, reaction progressed as shown in the hydrogen uptake curve (represented by red squares) in figure 3.1. This was considered to be a standard reaction with which all other reactions were compared. There are three distinct regions in the plot: an initial acceleratory period during the first five minutes or 10 % of reaction; a period of constant hydrogenation rate for 80 % of reaction; and then a sudden decline in the rate of hydrogen consumption. The initial rate of reaction, Ri, was measured during the second of these periods. In this case Ri was measured to be 1760 mols h^{-1} (g cat.)$^{-1}$. This is a 35 fold increase over the racemic reaction rate (measured according to the convention explained above). Catalysis in the presence of cinchonidine also produced an optical yield of 70 % (85 % R-(+)-methyl lactate, 15 % S-(-)-methyl lactate).

3.2 Mixed Modification

Modification of 100 mg EUROPT-1 with varied mole fractions of cinchonidine (mfcd) in cinchonine using the procedure explained in section 2.3.8 resulted in the initial rates of methyl pyruvate hydrogenation (represented by green squares) and the optical yields (represented by red squares) shown in figure 3.2. Reaction provides an excess of S-(-)-methyl lactate at low mole fractions cinchonidine and an excess of R-(+)-methyl

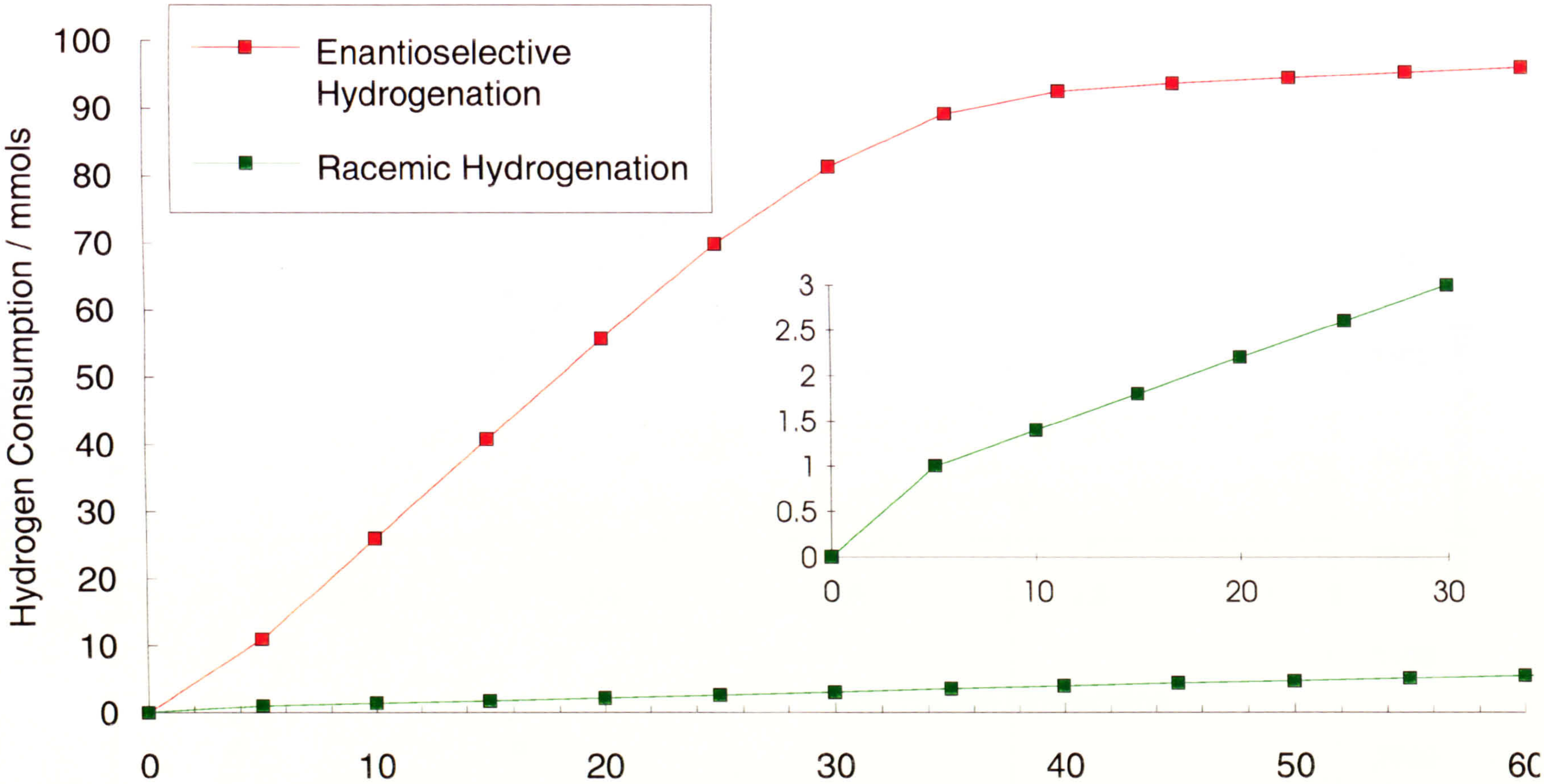

Figure 3.1
Methyl Pyruvate Hydrogenation over Modified and Unmodified EUROPT-1

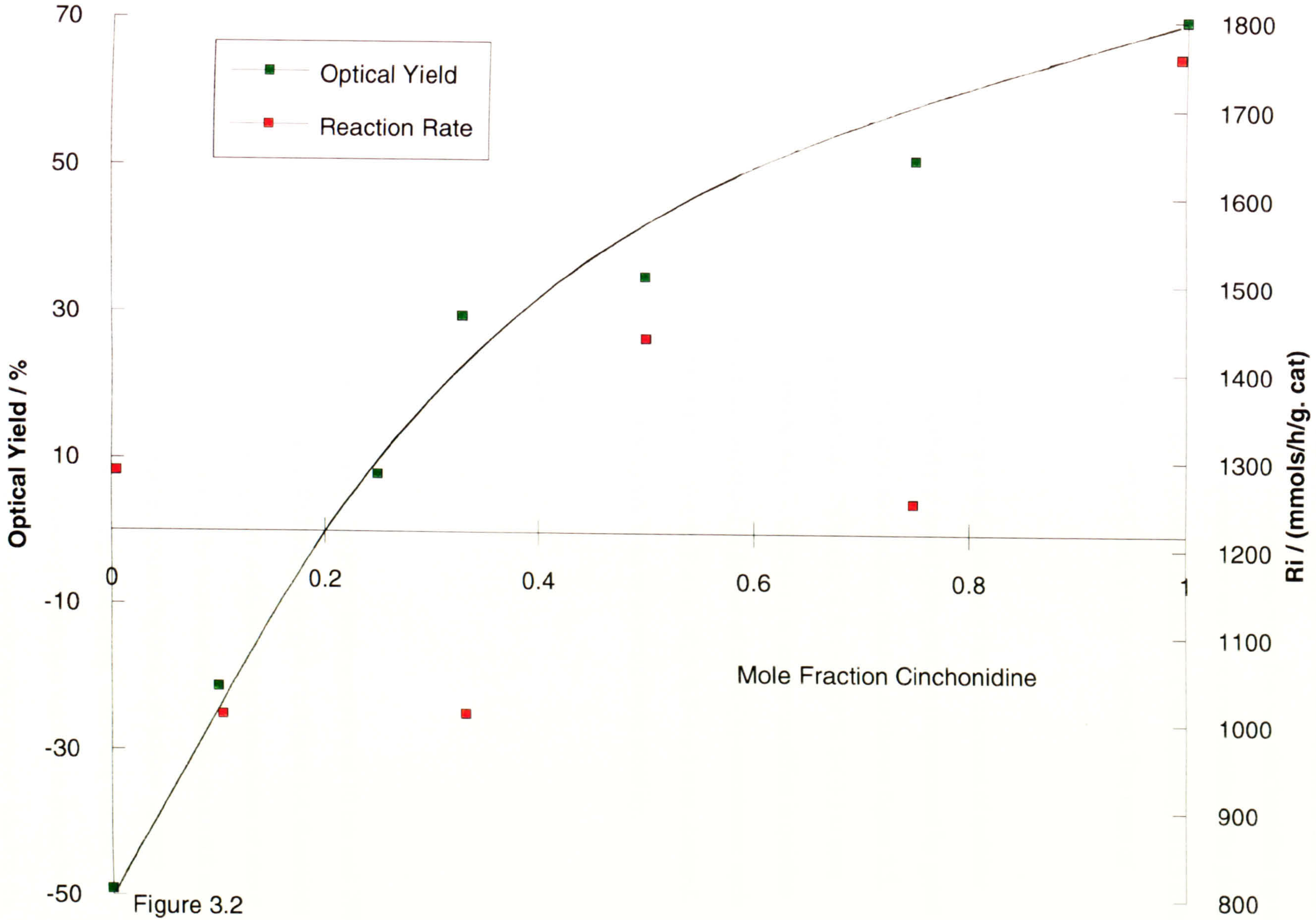

Figure 3.2
Variation of Optical Yield and Rate of Reaction for Methyl Pyruvate Hydrogenation at 298 K and 10 bar H2 over EUROPT-1 modified by varied Mole Fractions of Cinchonidine

lactate at high mole fractions of cinchonidine. The optical yield can be seen to increase steadily from - 50 % (25 % R-(-)-, 75 % S-(-)-) at zero mole fraction cinchonidine up to + 70 % (85 % R-(-)-, 15 % S-(-)-) when the modifier was pure cinchonidine. The plot is not linear, but weighted in favour of R-(+)-product formation. Consequently, at 0.5 mfcd an optical yield of 35 % (67.5 % R-(-)-, 32.5 % S-(-)-) was observed. The rates of reaction tended to be more erratic.

When these experiments were repeated, with varied mole fractions of quinine (mfqn) in quinidine initial rates of methyl pyruvate hydrogenation (represented by green squares) and optical yields (represented by red squares) resulted as shown figure 3.3. There is a steady rise in optical yield from -38 % (31 % R-(+)-, 69 % S-(-)-) at zero mole fraction quinidine to 60 % (80 % R-(+)-, 20 S-(-)-) when the modifier is quinine alone. The plot is not linear but again weighted in favour of the R-(+)-enantiomer such that at 0.5 mfqn an optical yield of 19 % (59.5 % R-(+)-, 40.5 % S-(-)-) was obtained. The initial rates of reaction are less erratic, and tend to increase more steadily.

3.3 Low Concentrations of Modifier

3.3.1 EUROPT-1

The variation of optical yield in methyl pyruvate hydrogenation at 10 bar and 298 K with the weight of cinchonidine added to EUROPT-1 is given in figure 3.4. Reactions provide an excess of R-(+)-methyl lactate. Optical yields reach a plateau value of about 66 % (83 % R(+)-, 17 % (S)-) as the amount of cinchonidine approaches about 0.8 mg per 100 mg catalyst. Results of experiments represented by blue and yellow squares (series III and IV as defined in table 2.5) fall on the same curve, indicating that the alkaloid is equally effective whether it is adsorbed on the catalyst initially in either the oxidised or reduced state. Similar optical yields are observed irrespective of whether the catalyst was stirred in air with the modifier (as recommended by Orito *et al.* for

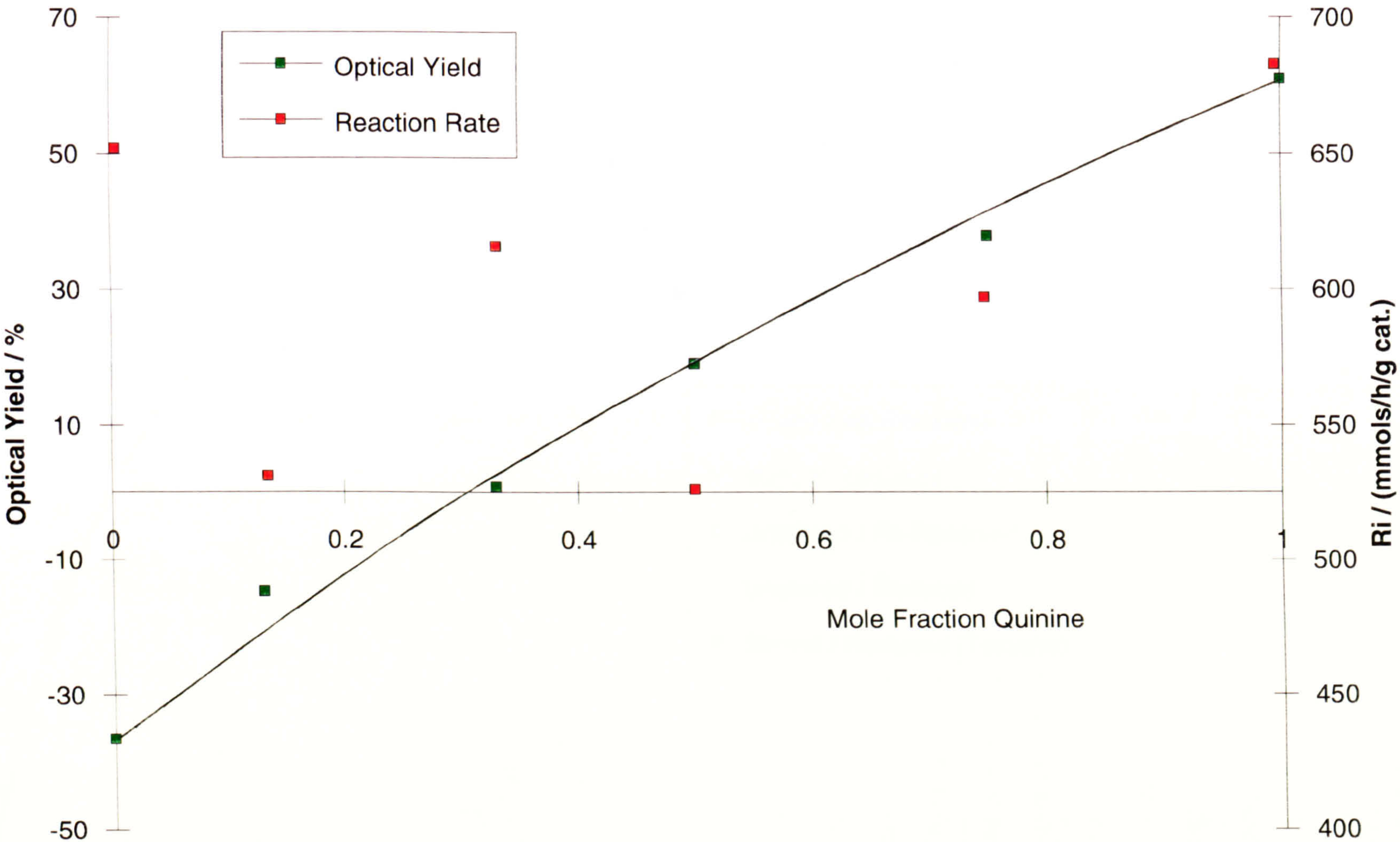

Figure 3.3
Variation of Optical Yield and Rate of Reaction with Mole Fraction of Quinine for Methyl Pyruvate Hydrogenation

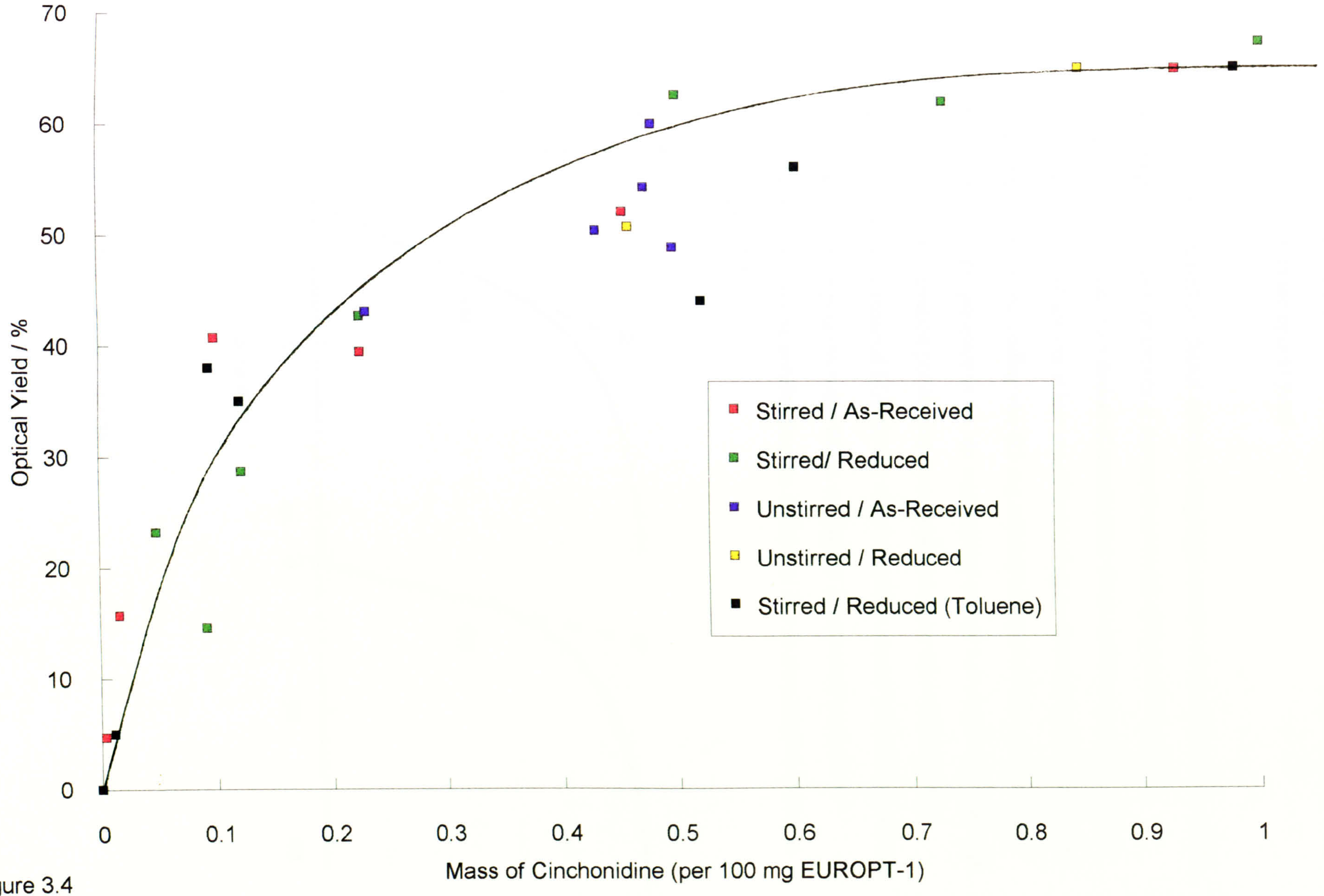

Figure 3.4
Variation of Optical Yield with Cinchonidine Loading for Methyl Pyruvate Hydrogenation over EUROPT-1 in Ethanol Solvent

modification at excess modifier concentrations[1]) or not. The use of ethanol or toluene as solvent does not affect the optical yield.

Reactions carried in ethanol solvent using high concentrations of modifier exhibit hydrogen uptake versus time curves as shown in curve (a) of figure 3.5 in which hydrogenation is preceded by a period of acceleration. Such uptake versus time curves were obtained in ethanol solvent at low modifier loadings in the range 0.7 to 1.0 mg per 100 mg catalyst. When the loading was 0.5 mg and the catalyst had been stirred in the modifier solution in the presence of air, the acceleratory period was absent. For loadings below 0.5 mg the acceleration period was short or absent under all conditions. For reactions carried out on reduced EUROPT-1 which had been stirred with toluene solvent in air at modifier loadings in the range 0.0 to 1.0 mg, no acceleratory period was observed. When there was no acceleration the initial rate R' was measured as shown in curve (b) of figure 3.5.

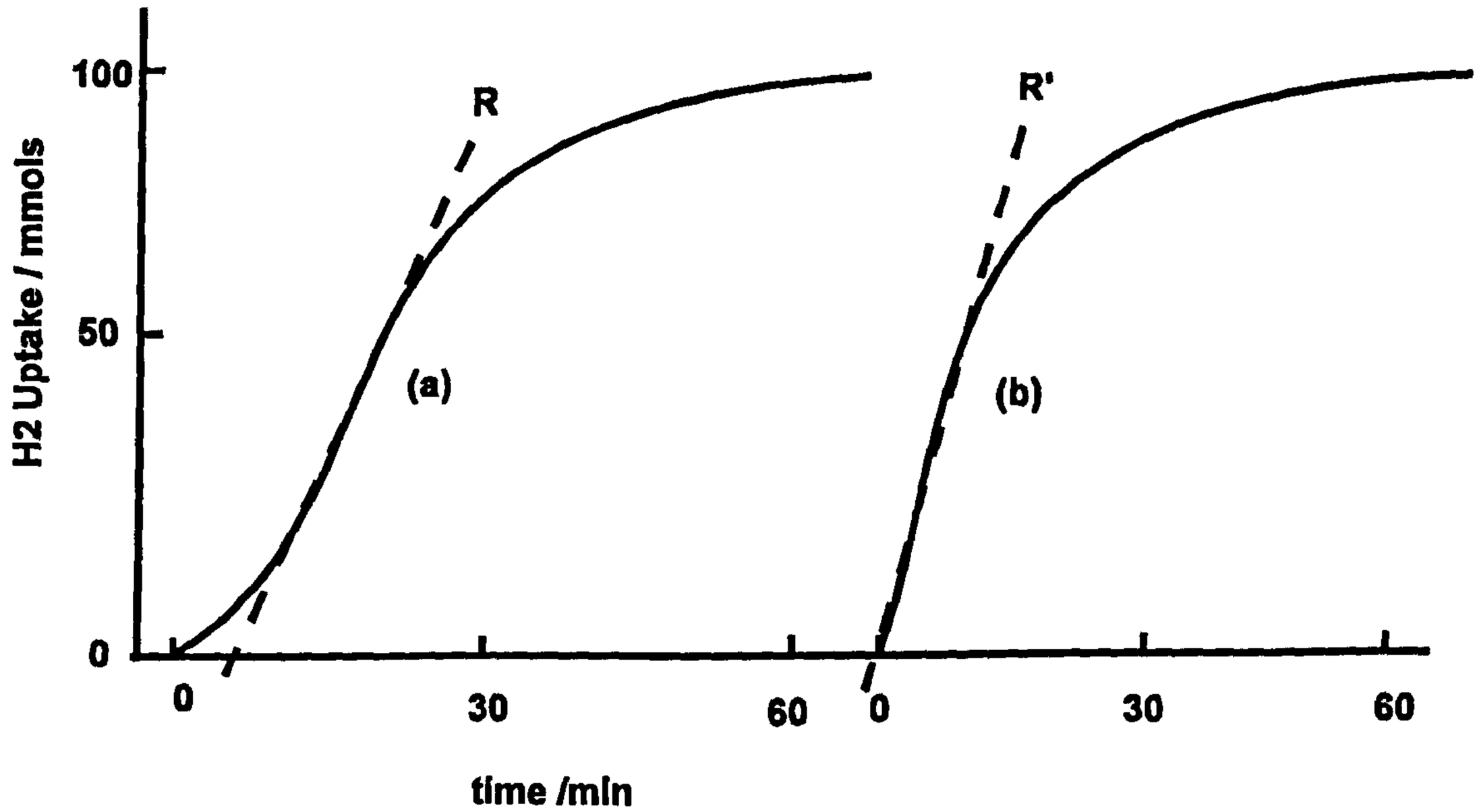

Figure 3.5

Two Types of Hydrogen Uptake Curves

The variation of R or R' with the weight of cinchonidine added to 100 mg catalyst is shown in figure 3.6. Reaction rate increased as the loading of the alkaloid increased. For the experiments conducted in ethanol, although there is experimental scatter, no plateau is observed. Rates of reaction in toluene solution were faster than those observed in ethanol (as has been reported by Wehrli *et al.*[2]) and a plateau was observed. The rate of reaction using a catalyst loaded with 1 mg of modifier exceeded that of an unmodified catalyst by a factor between 5 and 20 in ethanol solvent and between 20 and 90 in toluene depending on the value taken for initial rate under racemic conditions.

A plot of optical yield versus reaction rate under all the reactions performed in ethanol solvent is shown in figure 3.7. Although there is experimental scatter, there is a clear linear relationship between the two.

3.3.2 Degree of Modifier Adsorption

Two experiments were performed which involved a 1 h modification of reduced EUROPT-1 at low concentration in 40 ml ethanol, with the excess alkaloid decanted off before hydrogenation of methyl pyruvate at 298 K and 10 bar H_2 in 20 ml fresh ethanol. The results are summarised in table 3.1. When the values of optical yield and rate data are compared with the plots of optical yield and initial rates of reaction versus modifier loading in figures 3.4 and 3.6 respectively the values obtained are far less than would be expected had full adsorption of the alkaloid on the catalyst taken place. The results indicate that less than 10 % of the alkaloid was adsorbed on the catalyst.

3.3.3 Ultra-Violet Spectroscopy

Figure 3.8 shows a Beer-Lambert plot for absorbance vs. concentration at 210, 224, 284, 312 and 315 nm for cinchonidine dissolved in 20 ml ethanol. (These units are used as it corresponds to the quantities used for the modification of EUROPT-1 at low

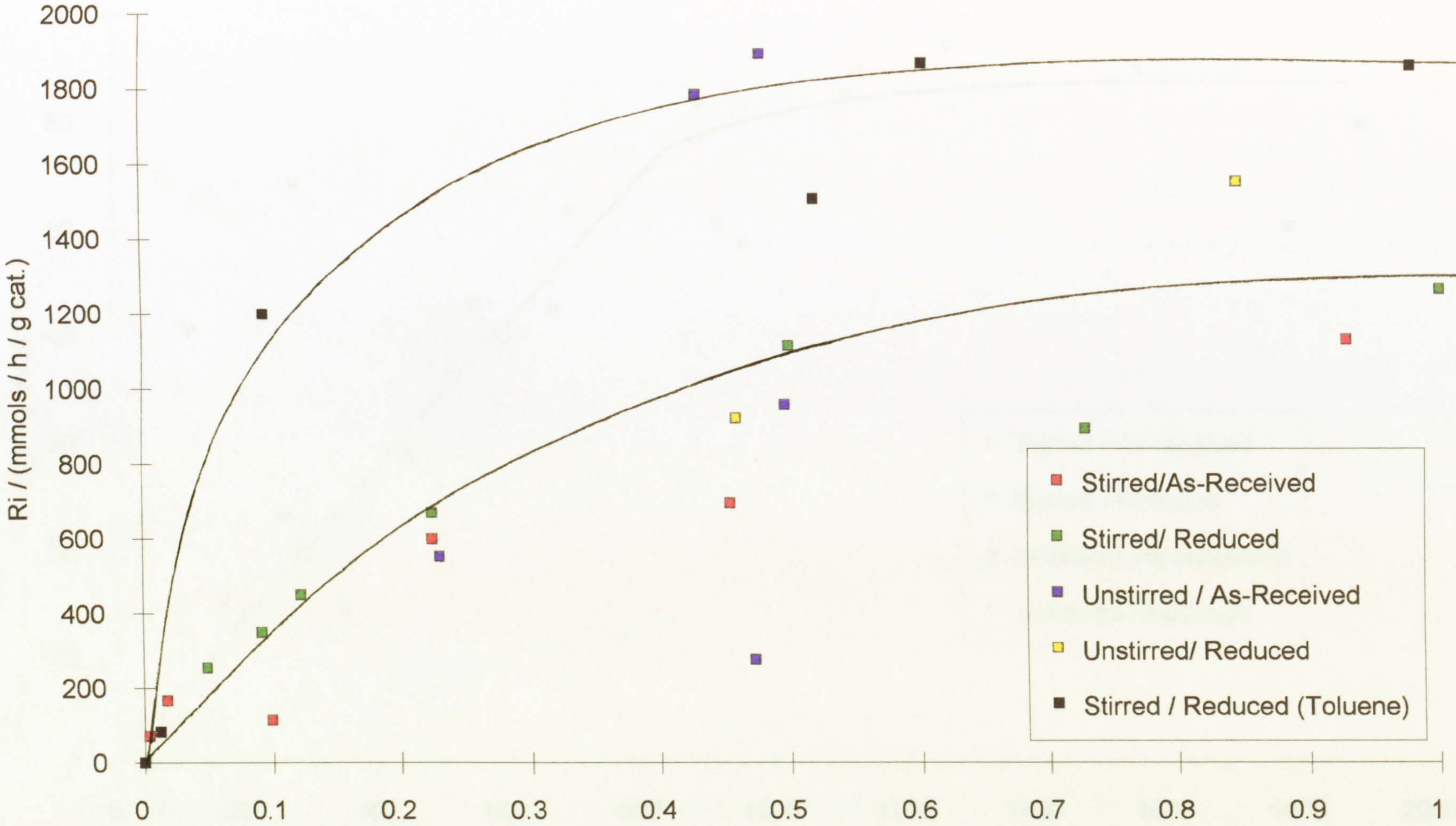

Figure 3.6
Variation of Initial Rate with Cinchonidine Loading for Methyl Pyruvate Hydrogenation over EUROPT-1 in Ethanol Solvent

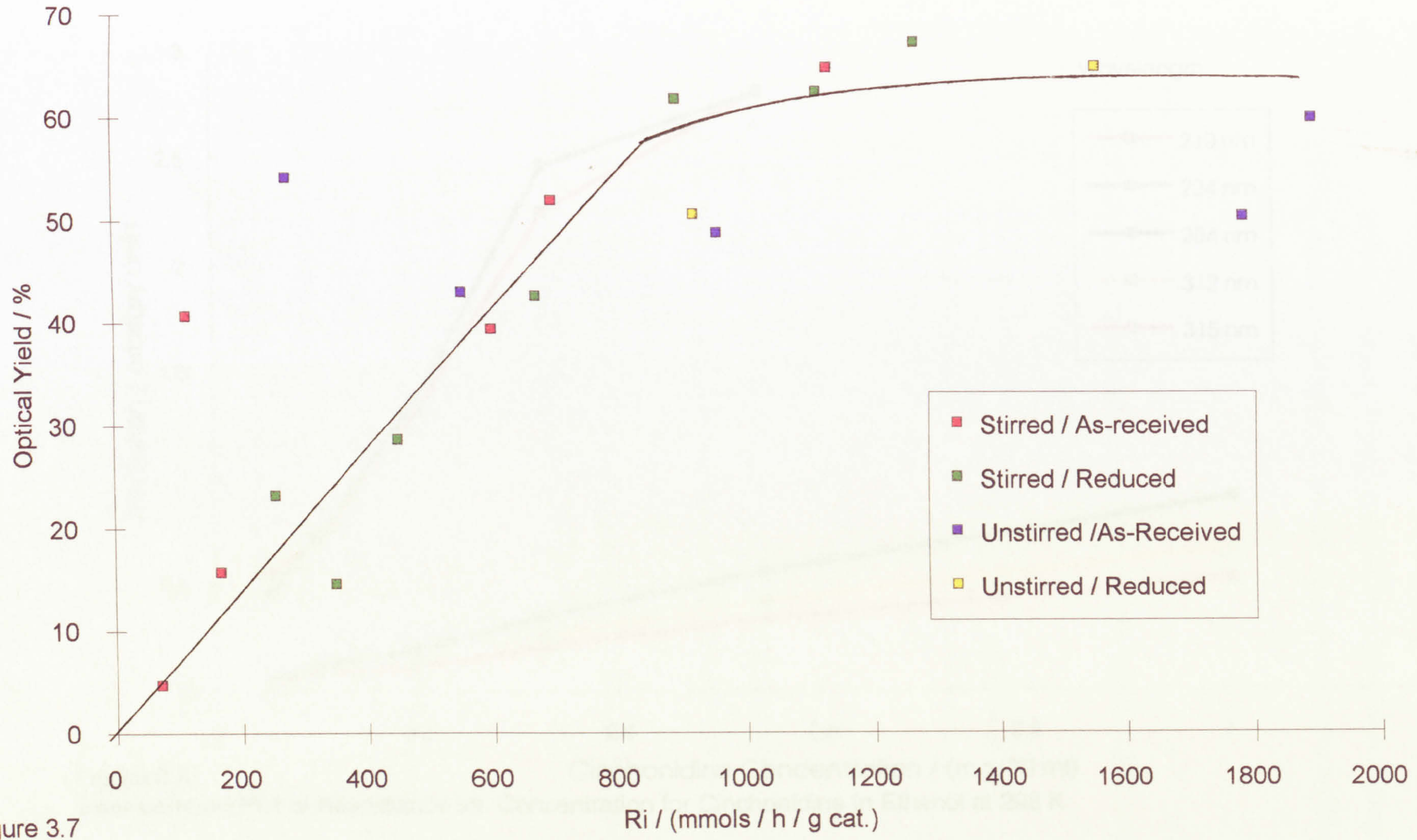

Figure 3.7
Plot of Optical Yield vs. Initial Rate for Methyl Pyruvate Hydrogenation at 298 K and 10 bar H2 in Ethanol

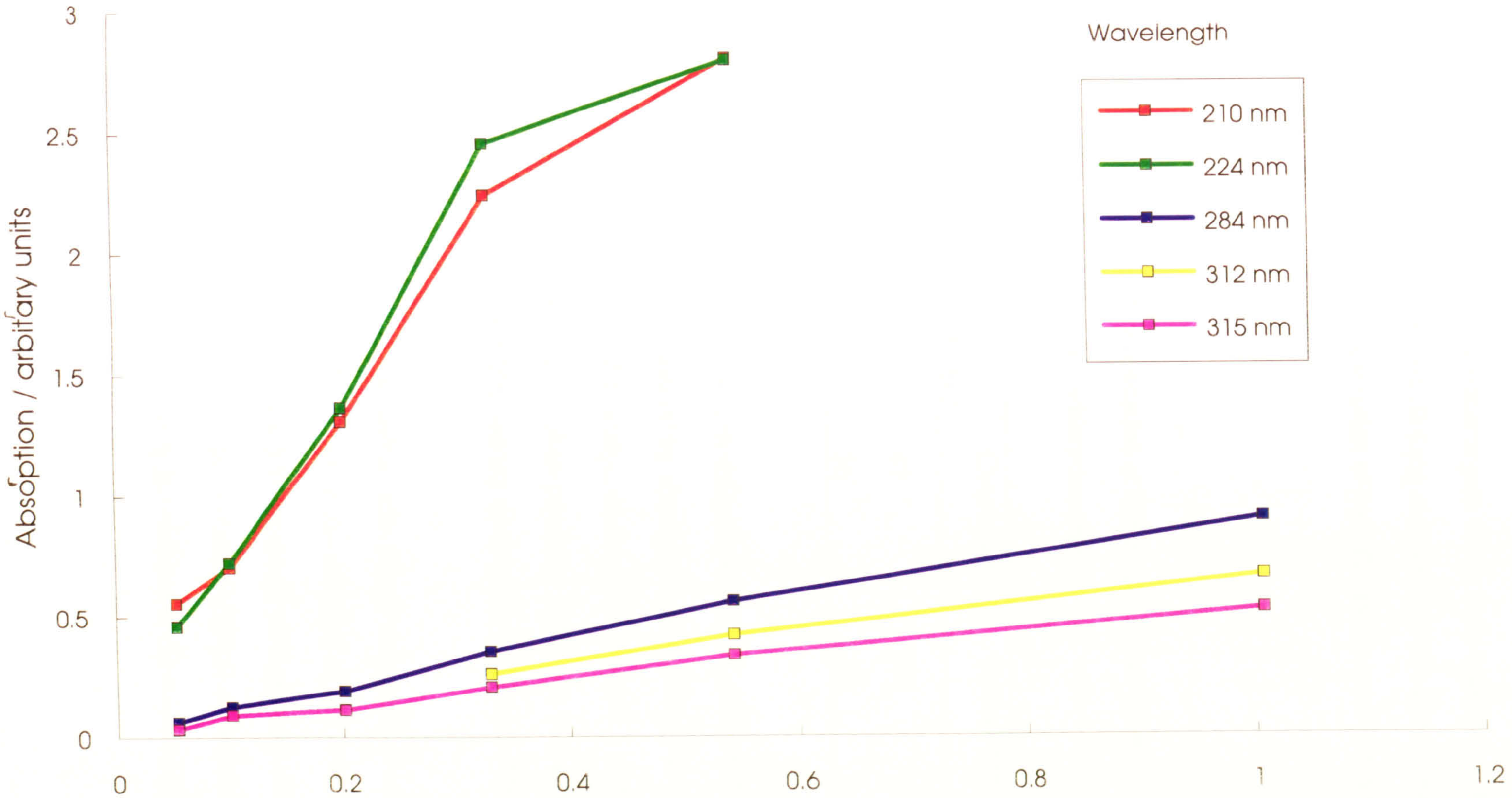

Figure 3.8
Beer-Lambert Plot of Absorbance vs. Concentration for Cinchonidine in Ethanol at 298 K

concentrations as explained in section 2.3.9). A concentration of 0.5 mg cinchonidine in 20 ml of solvent is just outside the linear region of the Beer-Lambert plot for the absorption band at 224 nm. However, 0.4 mg cinchonidine per 20 ml solvent is on the linear region, so any significant adsorption of modifier in the quantities studied in section 2.3.9 would be apparent.

Table 3.1

Effect on Methyl Pyruvate Hydrogenation at 298 K and 10 bar H_2 with Modification of Catalyst at Low Concentrations by Adsorption only.

Cinchonidine / mg	Ri / mmols h^{-1} (g cat.)$^{-1}$	Conversion / %	Optical Yield / %
11	810	47	49
1	450	26	30

When 100 mg EUROPT-1 was modified by 0.5 mg of cinchonidine in 20 ml of solvent, and then the solution examined by ultra-violet spectroscopy at varied times, the fraction of modifier adsorbed on the catalyst surface was between 5 and 15 %. This estimate was uncertain because of UV absorption due to the fine suspension of fine particulate catalyst was considerable, making quantitative assessment difficult.

The same experiment was attempted with toluene as solvent. Unfortunatly toluene is a poor chromatographic solvent[3], with a UV cut-off point at 285 nm . However, the broad adsorption band between 285 and 320 nm totally dissappeared when 100 mg EUROPT-1 was modified by 0.5 mg of cinchonidine in 20 ml of toluene. This was irrespective of whether the catalyst was in the reduced or the as received state.

3.3.4 Anaerobic Modification

One experiment was performed under the anaerobic modification conditions described in section 2.3.9a for EUROPT-1 catalyst which had been modified by 0.5 mg cinchonidine. Hydrogenation of methyl pyruvate at 298 K and 10 bar H_2 resulted in an initial rate if 275 mmols h^{-1} (g cat.)$^{-1}$ and an optical yield of 54 % at 14 % conversion. The optical yield is comparable to that obtained under the aerobic experiments performed at the same concentrations of modifier. However, the reaction rate was reduced to approximatly one third of that observed for the experiments where air was not excluded from the modification step. Reaction rate also fell away at 10 % conversion.

3.3.5 GHI Pt/silica

A brief study was undertaken of hydrogenation of methyl pyruvate at 298 K and 10 bar H_2 over 0.1 g GHI Pt/silica modified by cinchonidine at low concentration. The results are summarised in table 3.2. The initial rates quoted were calculated between 0-15 minutes, the reaction rate did however fall dramatically after this period. Also included is the result obtained by Meheux[4] when the catalyst was modified under the standard conditions of high cinchonidine concentration described in section 2.3.7.

The initial rates of reaction are similar and are very low under the modifier loadings examined. Comparison with the result obtained by Meheux for modification using standard conditions shows there to be an apparent 10 fold increase in reaction rate by lowering modifier concentration. However, the value quoted by Meheux is likely to be the residual reaction rate, which is of a similar magnitude to those observed for after modification at low concentrations of modifier. Optical yields were not improved by lowering the modifier concentration.

Table 3.2

Effect of Variation of Modifier Loading on Optical Yield and Initial Reaction Rate of Methyl Pyruvate Hydrogenation at 10 bar H_2 and 298 K

Modifier Loading / mg	Ri / mmols h^{-1} (g cat.)$^{-1}$	Conversion / %	Optical Yield / %
0.05	60	7	4
0.025	45	3	4
0.1	55	8[b]	1[b]
0-200[a]	6	4	8

[a] Modification as described in section 2.3.1.
[b] Estimated from H_2 Uptake Curve

3.4 Modification by Ephedrine and by Derivatives

Results obtained for the series of methyl pyruvate hydrogenations at 10 bar and 298 K in ethanol solvent by EUROPT-1 modified by various ephedrines are given in table 3.3. The experiments are sorted by the order in which they were performed using the experimental procedures explained in section 2.3.15.

Table 3.3

Variation of Reaction with choice of Ephedrine Modifier

Experiment	Ephedrine	Ri / mmols h^{-1} (g cat)$^{-1}$	Conversion / %	Optical Yield / %
1	1R,2S	-[a]	27	2.9
2	1R,2R	80	18	2.2
3	1S,2R	90	11	0.5
4	1S,2S	55	15	0.0
5	Deoxy	110	23	-1.1
6	1R,2S	65	15	0.0

[a]not determined

Rates of reaction are increased slightly by the presence of the ephedrine modifiers by a factor of between 1 and 2 when compared to the rate of reaction in the absence of any added modifier. The greatest increase in rate occurs for deoxyephedrine. No acceleratory period is observed and the rate of reaction is constant for the conversions studied. Greater increases in rates of reaction have been observed by other workers[5,6] upon the addition of other bases to the reaction.

Enantiomeric excesses obtained for three of the six experiments slightly favour R-(+)-methyl lactate formation and two show no preference. Only when deoxyephedrine is used as modifier is the enantiomeric excess in favour of S-(-)-product. This latter result should however be treated with caution as it is possible that the optical rotation measured by polarimeter resulted from low concentration of deoxyephedrine in the sample. This could have resulted during the product separation stage by rotary evaporation described in section 2.3.17. Deoxyephedrine unlike the other derivatives is a liquid and consequently its higher vapour pressure could have caused contamination of the sample.

Therefore, ignoring this result, it could be argued that the sense of the observed enantioselectivity is independent of the stereochemistry of the ephedrine at the C1 and C2 positions. However the trend is that the observed enantioselectivity in favour of R-(+)-lactate decreases with each experiment performed. When the first experiment was repeated with a fresh batch of 1R,2S-ephedrine no optical yield was obtained. It appears therefore that ephedrines *do not act as chiral modifiers for the reaction*, and that the observed enantiomeric excesses are as a result of slight traces of cinchonidine contaminant acting as a modifier in preference to the vast excess of ephedrine which is present.

For comparison, the results obtained by other workers for ephedrine modifiers, are given in table 3.4. For the reactions performed by Meheux[4] and Sutherland[7] the reactions were performed with identical choice of catalyst, pretreatment and reaction conditions.

The experiments performed by Blaser[6] and co-workers were similar, although 1.5 g Pt/Al_2O_3 catalyst was used and reaction was at 70 bar H_2, 298 K with 0.4 moles of ethyl pyruvate in 75 ml solvent (not explicitly stated but probably ethanol and/or toluene)

Table 3.4

Effect of Ephedrine Modifier on Reaction by various Workers

Worker	Ephedrine	Rate / mmols h^{-1} (g cat.)$^{-1}$	Conversion / %	O.Y. / %
Meheux[4]	1R,2S	117	37	13
Sutherland[7]	1R,2S	33	15	7
Blaser *et al.*[6]	varied	-	-	5-25

3.5 Modification by Benzyl Pyrrolidine Methanol

S-Benzyl pyrrolidine methanol had been found to be a catalyst modifier for methyl pyruvate hydrogenation at 10 bar and 298 K in ethanol solvent[4]. The experiments were repeated for EUROPT-1 and Ir/$CaCO_3$-1 and the results are summarised in table 3.5 which also includes the values found by Meheux for comparison.

The optical yield observed when EUROPT-1 is used as a catalyst is negligible and is indistinguishable from optical yields resulting from cinchonidine caused by contamination of the equipment. Although the rates of reaction are similar, the former observation is in contrast with that of Meheux. A reduction in the rate of reaction occurs when Ir/$CaCO_3$-1 is modified by S-benzyl pyrrolidine as opposed to cinchonidine and no optical yield is observed.

Table 3.5

Variation of Reaction for Modification by S-Benzyl Pyrrolidine Methanol

Catalyst	Ri /mmols h^{-1} (g cat.)$^{-1}$	Conversion / %	Optical Yield / %
EUROPT-1	90	27	0.03
$Ir/CaCO_3$-1	635	72	0.0
EUROPT-1[a]	111	28	8
EUROPT-1[a]	120	30	12

[a]Meheux[4]

3.6 Modification by Tryptophan and Histidine

When EUROPT-1 is pretreated as described in section 2.3.1 and 2.3.7 but modified by varied derivatives of tryptophan and histidine, hydrogenation of methyl pyruvate at 10 bar and 298 K gives results as described in table 3.6.

Modification by L-histidine, L-histidine methyl ester and L-tryptophan methyl ester gives product with R-(+)-methyl lactate in slight enantiomeric excess and D-histidine and D-tryptophan enantiomeric excess in the opposite sense. The optical yields are however very low. Rates of reaction are lower than the corresponding reaction in the absence of added modifier and no acceleratory period is observed.

The experiment described in section 2.3.10 whereby a mixed modification by L-histidine methyl ester and quinuclidinol is also give in table 3.6. The aim of the experiment was to induce enantioselectivity in the product at an enhanced rate as is the case when cinchonidine is used as a modifier. Although the rate of reaction was indeed enhanced, this was at the expense of the optical yield which was reduced to zero.

Table 3.6

Effect of Modification by Histidine and Tryptophan upon Reaction

Modifier	Rate / mmols h^{-1} (g cat.)$^{-1}$	Conversion / %	Optical Yield / %
L-(-)-Histidine	40	16	2.5
L-(-)-Histidine	50	14	2.0
D-(+)-Histidine	30	17	-1.5
L-Tryptophan Methyl Ester	35	20	1.5
D-Tryptophan Methyl Ester	40	22	-1.5
L-(-)-Histidine Methyl Ester	20	11	3.5
L-(-)-Histidine Methyl Ester/ Quinuclidinol	80	35	0.0

3.7 Modification by Cinchona Alkaloid Derivatives

Hydrogenation of methyl pyruvate by EUROPT-1 under the standard conditions described in section 2.3.15, but modified by cinchona alkaloids which had been derivatised by large bulky substituents at the C9 position resulted in initial rates of reaction and optical yields summarised in table 3.6. Each of the modifiers enhanced the hydrogenation rate over that observed in the absence of added modifier. No acceleratory period was observed in the hydrogen uptake curve, a feature which is in common with the observations of Meheux *et al.* when 10,11-dihydrocinchonidine is used as modifier[8]. In common with the natural alkaloids, quinine derivatives gave methyl lactate with the R-(+)-enantiomer in excess and quinidine derivatives the S-(-)-product in enantiomeric excess. The absolute magnitude of the optical yields were greater for modifier giving R-(+)-methyl lactate, in common with the observation for the natural alkaloids.

Table 3.7

Variation of Optical Yield and Initial Reaction Rate with choice of Modifier

Modifier	Ri / mmols h^{-1} (g cat.)$^{-1}$	Optical Yield / %	Conversion / %
10,11-dihydroquinine 4-methyl-2-quinoyl ether	160	22	94
10,11-dihydroquinidine 4-methyl-2-quinoyl ether	225	-1	94
10,11-dihydroquinine 9-phenanthryl ether	190	3	32
10,11-dihydroquinidine 9-phenanthryl ether	90	-1	21

Table 3.8

Hydrogenation of Methyl Pyruvate by Cinchonidine modified Rh/Al_2O_3

Rh/Al_2O_3	Modifier /mg	Modification time / h	Ri /mmols h^{-1} (g cat)$^{-1}$	Conversion / %	Optical Yield / %
Unsintered	0	-	415	95	0
Sintered	0	-	320	25	0
Unsintered	200[a]	1	470	70	3
Sintered	200[a]	1	610	50	4
Sintered[c]	200[a]	1	320	35	0
Sintered	200[b]	1	535	39	-0.15
Unsintered	0.5[a]	0	240	33	2
Sintered	0.5[a]	0	280	35	3
Sintered	0.5[a]	1	270	28	3

[a]Cinchonidine used as modifier
[b]Cinchonine used as modifier
[c]Hydrogenation at ca. 273 K

3.8 Rhodium Catalysts

Results of a short investigation as to the effectiveness of 5% Rh/Al_2O_3 as a catalyst for the asymmetric hydrogenation of methyl pyruvate at 10 bar are summarised in table 3.8. None of the reactions showed any acceleratory period hence the value for Ri is as given in curve (b) of figure 3.5.

In the absence of any added modifier, rates of reaction are ca. 6-8 times faster than the reaction over EUROPT-1 under equivalent conditions. The rate of reaction is however slightly reduced upon sintering the catalyst, caused by a reduction in the metal surface area.

Upon modification of the catalyst by a high concentration of cinchonidine using the procedure described in section 2.3.7, methyl pyruvate is hydrogenated to give R-(+)-methyl lactate in slight enantiomeric excess. The sintered Rh/Al_2O_3 catalyst gives product at a slightly greater rate and optical yield. Initial rates of reaction are faster for modified as opposed to unmodified catalysts, as is observed with Pt catalysts. Surprisingly, reducing the temperature to 273 K caused a loss in enantioselectivity, the opposite of the effect observed with Pt.

Modification by 200 mg of alkaloid using the procedure recommended by Orito *et al.* is in vast excess over that required for a monolayer surface coverage. On platinum it has been proposed that a 'non-close-packed array' of alkaloid molecules is required for the formation of an effective asymmetric hydrogenation site[9]. If the alkaloid molecules were to adsorb strongly in a close-packed manner then it would be expected that the reactant would be hindered from approaching the surface. To examine if this was indeed the case three experiments were performed with 0.5 mg of added modifier in the manner described in section 2.3.9.

Although there was enough alkaloid present to induce a slight degree of enantioselectivity in the product it was comparable in magnitude to experiments performed at high concentrations of alkaloid modifier. The reaction rate was however less than that observed in the racemic reaction. As observed with experiments performed at low concentrations of modifier with EUROPT-1, the results were the same whether or not the catalyst and modifer solution had been stirred in air for an hour during modification.

3.9 Iridium/alumina

Racemic hydrogenation of methyl pyruvate at 10 bar H_2 and 293 K over a 5 % Ir/alumina catalyst in ethanol solvent (in the absence of any added modifier) proceeded at an initial rate of 185 mmols h^{-1} (g cat.)-1 for up to 21 % conversion when the reaction was stopped. No optical yield was of course observed.

When the experiment was repeated with catalyst modified with cinchonidine (in the manner described in section 2.3.7) an enhanced initial rate of reaction of 425 mmols h^{-1} (g cat.)$^{-1}$ resulted. No acceleratory period, as observed with similar experiments conducted over cinchonidine modified EUROPT-1 (and described in figure 3.5 curve (a)) was present. A slight optical yield of 2 % was observed at 54 % conversion (51 % R-(+), 49 % S-(-)).

As larger metal crystallites appear to increase enantioselectivity to product over Pt catalysed reaction[10,11], the as received Ir/alumina catalyst was sintered in the manner described in section 2.3.5. Transmission Electron Micrographs of the Ir/alumina, as received and after sintering were of conventional appearance, although the particles in the former case we impossible measure to any accuracy. Heating the catalyst at 1223 K in flowing H_2 increased the average metal crystallite size, the size distribution for 90 metal particles (which were clearly in focus) is shown in figure 3.9 to be centred around 11 Å. Hydrogenation of methyl pyruvate over this cinchonidine-modified catalyst, under

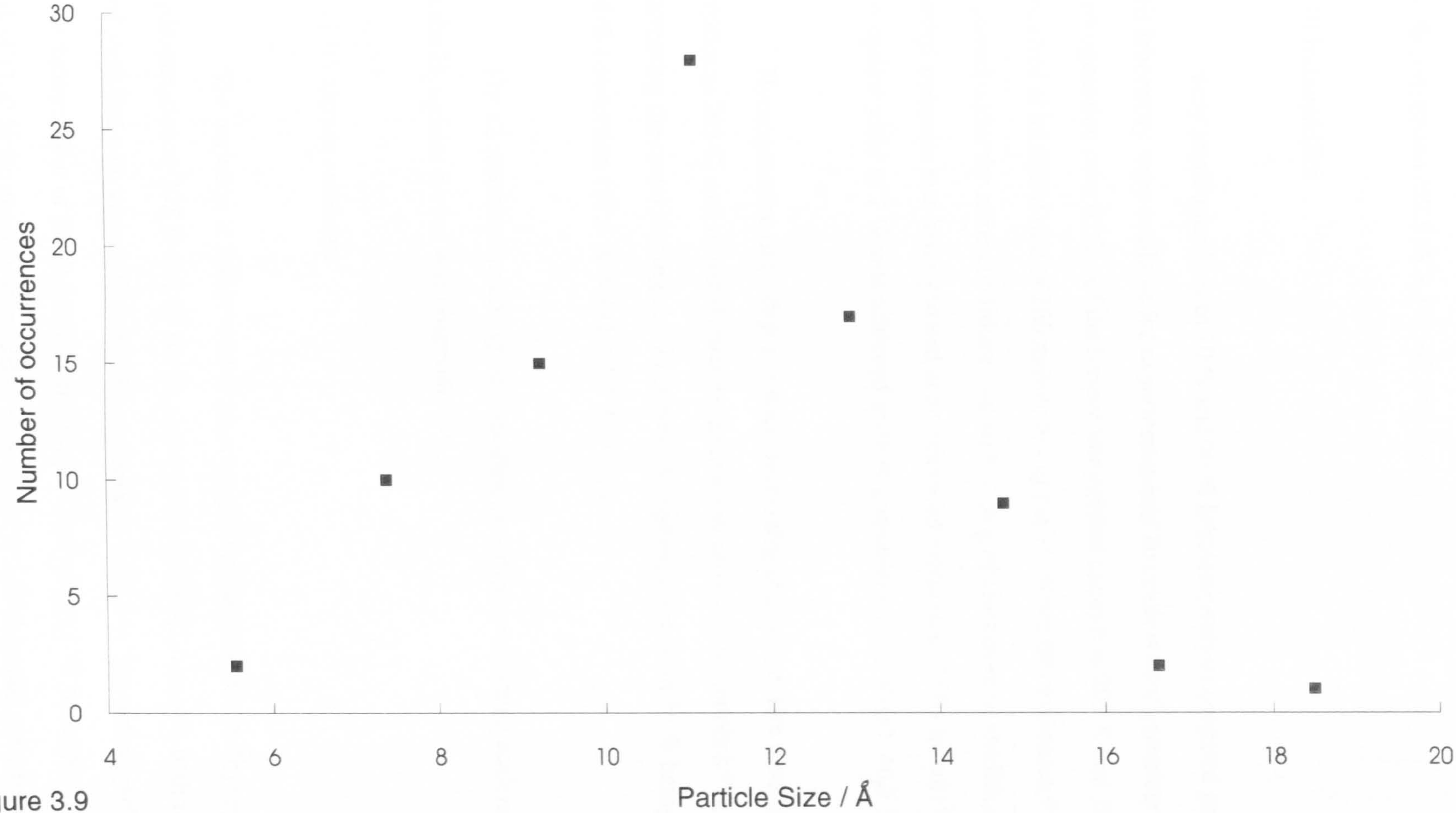

Figure 3.9
Particle Size Distribution for Sintered Iridium/alumina

the same conditions as above did indeed raise the optical yield slightly, but only to 5 % at 56 % conversion (52.5 % R-(+), 47.5 % S-(-)).

3.10 Iridium/silica

Very small quantities of 10 % and 20 % Ir/silica catalysts prepared previously in this laboratory were available for experimentation. Racemic methyl pyruvate hydrogenation over 0.02 g of the former unmodified catalyst at 293 K and 10 bar H_2 occurred at an initial rate of 260 mmols h-1 (g cat.)$^{-1}$. When this experiment was repeated under the same conditions, but with 0.04 g of cinchonidine modified catalyst methyl pyruvate was hydrogenated at an enhanced initial rate of 605 mmols h^{-1} (g cat.)$^{-1}$. An optical yield of 7 % was achieved at 46 % conversion (53.5 R-(+), 46.5 S-(-)).

Hydrogenation of methyl pyruvate over 0.03g of cinchonidine modified 20 % Ir/silica at 293 K and 10 bar H_2 proceeded at a rate of ca. 1800 mmols h^{-1} (g cat.)$^{-1}$. Increasing the metal loading also improved the optical yield, with 15 % being achieved at 84 % conversion (57.5 % R-(+), 42.5 % S-(-)).

For all reactions involving cinchonidine-modified catalysts no accleratory period in the H_2 uptake curves was observed.

3.11 Ir/calcium carbonate

The variation in initial rates of reaction and optical yield for methyl pyruvate hydrogenation at 293 K and 10 bar H_2 using a 5 % Ir/$CaCO_3$ catalyst, both unmodified and modified with varied alkaloids are displayed in table 3.9. The optical yield was found to be independent of the degree of conversion. Catalysis by 5 % Ir/$CaCO_3$-1 and Ir/$CaCO_3$-2 in the absence of modifier is different to that observed for other catalysts in as much as very fast rates of racemic hydrogenation of 1270 and 1680 mmols h^{-1} (g cat.)$^{-1}$ respectively were observed. The rates of reaction for the enantioselective reaction

when the catalysts were modified by cinchonidine were not as fast using Ir/$CaCO_3$-1; and identical using Ir/$CaCO_3$-2. Nevertheless moderate optical yields of 23 % (61.5 % R-(+), 38.5 % S-(-)) were achieved with the former catalyst and 39 % (69.5 % R-(+), 30.5 % S-(-)) under these conditions. (Ir/$CaCO_3$-2 did not become available until the end of period of study. Subsequently the majority of the work reported for Ir/$CaCO_3$-1, even though Ir/$CaCO_3$-2 gives product with higher optical yield.)

Table 3.9

Initial Rates and Optical Yields in Methyl Pyruvate Hydrogenation over 5 % Ir/$CaCO_3$ at 10 bar H_2 and 293 K

Catalyst	Modifier	Ri / mmols h^{-1} (g cat.)$^{-1}$	Conversion / %	Optical Yield /%
1	none	1270	80	0
1	cinchonidine	892	81	23
1	dhc	675	75	19
1	quinine	525	76	17
1	cinchonine	675	67	-9
1	quinidine	370	51	-6
2	none	1680	80	0
2	cinchonidine	1680	90	39

dhc = 10,11-dihydrocinchonidine

When cinchonidine, 10,11-dihydrocinchonidine or quinine were used as modifiers selective formation to R-(+)-methyl lactate occurred. Modification of the catalyst by cinchonine or quinidine resulted in enantioselectivity to S-(-)-methyl lactate. Hydrogenation of methyl pyruvate over alkaloid modified Ir/$CaCO_3$-1 occurred at a moderate rate which was lower than that for the racemic hydrogenation over unmodified catalyst. No acceleratory period in the H_2 uptake curves was present.

3.11.1 Solvent Effects on the Reaction

The effect of varied solvents on methyl pyruvate hydrogenation at 10 bar H_2 and 293 K over Ir/$CaCO_3$-1 both in the absence and presence of cinchonidine modifier are shown in table 3.10. The very fast racemic rates experienced over unmodified Ir/$CaCO_3$ in ethanol solution were not seen for the other solvents examined. The next fastest initial rate of hydrogenation was observed for dodecanol which was one third that of reaction in ethanol. Racemic hydrogenation in toluene solvent is very slow, as is the case in dichloromethane (although no 'apparent rate' of reaction was observed due to the H_2 uptake being less than the vapour pressure of the solvent - a feature which the dosing system can not compensate for).

Table 3.10

Initial Rates and Optical Yields in Methyl Pyruvate hydrogenation over 5 % Ir/$CaCO_3$-1 at 10 bar H_2 and 293 K

Solvent	Modifier	Ri / mmols h^{-1} (g cat.)$^{-1}$	Conversion / %	Optical Yield / %
ethanol	none	1270	80	0
ethanol	cinchonidine	895	81	23
dodecanol	none	440	68	0
dodecanol	cinchonidine	270	73	13
toluene	none	80	10	0
toluene	cinchonidine	110	12	14
dichloromethane	none	-	9	0
dichloromethane	cinchonidine	-	8	5

Modification of Ir/$CaCO_3$-1 with cinchonidine reduced the initial rates of hydrogenation in dodecanol solvent. This effect was, however not seen in toluene solvent where the rates are identical within experimenal error. No difference in the reaction rates

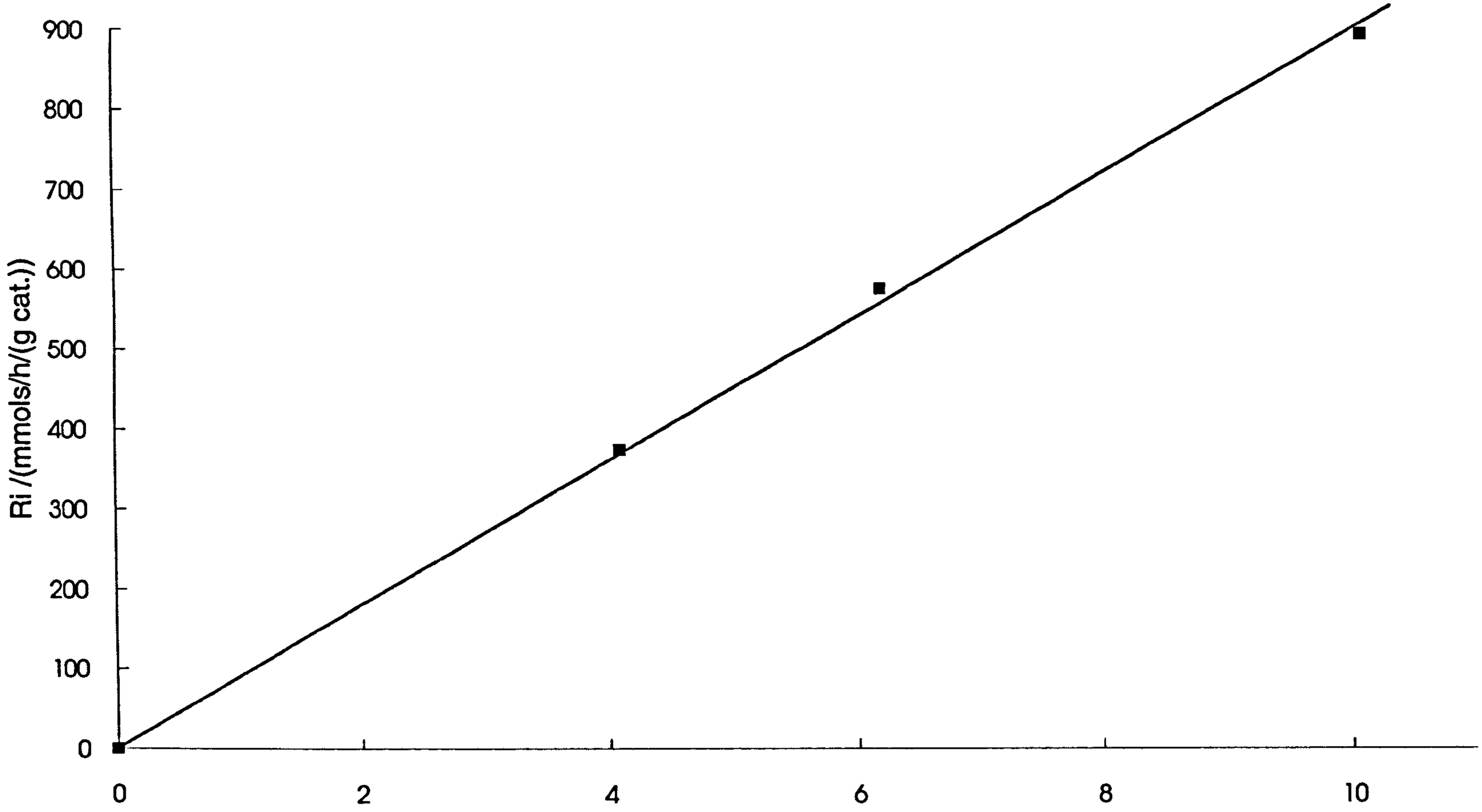

Figure 3.10
Plot of Reaction Rate vs. Hydrogen Pressure for Methyl Pyruvate Hydrogenation over Ir/CaCO3-1 at 298 K

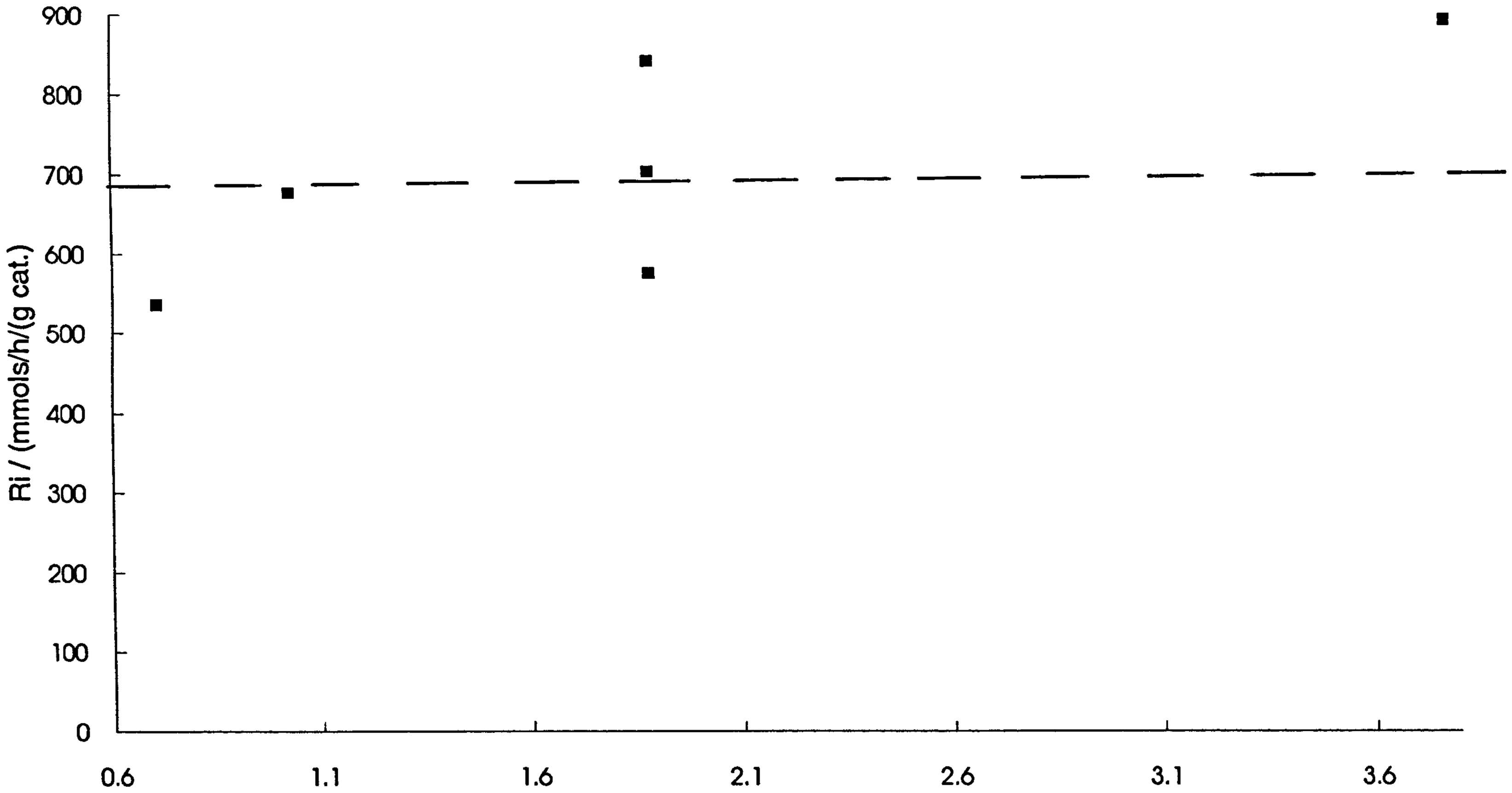

Figure 3.11
Variation of Reaction Rate with Modifier Concentration

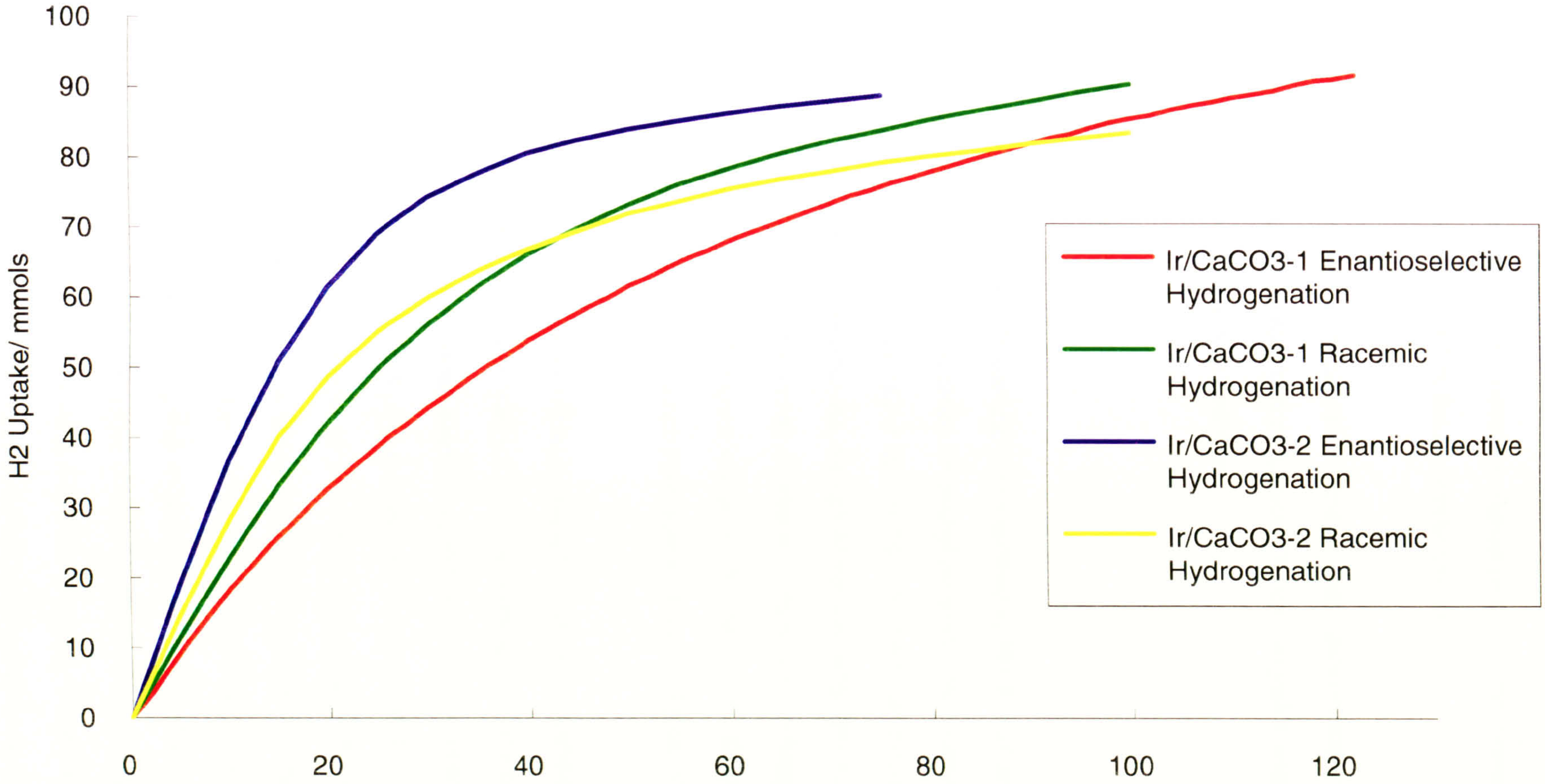

Figure 3.12
Hydrogen Uptake Curve for Reaction Catalysed by Ir/CaCO3 at 10 bar Hydrogen and 293 K

is apparent in dichloromethane solvent either (based on the overall conversion). No acceleratory period was observed in the H_2 uptake curves.

For all solvents, modification of the catalyst with cinchonidine resulted in product with R-(+)-methyl lactate in enantiomeric excess. The optical yields were, however, not as great as that observed for ethanol solvent.

3.11.2 Orders of Reaction

The orders of reaction by the initial rate method at 293 K was zero order with respect to enantioselective hydrogenation of methyl pyruvate over cinchonidine modified $Ir/CaCO_3$-1, (initial concentration varied from 0.7 to 3.8 mol l^{-1} as shown in figure 3.11). The experimental scatter in reaction rate, though apparently large has been observed before in figure 3.2. This reaction was first order with respect to hydrogen (pressure varied from 4.1 to 10.1 bar, initial concentration = 1.9 mol l^{-1}). The first order plot of enantioselective hydrogenation rate versus pressure is shown in figure 3.10.

Reaction catalysed by cinchonidine modified $Ir/CaCO_3$-1 would therefore be expected to be first order overall. Examination of the hydrogen uptake curve for this reaction shown in figure 3.12, has the appearance of a first order reaction which is confirmed by the fitting the points to a plot of ln(a-x) vs. t in figure 3.13. (Where a is the initial concentration of methyl pyruvate of 110 mmols assuming 97 % purity of reactant and x is the methyl pyruvate concentation at time t). The line through the points produced by this method is almost linear, indicating the process to be nearly first order overall. When the same treatment is given to the hydrogen uptake curve produced by racemic hydrogenation of methyl pyruvate over $Ir/CaCO_3$-1 the resulting points are non-linear, suggesting that this reaction is not a first order process. When the hydrogen uptake curves for both racemic and enantioselective hydrogenation are fitted to the equation 1/(a-x) vs. t (not shown) neither of the plots produce a linear line, indicating that neither reaction is second order.

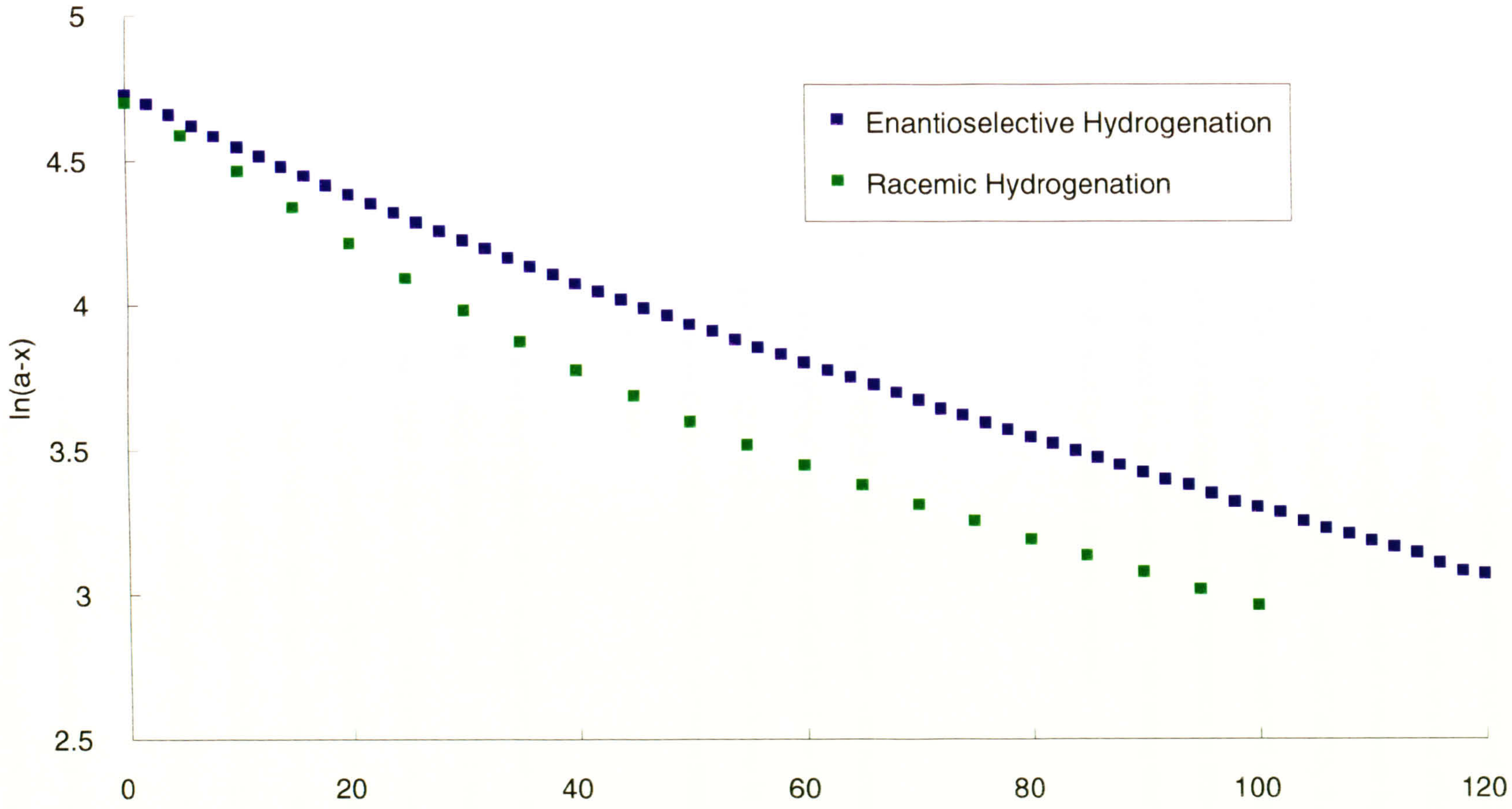

Figure 3.13
First Order Plot of Methyl Pyruvate Hydrogenation over Ir/CaCO3-1 at 10 bar Hydrogen and 293 K

Meheux[4] showed that the hydrogen uptake curves produced by enantioselective hydrogenation of methyl pyruvate over dihydrocinchonidine modified EUROPT-1 could be fitted to the Hinshelwood equation[12], linearity in which shows the effect of poisoning by reaction products. The hydrogen uptake curves for methyl pyruvate hydrogenation over unmodified and cinchonidine modified $Ir/CaCO_3$-1 and $Ir/CaCO_3$-2 are fitted to the Hinshelwood equation and shown in figure 3.14. (For data collected after 20 and 10 minutes respectively). The plot for enantioselective hydrogenation is non-linear, unlike that for racemic hydrogenation which is reasonably linear, indicating that the enantioselective reaction is inhibited by methyl lactate product.

3.11.3 Activation Energy

The affect of temperature on initial rate of reaction for both racemic and enantioselective methyl pyruvate hydrogenation over $Ir/CaCO_3$-1 (in the absence and presence of cinchonidine modifier respetively) at 10 bar H_2 are shown in the form of an Arhenius plot in figure 3.15. The data shown is taken from reactions performed both in the Büchi and the Fischer Porter reactor.

Initial rates of racemic reaction increases with temperature over the range 273 K to 338 K. The apparent activation energy for the reaction is 11 ± 2 kJ mol^{-1}. This value is quite low, and can be representative of diffusion control. However, the two identical points at 298 K represent one reaction performed in the Fischer Porter reactor vessel with 0.1 g of catalyst and a reaction performed on the Büchi reactor with 0.05 g of catalyst at a stirrer speed of 1400 rpm. The three other points at 273 318 and 338 K were also performed under the latter conditions which should inhibit diffusion control.

For the enantioselective reaction, the initial rate increases with temperature over the range 263 to 295 K, but collapses above 318 K. From the linear points of increasing reaction rate, an apparent activation energy of 22 ± 2 kJ mol^{-1} has been calculated. This is again quite low, but the points over which the calculation was made are quite linear.

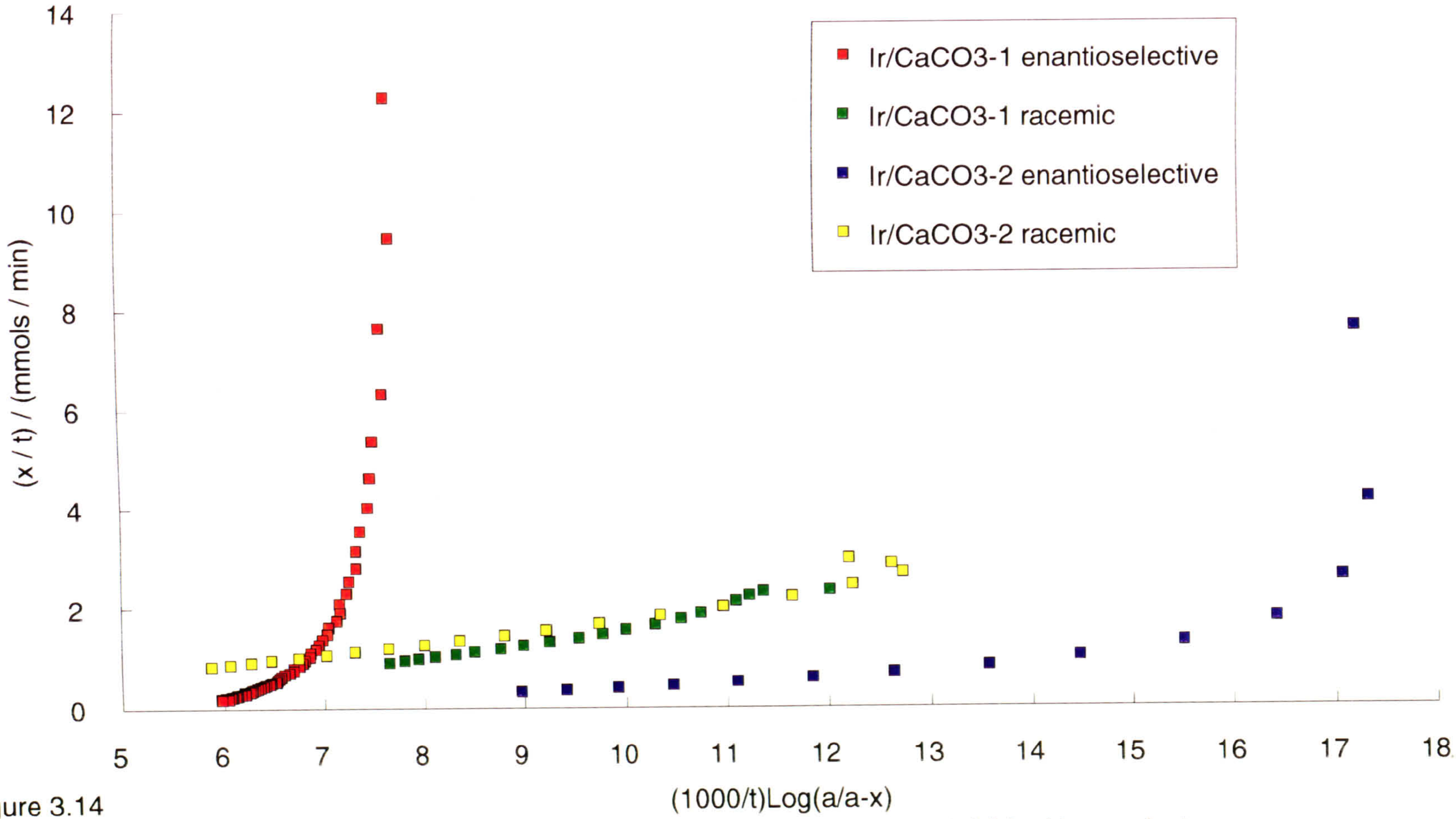

Figure 3.14
Plot showing non-conformity to the Hinshelwood Equation for catalysed reaction inhibited by products

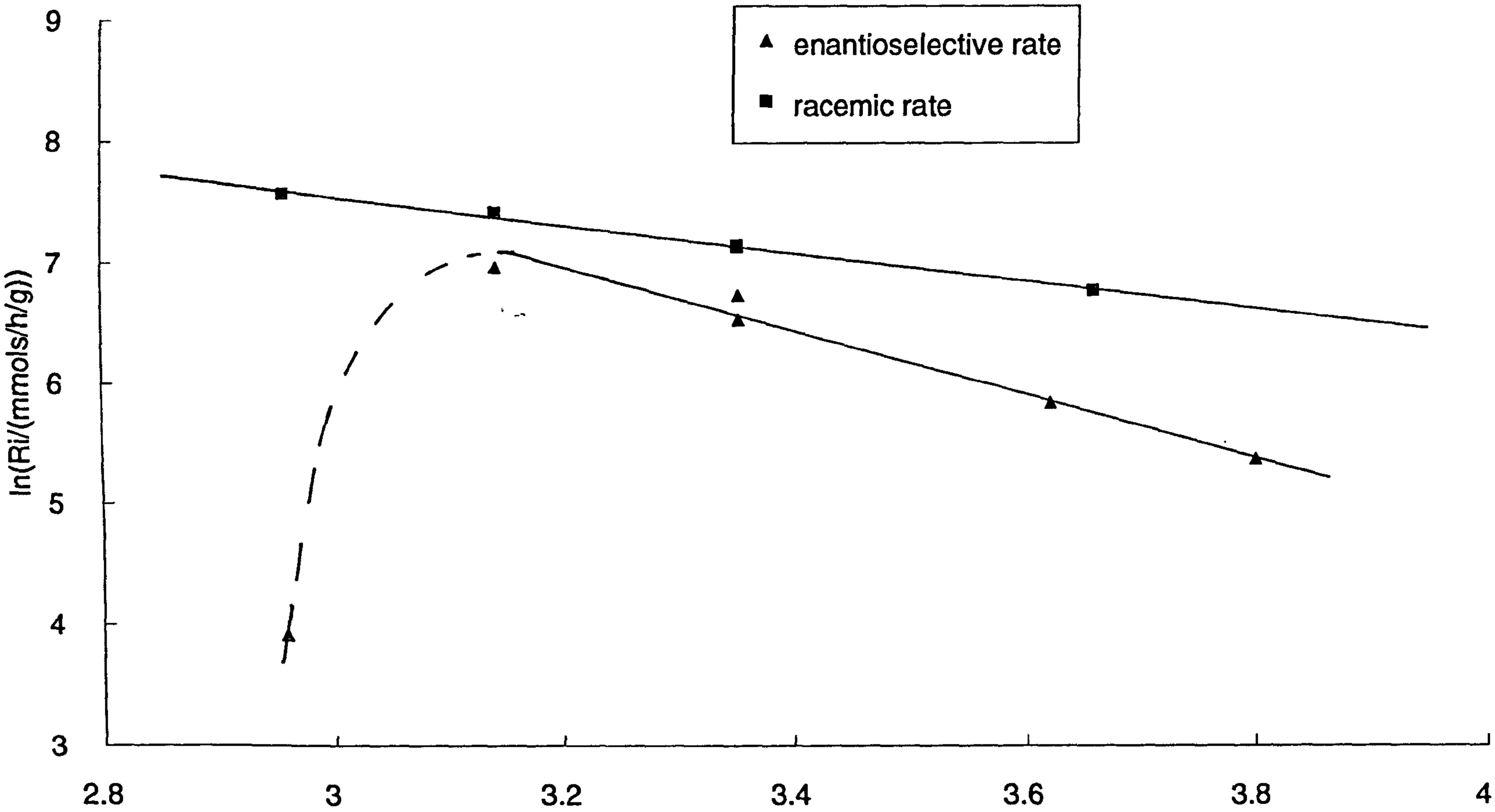

Figure 3.15
Arhenius Plot for Methyl Pyruvate Hydrogenation over Ir/CaCO3-1 at 10 bar H2

The effect of temperature on optical yield is shown in figure 3.16. There is a gradual decline in optical yield with increasing temperature. The optical yield does not collapse above 318 K in the same manner as the initial rate of reaction. The highest optical yield of 31 % (65.5 % R-(+), 34.5 % S-(-)) observed for $Ir/CaCO_3$-1 was for reaction at 273 K. The slight decrease in optical yield noticed at 263 K could be due to experimental error. Maintenance of constant temperature, before and during reaction was not easy, and a fluctuating temperature could have affected the result. It was not possible to go to a temperature below this value and still to maintain pressure integrity of the Fischer Porter reactor.

3.11.4 Deuterium Tracer Study

The amount of exchange of H for D in 10,11-dihydrocinchonidine over $Ir/CaCO_3$-1 after 18 h and 9 days at 293 K as described in section 2.3.23 occurred as shown in figure 3.17 and 3.18 respectively. Ambiguity in the assignment of the protons at C5' and C8' positions were confirmed by use of the Nuclear Overhauser Effect by irradiation of the proton at C9'. For comparison the amount of exchange of H for D in 10,11-dihydrocinchonidine over EUROPT-1 after 5 days obtained by Bond *et al.*[13] in this laboratory using the same procedure are given in figure 3.19.

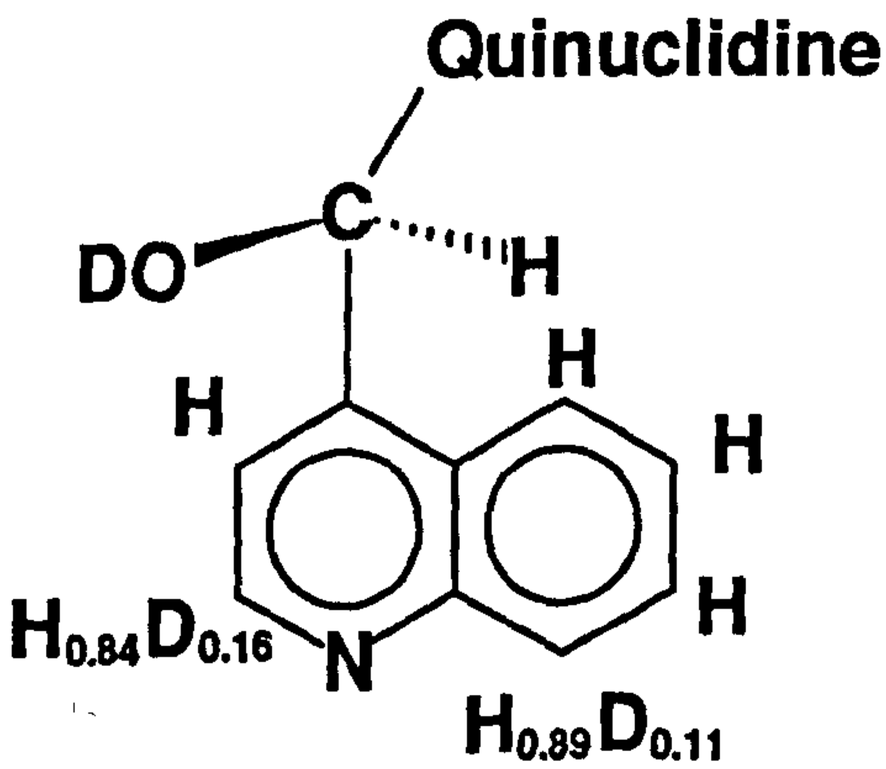

Figure 3.17

Degree of Deuterium Exchange in DHC in EtOD and D_2 at 298 K after 18 h over $Ir/CaCO_3$-1

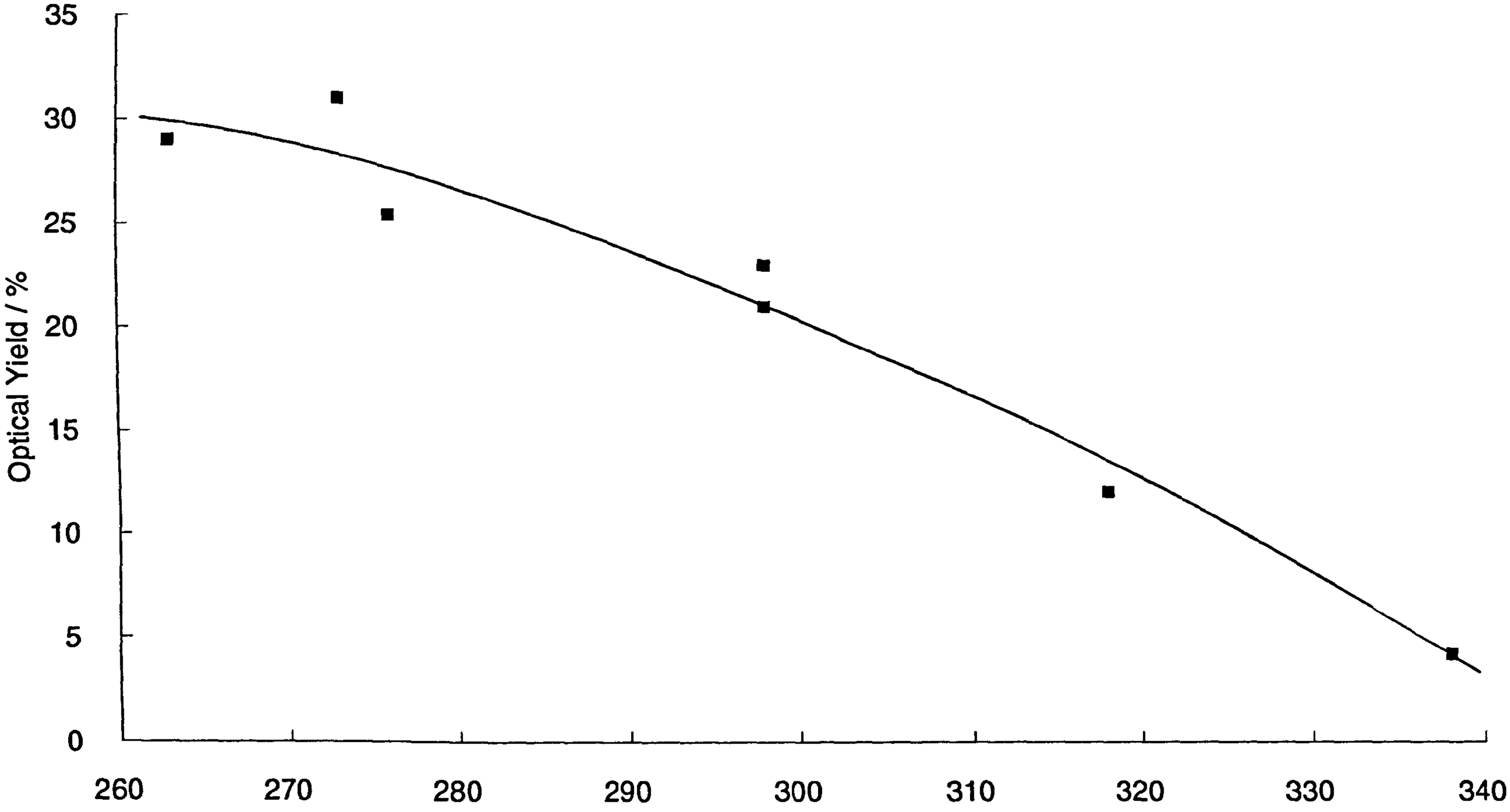

Figure 3.16
Variation of Optical Yield with Temperature for Methyl Pyruvate Hydrogenation over Ir/CaCO3 at 10 bar H2

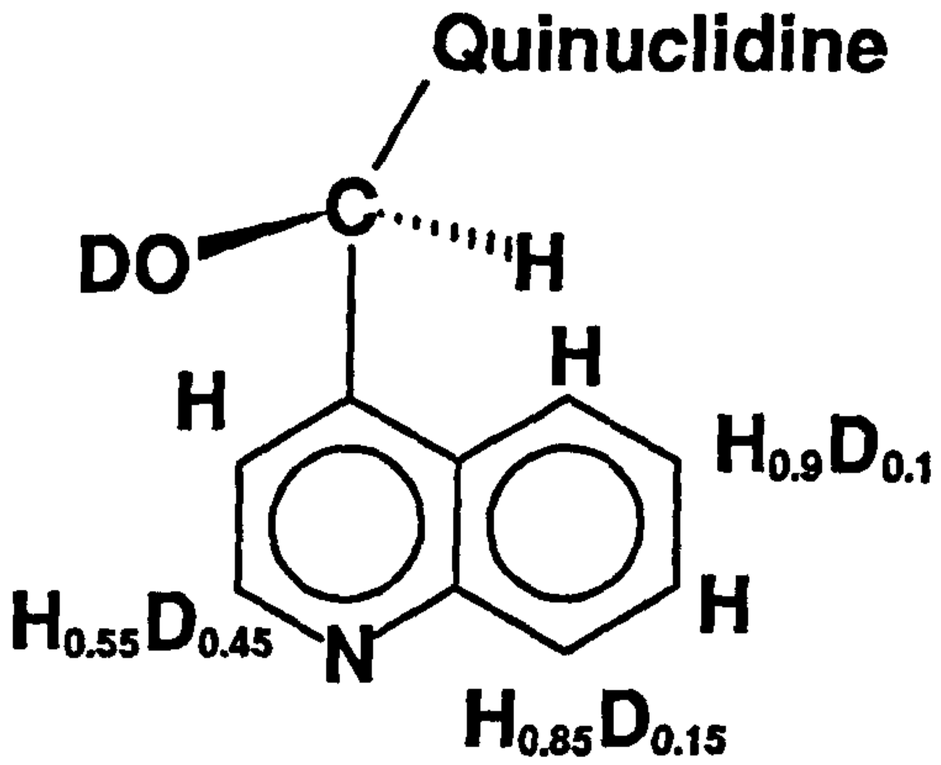

Figure 3.18

Degree of Deuterium Exchange in DHC in EtOD and D_2 at 298 K after 9 days over $Ir/CaCO_3$-1

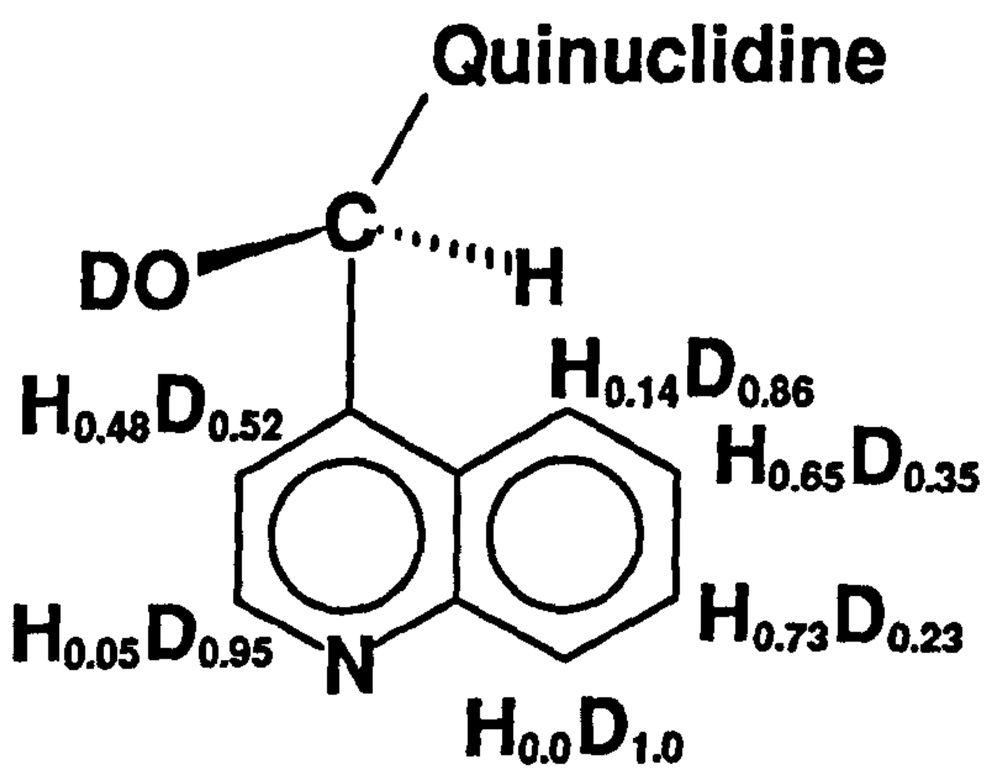

Figure 3.19

Degree of Deuterium Exchange in DHC in EtOD and D_2 at 298 K over EUROPT-1

After 18 h exchange occurred at the C2', and C8' positions. No hydrogenolyis or hydrogenation occurred according to mass spectrometry, which was consistent with the slight increase in molecular mass caused by deuterium exchange. Unfortunately the small amount of exchange observed makes these figures inaccurate. However, after 9 days exchange occurred at the same positions and also C6', the greater extent of exchange improving the accuracy of the interpretation. In contrast, deuterium exchange over EUROPT-1 occurs to a large extent at all other aromatic protons.

3.12 Other Catalyts

Three other cinchonidine modified catalysts were briefly studied for the enantioselective hydrogenation of methyl pyruvate at 10 bar H_2 and 298 K, the values of initial rate of reaction and optical yield are summarised in table 3.11. Modification of $Pt/CaCO_3$ by cinchonidine resulted in a slightly enhanced rate of reaction and modest optical yield in favour of R-(+)-methyl lactate. No acceleratory period in the hydrogen uptake curve was observed for the enantioselective reaction.

Neither of the osmium or rhenium catalysts was active for methyl pyruvate hydrogenation under the conditions studied.

Table 3.11

Variation in Optical Yield and Initial Reaction Rate for Three Catalysts

Catalyst	Ri /mmols h^{-1} (g cat.)$^{-1}$	Conversion / %	Optical Yield / %
$Pt/CaCO_3$[a]	70	5	0
$Pt/CaCO_3$	120	13	41
3 % Os/Al_2O_3[b]	-	-	-
20 % Re_2O_3/Al_2O_3[b]	-	-	-

[a] Unmodified Catalyst
[b] No reaction observed after 1 h

3.13 Benzil Hydrogenation

Benzil was successfully hydrogenated to benzoin at a rate of 200 mmols h^{-1} (g cat)$^{-1}$.The product was a white crystalline solid of melting point 402-407 K (lit. 405 K). However, no optical rotation of the product was observed, indicating no enantiomeric excess.

---

[1] Y.Orito, S. Imai and S. Niwa, Nippon Kagaku Kaishi 1979 8

[2]J.T. Wehrli, A. Baiker, D.M. Monti, H.U. Blaser and H.P. Jalett, J.Mol. Cat. 57 (1989) 245.

[3]Pye Unicam LC-UV Detetector technical Manual, Pye Unicam Ltd., Publication No. 4013 229 97531

[4]P.A. Meheux, Ph.D Thesis, University of Hull, 1991.

[5]G. Bond, P.A. Meheux, A. Ibbotson and P.B. Wells, Catal. Today, 10 (1991) 371.

[6]H.U. Blaser, H.P. Jalett, D.M. Monti, J.F. Reber, and J.T. Wehrli, Stud. Surf. Sci Catal., 41 (1988) 153.

[7]I.M. Sutherland, Ph.D. Thesis, University of Hull, 1989.

[8]P.A. Meheux, A. Ibbotson and P.B. Wells, J. Catal, 128 (1991) 387.

[9]I.M. Sutherland, A.Ibbotson, R.B. Moyes and P.B. Wells, J.Catal 125 (1990) 77.

[10]S.D. Jackson, M.B.T. Keegan, G.D. McLellan, P.A. Meheux, R.B. Moyes, G. Webb, P.B. Wells, R. Whyman and J. Willis, Preparation of Catalysts V, (G. Poncelet, P.A. Jacobs, P. Grange and B. Delmon (Eds)), pp 135-144, Elsevier, Amsterdam, 1991.

[11]J.T. Wehrli, A. Baiker, D.M. Monti and H.U. Blaser, J. Mol. Catal, 49 (1989) 195.

[12]C.N. Hinshelwood, in 'The Kinetics of Chemical Change', Clarendon Press, Oxford, 1940, p.193.

[13]G. Bond and P.B. Wells, unpublished results.

Chapter 4

Discussion

4.1 Mathematical Modelling of Mixed Modification

Both the original[1] and the revised template model[2] conceives of modification as involving an ordered non-close-packed adsorption of alkaloid molecules at the Pt surface. The use of alkaloids of opposite configuration enables this concept to be tested.

Because the enantioselective reaction is faster than racemic reaction and because the former requires a specific chemical reaction between the adsorbed modifier and reaction intermediate[3], the optical yield obtained in a mixed-modified reaction may be influenced both by the optical yield and the rate afforded by each pure modifier. Supposing this to be so, the expected optical yields can be calculated for various modifier concentrations, using the various mathematical models for the asymmetric hydrogenation site and the calculations compared to the results obtained in figures 3.2 and 3.3.

The mathematical model of expected optical yield versus mole fraction of cinchonidine (mfcd) and mole fraction of cinchonine (mfcn) for different possible models of the asymmetric hydrogenation site is explained below. An identical model is achievable when the data is taken from the quinine and quinidine mixed modifier system, the mole fractions being denoted as mfqn and mfqd, respectively. An equivalent explanation is therefore not given, although parameters used for the calculations are shown in table 4.2. A number of assumptions as to the nature of the system were necessary and these are noted below.

4.1.1 1:1 Interaction Model

If the asymmetric hydrogenation site consists of only one alkaloid molecule interacting with one methyl pyruvate molecule, then

$$\text{Optical Yield} \propto (\text{mfcd} + \text{mfcn})$$

For the cinchonidine-cinchonine system, assuming (i) that: the mfcd and mfcn in solution is representative of the probability of finding the alkaloid on the surface (i.e. the heats of adsorption are identical):

$$\text{mfcd} = \frac{[\text{cd}]_{\text{solution}}}{[\text{cd}+\text{cn}]_{\text{solution}}} = \frac{[\text{cd}]_{\text{surface}}}{[\text{cd}+\text{cn}]_{\text{surface}}}$$

where,

cd = cinchonidine
cn = cinchonine

and (ii) that the rate and ratio of R-(+)- and S-(-)-methyl lactate formation from each alkaloid alone remains the same in a mixture at a rate proportional to its mole fraction then, disregarding any racemic reaction:

$$R^{+}_{Tot} = (\text{mfcd} \times \text{Rate}_{cd} \times R^{+}_{cd}) + (\text{mfcn} \times \text{Rate}_{cn} \times R^{+}_{cn})$$

$$S^{-}_{Tot} = (\text{mfcn} \times \text{Rate}_{cn} \times S^{-}_{cn}) + (\text{mfcd} \times \text{Rate}_{cd} \times S^{-}_{cd})$$

$$\text{Optical Yield} = \frac{R^{+}_{Tot} - S^{-}_{Tot}}{R^{+}_{Tot} + S^{-}_{Tot}} \times 100 \qquad (1)$$

where,

mfcn = (1 - mfcd)
Rate_{cd} = Reaction rate from cinchonidine alone
Rate_{cn} = Reaction rate from cinchonine alone
R^{+}_{cd} = % R-(+)-product from cinchonidine
R^{+}_{cn} = %R-(+)-product from cinchonine
R^{+}_{Tot} = Total amount of R-(+)- product
S^{-}_{cd} = % S-(-)-product from cinchonidine
S^{-}_{cn} = %S-(-)-product from cinchonine
S^{-}_{Tot} = Total amount of S-(-)- product

Using the assigned values given in table 4.1, a plot of optical yield versus mfcd as shown in the green squares of figure 4.1 is achieved. Optical yield increases steadily from -50 % to +70 % with increasing mole fraction of cinchonidine. The plot is not linear, but weighted in favour of R-(+)-product formation because the rate of formation of this enantiomer resulting from the presence of cinchonidine proceeds at a faster rate than the formation of S-(-)-product from cinchonine. Although the fit to the experimental points is not excellent, the general trend is supported.

Table 4.1

Values used in mathematical model for cinchonidine and cinchonine

Parameter	Value
$Rate_{cd}$	1755 / mmols h^{-1} g^{-1}
$Rate_{cn}$	1280 / mmols h^{-1} g^{-1}
R^{+}_{cd}	0.85
R^{+}_{cn}	0.25
S^{-}_{cd}	0.15
S^{-}_{cn}	0.75

Table 4.2

Values used in mathematical model for quinine and quinidine

Parameter	Value
$Rate_{qn}$	685 / mmols h^{-1} g^{-1}
$Rate_{qd}$	650 / mmols h^{-1} g^{-1}
R^{+}_{qn}	0.80
R^{+}_{qd}	0.31
S^{-}_{qn}	0.20
S^{-}_{qd}	0.69

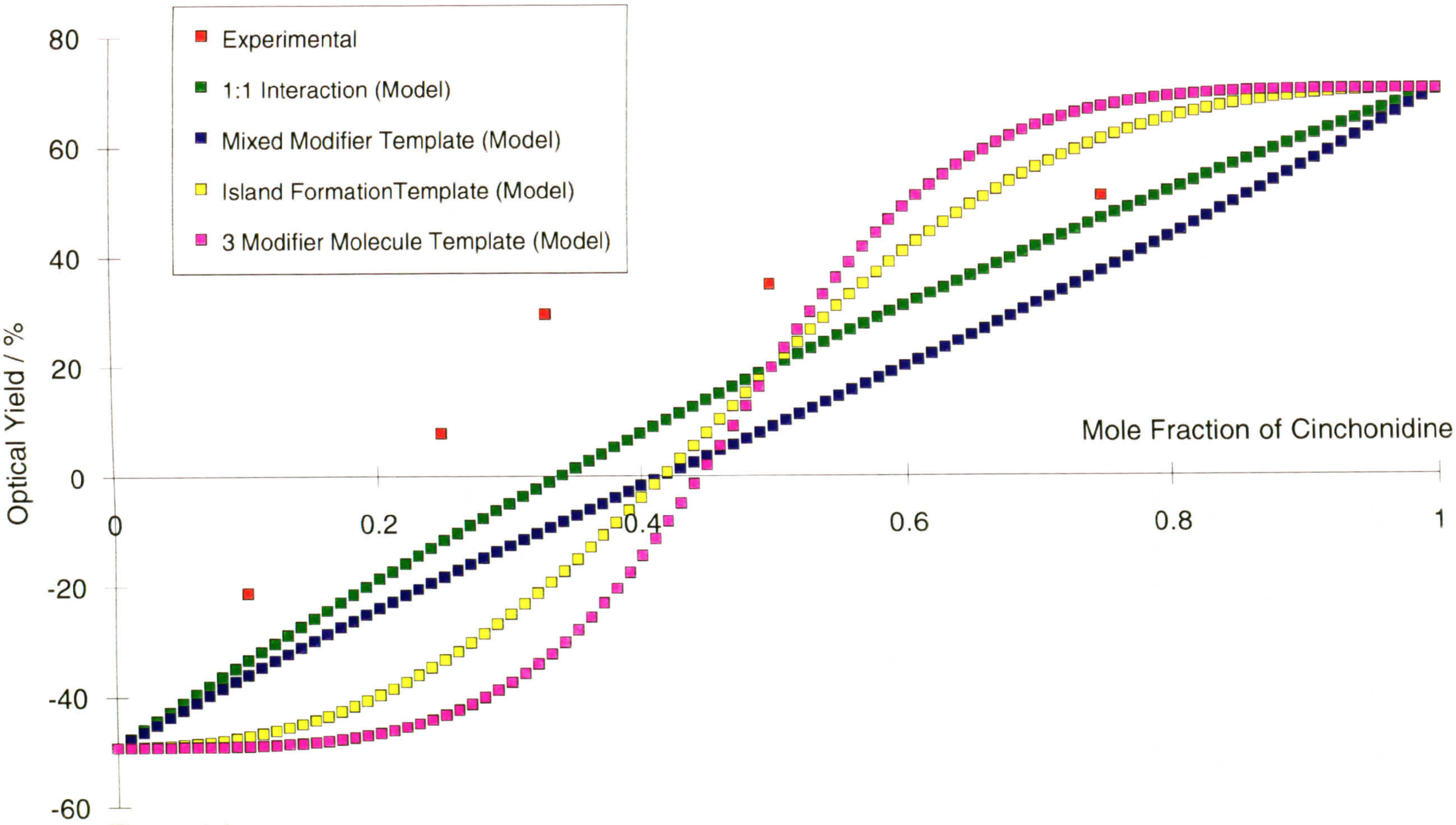

Figure 4.1
Variation of Optical Yield with Mole Fraction of Cinchonidine for Methyl Pyruvate Hydrogenation at 10 bar and 298 K

4.1.2 Template Site Model

If the asymmetric hydrogenation site consisted of two alkaloid molecules, and the racemic reaction can again be disregarded then, under the conditions of mixtures of modifiers being present, one of two situations can be envisaged. If alkaloid molecules adsorb such that the asymmetric hydrogenation site consisted of like molecules alone then, a plot of optical yield (calculated from equation 1) versus mfcd would obey the relationship viz.:

$$\text{Optical Yield} \propto (\text{mfcd}^2 + \text{mfcn}^2)$$

$$R^+_{Tot} = (\text{mfcd}^2 \text{ x } \text{Rate}_{cd} \text{ x } R^+_{cd}) + (\text{mfcn}^2 \text{ x } \text{Rate}_{cn} \text{ x } R^+_{cn})$$

$$S^-_{Tot} = (\text{mfcn}^2 \text{ x } \text{Rate}_{cn} \text{ x } S^-_{cn}) + (\text{mfcd}^2 \text{ x } \text{Rate}_{cd} \text{ x } S^-_{cd})$$

The above model therefore assumes 'island formation' of like alkaloid molecules. The 'S-shaped' plot (yellow squares, figure 4.1) results as enantiomeric excess remains high at low values of mfcd or mfcn as there is insufficient alkaloid present to form sites giving the opposite enantiomer to that produced by the majority of the sites. As the values of mfcd and mfcn approach each other the optical yield falls rapidly. Using the same argument the effect of requiring three alkaloid molecules to form the asymmetric hydrogenation site can be modelled by cubing the values of mfcd and mfcn. This is also shown in figure 4.1 (purple squares) and shows that enantiomeric excesses would remain very high until the values mfcd and mfcn approach each other.

If however the asymmetric hydrogenation site could consist of either molecules, then a plot of optical yield versus mfcd as shown in figure 4.1 can be calculated according to the equations, viz.:

$$\text{Optical Yield} \propto (\text{mfcd}^2 + \text{mfcn}^2) + 2(\text{mfcd x mfcn})$$

$$R^{+}_{Tot} = (mfcd^2 \times Rate_{cd} \times R^{+}_{cd}) + (mfcn^2 \times Rate_{cn} \times R^{+}_{cn}) + (mfcd \times mfcn) \times ((Rate_{cd} \times R^{+}_{cd}) + (Rate_{cn} \times R^{+}_{cn}))$$

$$S^{-}_{Tot} = (mfcn^2 \times Rate_{cn} \times S^{-}_{cn}) + (mfcd^2 \times Rate_{cd} \times S^{-}_{cd}) + (mfcn \times mfcd) \times ((Rate_{cn} \times S^{-}_{cn}) + (Rate_{cd} \times S^{-}_{cd}))$$

the optical yield is then calculated according to equation 1. This is an extension of the model of preferential adsorption of the molecules but also takes into account mixed alkaloid sites which are assumed to give fast and racemic reaction. The result is the blue-squared curve of figure 4.1. The plotted line is nearly linear in nature but has a slight 'S-shape', indicating that the faster racemic sites tend to dominate.

These results, particularly those for the case of modelling the quinidine-quinine mixed modifier system (figure 4.2) support a mechanism based on a 1:1 interaction model as the behaviour expected of the other models is not observed.

4.2 Low concentrations of Modifier

4.2.1 Mathematical Modelling

It was possible to create a mathematical model of the expected variation of optical yield with increasing coverage of alkaloid modifier. Various numbers of alkaloid molecules in the asymmetric hydrogenation site were introduced into the calculation for comparison with the observed results. The models were generated using the method and assumptions outlined below.

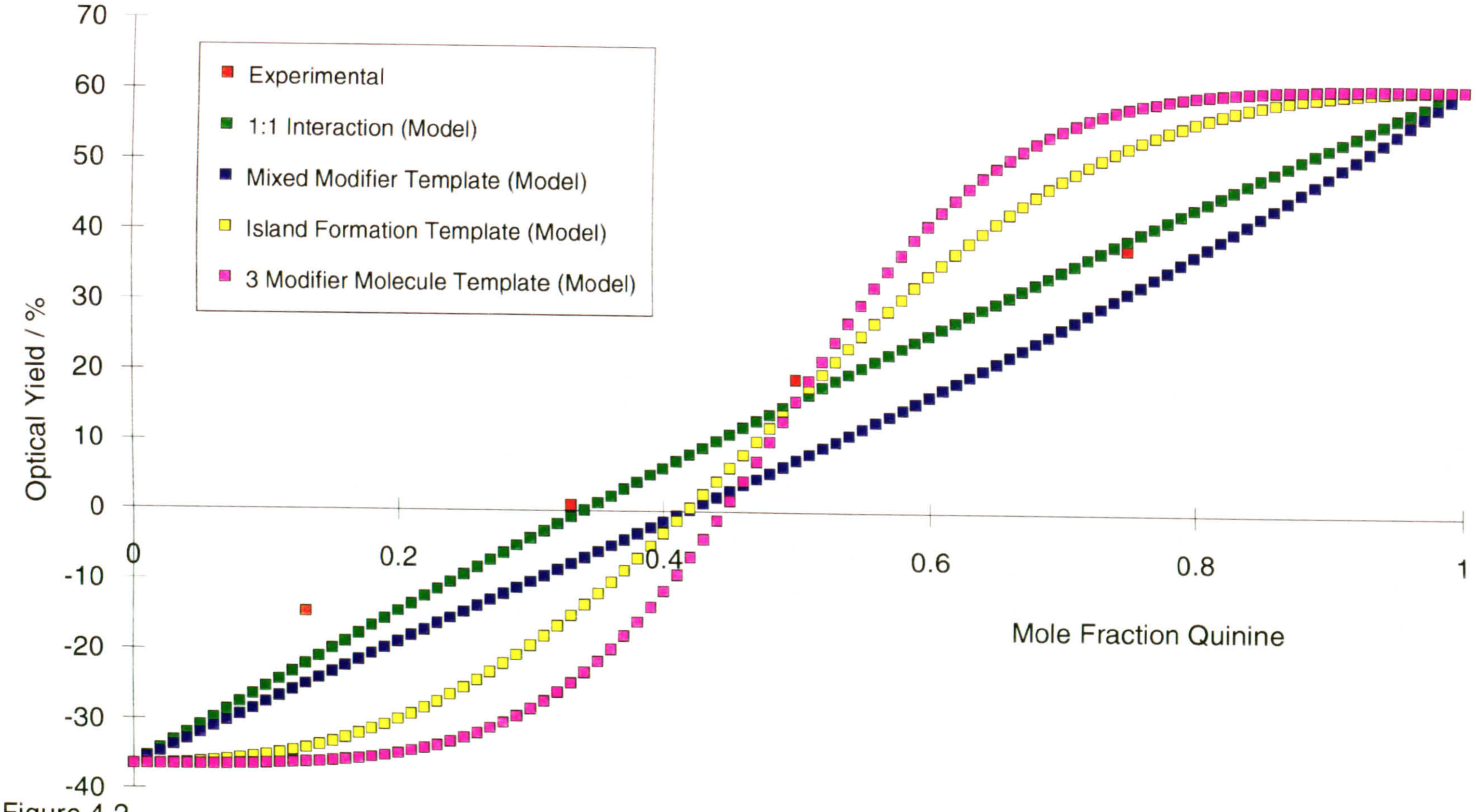

Figure 4.2
Variation of Optical Yield with Mole fraction of Quinine for Methyl Pyruvate Hydrogenation at 10 bar and 298 K

Common to all of the models was the assumption as to the metal surface coverage of alkaloid molecules. Assuming that x is the amount of alkaloid adsorbed on the catalyst, and that x_{max} is the maximum amount that the surface can take up, then

$$x/x_{max} = \theta$$

where θ is the fractional surface alkaloid coverage which is equal to 1 at maximum coverage. The amount of surface not covered in alkaloid is therefore 1-θ. For the purpose of evaluating the model the value at which θ is equal to 1 is a variable and the amount of the Pt surface which can actually be physically modified by the alkaloid does not have to be considered.

Methyl pyruvate is hydrogenated by both an alkaloid covered site and by a non-alkaloid covered site, but at different rates and with different enantioselectivity to product. The contribution of each site to R-(+)- and S-(-)-methyl lactate can be combined in the following equations which assume that there is 1:1 interaction of alkaloid and methyl pyruvate molecule. The values for the rates of reaction and enantiomeric excesses are variables which can be changed as necessary or based on experimental values taken at high concentrations of added modifier. The optical yield for a given coverage can therefore be calculated, viz.:

$$R^{+}_{Tot} = ((1-\theta) \times Rate_{rac} \times R^{+}_{rac}) + (\theta \times Rate_{cd} \times R^{+}_{cd})$$

$$S^{-}_{Tot} = ((1-\theta) \times Rate_{rac} \times S^{-}_{rac}) + (\theta \times Rate_{cd} \times S^{-}_{cd})$$

Where

$Rate_{rac}$ = Racemic Rate of Reaction

R^{+}_{rac} = % R-(+)-product from Racemic Reaction

S^{-}_{rac} = % S-(-)-product from Racemic Reaction

$$\text{Optical Yield} = \frac{R^{+}_{Tot} - S^{-}_{Tot}}{R^{+}_{Tot} + S^{-}_{Tot}} \times 100 \qquad (1)$$

If, however, the asymmetric hydrogenation site consists of a shaped ensemble or template formed by 2 alkaloid molecules the selectivities to R-(+)- and S-(-)- product are calculated by the equations

$$R^{+}_{Tot} = ((1-\theta) \times Rate_{rac} \times R^{+}_{rac}) + (\theta^2 \times Rate_{cd} \times R^{+}_{cd})$$

$$S^{-}_{Tot} = ((1-\theta) \times Rate_{rac} \times S^{-}_{rac}) + (\theta^2 \times Rate_{cd} \times S^{-}_{cd})$$

the optical yield being calculated from equation 1.

Following on in the same manner, an asymmetric hydrogenation site consisting of a template formed by 3 alkaloid molecules can be calculated to give product in amounts defined by the equations, viz.:

$$R^{+}_{Tot} = ((1-\theta) \times Rate_{rac} \times R^{+}_{rac}) + (\theta^3 \times Rate_{cd} \times R^{+}_{cd})$$

$$S^{-}_{Tot} = ((1-\theta) \times Rate_{rac} \times S^{-}_{rac}) + (\theta^3 \times Rate_{cd} \times S^{-}_{cd})$$

with optical yield again being found by equation 1

Figure 4.3 shows the theoretical behaviour for each of these cases with purple, cyan and red squares, respectively. The theoretical curves utilise the variable values in table 4.3. The experimental behaviour accords with the case of a 1:1 interaction of pyruvate with the modifying alkaloid as envisaged in chapter 5. (The model requires a racemic rate of 150 mmols h^{-1} g^{-1}, whereas experimental values recorded were 30 to 50 mmols h^{-1} g^{-1}. As mentioned in section 3.1, the experimentally observed value of initial rate may be lower than is actually the case. The value of θ=1 is taken at the modifier loading of 1 mg as this is where the plateau in optical yield is fully achieved. The remaining values were found experimentally.)

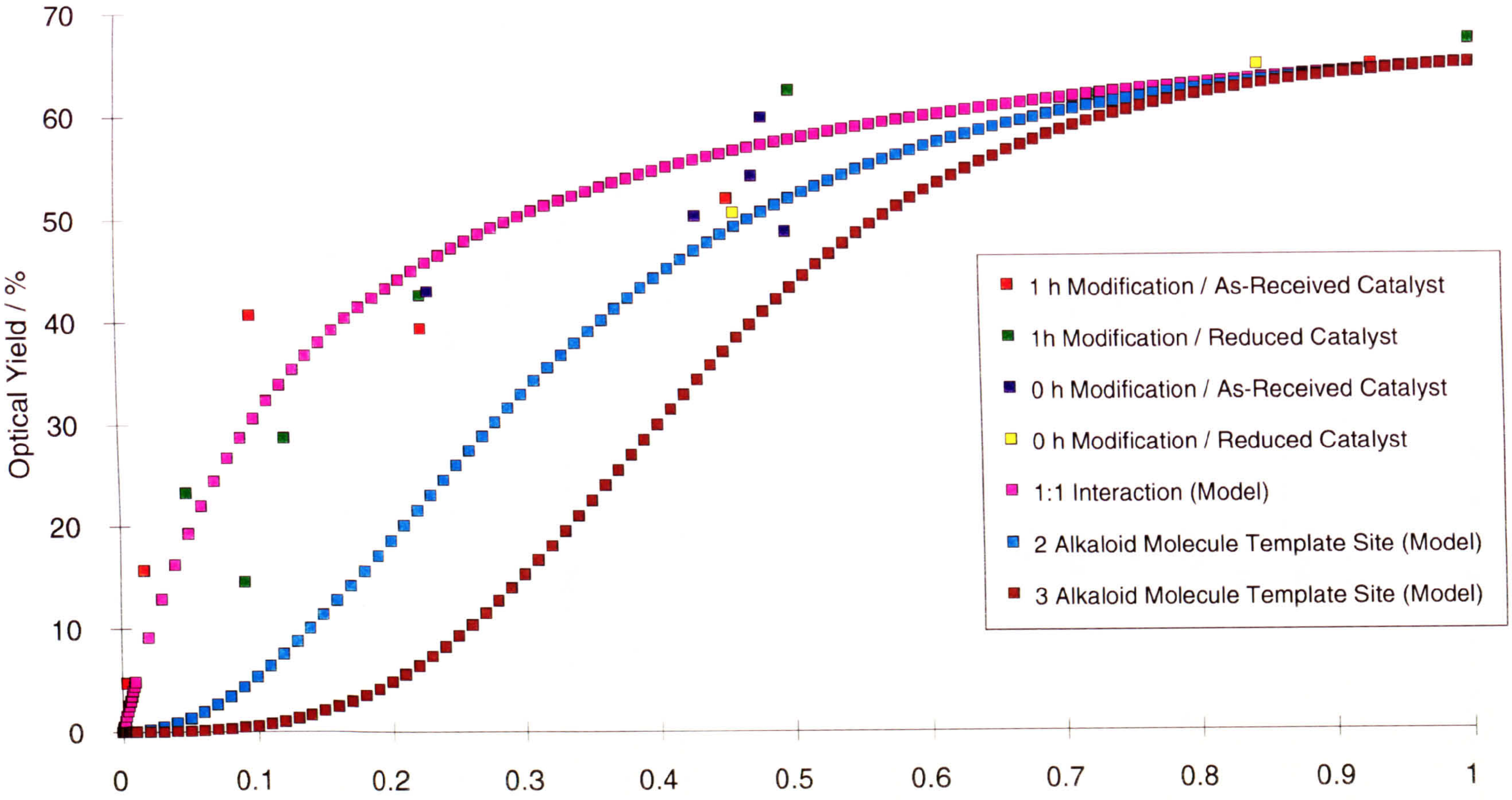

Figure 4.3
Variation of Optical Yield with Modifier loading for Methyl Pyruvate Hydrogenation at 10 bar and 298 K

Table 4.3

Values used in Mathematical Model of Different Hydrogenation Sites at Low Concentration

Parameter	Value
$\theta = 1$	1 / mg
$Rate_{rac}$	150 / mmols h^{-1} g^{-1}
R^{+}_{rac}	0.5
$Rate_{cd}$	1200
R^{+}_{cd}	0.825
S^{-}_{rac}	0.5
S^{-}_{cd}	0.175

4.2.2 Other Models

At this point the work of Blaser *et al.* is worthy of mention. In a series of papers published after the above work was performed,[4,5,6] similar experimental results were observed and a model developed which again explained the mechanism of the reaction in terms of a 1:1 interaction, though no *formal* mechanism was suggested. Based on the mathematical model of Jacobsen *et al.*[7] for the dihydroxylation of alkenes catalysed by the presence of osmium-alkaloid complexes, Blaser *et al.* published a model for the enantioselective hydrogenation of α-ketoesters by cinchona alkaloid modified Pt catalysts.

The first two publications by Blaser *et al.* describe a 'Two-Site Model' of fast enantioselective reactions and slow racemic reactions in an identical manner as independently developed by the author. Where the two models differ is in the manner in which the surface coverage is determined. Blaser *et al.* consider (quite rightly) that an equilibrium exists between the amount of modifier in solution and on the Pt surface. Instead of assuming when maximum surface alkaloid coverage ($\theta = 1$) has been reached

by the plateau in optical yield as in the model above, Blaser *et al.* varied the values for the equilibrium-adsorption constant and θ until a good fit with experimental data was obtained. With the author's method, only the point at which $\theta = 1$ is adjustable and closely related to the experimentally observed plateau of optical yield. Otherwise, the models are mathematically closely related. Indeed, Blaser was able to fit the author's data for toluene[8] to his model and arrive at a good fit for a 1:1 interpretation of the mechanism[9]. Experimentally determining the equilibrium-adsorption constant is very difficult. The results presented in section 3.3.3, where measurement of the degree of adsorption has been attempted, still only afford the answer for adsorption on the metal *and* support. Moreover the degree to which the Pt surface can be physically modified by the cinchonidine is still unknown.

In his latest publication, Blaser *et al.* derived a "Three-Site Model" in order to explain the experimental observation that at higher coverage the reaction rate started to fall. This involved the assumption that two different sites for enantioselective hydrogenation exist, each with a different selectivity and equilibrium-adsorption constant, increasing the number of parameters. The amount of surface modifiable Pt was also brought into the calculation. Although a good fit was obtained to experimental observations, the parameters were varied until a good fit was obtained. The sensitivity of these parameters to slight changes was not given. Although all of the phenomena used in that model are known to exist in catalysis, until some of the unknown parameters can be experimentally checked, having such a complex mathematical model with too many unknown parameters, chosen to fit the model is pure scientific speculation.

One further difference between the models is that Blaser *et al.* state that "it is only the formation of the R-enantiomer that is accelerated by the modifier." However, in the author's model, a good fit to experimental data is obtained above by including a rate enhancement for the S-enantiomer also. As the enantiomeric excess observed for cinchonidine is high, this effect can be hidden by the choice of adjustable parameters in both cases.

4.2.3 GHI Pt/SiO_2

The attempts to render the GHI Pt/SiO_2 catalysts effective for enantioselective hydrogenation by use of low concentrations of modifiers failed as the average particle size was too small to accommodate both the alkaloid and the pyruvate[10]. The low enantioselectivities observed were probably due to alkaloid adsorption on the larger particles of the size distribution. This contrasts with the original conclusion that perhaps the non close-packed-array of alkaloid molecules required for the template model was not achievable due to the high concentrations of modifier used as standard conditions.

This accords with the findings that metal particles at least 2 nm in size are required for high optical yields[11,1]. It would however be interesting to construct a raft-like catalyst (1 nm^2) which could only accommodate one alkaloid molecule and reactant molecule and try to limit the competitive adsorption of modifier, reactant and probably solvent. This would provide further evidence against the size requirements of the template theory.

4.3 Iridium

Supported iridium catalysts were found to be very active for racemic α-keto ester hydrogenation. Modification by cinchona alkaloids rendered the catalyst effective for enantioselective α-keto ester hydrogenation. This result is significant as few experimental difficulties attend the catalysis of this reaction by Pt, provided the metal particle size is not too small[10], but attempts to use other Group VIII metals frequently, indeed normally fail. Blaser and co-workers have reported optical yields of 20-30 % in ethyl pyruvate hydrogenation over modified Rh/Al_2O_3 at 75 bar hydrogen pressure[12], but the study presented in section 3.8 failed to register enantioselectivities greater than 4 %.

The investigation into the Ir-catalysed reaction showed similarities and some differences by comparison with the more extensively studied Pt-catalysed reaction. The

reactions are similar in that modification by adsorption of cinchonidine or quinine onto each metal induces enantioselectivity in favour of R-(+)-methyl lactate, whereas modification by cinchonine or quinidine provides an excess of the S-enantiomer.

4.3.1 Temperature and Adsorption

The study of the effect of temperature on the enantioselective reaction showed an overall similarity to the Pt-catalysed reaction[13] in that activity collapsed above ca. 320 K. However for Ir-catalysed reaction, the enantioselectivity decreased gradually with increasing temperature, or conversely, increased with decreasing temperature. Higher optical yields would be expected to be theoretically achievable at temperatures below that studied. Practical considerations were the limiting factor (i.e. freezing point of liquid mixture, very slow reaction rate, and maintenance of temperature and pressure integrity of reactor).

The interpretation of this subtle difference in the manner in which enantioselectivity is lost over each catalyst is attributed to the effect of temperature on the mode of adsorption and reducibility of the quinoline ring of the alkaloid. Adsorption of the cinchona alkaloids with the aromatic function parallel to the metal surface has been suggested by Wehrli *et al.*[14,15] and Sutherland *et al.*.[1] It is also a necessary pre-requisite for the induction of enantioselectivity as envisaged in the mechanism previously proposed[2], and further developed in this thesis (in chapter 5). Such adsorption geometry also permits the establishment of the H-bonding interaction between the N-atom of the quinuclidine system and the hydroxyl group of the half-hydrogenated state (hhs) proposed to be responsible for the enhanced rate over Pt[3].

Hydrogen-deuterium exchange in the alkaloid modifier may, under favourable conditions, provide information concerning its mode of adsorption. The observed exchange at the 2-, 6- and 8- positions in the quinoline ring system of dihydrocinchonidine establishes that the molecule adsorbs on iridium by interaction of the

aromatic function with the metal surface, and the pattern of exchange suggests that the quinoline ring system may be adsorbed approximately parallel to the surface. Such a conclusion would indicate that the adsorbed state is similar to that on the Pt surface where a comparable experiment by Bond and Wells produced exchange at all 6 positions[16]. The less extensive exchange at the Ir surface may simply imply that the adsorbed alkaloid is less reactive towards adsorbed deuterium, or that the concentration of adsorbed-D derived from $D_{2(g)}$ or C_2H_5OD is lower, or that the alkaloid forms other adsorbed states, perhaps inclined to the surface and adsorbing predominantly through the quinoline nitrogen. Bond and Wells also found that at temperatures above ca. 320 K reduction of the aromatic function of dihydrocinchonidine occurred, resulting in adsorption through the quinoline-N alone. A possible interpretation for the gradual decline in enantioselectivity with increasing temperature over $Ir/CaCO_3$ discussed above could be that there is competition between these two modes of adsorption for the alkaloid, or that the reduction of the aromatic ring is not as sudden over Ir as over Pt.

4.3.2 Reaction Rate and Kinetics

An important difference between the Ir- and Pt-catalysed reaction relates to the relative magnitudes of the racemic and enantioselective reaction rates. Ir catalysts provided rapid racemic reaction under standard reaction conditions (185 mmols h^{-1} g^{-1} over 5 % Ir/Al_2O_3, 260 mmols h^{-1} g^{-1} over 10 % Ir/SiO_2, 605 mmols h^{-1} g^{-1} over 20 % Ir/SiO_2 1270 mmols h^{-1} g^{-1} over $Ir/CaCO_3$-1 and 1680 mmols h^{-1} g^{-1} over $Ir/CaCO_3$-2). These values compare with 50 mmols h^{-1} g^{-1} over EUROPT-1. However, the latter value is the racemic rate measured after several minutes of reaction, not the true initial reaction rate. In section 3.11.2 it was shown that the racemic reaction could be fitted to a Hinshelwood equation for product-inhibited reaction. Although at first glance the racemic rates observed over non-carbonate-supported Ir-catalysts are faster than Pt catalysts by a factor of 3 (normalising for wt. percentage of metal content) it is argued elsewhere in this thesis that in the latter case, initial rates 2-4 times greater may be occurring. Therefore it can be argued that for non-carbonate-supported Ir initial activities

are identical, but that the Pt-catalysed reaction is poisoned more quickly than the Ir-catalysed reaction.

For racemic hydrogenation, the apparent activation energy of 11 kJ mol^{-1} when iridium is supported on calcium carbonate is lower than that of ca. 30 kJ mol^{-1} obtained for silica-supported platinum[13]. However, it should be noted that the latter apparent activation energy was obtained using the 'classical' method for finding initial rates of reaction, making any comparison difficult.

The fast racemic hydrogenation rates obtained over 5% $Ir/CaCO_3$ is attributed to an effect of the basic nature of the support. The racemic rate over Pt was enhanced up to ten fold by the addition of nitrogen containing bases to the reaction mixtures[3] and it is this observation that leads to the proposed interpretation of the enhanced rate. The fast racemic rates over 5% $Ir/CaCO_3$ suggest that the catalyst morphology is such that the OH group of the hhs of Me(C*)(OH)COOMe adsorbed on iridium undergoes a H-bonding interaction with carbonate ions in the support surface leading again to the stabilisation of the hhs and hence to an enhanced rate. A schematic representation of this interaction is given in figure 4.4. This interpretation of rate enhancement rests on the assumption that the rate determining step in the reaction is the removal of the hhs states from the surface by adsorbed hydrogen atoms and that the surface concentration of hhs is low. Any process such as that shown in figure 4.4 which stabilises a hhs sufficiently to increase its instantaneous concentration serves thereby to enhance the overall reaction rate.

Following the modification procedure in which the reduced catalyst is stirred in a solution of alkaloid (17 mM) in appropriate solvent (ethanol), the catalyst is capable of enantioselective hydrogenation. Adsorption of alkaloid onto silica- or alumina-supported Ir catalysts induces enantioselectivity and also enhances the reaction rate by a factor of 2-3. This is comparable in value to the rate enhancement observed in a more extensive study performed in this laboratory for silica supported catalysts[17]. This rate enhancement

upon addition of alkaloid to Ir/SiO_2 and Ir/Al_2O_3 is similar to, though less pronounced than, that observed over Pt/SiO_2 catalysts, for which a typically 30-fold rate enhancement is observed (taking the "classical" view for rate enhancement)[1]. The rates of enantioselective reactions over silica or alumina-supported Ir catalyst are less (taken on wt% metal terms) than that observed for Pt. The enantiomeric excesses recorded over Ir (up to 39 %) are poorer than those over Pt (up to 90 %) because of rapid racemic reaction that occurred over those areas of the active metal surface not effectively modified by the catalyst.

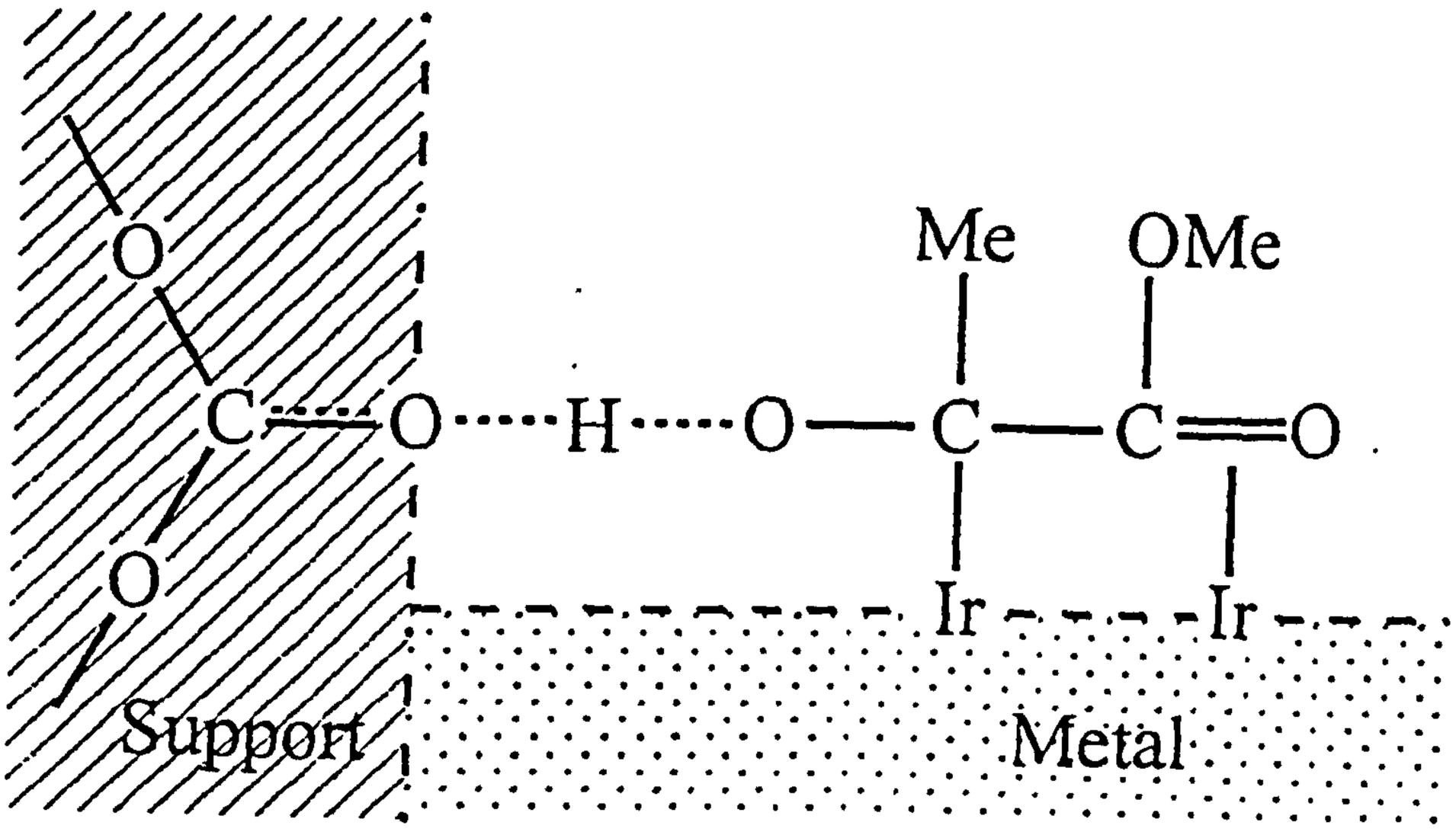

Figure 4.4

A representation of the proposed interaction of the half-hydrogenated state of methyl pyruvate with carbonate ion of the support in $Ir/CaCO_3$

Chiral hydrogenations over both Pt and Ir is zero order in ester and first order in hydrogen (for the ranges studied), with similar forms of the hydrogen uptake against time curves and optical yields are almost independent of conversion. The apparent activation energy for chiral hydrogenation over $Ir/CaCO_3$ (22 kJ mol^{-1}) is lower than that over Pt/SiO_2 (42 kJ mol^{-1})[13]. Only limited efforts were made to optimise the Ir system by variation of metal particle morphology and calcination and reduction temperatures (much variation of the temperature in the case of $Ir/CaCO_3$, the best system found, would have proved impossible due to the thermal instability of the support at high temperatures); no attempt was made to optimise the modifier or reactant concentrations, reactor pressure or the condition of the catalyst by desorption of adsorbed hydrogen before modification, all of which were found to improve the performance of the Pt catalysts[1].

The slower rates of enantioselective reaction over quinine- and quinidine-modified $Ir/CaCO_3$, by comparison with those observed over cinchonidine- and cinchonine-modified catalysts respectively, accords with experience over Pt (see section 3.2) and is attributable at least in part to the smaller numbers of quinine and quinidine molecules that can be accommodated per unit area of surface, and hence to the smaller numbers of enantioselective sites that are thereby created.

4.3.3 Morphological Effects

The poor enantioselectivity obtained upon unsintered 5% Ir/Al_2O_3 indicates that very small Ir particles accommodate alkaloid, methyl pyruvate and hydrogen less efficiently; this accords with the experiments performed using a 0.6 % Pt/SiO_2 catalysts having a majority of the active phase present largely as clusters typically 0.7 nm which also showed very little activity for enantioselective hydrogenation, presumably because the Pt particles were too small to provide for the adjacent adsorption of both alkaloid and methyl pyruvate[10]. Sintering Ir/Al_2O_3 at 1223 K served to increase the Ir particle size sufficiently, such that improved enantioselectivities were observed. Burkhardt and Schmidt sintered Ir/SiO_2 in hydrogen at 1073 K for 4 h; TEM micrographs obtained

demonstrated that the resultant metal particles had smooth faceted surfaces[18] which would be suitable for the adsorption of alkaloid and pyruvate, as presented in chapter 5.

4.4.4 Effect of Solvent

Fastest rates were observed in ethanol as solvent, with poorer rates in dodecanol and toluene. Very poor conversion of methyl pyruvate and low optical yields were obtained when dichloromethane was used as solvent, unlike that observed using silica-supported Pt[19]. The highest optical yields observed to date were obtained by Blaser using acetic acid as solvent[20]. This solvent is missing from the list of those tried with $Ir/CaCO_3$ as it would be expected to react with the basic carbonate support. Adsorption of alkaloid onto the metal particles leads to a decrease in metal surface area available for hydrogenation, consequently a decrease in racemic rate is expected following modification. However, as the enantioselective rate is enhanced due to the presence of alkaloid, the overall rate depends on the relative magnitudes of racemic and enantioselective components and the observed rate may, depending on the circumstances, be faster or slower than the racemic hydrogenation rate.

4.4.5 Effect of Chlorine

The possibility has been considered that the observed rates and enantioselectivities were affected by the presence of chloride ion remaining in the Ir/SiO_2 and $Ir/CaCO_3$ catalysts from their preparation. (The EUROPT-1 catalyst cited above as comparator was virtually Cl-free). A study performed in this laboratory, using four chloride-free silica-supported catalysts showed lower enantioselectivities and than the chloride containing equivalents[17]. Improved optical yields were obtained for $Ir/CaCO_3$-2 which contains significantly more chloride. Clearly, the presence of chloride ions in these iridium catalysts promotes enantioselectivity.

4.4 Role of Oxygen

The original recommendation of Orito and co-workers was to stir the catalyst in a modifier solution, in air for 20 h[21], the practice in this laboratory was to reduce that time to 1 h which provided similar enantioselectivity, but a slightly reduced rate. When the conditions of low concentrations of modifier were applied, it was found that the aerobic modification was not required and that the same results for reaction rate and enantioselectivity could be obtained, irrespective of whether the catalyst had been stirred in air or not, prior to reaction. When an attempt was made at anaerobic modification at low concentrations the effect was to reduce the reaction rate, but the optical yield remained at the same level as for aerobic conditions.

Clearly at conditions of low modifier concentrations enough air (or more probably oxygen) is present dissolved in solvent and reactant to be effective. Recent findings in this laboratory have shown that if this dissolved air can be completely removed by successive freeze/thaw cycles reaction rate and enantioselectivity can be almost reduced to almost negligible values[22].

As noted earlier in this Discussion, Blaser and co-workers have proposed a 'Three-Site Model' to explain their experimental observations when using low concentrations of modifier[6]. On the first site racemic hydrogenation occurs, these sites are reduced with increasing quantities of modifier added to the reaction mixture and enantioselective hydrogenation occurs reaching a plateau in enantiomeric excess. Increasing the amount of modifier further has no effect on the enantiomeric excess, but serves to decrease the reaction rate. This has been fitted to a Three-Site mathematical model in which a third site begins to predominate at higher values of modifier loading with different properties of rate enhancement which explains a decrease in the reaction rate. It is proposed by the author that at higher values of modifier loading the oxygen:modifier ratio is decreasing such that the reaction rate is decreased. This conclusion can be drawn from the experimental finding presented in section 3.3.4.

Though no explanation as to the exact role of oxygen is given in this thesis, a paper based on more recent work that will shed light on this issue is in preparation[23].

4.5 Other Modifiers

Attempts to diversify the reaction by using alternatives to the cinchona alkaloids as modifiers met with only limited success. These cinchona alkaloids are effective because (i) they contain a moiety that provides for strong adsorption (the quinoline ring) which is not sterically hindered by any other functional group (the hydroxyl group of the alkaloids can easily rotate away from the surface upon adsorption as shown in figure 5.10) (ii) the conformation has a crucial energetic relationship with that of the reactant (see chapter 5), (iii) the enantioselective reaction exhibits an enhanced rate (due to the action of the quinuclidine-N) and (iv) rotational flexibility in the modifier permits the 1:1 interaction to be achieved to maximum effect.

The best alternative found was for the cinchona alkaloid derivative, 10,11-dihydroquinine 4-methyl-2-quinoyl ether which gave an optical yield of 22 %. The 10,11-dihydroquinine phenanthryl ether also produced product with a slight enantiomeric excess in favour of the R-(+)-enantiomer and the dihydroquinidine analogues gave negligible enantiomeric excesses in favour of the S-(-)-enantiomer. The ability to direct the enantioselectivity in each direction is important as it confirms that the observations are genuine, and not a result of contamination.

Quite why the optical yield achieved with 10,11-dihydroquinine 4-methyl-2-quinoyl ether was as high as 22 % is not clear; generally low values for enantiomeric excess indicate that the modifier does not have all the properties outlined above.

The ability of tryptophan and histidine to exhibit slight enantio-differentiating properties is encouraging as there are many amino acids available, some of which may have some of the crucial properties found in the alkaloids.

The lack of enantioselectivity observed for the ephedrines and benzyl pyrrolidine methanol indicates how crucial it is in this work to use absolutely clean apparatus. Although these alkaloids have been reported to give modest enantio-differentiation in the products, the lack of reproducibility suggests that this was a result of contamination.

4.6 Benzil

The lack of any enantiomeric excess observed when benzil was successfully hydrogenated to benzoin over cinchonidine-modified EUROPT-1 was disappointing considering the fact that it was later discovered that a variety of other diketones could be hydrogenated with moderate degrees of optical yield.[24] However, unlike the 2,3-butadione used in that study which has a dihedral angle between the two carbonyl groups of 180° (at 261 K)[25], the crystal structure of benzil[26] contains a dihedral angle of 107° between these groups which means that planar adsorption of the molecule, as envisaged to occur for pyruvate, is sterically hindered. Another possibility is that the method of hot filtration, used to recover the product from the catalyst may have racemised any chiral product.

---

[1]I.M. Sutherland, A. Ibbotson, R.B. Moyes and P.B. Wells, J. Catal. 125 (1990) 77.

[2]G. Webb and P.B. Wells, Catal. Today 12 (1992) 319.

[3]G. Bond, P.A. Meheux, A. Ibbotson and P.B. Wells, Catal.Today, 10 (1991) 371.

[4]M. Garland and H.U. Blaser, J. Am. Chem. Soc. 112 (1990) 7048.

[5]M. Garland, H.P. Jalett and H.U. Blaser, Prepr. Pap. Am. Chem. Soc. Div. Fuel. Chem. 37 (1992) 320.

[6]H.U. Blaser, M. Garland and H.P. Jalett, J. Catal., 144 (1994) 569.

[7]E.N. Jacobsen, I. Marko, W.S. Mungall, G. Schröder and K.B. Sharpless, J. Am. Chem. Soc. 110 (1988) 1968.

[8]G. Bond, K.E. Simons, A. Ibbotson, P.B. Wells and D.A. Whan, Catal. Today, 12 (1992) 421.

[9]H.U. Blaser, personal communication.

[10]S.D. Jackson, M.B.T. Keegan, G.D. McLellan, P.A. Meheux, R.B. Moyes, G. Webb, P.B. Wells, R. Whyman and J. Willis, "Prepαration of Catalysts V", G. Poncelet et al, eds, Elsevier, Amsterdam, 1991, p. 135.

[11]J.T. Wehrli, A. Baiker, D.M. Monti and H.U. Blaser, J. Mol. Catal., 61 (1990) 207.

[12]H.U. Blaser, H.P. Jalett, D.M. Monti, J.F. Reber, and J.T. Wehrli, Stud. Surf. Sci Catal., 41 (1988) 153.

[13]P.A. Meheux, A. Ibbotson and P.B. Wells, J. Catal., 128 (1991) 387.

[14]J. Wehrli, Ph.D. Thesis No.8833, (1989) ETH, Zürich

[15]J.T. Wehrli, A. Baiker, D.M. Monti, H.U. Blaser and H.P. Jalett, J. Mol. Catal. 57 (1989) 245.

[16]G. Bond and P.B. Wells unpublished results.

[17]K.E. Simons, A. Ibbotson, P. Johnston, H. Plum and P.B. Wells, submitted for publication.

[18]J. Burkhardt and L.D. Schmidt J. Catal., 116 (1989) 240.

[19]W.A.H. Vermeer and P.B. Wells, unpublished results.

[20]H.U. Blaser, H.P. Jalett and J. Wiehl, J. Mol. Catal., 68 (1991) 215.

[21]Y.Orito, S. Imai and S. Niwa, Nippon Kagaku Kaishi 1979 8.

[22]K.E. Simons, P.A. Meheux, S.P.Griffiths, I.M. Sutherland, P. Johnston, P.B. Wells, A.F. Carley, M.K. Raujumon, M.W. Roberts and A. Ibbotson, accepted for publication.

[23]B. Minder, T. Mallat and A. Baiker, manuscript in preparation.

[24]W.A.H. Vermeer, A. Fulford, P. Johnston and P.B. Wells, J. Chem. Soc., Chem. Commun., 1053 (1993).

[25]K. Eriks, T.D. Hayden, S. Hsi, Yang and I.Y. Chan, J. Am. Chem. Soc., 105 (1983) 3940.

[26]C.J. Brown and R. Sadanga, Acta. Crystallogr., 18 (1965) 158.

PAGE NUMBERING AS ORIGINAL

Chapter 5

Molecular Modelling

5.1 Molecular Modelling and Reaction Mechanism

Although molecular modelling studies were performed using a variety of packages, only the results of the extensive work performed using HyperChemII are presented. The studies performed using CHEM-X allowed the same conclusions to be drawn, and are therefore not formally presented.

All energy values are quoted in kcal mol^{-1}, as opposed to kJ mol^{-1} as this is the convention in computational chemistry. Although the values could have been converted to kJ mol^{-1} by multiplication by 4.1868, comparison with any other published results could lead to confusion.

5.1.1 Methyl Pyruvate

The molecule methyl pyruvate was constructed and optimised using both molecular dynamics and molecular mechanics to give the minimum energy conformation shown in figure 5.1a. The molecule is planar and orientated in an anti-conformation. The plot of potential energy versus torsion angle for rotation about the central carbon-carbon bond, C_1C_2 in methyl pyruvate is depicted in figure 5.2. An energy barrier of ca. 5 kcal mol^{-1} exists against a rotation from the anti- to the syn-conformation, although there is a shallow energy minimum for the latter orientation (see figure 5.1b).

Planar adsorption of the methyl pyruvate molecule can therefore occur in one of two orientations, each presenting a different enantio-face to the platinum surface: with the carbonyl groups *top-left bottom-right* relative to the central carbon-carbon bond; and *bottom-left top right* relative to this central bond. Assuming that the hydrogen addition is from the platinum surface, adsorption of the molecule in the former case would achieve R-(+)-product and in the latter case S-(-)-product. Unhidered adsorption of the molecule results in racemic product, upon hydrogenation.

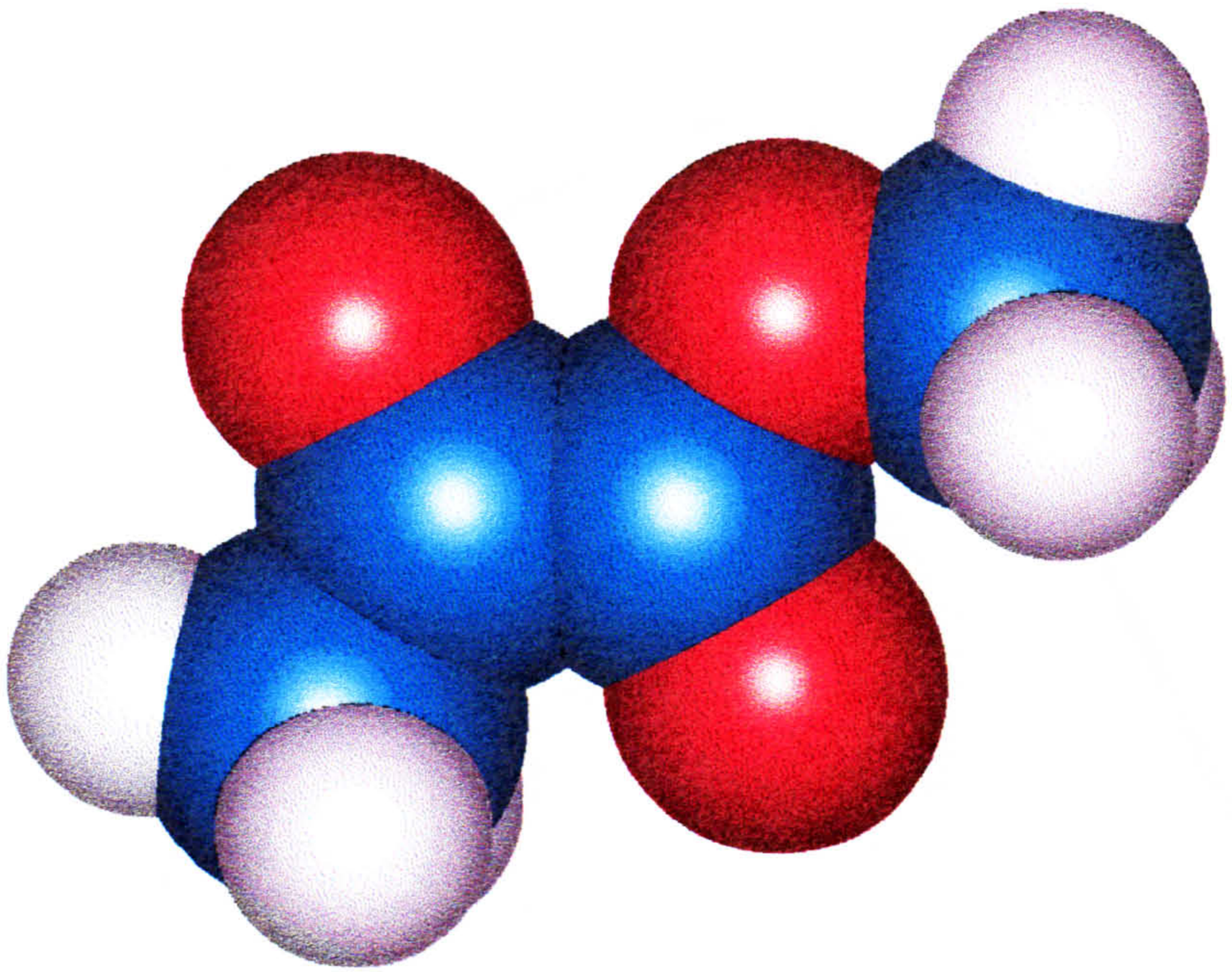

Figure 5.1a
Methyl Pyruvate in Anti-Conformation

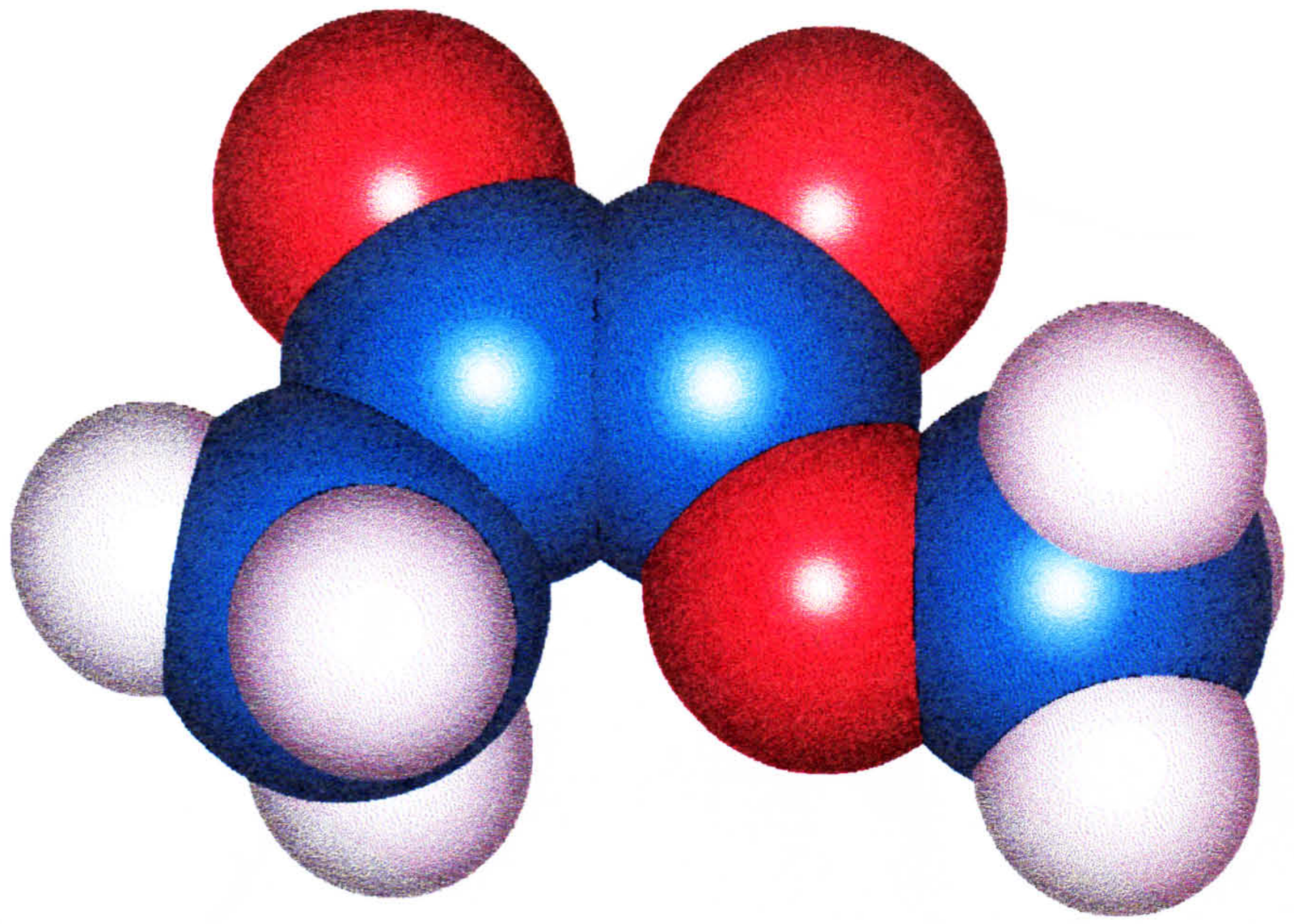

Figure 5.1b
Methyl Pyruvate in Syn-Conformation

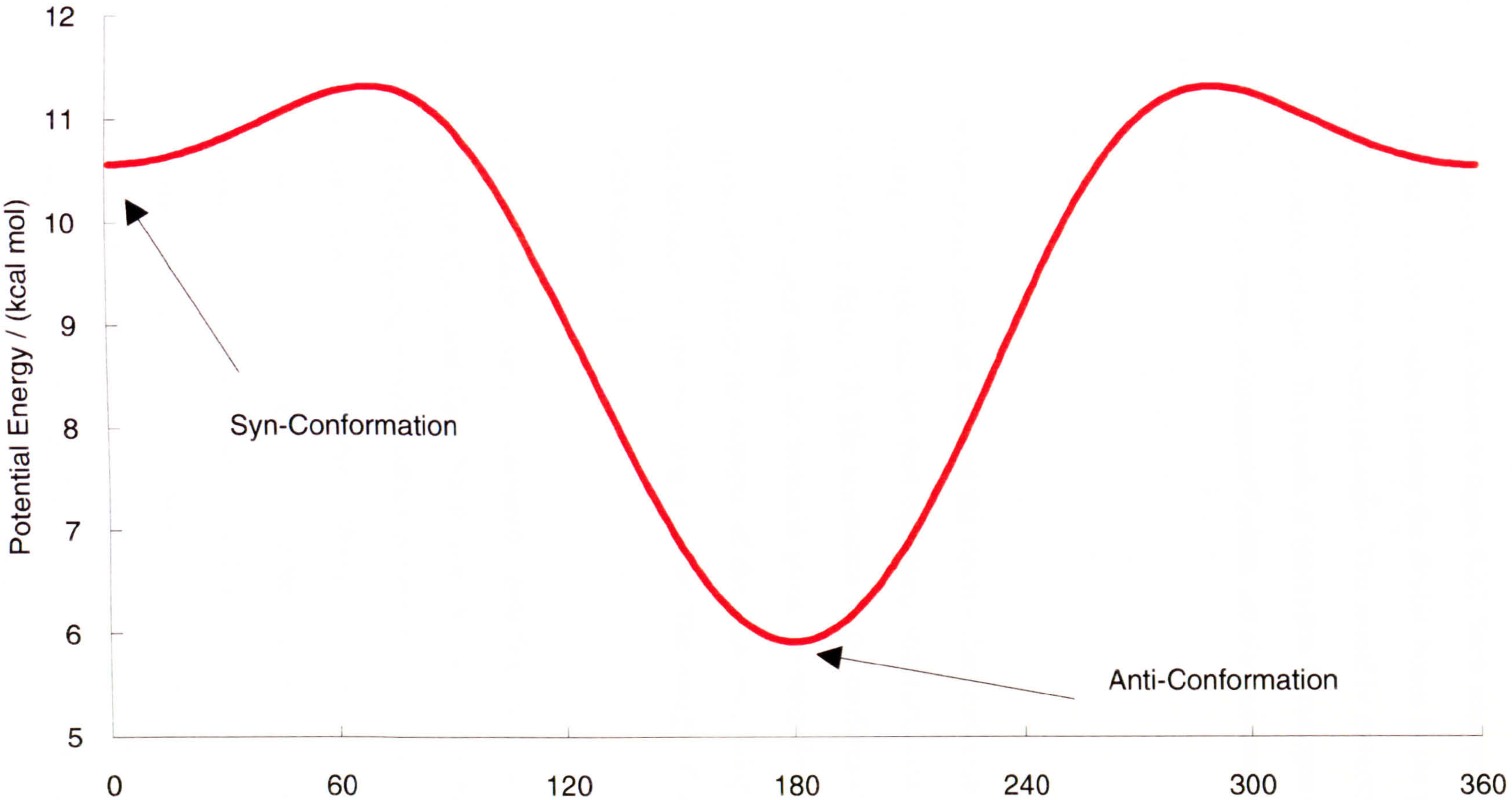

Figure 5.2
Effect on Potential Energy of Rotation about Central C-C Bond of Methyl Pyruvate

The pyruvate molecule can be manually positioned with the carbonyl groups over two adjacent platinum atoms as shown in figure 5.24. Such adsorption would have the regions of greatest electron density, namely the double bonds in the pyruvate and the centres of the Pt atoms in the closest proximity. This would be expected to be the most energetically favourable situation. This mode of adsorption is analogous to that reported for alka-1,3-dienes in a trans-conformation[1,2],which are also assumed to adsorb via the unsaturated bonds.

5.1.2 Cinchonidine

A conformational analysis study of the cinchonidine molecule was undertaken. After constructing the molecule, the first optimised structure, *conformation A* was achieved and is shown in figure 5.3. The orientation of the conformation was such that the molecule was 'L-shaped' with the hydroxyl group pointing down, away from the quinoline and quinuclidine rings, the nitrogen of the latter ring being orientated in the opening formed between the the two ring systems. The energy of the molecule was calculated to be 28.9 kcal mol^{-1}.

Molecular mechanics energy calculations resulting from full rotation of the molecule around the $C_{4'}C_9$ and C_9C_8 bonds (i.e. the torsion angles of the atoms $C_{3'}C_{4'}C_9C_8$ and $C_7C_8C_9C_{4'}$ respectively, using the numbering as in figure 2.1) in 1° steps are shown in figures 5.4 and 5.5 respectively. This can be considered to be the effect of rotating about the bond to the quinoline ring, but keeping the quinuclidine ring fixed in space for the former case and vice-versa in the latter case. Three energy minima are observed for the rotation about the former bond in *conformation A*, at torsion angle 97° (28.9 kcal mol^{-1}), 178° (162.5 kcal mol^{-1}) and 275° (34.7 kcal mol^{-1}). The first of these energy minima occurs for the starting conformation, the second of these is too high in energy to be viable, but the third is a possible conformation which also has the molecule 'L-shaped', but in the opposite sense to *conformation A*. The effect of rotation about the bond to the quinuclidine ring is four energy minima at 6° (35.2 kcal mol^{-1}), 97° (56.1 kcal

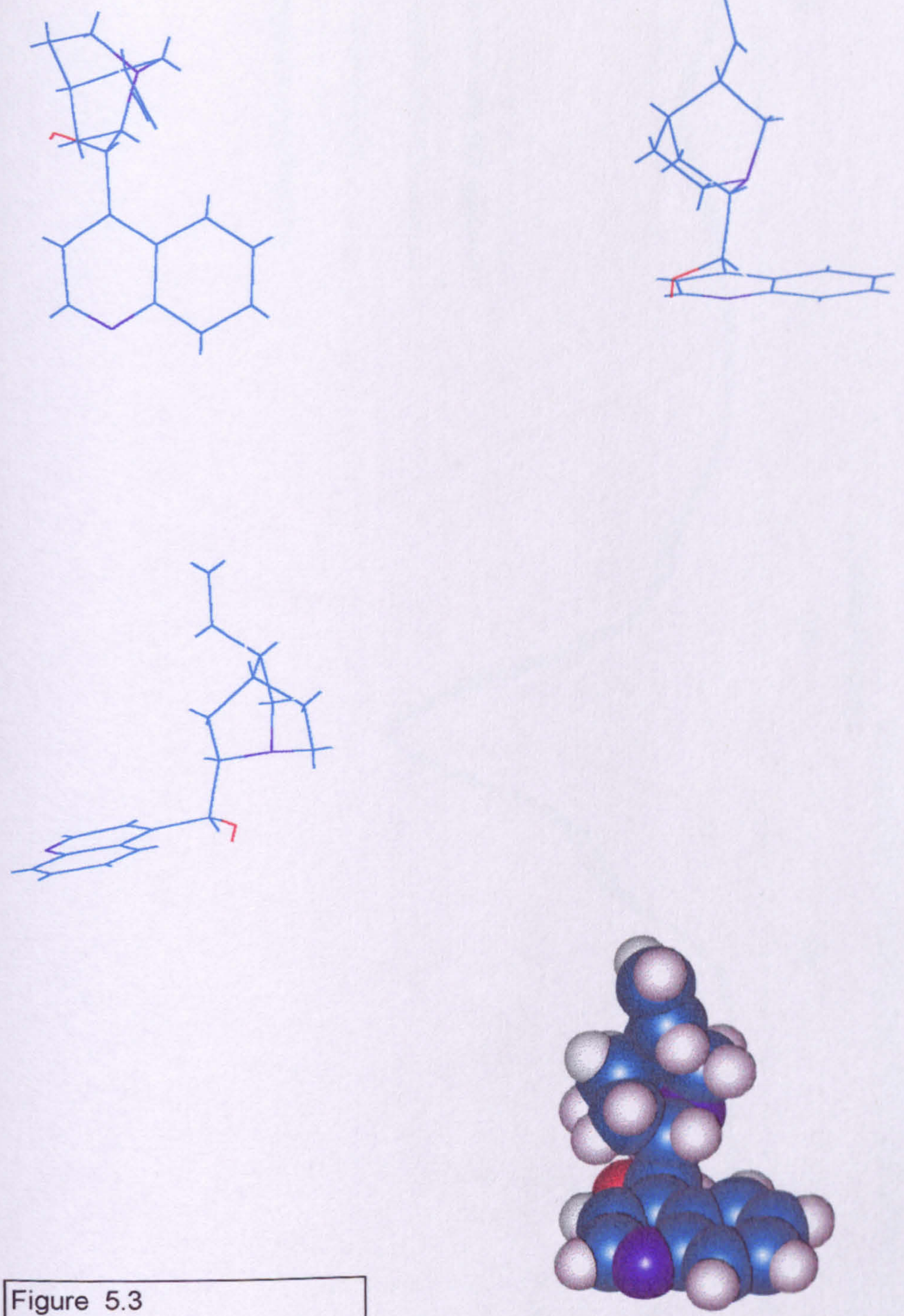

Figure 5.3
Conformation A
for Cinchonidine

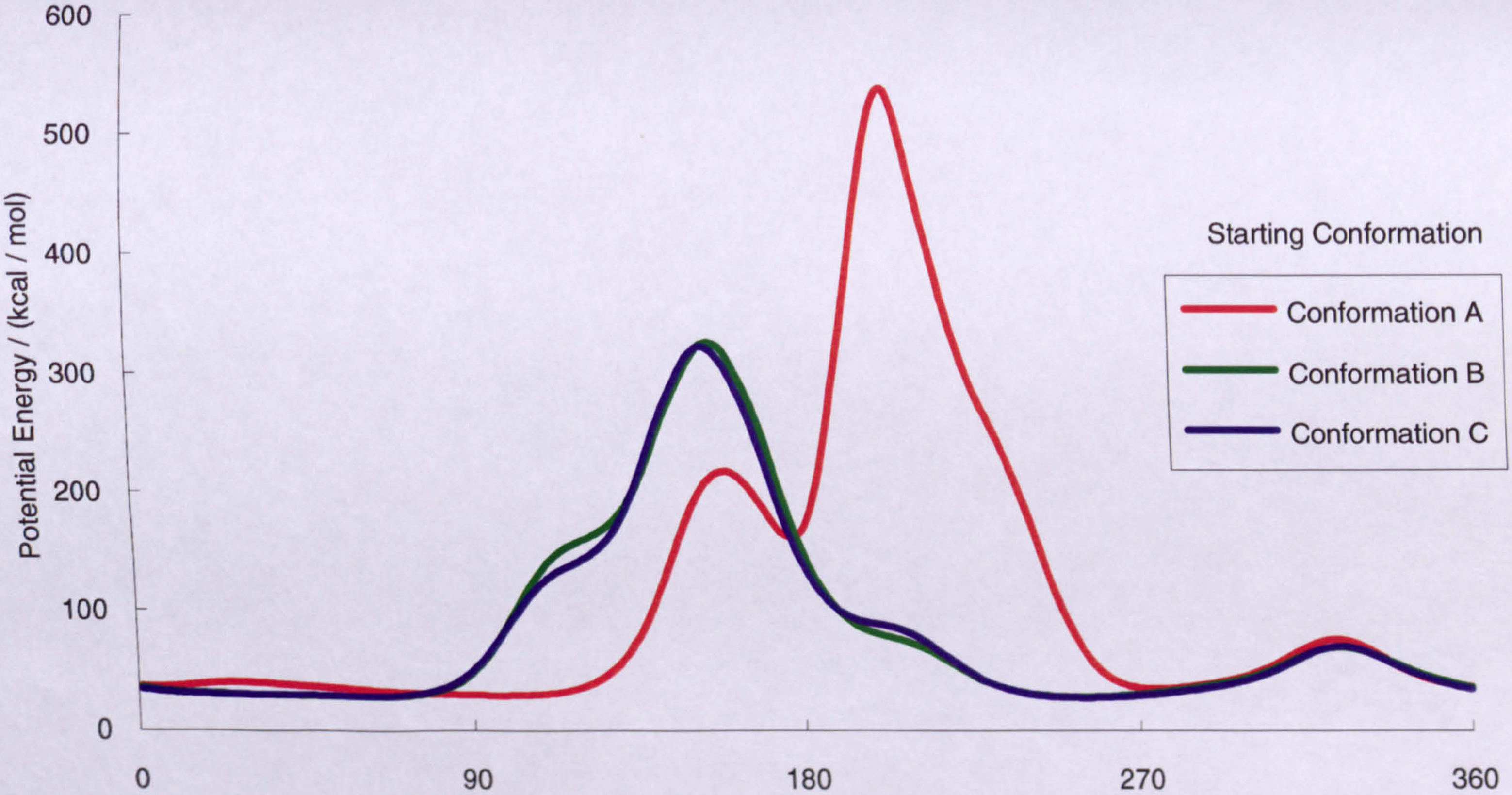

Figure 5.4
Variation of Potential Energy with Rotation of Bond C4'C9

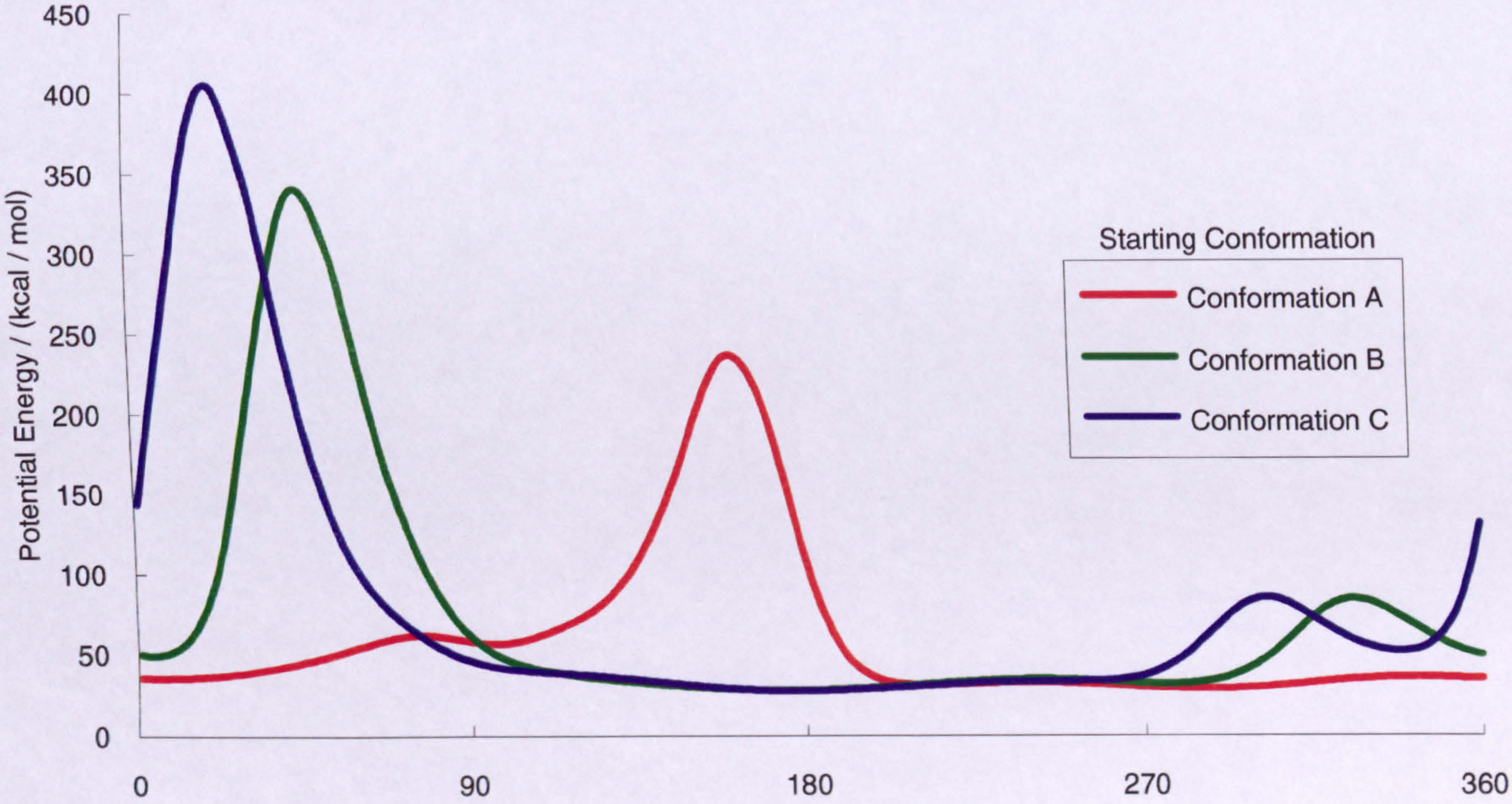

Figure 5.5
Variation of Potential Energy with Rotation of Bond C9C8

mol^{-1}), 211° (31.0 kcal mol^{-1}) and 286° (28.9 kcal mol^{-1}). Of these conformations the first two are slightly too high in energy to be viable, unlike the third which has the nitrogen of the quinuclidine ring positioned over the quinoline ring system. The latter is the starting, lowest energy conformation.

Both of these potential energy plots for *conformation A* have regions of similar energies for large changes in torsion angle. This causes problems for minimisation algorithms, explaining why past attempts to model the alkaloid molecule have only achieved inconclusive minimum energy conformations. When the above plots are compared to those obtained by Sutherland[3] who used CHEM-MOD it is observed that although the minimum energy conformations are at co-incident values of torsion angle, the gradient to those minima are much less steep. This implies that either the starting structure Sutherland used for his calculations was not fully optimised or that the default paramaters were different. The most probable explanation being that the values for van der Waals radii were much greater and that a slightly different starting conformation was used in the calculations.

Figure 5.6 is an energy contour map showing the effect of rotation about both of the aforementioned bonds with respect to each other through 360° in 5° steps, the remainder of the molecule being fixed in the optimised geometry found for *conformation A*. (It should be noted that for ease of interpretation, values of potential energy above 101 kcal mol^{-1} are not displayed). From the plot it can be seen that there are three minimum energy conformations, all with a very similar energy. Starting from these approximate minimum energy conformations, optimisation of the cinchonidine molecule by molecular mechanics calculations resulted in the two further minimum energy conformations *B* and *C* depicted in figures 5.7 and 5.8 respectively. The energies of these molecules being 27.8 and 27.5 kcal mol^{-1} respectively. *Conformation C* was also found to be the global minimum energy conformation by a molecular dynamics calculation using the method of simulated annealing at 400 K, before cooling to 0 K.

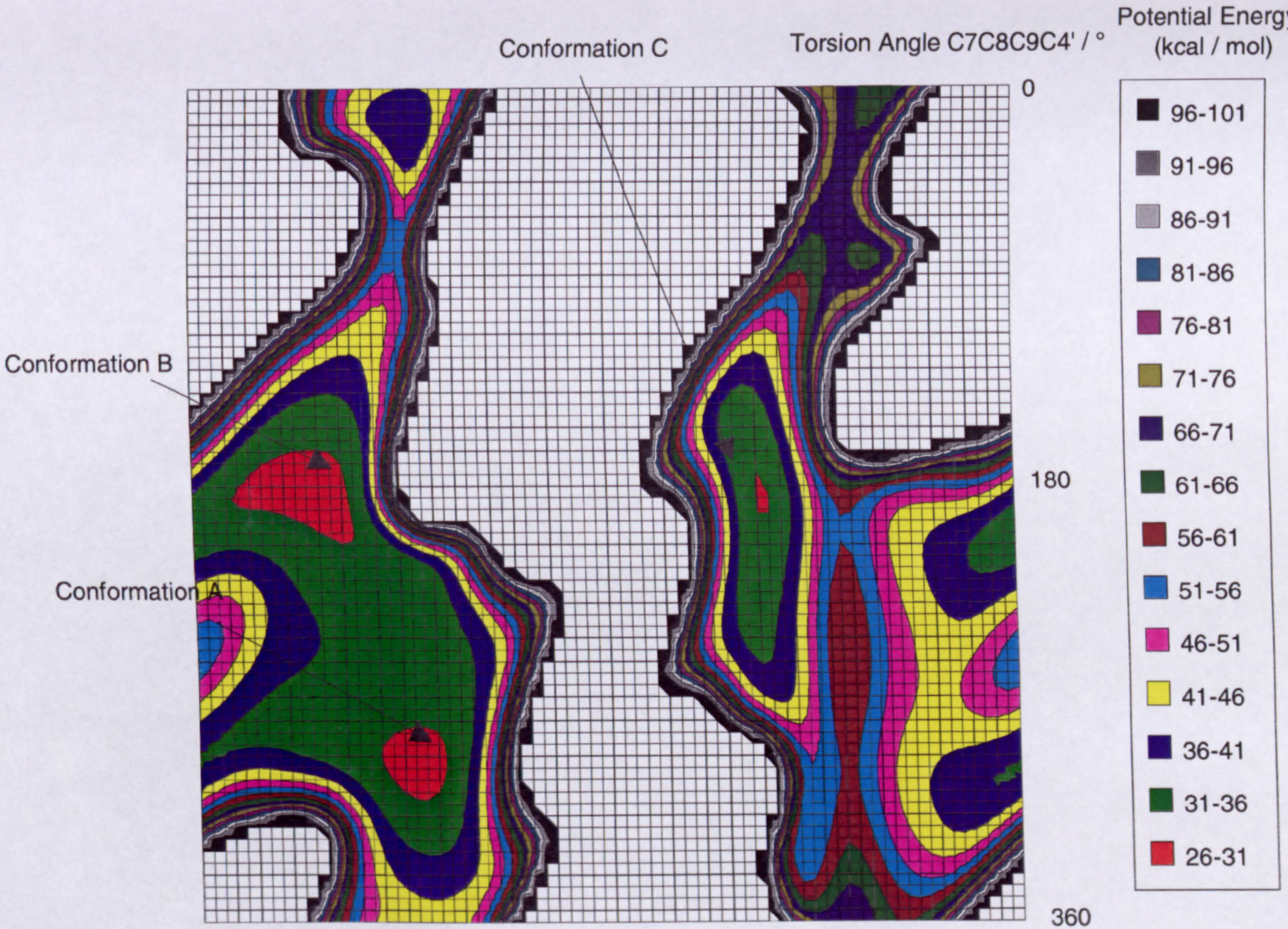

Figure 5.6
Effect on Potential Energy of Rotation around Bonds C4'C9 and C8C9

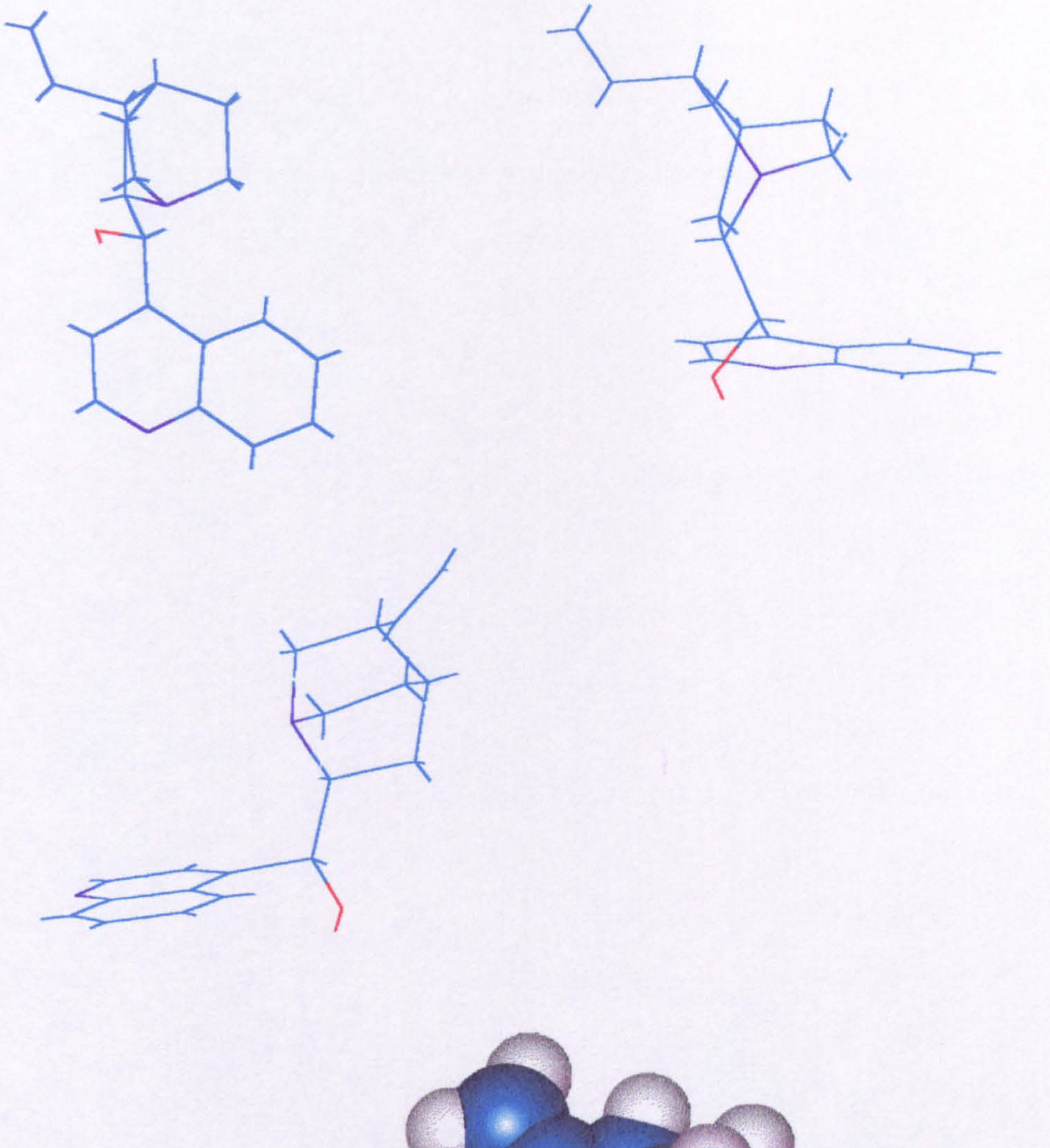

Figure 5.7
Conformation B
for Cinchonidine

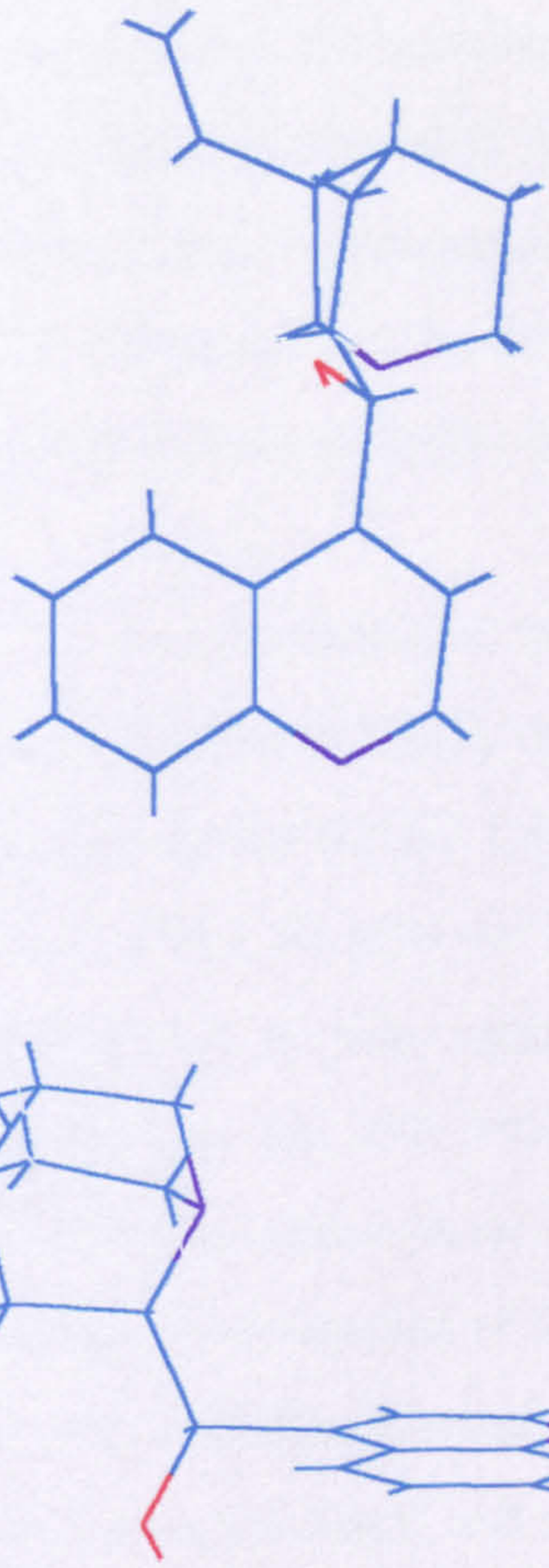

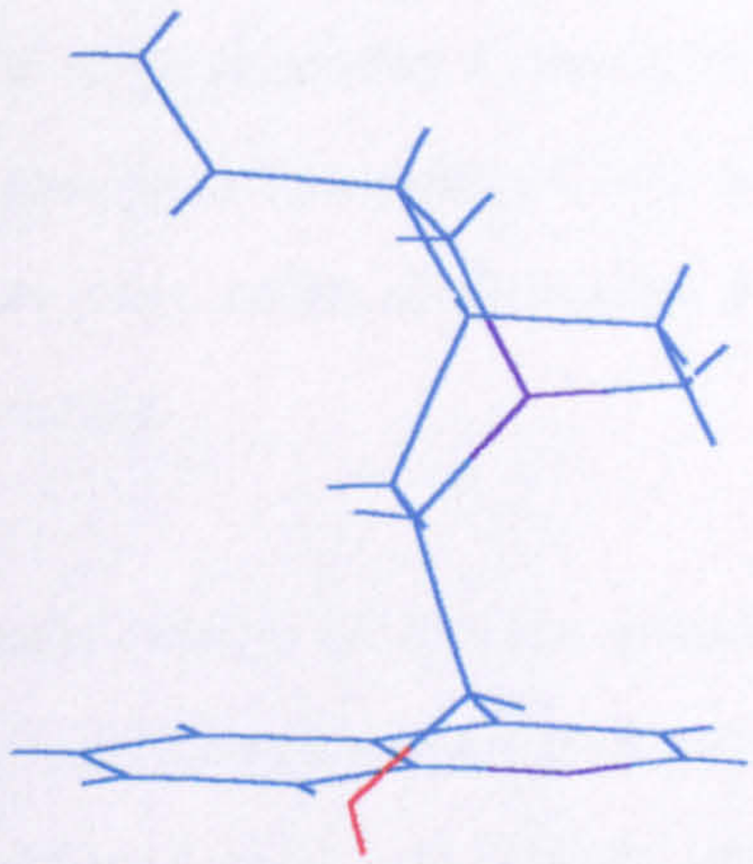

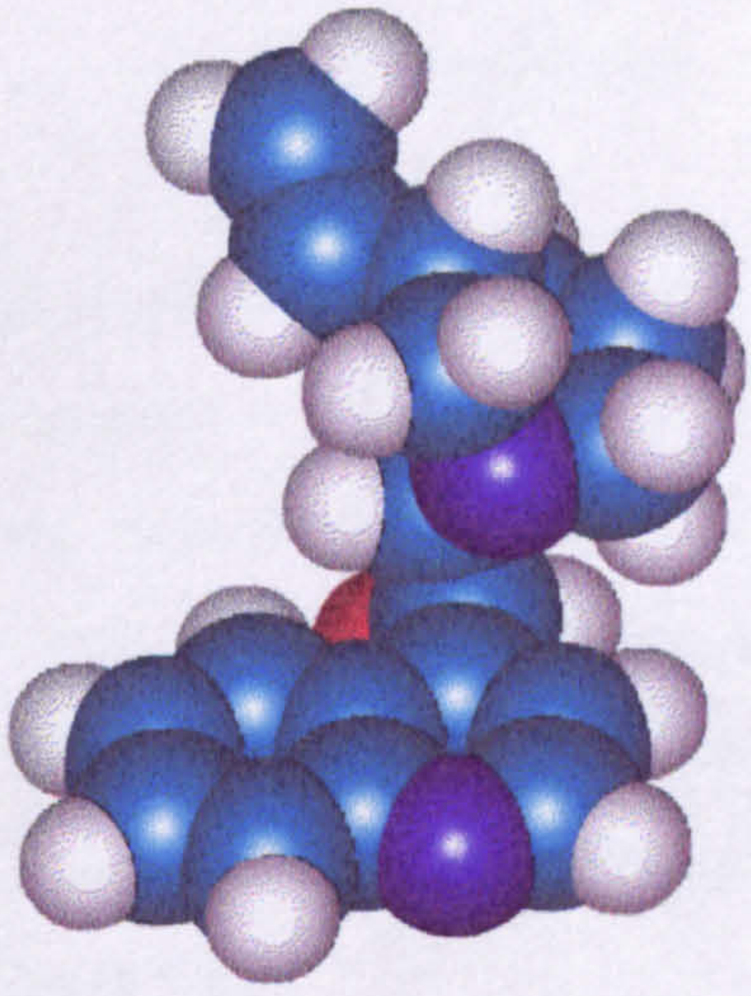

Figure 5.8
Conformation C
for Cinchonidine

Conformations B and *C* both have the nitrogen of the quinuclidine ring system orientated over the quinoline ring. If the molecule was to adsorb flat via the aromatic ring system, the 'L-shaped' adsorption shadow of *conformation C* would be the mirror image of that of *conformations A* and *B*. However, *conformation C* has the hydroxyl group orientated into the area between the two rings, unlike *conformation B* which has the hydroxyl group on the other side of the molecule.

For completeness, the effect on potential energy of rotation around the bond $C_{4'}C_9$ whilst keeping C_9C_8 constant and vice-versa for *conformations B* and *C* are also shown in figures 5.4 and 5.5. As the *conformations B* and *C* are virtually mirror images of each other, the plots are nearly identical. The plots do however differ from that for *conformation A* quite significantly. When the 2-D plots in figures 5.4 and 5.5 are compared to the 3-D contour plot in figure 5.6, the importance of considering simultaneous rotation about all possible bonds becomes important. The 3-D contour plot is still an approximation of the minimum potential energy of the cinchonidine molecule for two constrained dihedral angles. In theory the remainder of the molecule should have been allowed to 'relax', and the results plotted as a multi-dimensional hyper-surface. In practice, this calculation is difficult and the representation impossible!

The energy barrier between *conformations A* and *B* is seen to be quite small in figure 5.6. To determine the size of this barrier to a greater accuracy the torsional bonds $C_{3'}C_{4'}C_9C_8$ and $C_7C_8C_9C_{4'}$ were rotated through 26° to 112° and 156° to 302° respectively in 2° steps. The results of these calculations are given in figure 5.9. The energy barrier for rotation between the two *conformations A* and *B* was found to be 4.8 kcal mol^{-1}. The energy barrier between *conformations A* and *C*, is found to be ca. 30 kcal mol^{-1} (based on the results presented in figure 5.6).

There is also a degree of rotation possible about the hydroxyl group, $C_{4'}C_9OH$. The plot of energy versus torsion angle in 1° steps for this group is given in figures 5.10 for each minimum energy conformation. Rotation of the hydroxyl group in *conformation*

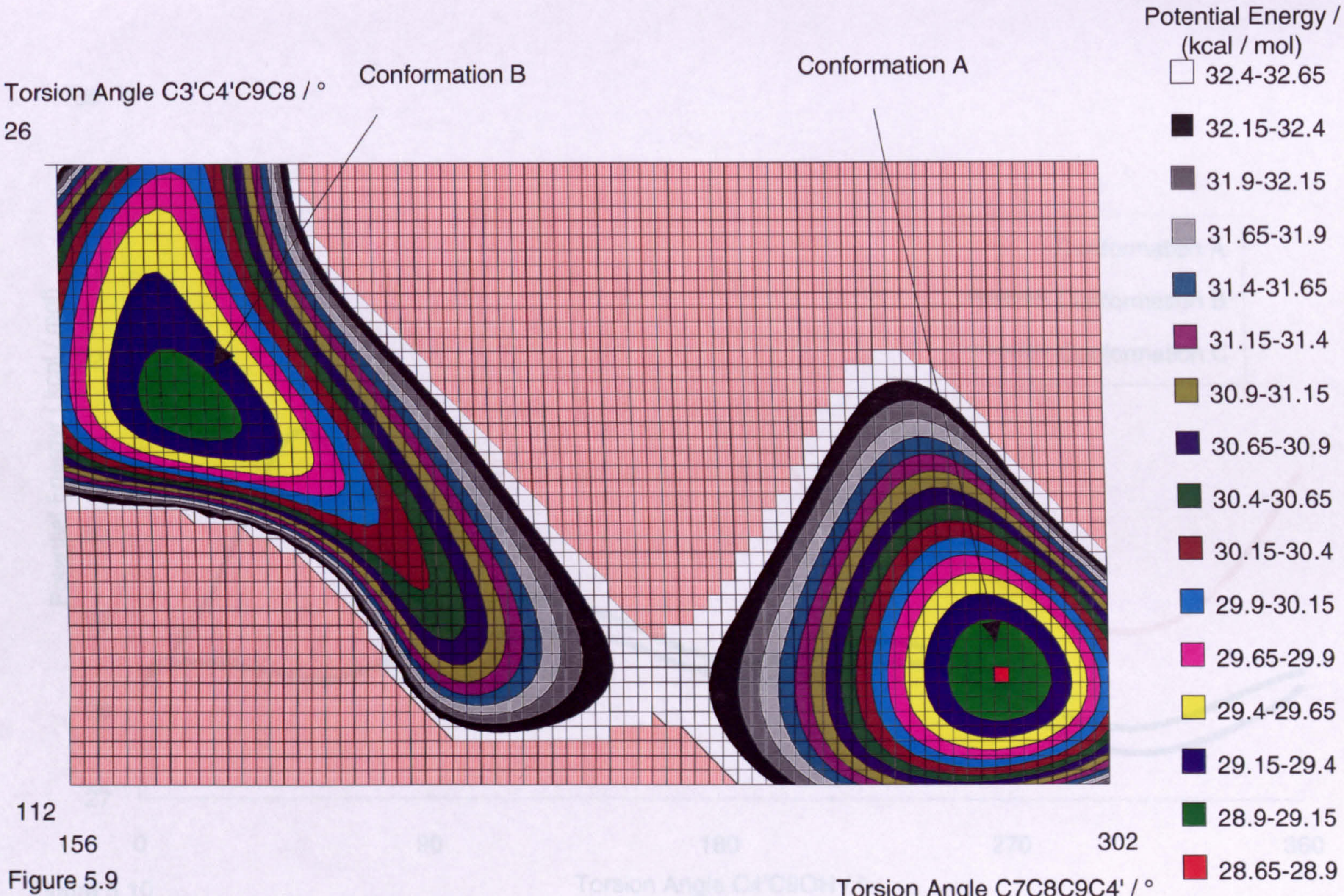

Figure 5.9
Plot Showing Potential Energy Barrier between Conformations A and B

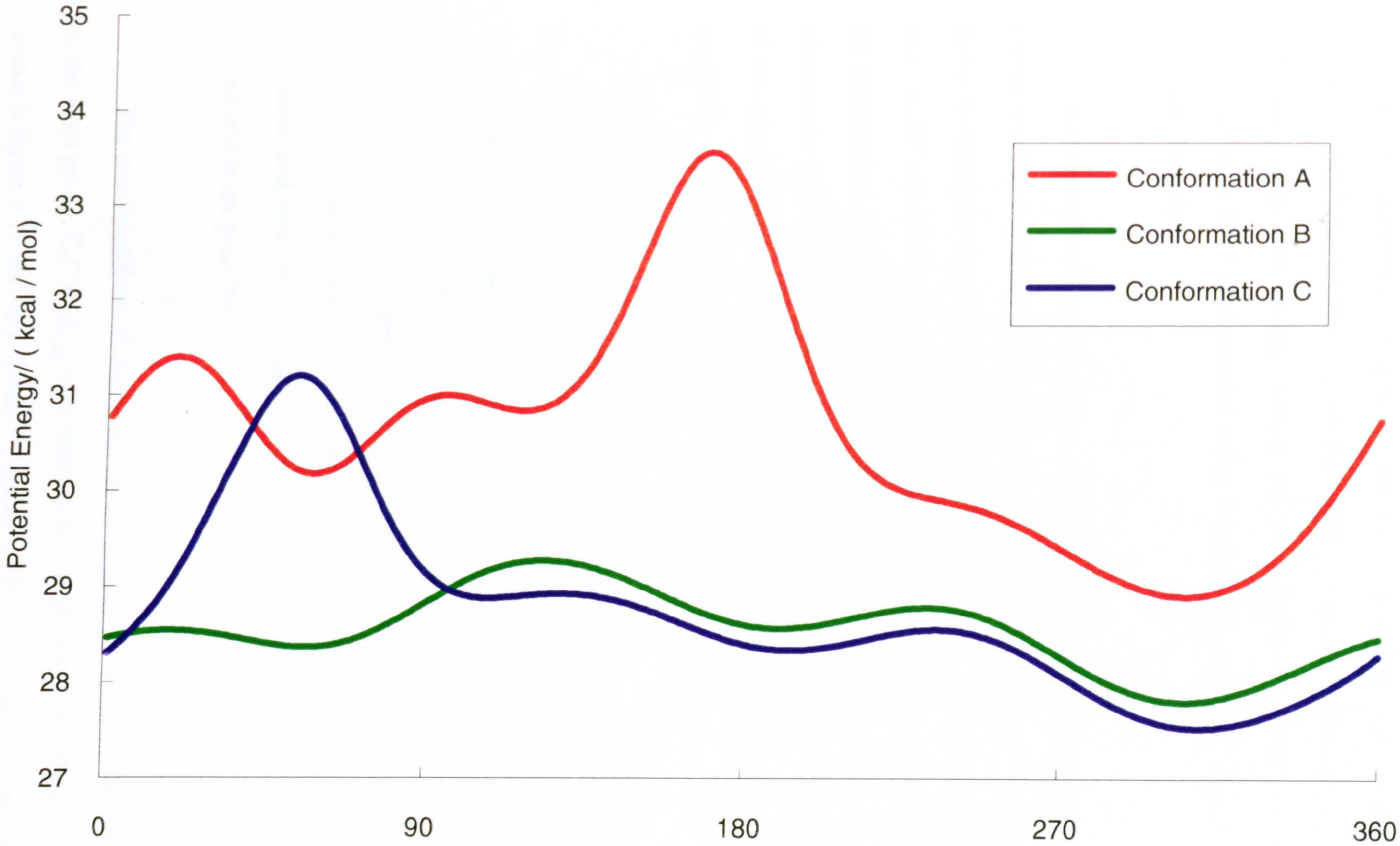

Figure 5.10
Effect on Potential Energy of Rotation of the Hydroxyl Group in Cinchonidine

A shows two energy minima, one global minimum at 306° where the hydroxyl group is orientated down away from the quinoline and quinuclidine ring and a local minimum at 62° where the hydroxyl group is pointing away from the quinoline ring towards the quinuclidine ring. The energy barriers for the rotation from the minimum energy conformation to the higher minima being 2.5 and 4.7 kcal mol^{-1}, depending on the direction of rotation.

Rotation of the hydroxyl groups of *conformation B* through 360° results in three energy minima. A global energy minima of 27.5 kcal mol^{-1} at 310° when the hydroxyl group is orientated away from the molecule and two local energy minima of 28.4 kcal mol^{-1} at 56° and 28.5 kcal mol^{-1} at 190° when the hydroxyl group is orientated towards the quinuclidine. The energy barriers to rotation of the hydroxyl group from the global minimum to these local minima being 1.0 and 1.2 kcal respectively. Within the accuracy of the calculations these energy minima become indistinguishable and energy barriers negligible.

The energy plot for rotation of the hydroxyl group in *conformation C* is similar to that for *conformation B*, the global energy minimum of 27.5 kcal mol^{-1} is also at 310°, when the hydroxyl group is orientated away from the molecule. However, there is only one local minimum of 28.3 kcal mol^{-1} at 193° to which there is an energy barrier of 1.0 kcal mol^{-1}. The energy maximimum of 31.2 kcal mol^{-1} at 53° occurs when the hydroxyl group is orientated towards the quinoline ring. Once again within the accuracy of calculation and with such a small energy barrier, either of these two minimum energy conformations are possible.

The remaining bond about which there is a degree of freedom for rotation is that of the vinyl group, $C_2C_3C_{10}C_{11}$. Unsurprisingly, the plots of energy versus torsion angle, shown in figure 5.11 are very similar for *conformations A, B* and *C* as the vinyl group is only influenced by the presence of the quinuclidine. The global energy minimum is ca. 28 kcal mol^{-1} at ca. 143° with a local minimum at ca. 335° of ca. 33 kcal mol^{-1}. The subtle

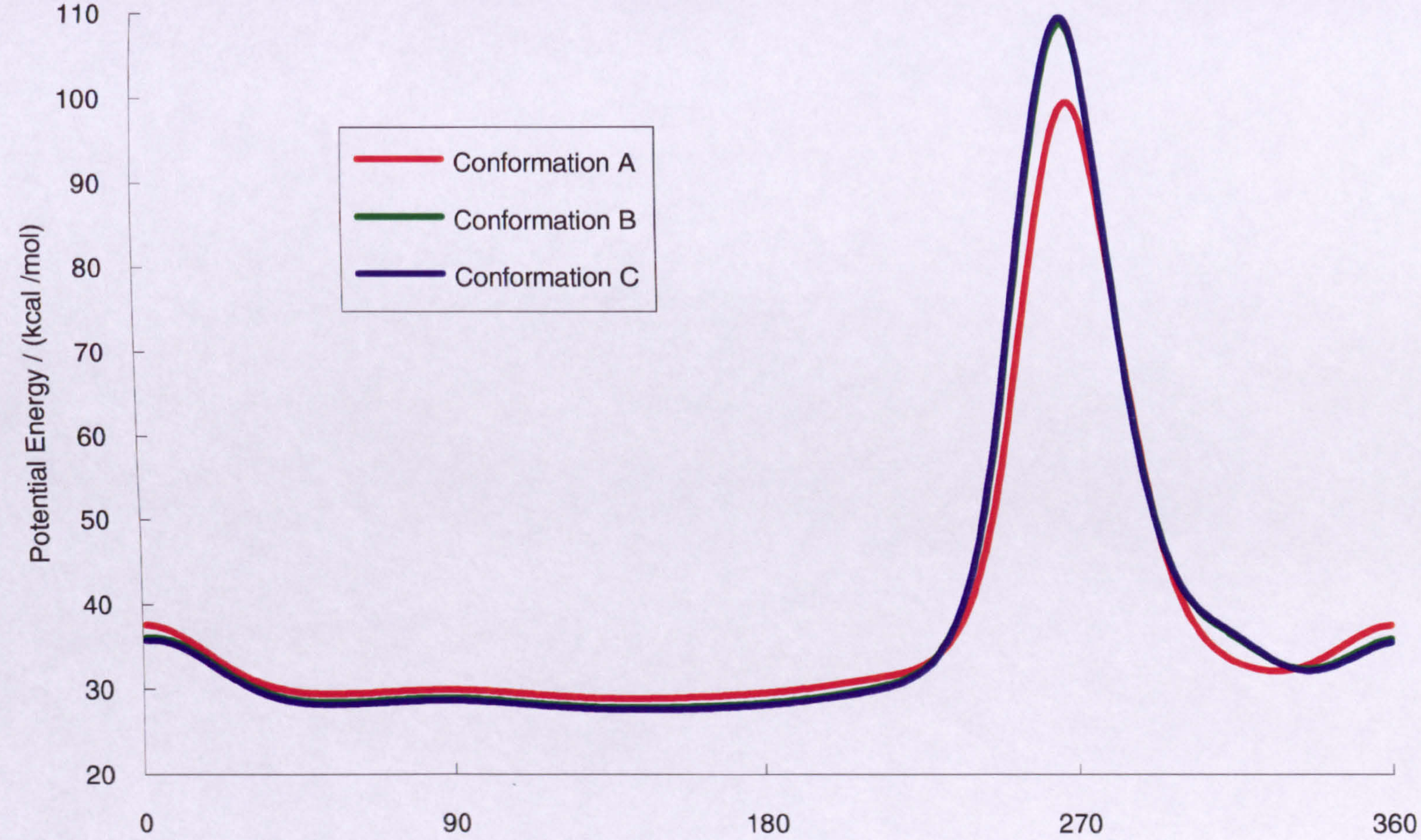

Figure 5.11
Effect on Potential Energy of Rotation of the Vinyl Group in Cinchonidine

differences in the magnitudes of the potential energy for each conformation is accounted for by the differences in the global potential energies.

Table 5.1

Angles of Principle Torsion Bonds in Minimum Energy Conformations for Cinchonidine

Conformation	$C_{3'}C_{4'}C_9C_8$/°	$C_7C_8C_9C_{4'}$/°	$C_{4'}C_9OH$/°	$C_2C_3C_{10}C_{11}$/°	Energy / kcal mol^{-1}
A	97	286	306	141	28.9
B	63	176	310	144	27.8
C	255	177	310	145	27.5
Crystal Structure	101	287	299	125	-

Dihedral angles for the four bonds at which the cinchonidine molecule is calculated to be at a minimum minimum energy conformation are summarised in table 5.1 for comparison with the dihedral angles found for the crystal structure[4]. The crystal structure is also shown in figure 5.12 and is close to that calculated to be conformation A (RFAC = 4.9 %). These authors also claim that two inter-molecular hydrogen bonds exist between the hydroxyl groups and alicyclic nitrogens of neighbouring molecules in the crystal as shown in figure 5.12.

All three minimum energy conformations are calculated to be within 2 kcal mol^{-1} of each other, which are identical within the accuracy of the program. Rotation between *conformation C* and *A* or *B* is not easily achievable due to the energy barrier which is required to be summounted (ca. 30 kcal mol^{-1}). As the R-factor of the crystal structure found for cinchonidine was small, it is suggested that little or no cinchonidine exists in conformation C. It is impossible to state categorically whether or not *A* or *B* is the true minimum energy conformation, even though calculation suggests it to be *B*. In any case, the energy barrier to rotation from *conformation A* to *B* is small and easily summountable. All molecular mechanics calculations assume the the molecule was in

vacuo and at 0 K. Stabilisation of *conformation A* may be assisted by solvation. It is interesting to note therefore that Wehrli *et al.*[5] found that enantioselectivity of product decreased with increasing di-electric constant of solvent.

The accessibility of the alicyclic nitrogen is important. With the molecule in *conformation A* interaction with co-adsorbed species is much more easily achieved .When the alicyclic nitrogen of cinchonidine is alkylated[6] or quaternerised[7] to yield N-benzylcinchonidium chloride, rate enhancement and enantioselectivity to product was all but removed.

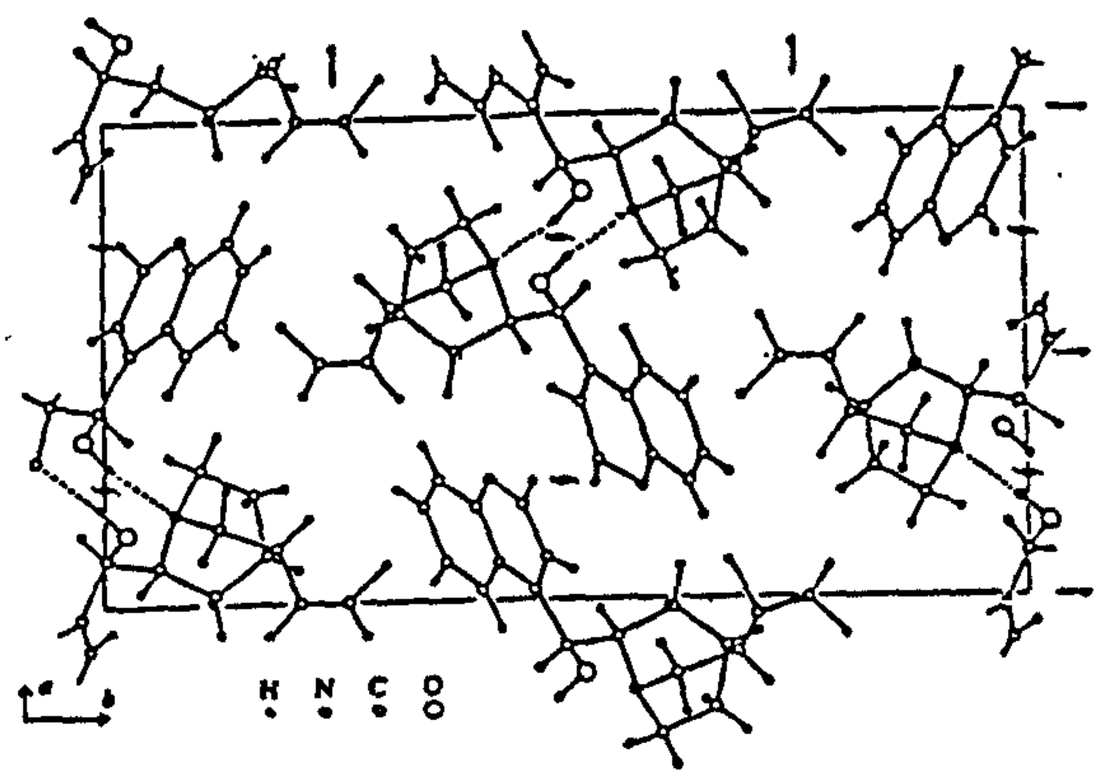

Figure 5.12

The crystal structure of cinchonidine showing the packing of the molecules (reproduced from reference 9)

Adsorption of the molecule is assumed to be through the aromatic ring system of the quinoline ring. (Deuterium tracer studies have lead to evidence to support this assumption[8]). The hydroxyl group in all three minimum energy conformations would hinder such adsorption. However, the energy barrier for rotation of the hydroxyl group (shown in figure 5.10) from the global minimum to further energy minima which could easily accommodate adsorption via the quinoline ring is small. This relatively strong adsorption of the molecule would help overcome the barriers, thus allowing unhindered flat adsorption of the cinchonidine molecule.

Adsorption of the cinchonidine is also possible via the vinyl group. However, in the presence of dissociated hydrogen on the platinum surface this would be expected to quickly hydrogenate to produce 10,11-dihydrocinchonidine. As shown in figure 5.3, the vinyl group is orientated such that it will not hinder the approach of reactant molecules to the important alicyclic nitrogen.

5.1.3 Cinchonine

Cinchonine, the near enantiomer of cinchonidine, (which differs only in the position at which the vinyl group is attached) was found to have very similar properties to cinchonidine. The effect on energy of rotating the bonds $C_{3'}C_{4'}C_9C_8$ and $C_7C_8C_9C_{4'}$ in 5° steps is shown in figure 5.13. The result is very similar to that for cinchonidine, and further minimisation using molecular mechanics again resulted in three minimum energy conformations, *A**, *B** and *C** as shown in figures 5.14 to 5.16. However, there is a further minimum energy region (as opposed to a distinct energy minima) at about $C_{3'}C_{4'}C_9C_8 = 105°$, $C_7C_8C_9C_{4'} = 90°$. The energy barrier between conformation *B** to *A** is ca. 5.5 kcal mol^{-1} and between *C** and *A** or *B** is ca. 46 kcal mol^{-1}. The dihedral angles of the four principle bonds for each minimum energy conformation are given in table 5.2 along with the values from the crystal structure[9].

Table 5.2

Angles of Principle Torsion Bonds of Minimum Energy Conformations for Cinchonine

Conformation	$C_{3'}C_{4'}C_9C_8$ / °	$C_7C_8C_9C_{4'}$ / °	$C_{4'}C_9OH$ / °	$C_2C_3C_{10}C_{11}$ / °	Energy / kcal mol^{-1}
A*	263	72	61	141	31.0
B*	298	186	60	140	29.4
C*	105	185	58	138	29.3
Crystal Structure	260	73	86	123	-

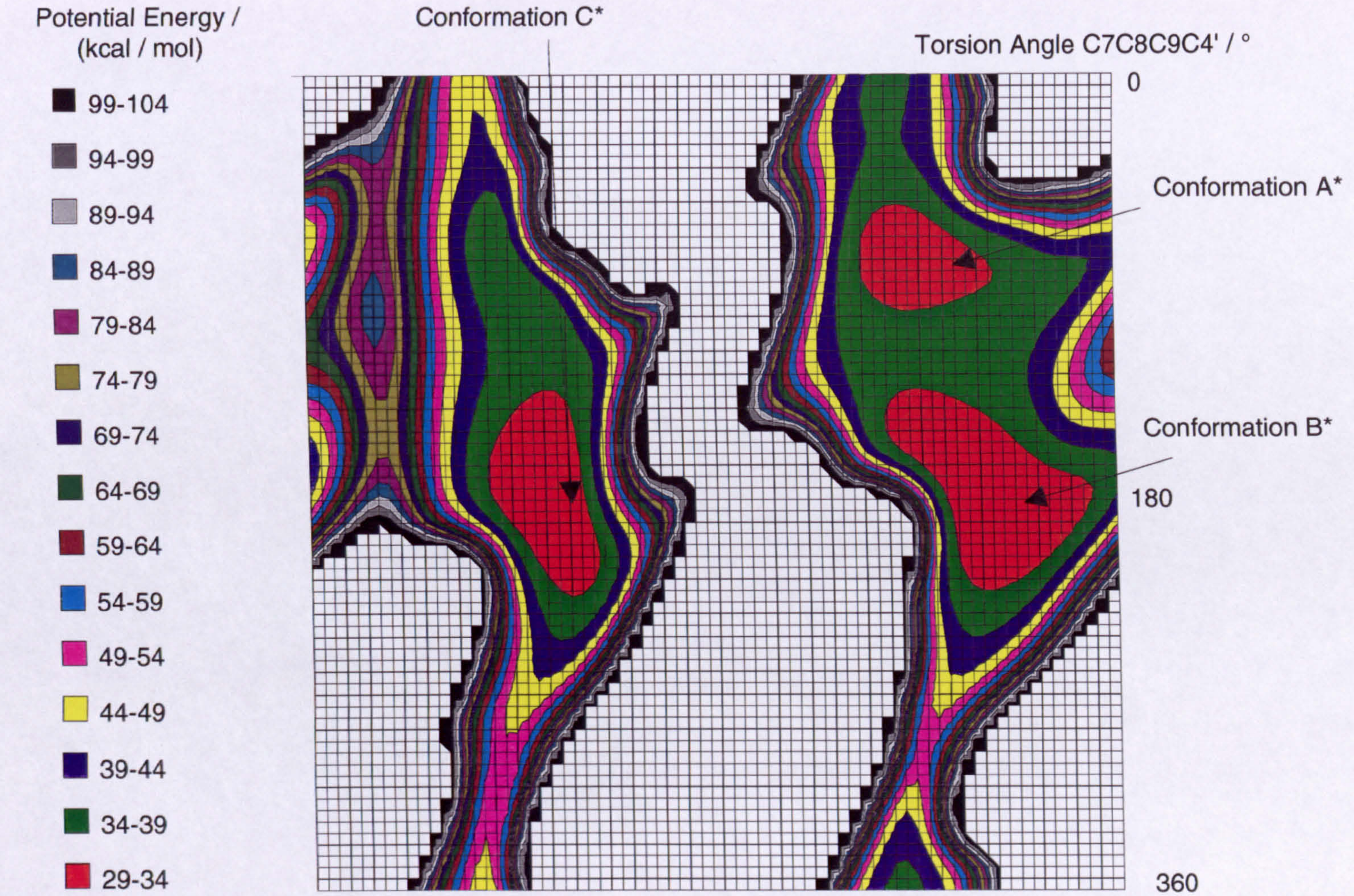

Figure 5.13
Effect on Potential Energy of Rotation around Bonds C4'C9 and C8C9 in Cinchonine

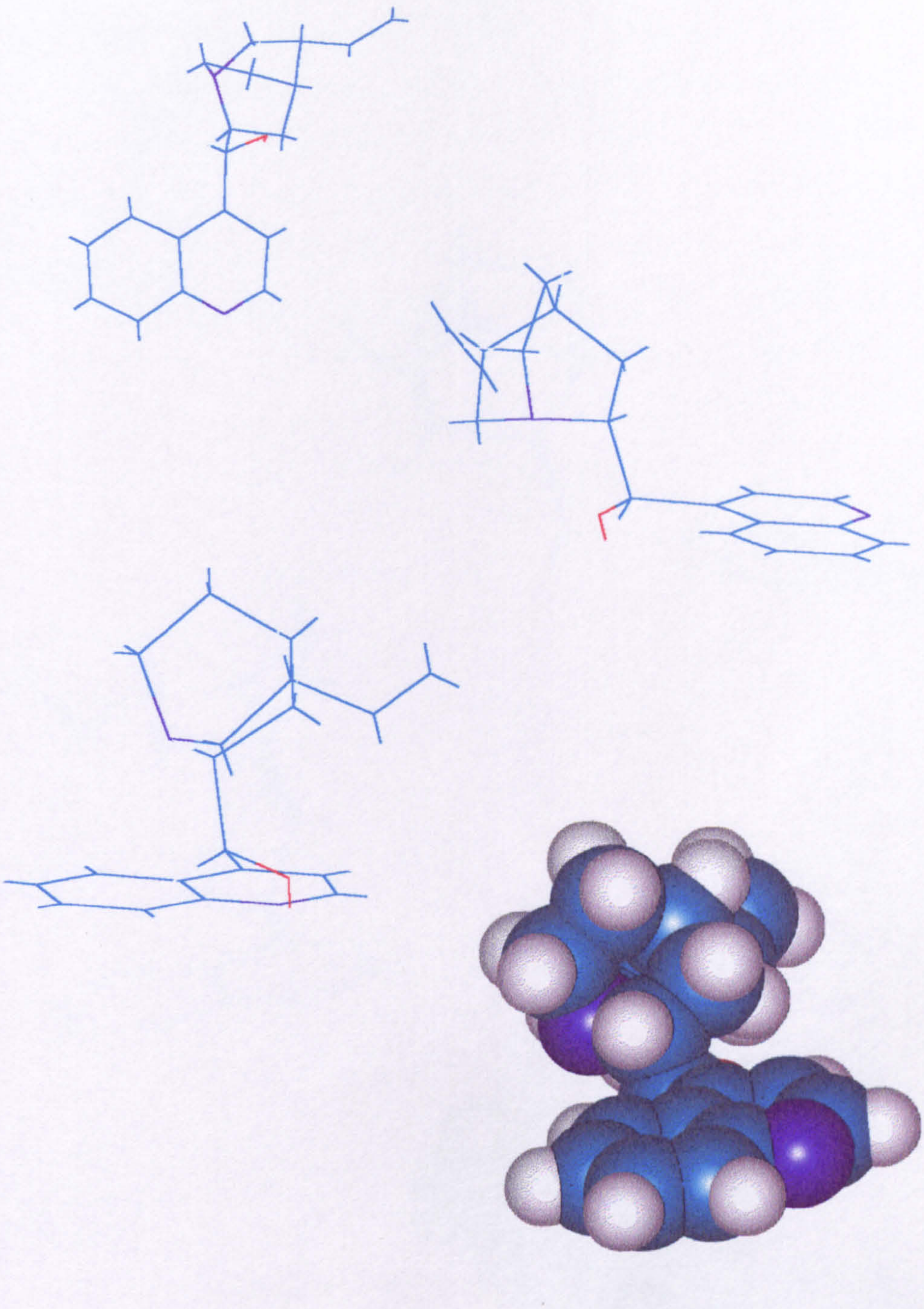

Figure 5.14
Conformation A*
for Cinchonine

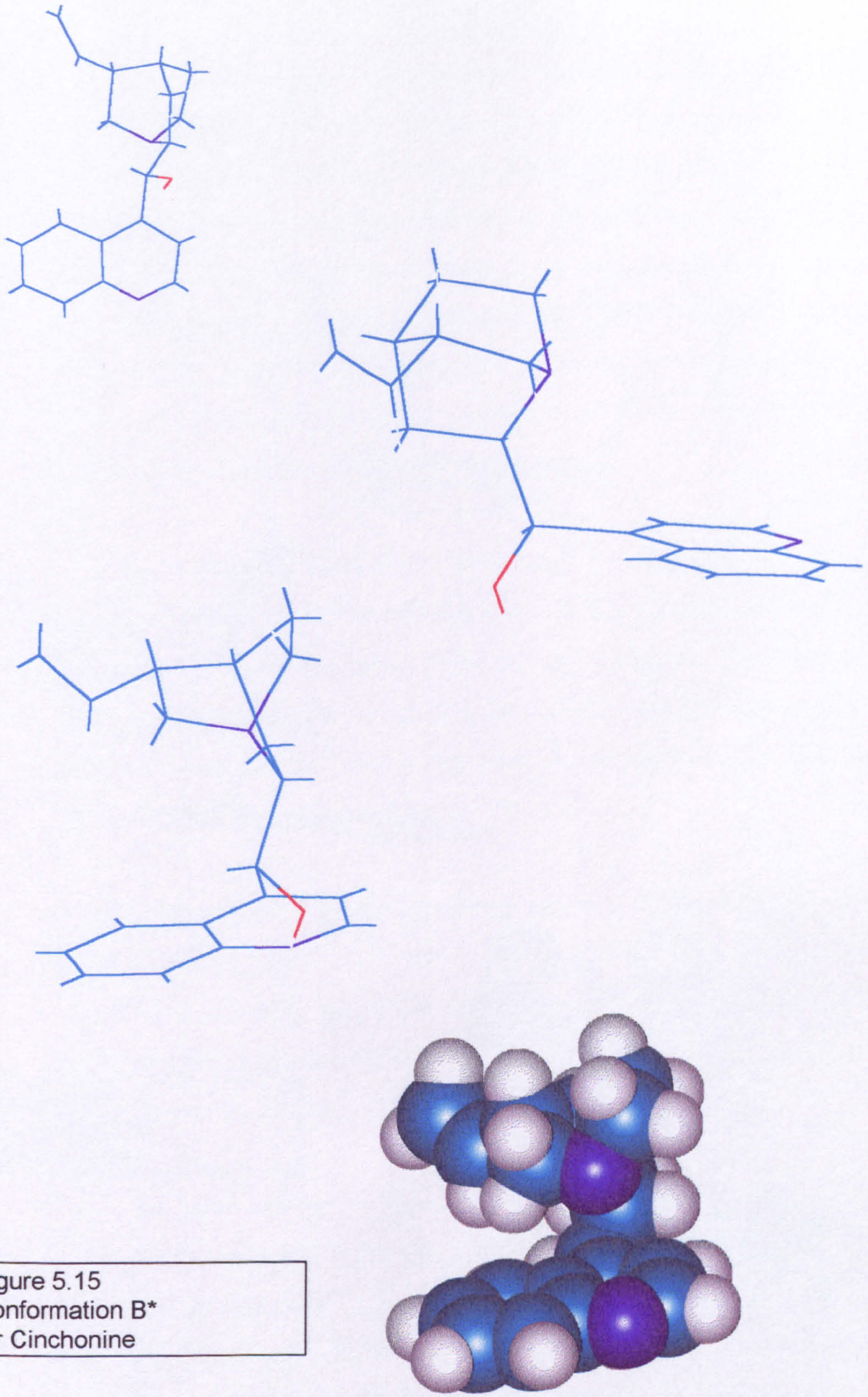

Figure 5.15
Conformation B*
for Cinchonine

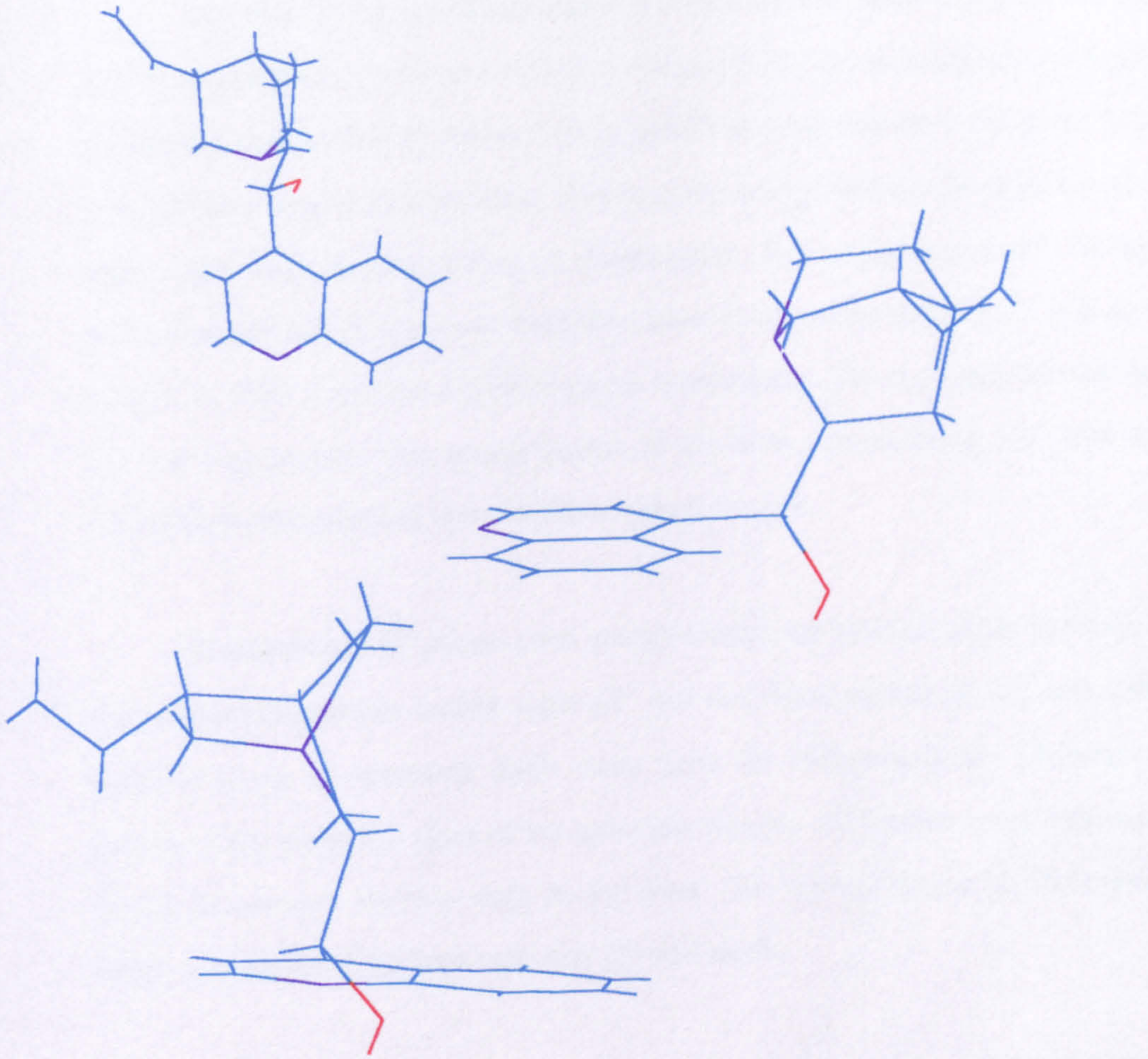

Figure 5.16
Conformation C*
for Cinchonine

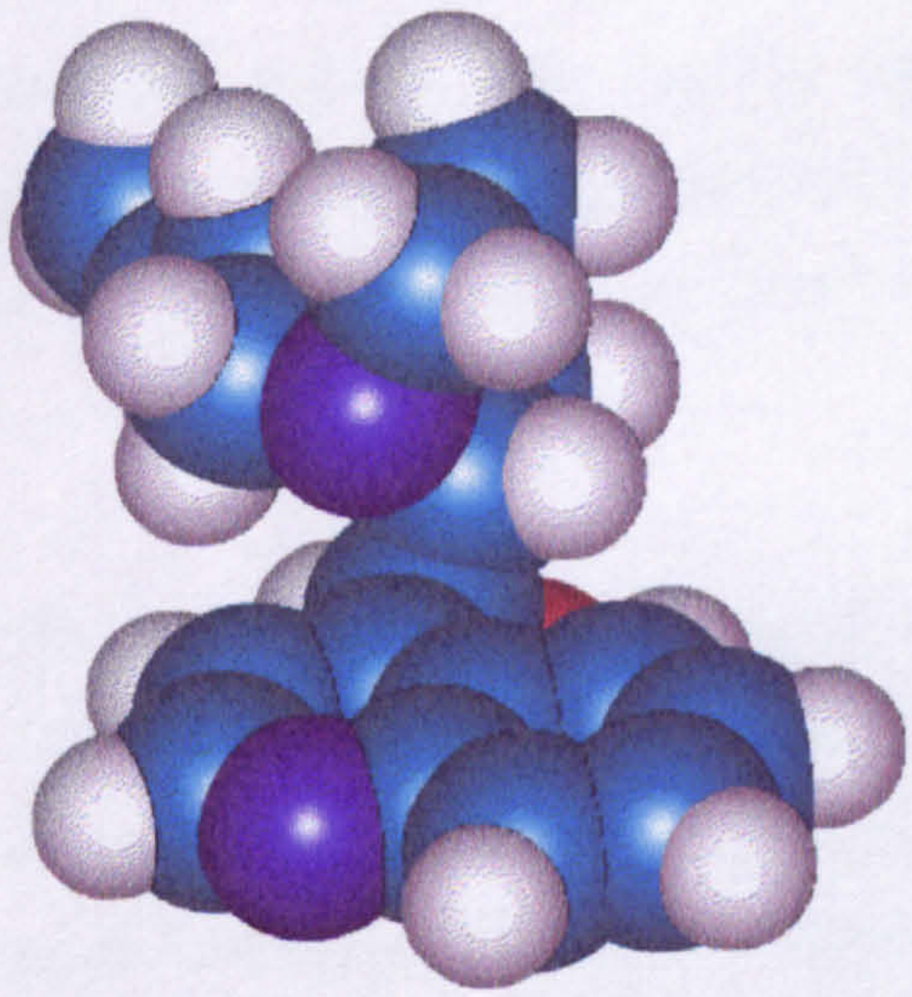

The plot of energy versus rotation of the torsion bond C_4C_9OH for the three minimum energy conformations is shown in figure 5.17. The plot is nearly a mirror image to that for cinchonidine in figure 5.10 as would be expected for a molecule which is a near-mirror image to cinchonidine. However the energy barriers for rotation are much higher than those corresponding to cinchonidine. For *conformation A**, the hydroxyl group is orientated down, away from the molecule at torsion angle 62°, with an energy minima at 302° where the hydroxyl group is orientated into the space formed between the two ring systems. The energy barrier to the local minima being 10.3 kcal mol^{-1} or 18.7 kcal mol^{-1} depending upon the direction of rotation.

*Conformation B** posses three energy minima for rotation of the hydroxyl group. One global minimum at torsion angle 62° and two local minima at 172 and 298°. The hydroxyl group is orientated down away from the molecule in the minimum energy conformation, along the plane of the quinoline ring for the former energy minimum and orientated between the two rings in the latter. The energy barrier to these two local energy minima being 2.8 kcal mol^{-1} and 3.7 kcal mol^{-1}.

*Conformation C** has a global energy minima at torsion angle 58° with a local minima at 169°. There is no corresponding minimum near 298° as found in *conformations A and B* which would have the hydroxyl group orientated towards the quinuclidine ring system. Energy barriers of 10 and 20 kcal mol^{-1} exist to rotation of the hydroxyl group in this conformation.

The effect on energy of rotating the bonds $C_2C_3C_{10}C_{11}$ for all minimum energy conformations is given in figure 5.18. The plot is very similar to that calculated for cinchonidine with the exception that the there is no minimum energy conformation at ca. 323° for *conformation A**. As shown in figure 5.14, the vinyl group is orientated to 'the side' of the quinuclidine ring whereas in cinchonidine the vinyl group is orientated 'up' from the quinuclidine and quinoline ring.

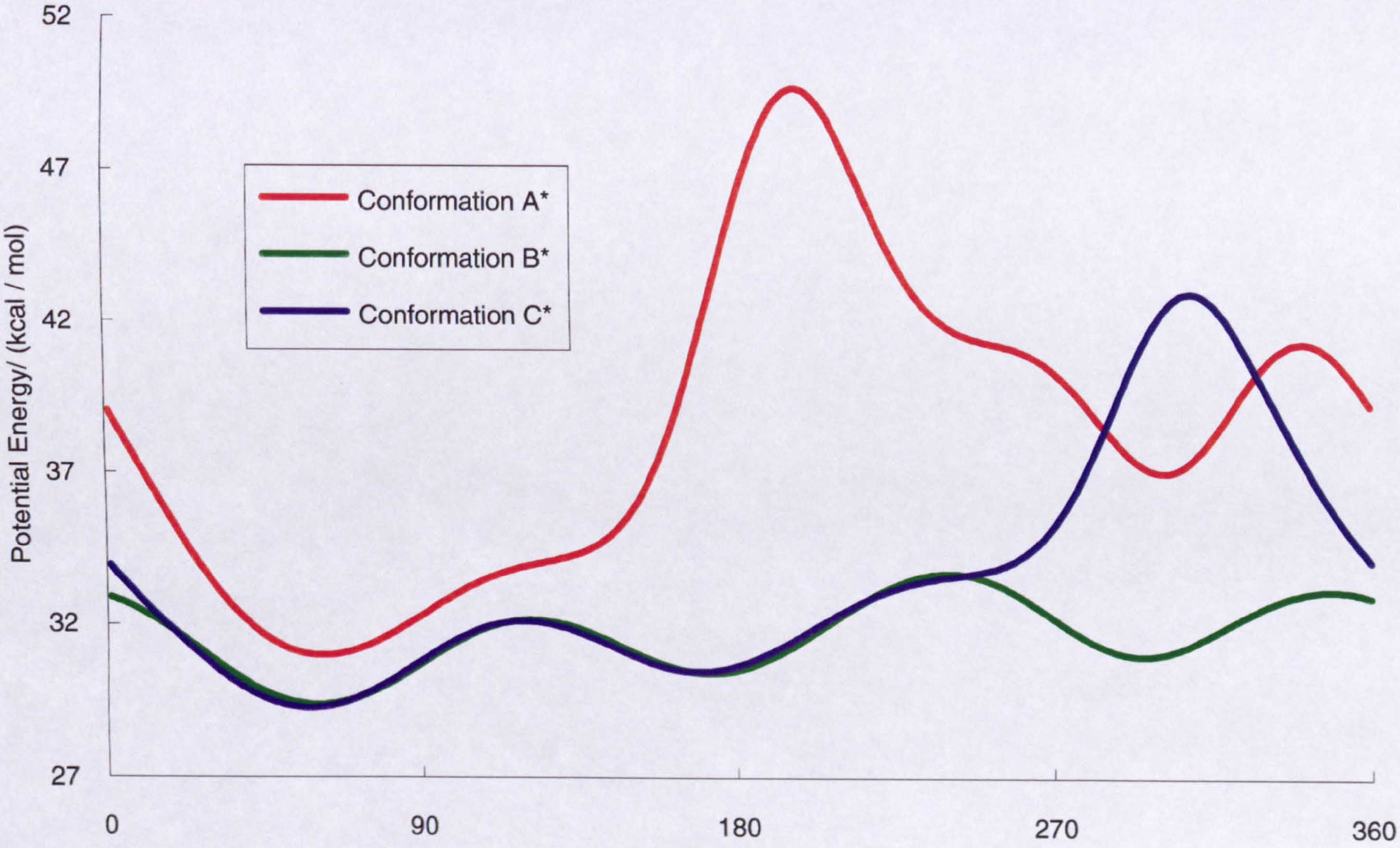

Figure 5.17
Effect on Potential Energy of Rotation of the Hydroxyl Group in Cinchonine

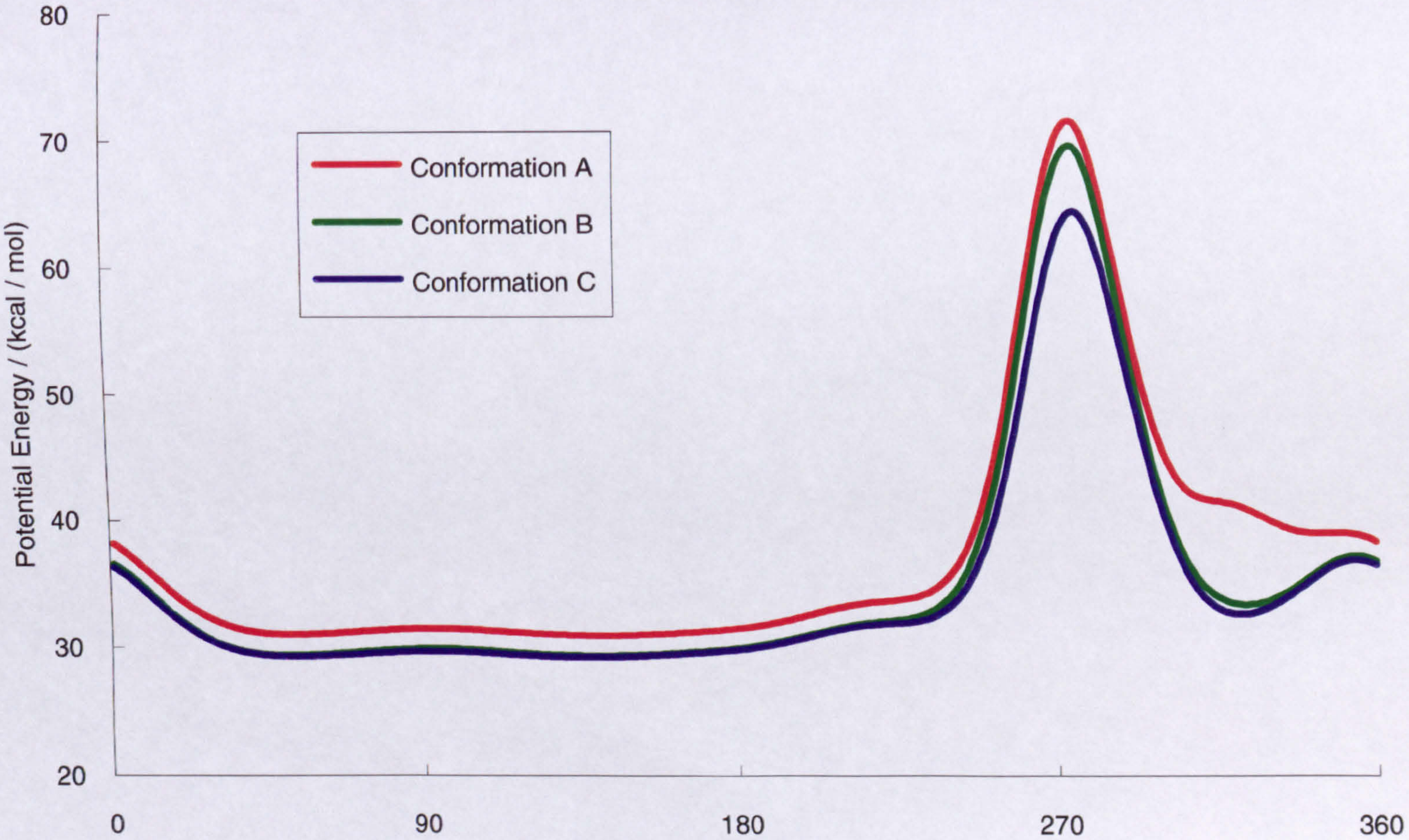

Figure 5.18
Effect on Potential Energy of Rotation of the Vinyl Group in Cinchonine

Again the minimum energy conformations found were to be very similar, being within 2 kcal mol^{-1} of each other. The crystal structure was found to resemble *conformation A**, which again would include the effect of crystal packing forces. The 'L-shaped' adsorption shadow of *conformations A** and *B** would also the mirror image of that formed by *conformations A* and *B* for cinchonidine.

The adsorption characteristics of cinchonine could be expected to differ from that for cinchonidine in two subtle ways. The hydroxyl group would be expected to rotate around to allow adsorption of the molecule via the aromatic ring. The energy barriers for this are slightly higher than that for cinchonidine, suggesting that adsorption may be slightly more hindered. Adsorption of the molecule via the aromatic ring brings the vinyl group close to the surface, implying that simultaneous adsorption is possible via both moities. The vinyl group would however be able to desorb rapidly on hydrogenation. The orientation of the group would also be expected to hinder slightly the adsorption of further cinchonine molecules, thus reducing the surface concentration. From figure 3.6 it is observed that the rate of reaction increases with increasing concentration of alkaloid modifier. Cinchonine typically enhances the rate of reaction to a lesser degree than cinchonidine, possibly due to this reduced surface concentration.

The energy barrier for rotation of the quinuclidine ring from *conformation B** to *A** is also calculated to be slightly greater than that for cinchonidine. If *A** is indeed the active conformation, the reduced optical yields and reaction rates observed could also be due to a reduced surface concentration of this conformation.

5.1.4 Epiquinidine

Epiquinidine differs from the other alkaloids studied by nature of having the R configuration at both C_8 and C_9 positions. The plot of energy versus rotation for the two torsion angles $C_{3'}C_{4'}C_9C_8$ and $C_7C_8C_9C_{4'}$ is displayed in figure 5.19. The alkaloid again has three principle energy minima giving three different *conformations* $A^{\dagger}$, $B^{\dagger}$ and $C^{\dagger}$

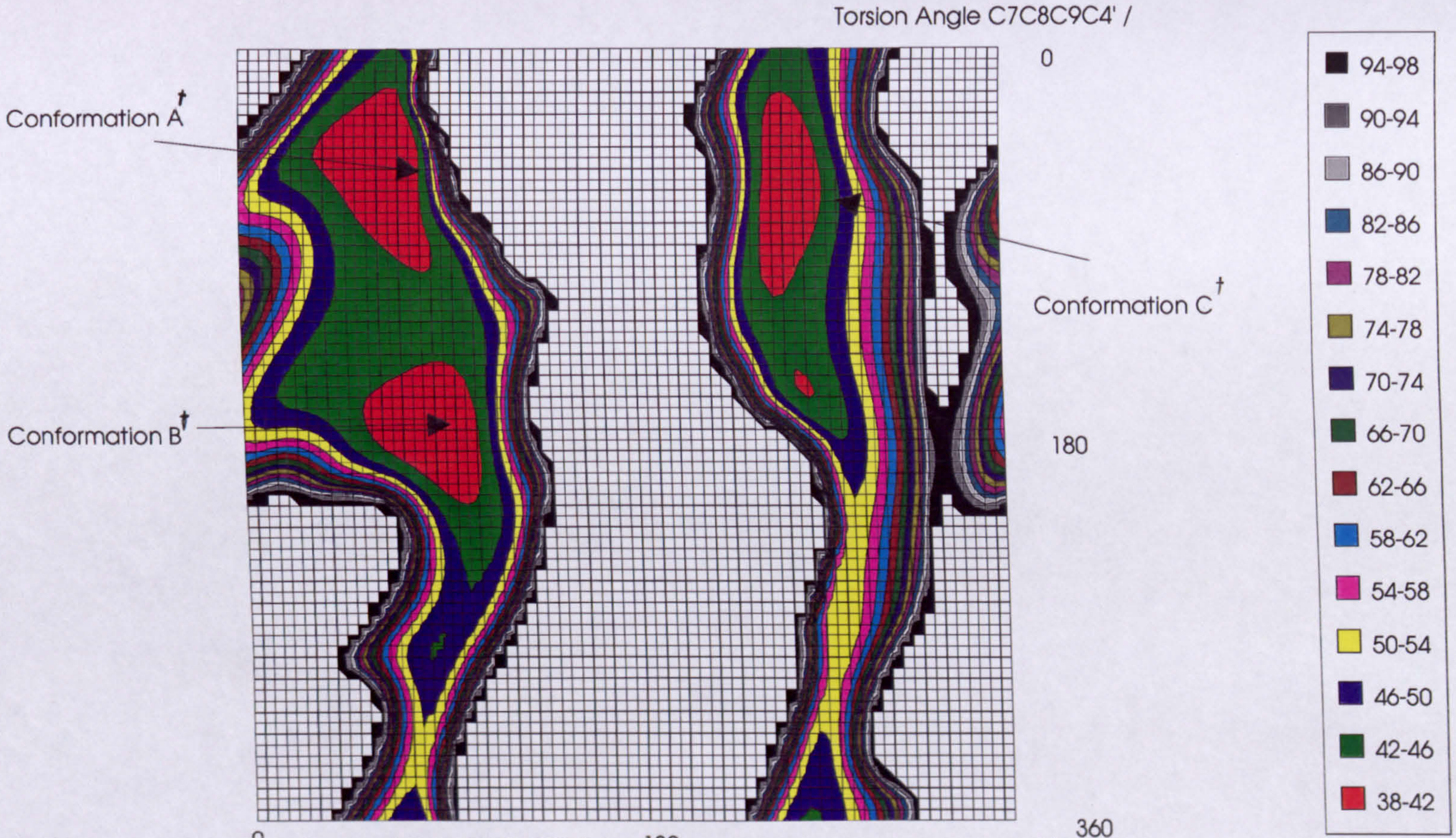

Figure 5.19
Effect on Potential Energy of Rotation about Bonds C4'C9 and C8C9 in Epiquinidine

which are shown in figures 5.20 to 5.22. The angles of the principle torsion bonds are given in table 5.3. No crystal structure for the molecule was available on the Cambridge Crystal Structure Database. In each case the nitrogen of the quinuclidine ring system is orientated to be adjacent to the hydroxyl group.

The remaining bond about which there is a degree of possible rotation is that belonging to the methoxy group attached to the quinoline ring. The plot of potential energy versus dihedral angle for $C_7C_{6'}OMe$ is displayed in figure 5.23. The favoured position for the group is at a dihedral angle of 180°.

Table 5.3

Angles of Principle Torsion Bonds of Minimum Energy Conformations for Epiquinidine

Conformation	$C_{3'}C_{4'}C_9C_8$ / °	$C_7C_8C_9C_{4'}$ / °	$C_{4'}C_9OH$ / °	$C_2C_3C_{10}C_{11}$ / °	Energy / kcal mol^{-1}
A†	74	56	298	173	37.4
B†	93	181	298	176	38.4
C†	251	66	300	176	37.9

5.1.5 Template Model

It was proposed by Wells and co-workers that the site for asymmetric hydrogenation of methyl pyruvate to methyl lactate consisted of a non-close-packed ordered array of cinchonidine molecules adsorbed through their quinoline rings on a Pt crystallite[10]. The shaped ensembles of Pt atoms remaining on the catalyst surface being such that pyruvate adsorption was only possible in an orientation which produces R-(+)-product upon hydrogenation. Although the model was based upon cinchonidine molecules adsorbed upon a Pt surface in a (100) configuration, it was later found that the Pt particles in EUROPT-1 at least in some circumstances of reduction, exhibit preferential exposure of (111) faces[11].

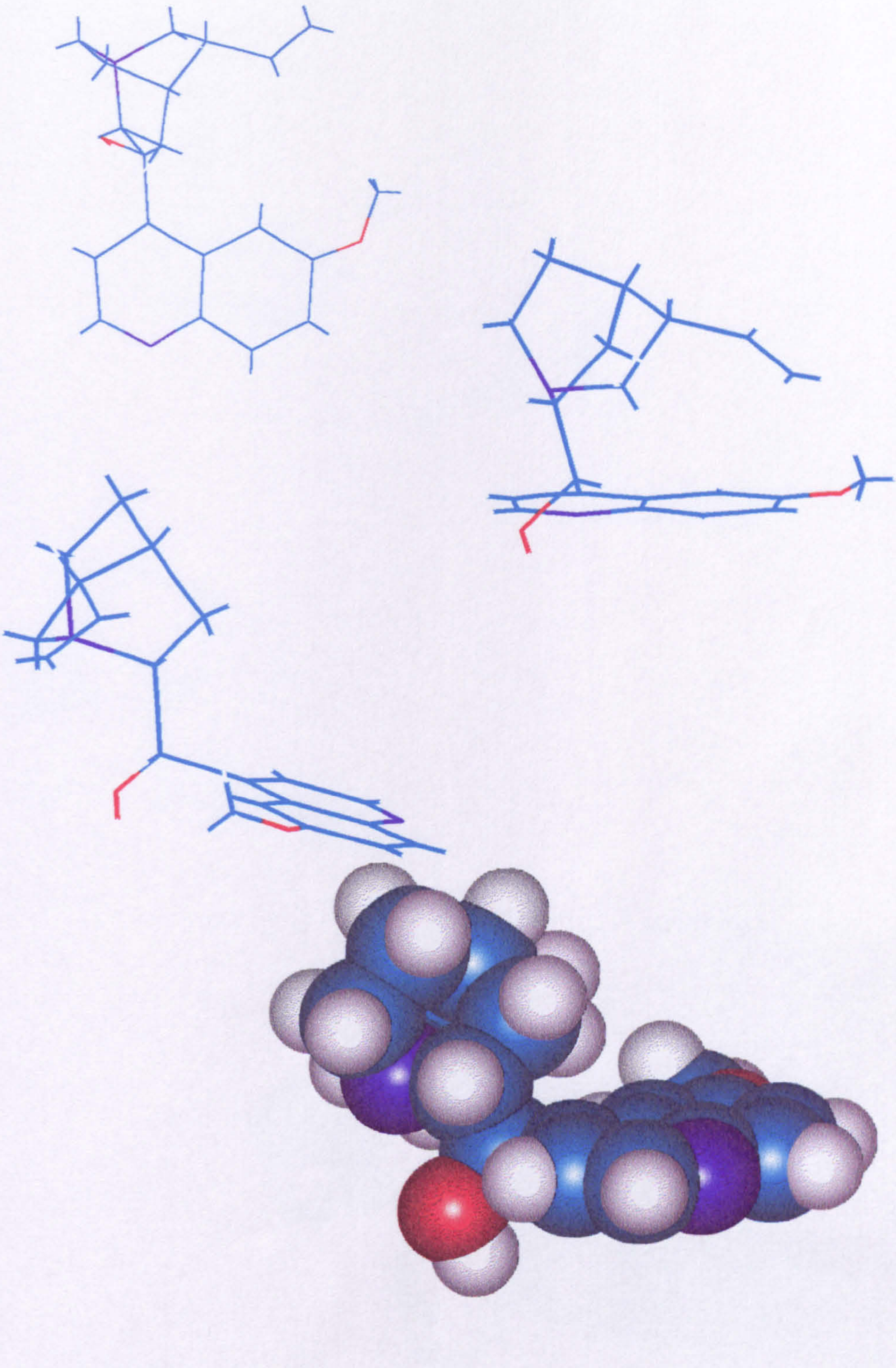

Figure 5.20
Conformation A† of Epiquinidine

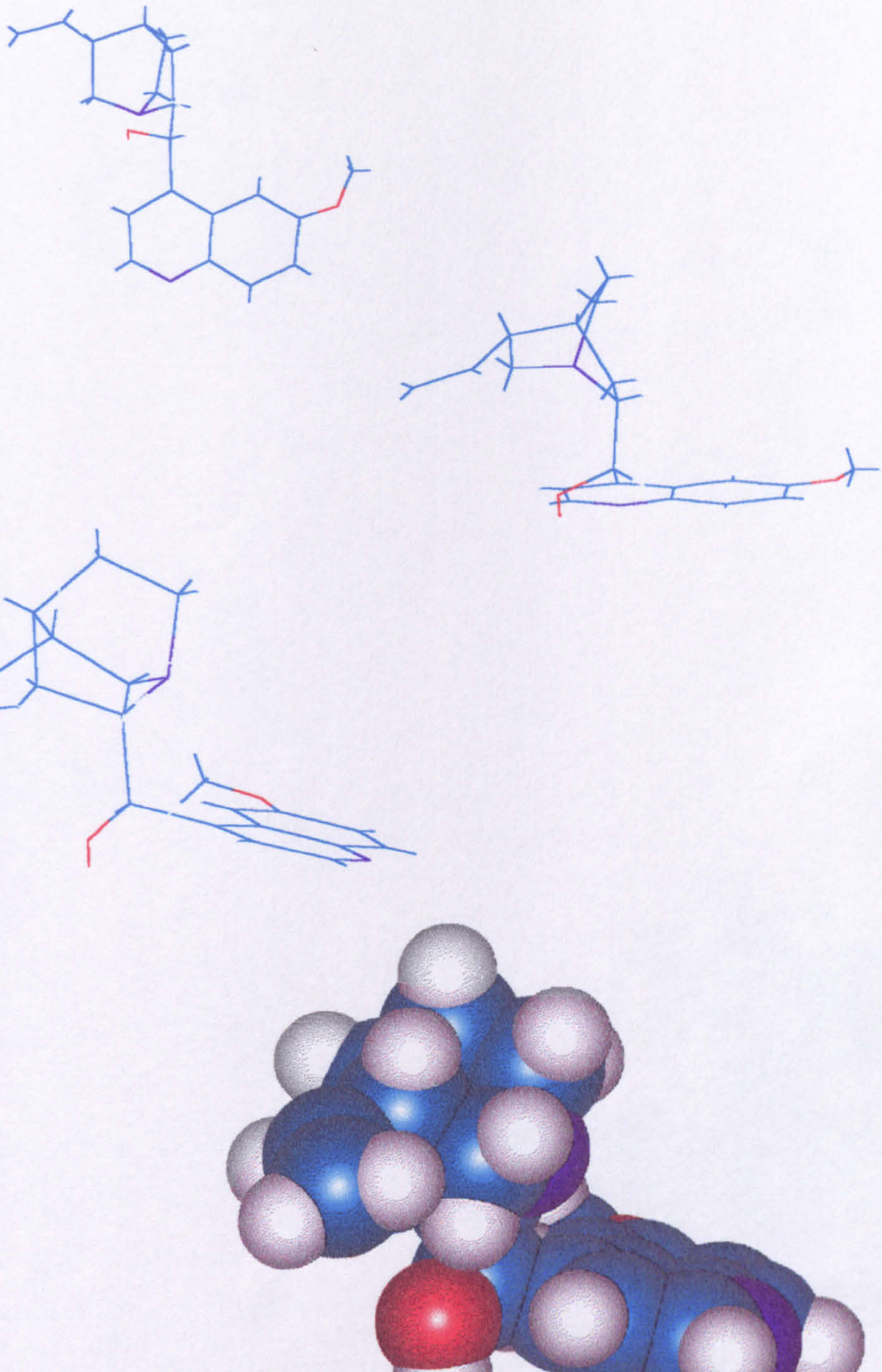

Figure 5.21
Conformation B†
of Epiquinidine

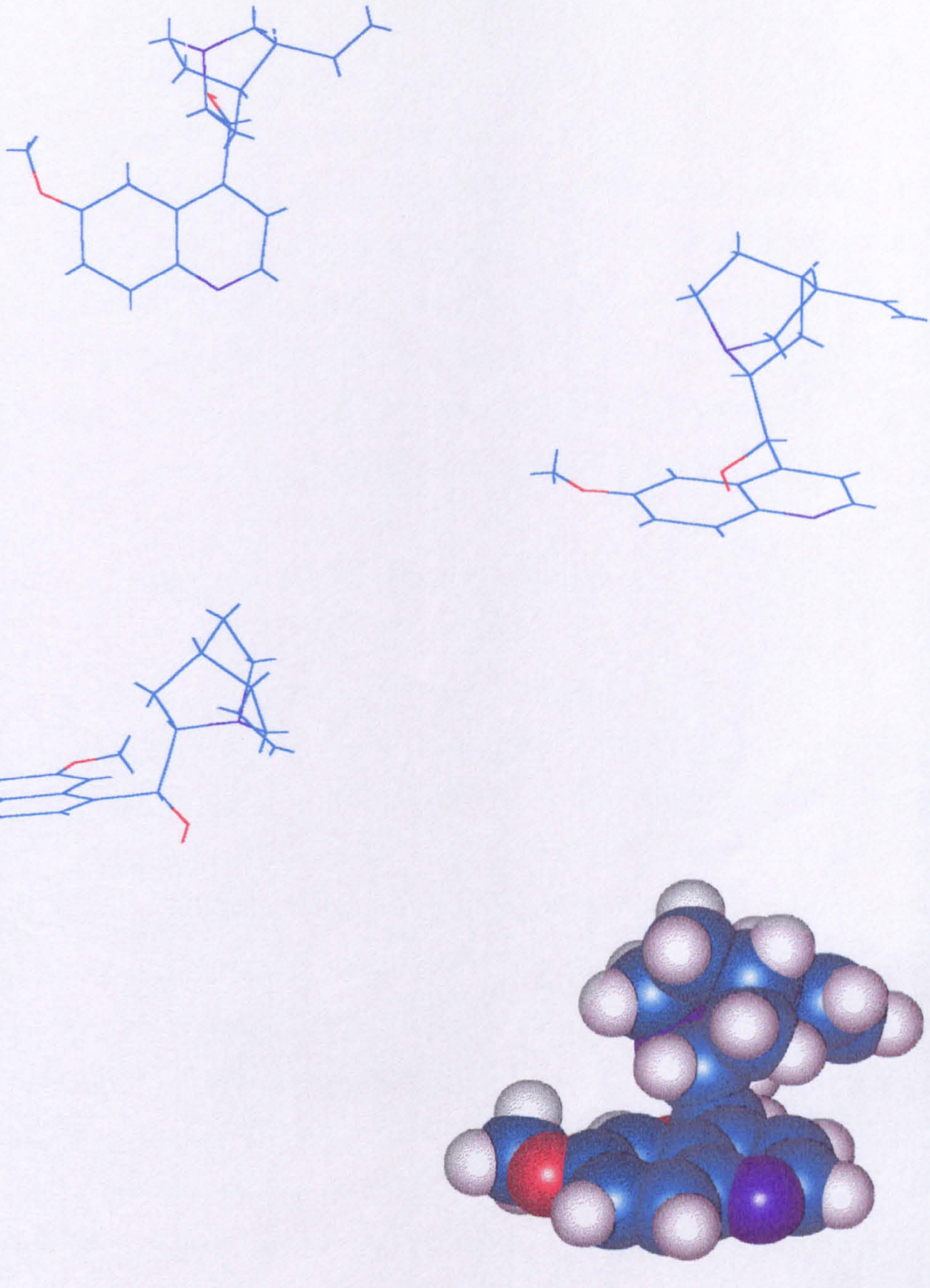

Figure 5.22
Conformation C†
of Epiquinidine

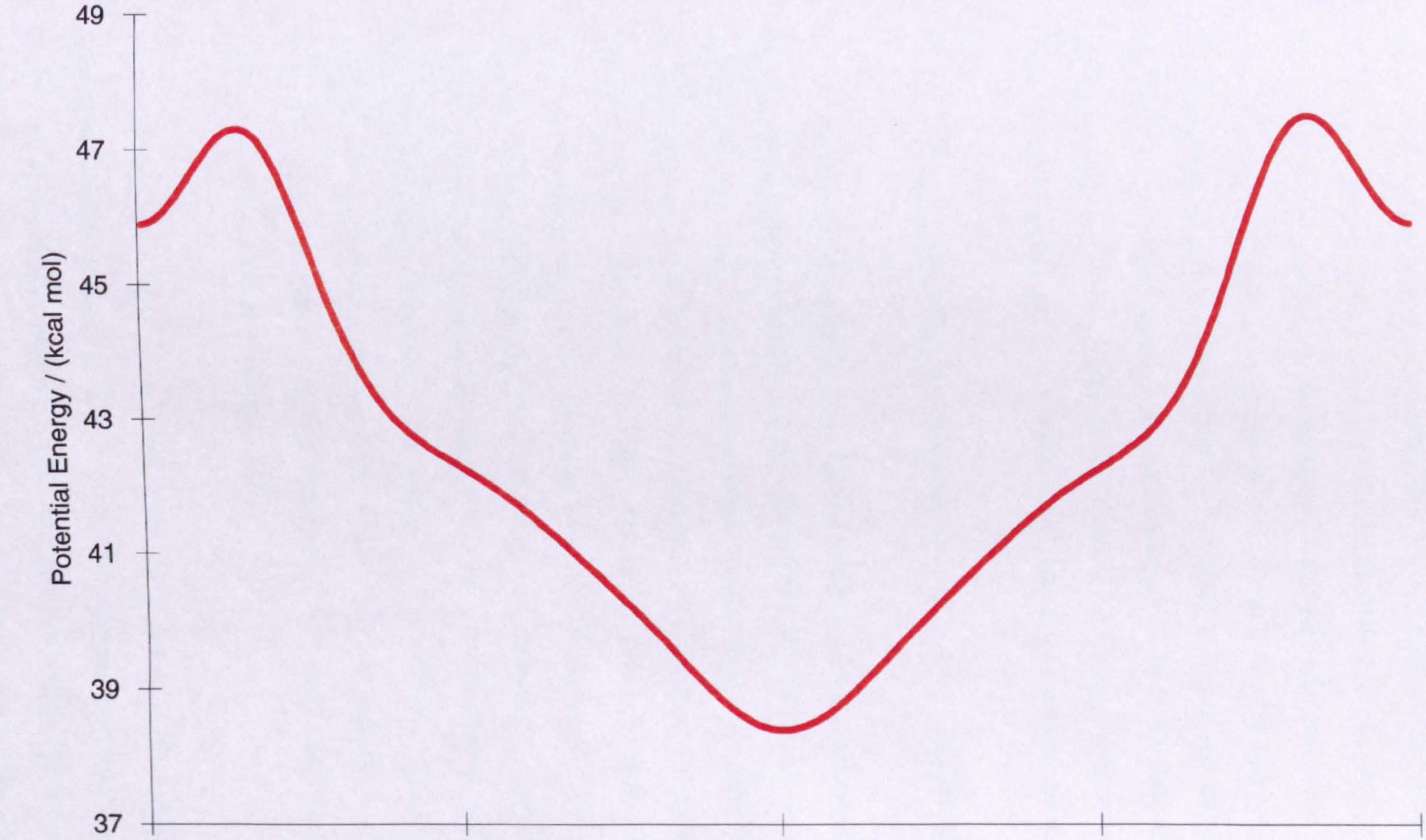

Figure 5.23
Effect on Potential Energy on Rotation of Methoxy Group in (8R,9R)-Epiquinidine

Consequently the so-called 'Template Model' is re-described in figures 5.24 and 5.25 for cinchonidine molecules adsorbed on a Pt(111) crystallite for pyruvate adsorbing in a manner to give R-(+)- and S-(-)- product respectively. It was necessary to assume *conformation A* as being the correct form for cinchonidine adsorbed on the surface as the carbonyl group to be hydrogenated is required to be in close proximity to the nitrogen of the quinuclidine ring. It is apparent that it is not possible to pack the alkaloid molecules as close as occurs in the simplistic published models. However, the same principle is still valid that adsorption of the pyruvate is less hindered for hydrogenation to R-(+)- product than to S-(-)-product as the latter is blocked by a second alkaloid molecule.

5.1.6 A 1:1 Interaction Model as a Superior Alternative to the Template Model

Meheux proposed that the there was no requirement for the formation of ordered arrays of cinchonidine molecules on a Pt crystallite but that the mechanism could be fully explained in terms of a 1:1 interaction between alkaloid and pyruvate. The hydroxyl group of the half-hydrogenated product intermediate is stabilised via hydrogen bonding with the nitrogen of the quinuclidine ring[12]. This requires the quinuclidine ring system to be rotated such that its nitrogen is directed away from the space formed in between the ring systems as described in figure 5.26. If figure 5.6 is examined it can be seen that this rotation would raise the potential energy of the molecule to a higher value by 15 - 25 kcal mol^{-1}. Meheux's description of 1:1 interaction is modelled in figure 5.26. It can be seen that the two molecules are very close to each other and large inter-molecular forces of repulsion give the system a very high energy of ca. 1000 kcal mol^{-1}. This is too high a value to make the model as presented viable.

However, the idea of the mechanism being due to a 1:1 interaction via the stabilisation of the half-hydrogenated state by the quinuclidine-N remains valid. Figure 5.25 which shows an ordered array of alkaloid molecules with pyruvate adsorbed to give S-(-)-product on hydrogenation; this shows that not only is the adsorption of the reactant hindered by a second alkaloid molecule but also by the first.

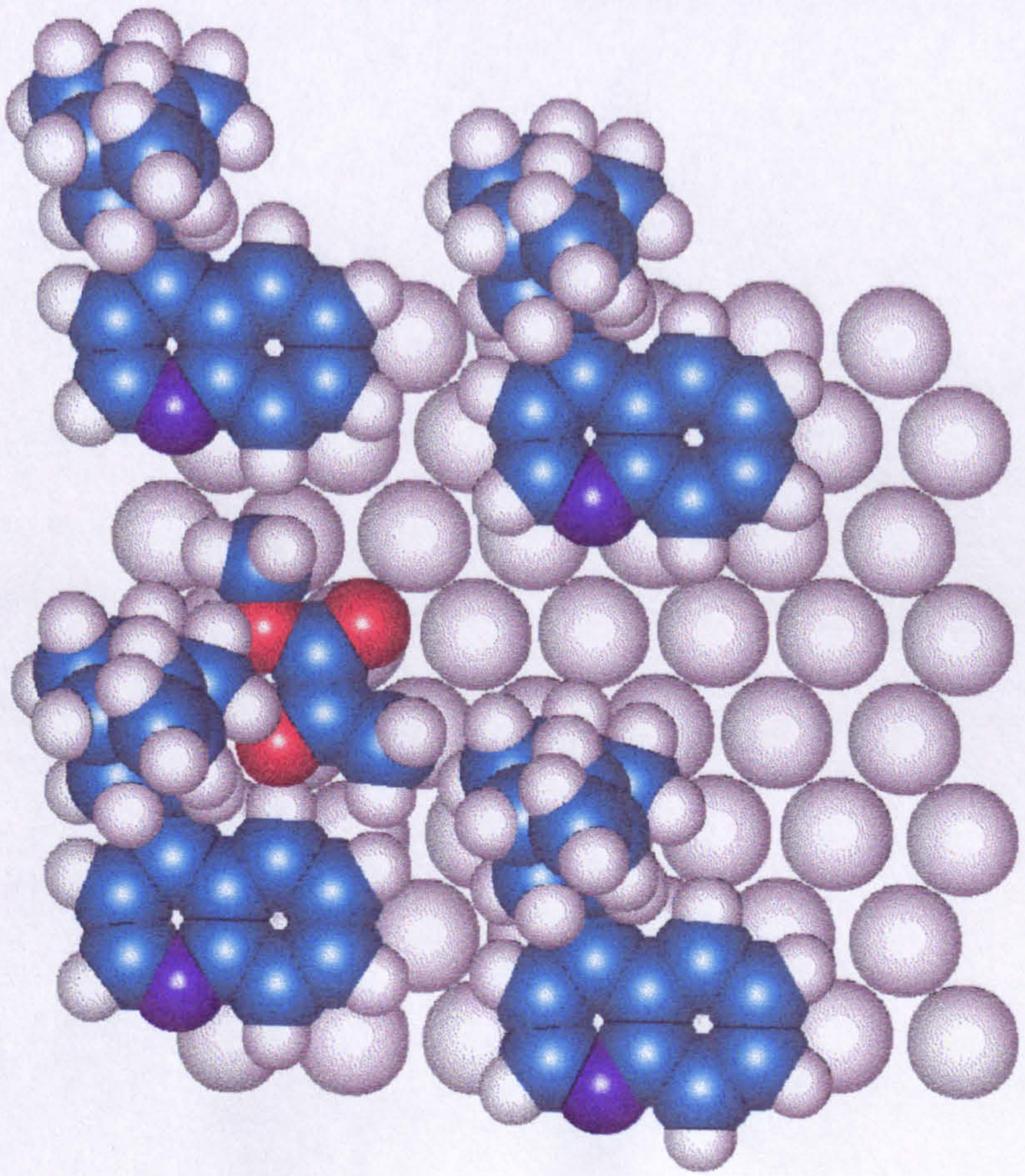

Figure 5.24
Methyl Pyruvate on Pt(111) Templated by Cinchonidine Molecules to give R-(+)-Lactate

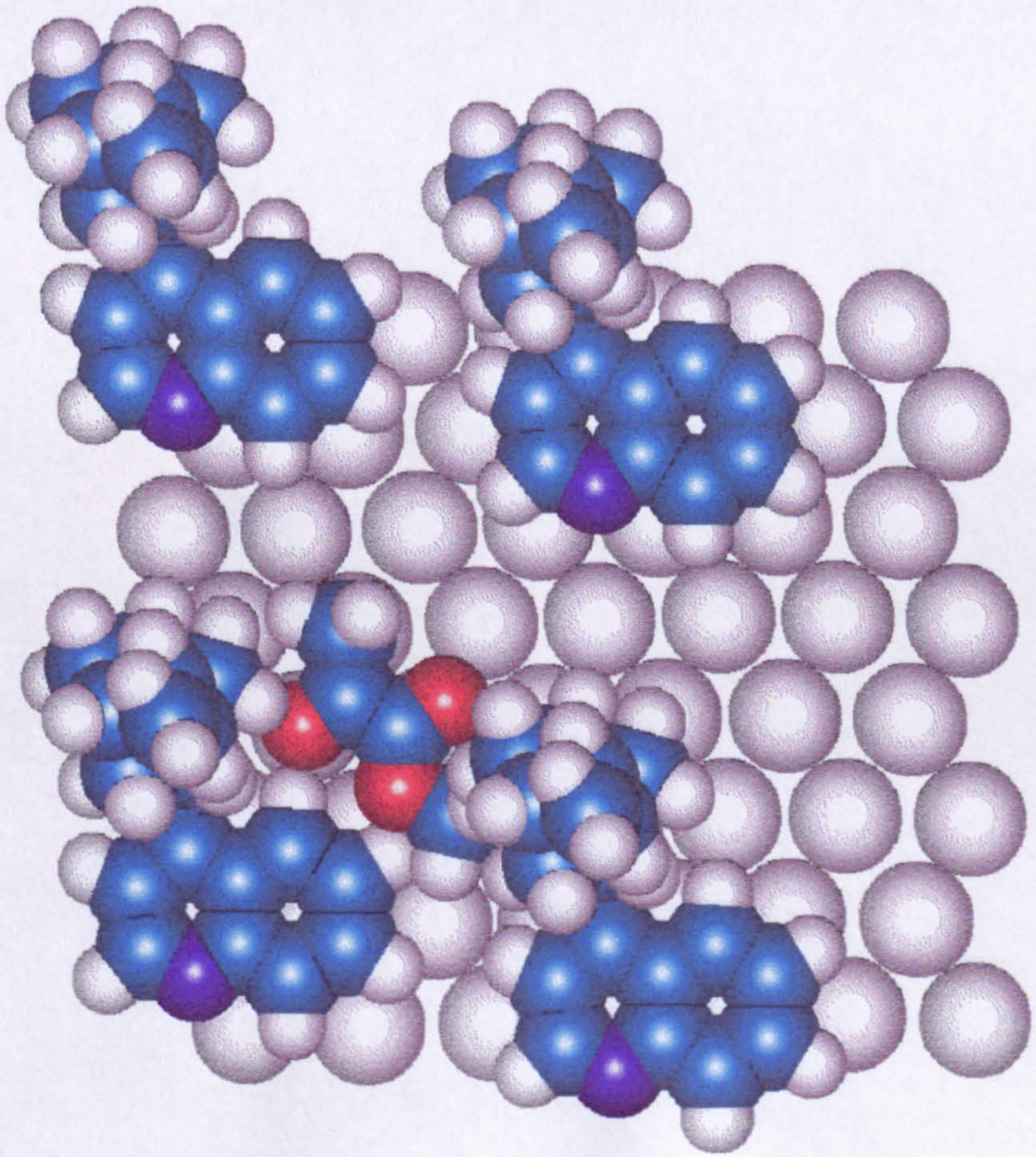

Figure 5.25
Methyl Pyruvate unable to adsorb on Pt(111)Templated by Cinchonidine Molecules to give S-(-)Methyl Lactate

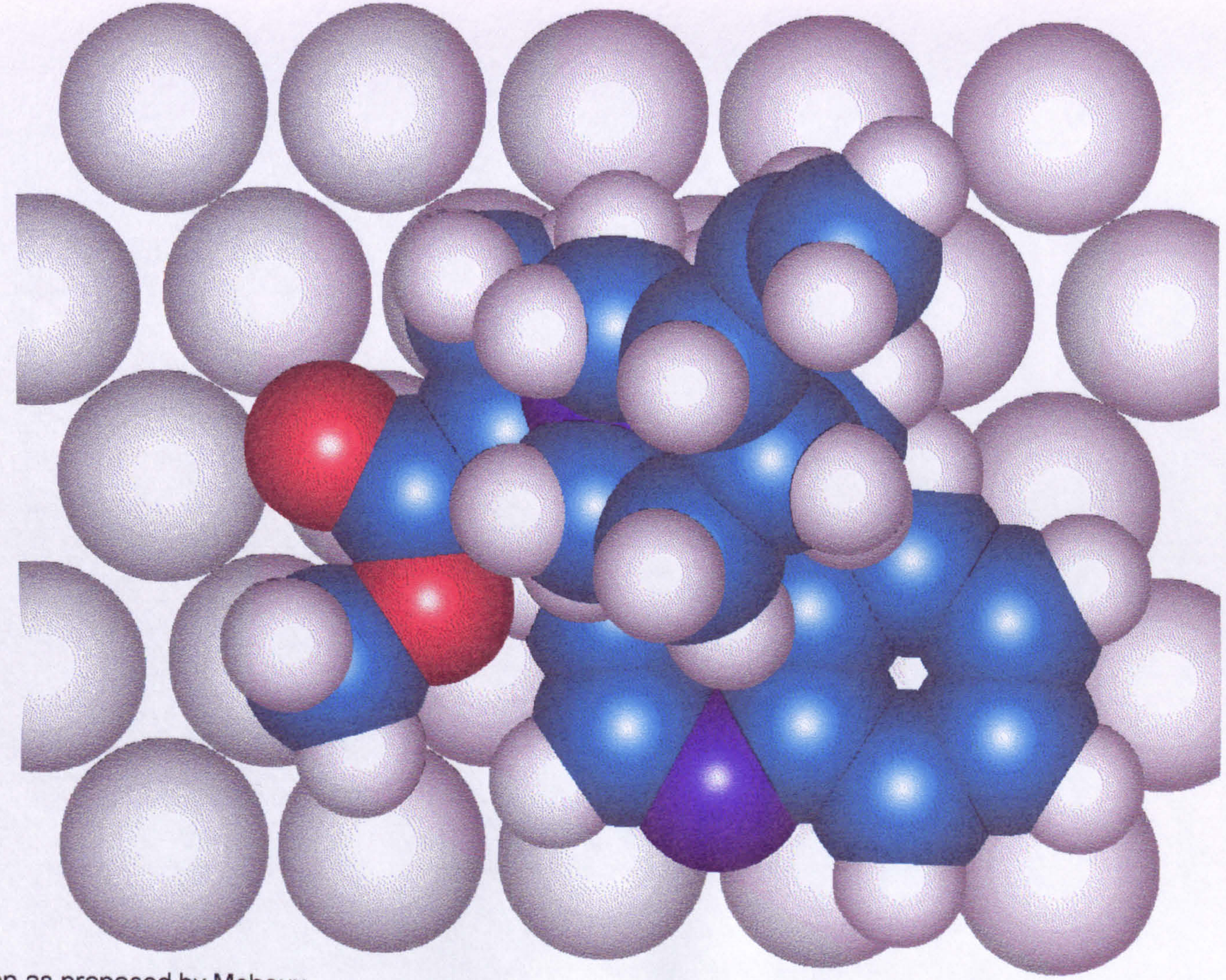

Figure 5.26
1:1 Interaction as proposed by Meheux

A mechanism is therefore proposed by which pyruvate approaches adsorbed cinchonidine such that the enantio-face to the surface that forms R-(+)-lactate on hydrogenation is energetically more favourable than that which gives S-(-)-lactate. When the total potential energy of each possible interaction is calculated, the former case gives lower, more favourable energy values. It is also easier to position the cinchonidine and carbonyl groups over Pt atoms in the case which gives R-(+)-product on hydrogenation of the pyruvate. These two forms of interaction are represented in figures 5.27 and 5.28, the exact magnitude of interaction energy depending on the exact positioning of the two molecules relative to one and other. (The same arguments could would also be able to explain S-(-)-lactate formation when cinchonine is used as modifier).

Figure 5.29 shows how the hhs of methyl lactate can be stabilised by the nitrogen of quinuclidine. (The dotted line, is generated by HyperChem as a valid hydrogen bond, i.e. not arbitarily drawn). The effect of rotation of the hhs of lactate about this H-bond is represented in figure 5.30. The calculation excludes any affect of the Pt surface, which would in fact create large energy barriers to rotation.

There are therfore only two 'sensible' regions at ca. 110° and 270° at which it is possible to have the hhs adsorbed in a planar fashion on a Pt surface. The energy of interaction of the orientation to give R-(+)-products is ca. 60 kcal mol^{-1} less than that required to give S-(-)-product. Not only is there less steric hinderance to the former adsorption, but also less electrostatic repulsion expected than would occurr between the lone pairs of the ester group and the quinoline ring system. Modelling with the package CHEM-X also showed that there were larger intermolecular repulsive forces in the latter case.

5.1.6a Evidence in Support of this Mechanism

The use of low concentrations of cinchonidine to study the kinetics of enantioselective hydrogenation of methyl pyruvate presented in this thesis and by other

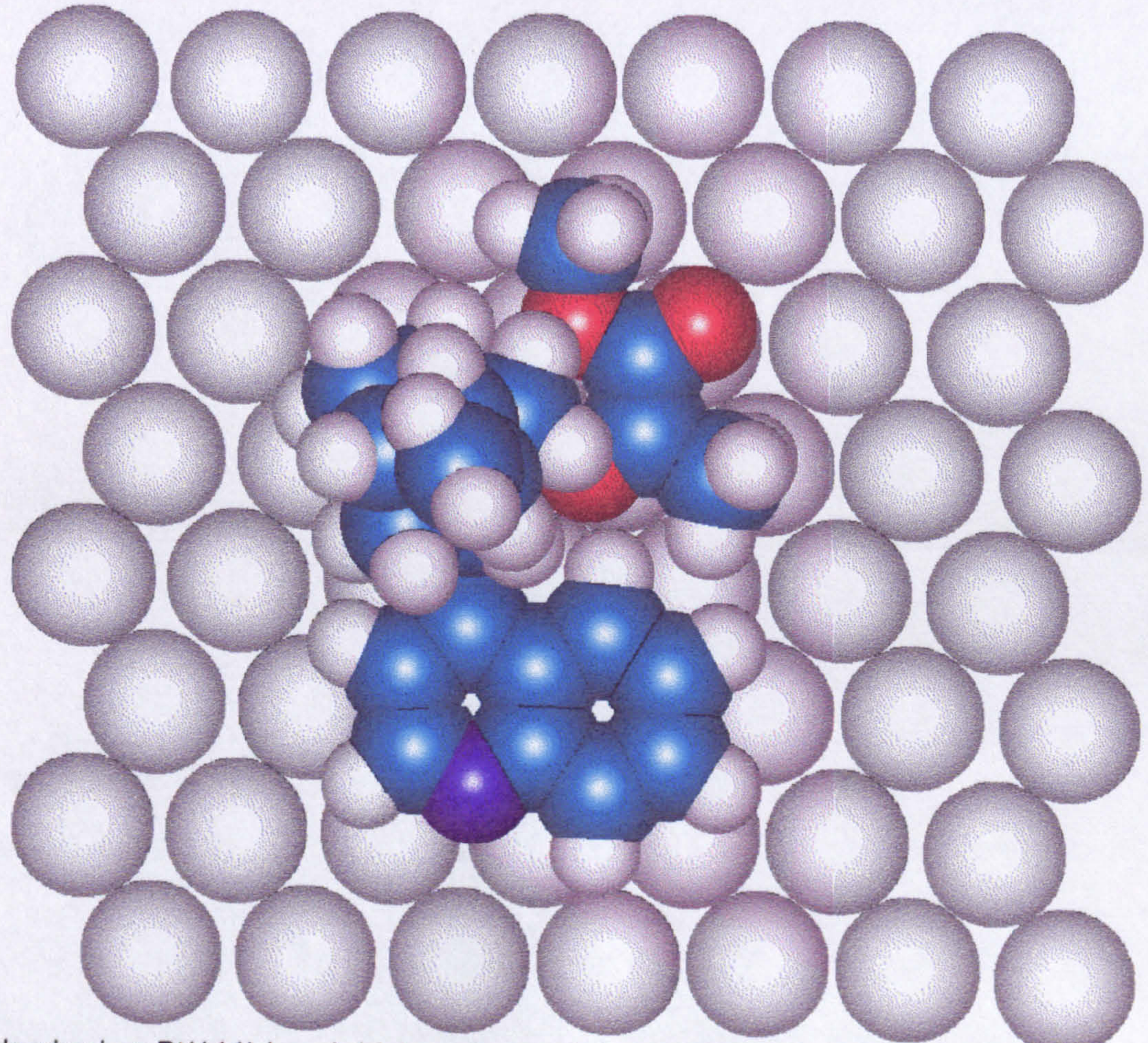

Figure 5.27
Methyl Pyruvate adsorbed on Pt(111) in a 1:1 Interaction with Cinchonidine to give R-(+)-Methyl Lactate on Hydrogenation

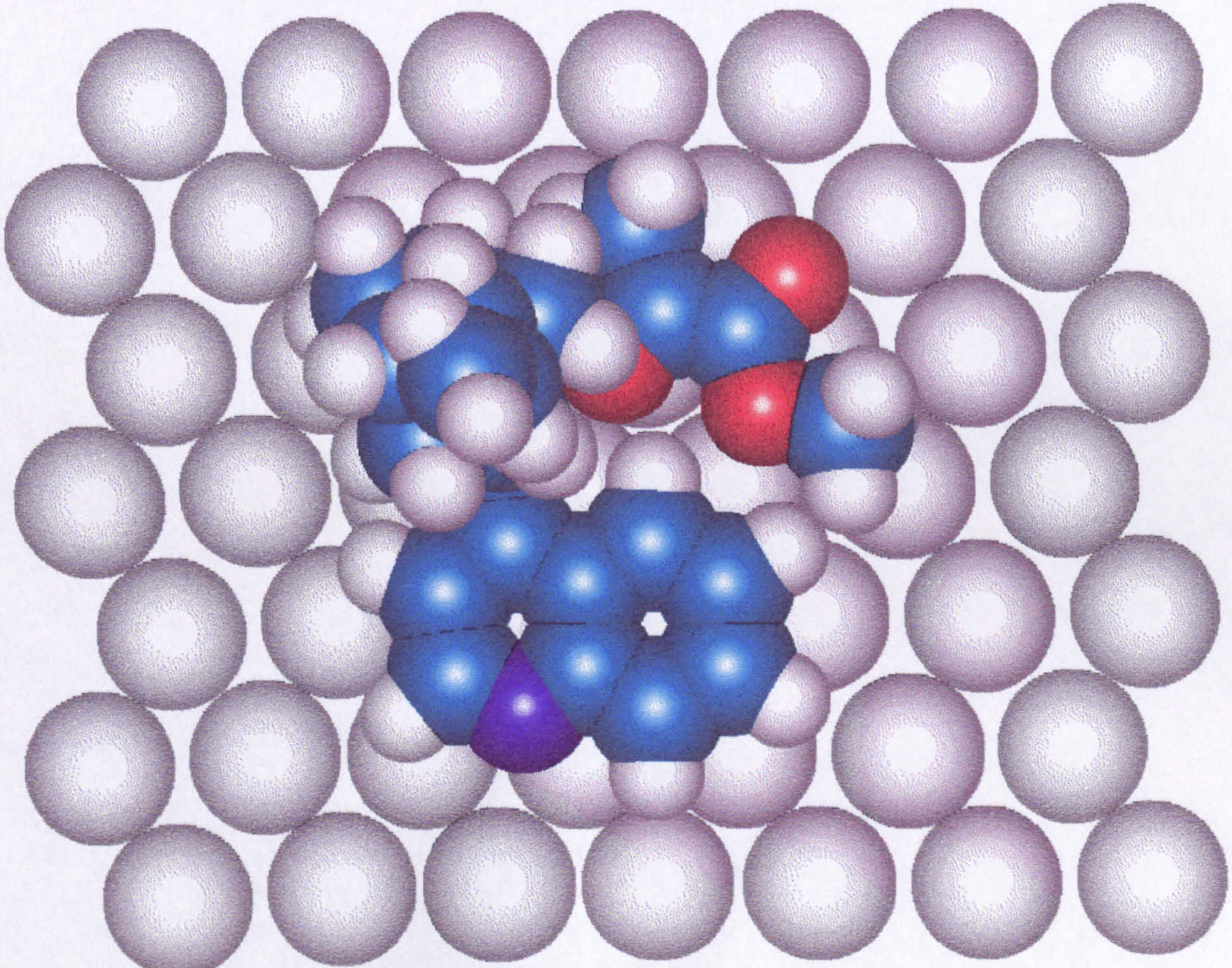

Figure 5.28
Hihdered adsorption of Methyl Pyryuvate on Pt(111) in a 1:1 Interaction with Cinchonidine to give S-(-)-Methyl Lactate on Hydrogenation

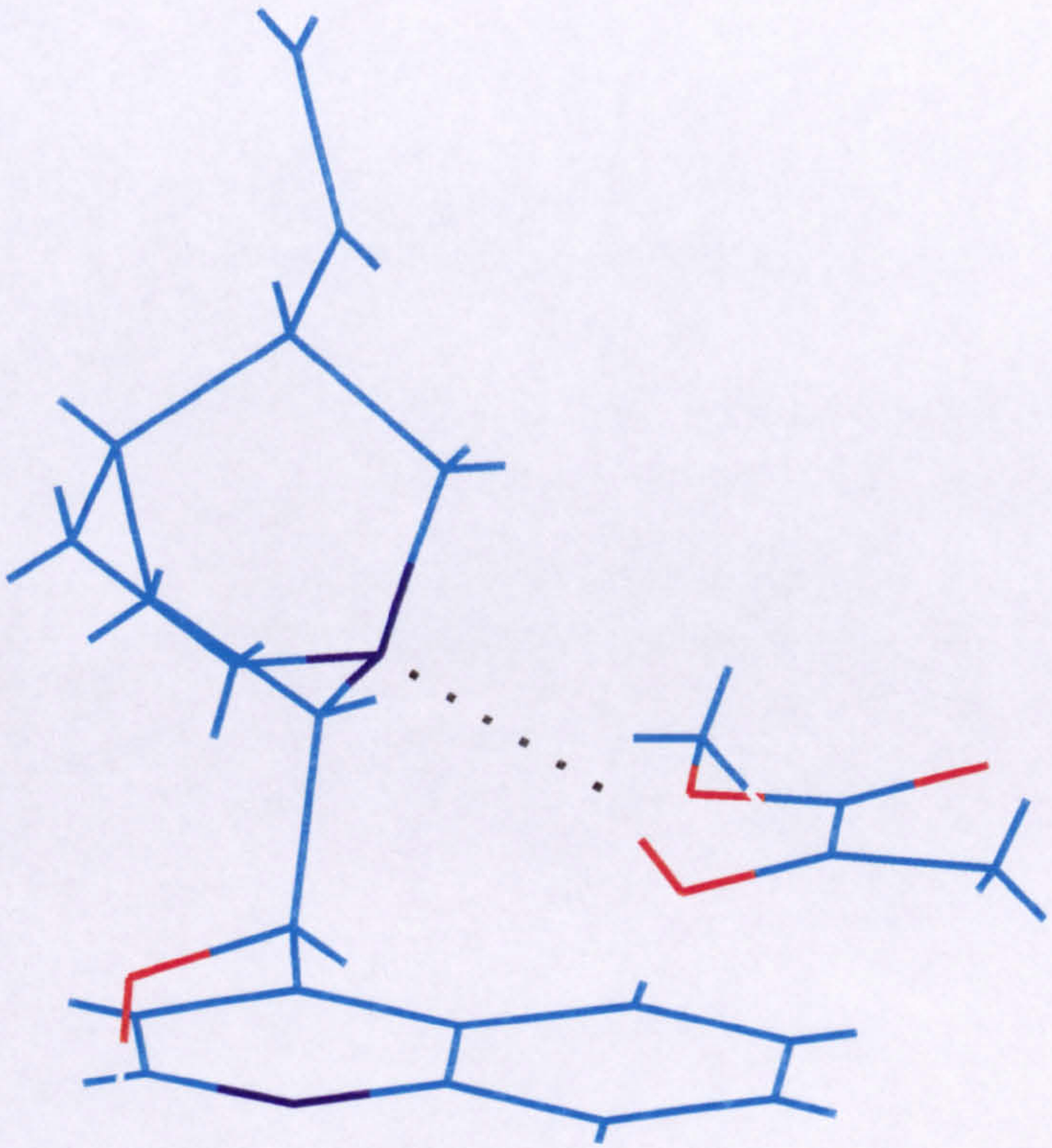

Figure 5.29
Half-Hydrogenated State Stabilised by Hydrogen Bond to Alicyclic Nitrogen of Cinchonidine R-(+)-Methyl Lactate on Hydrogenation

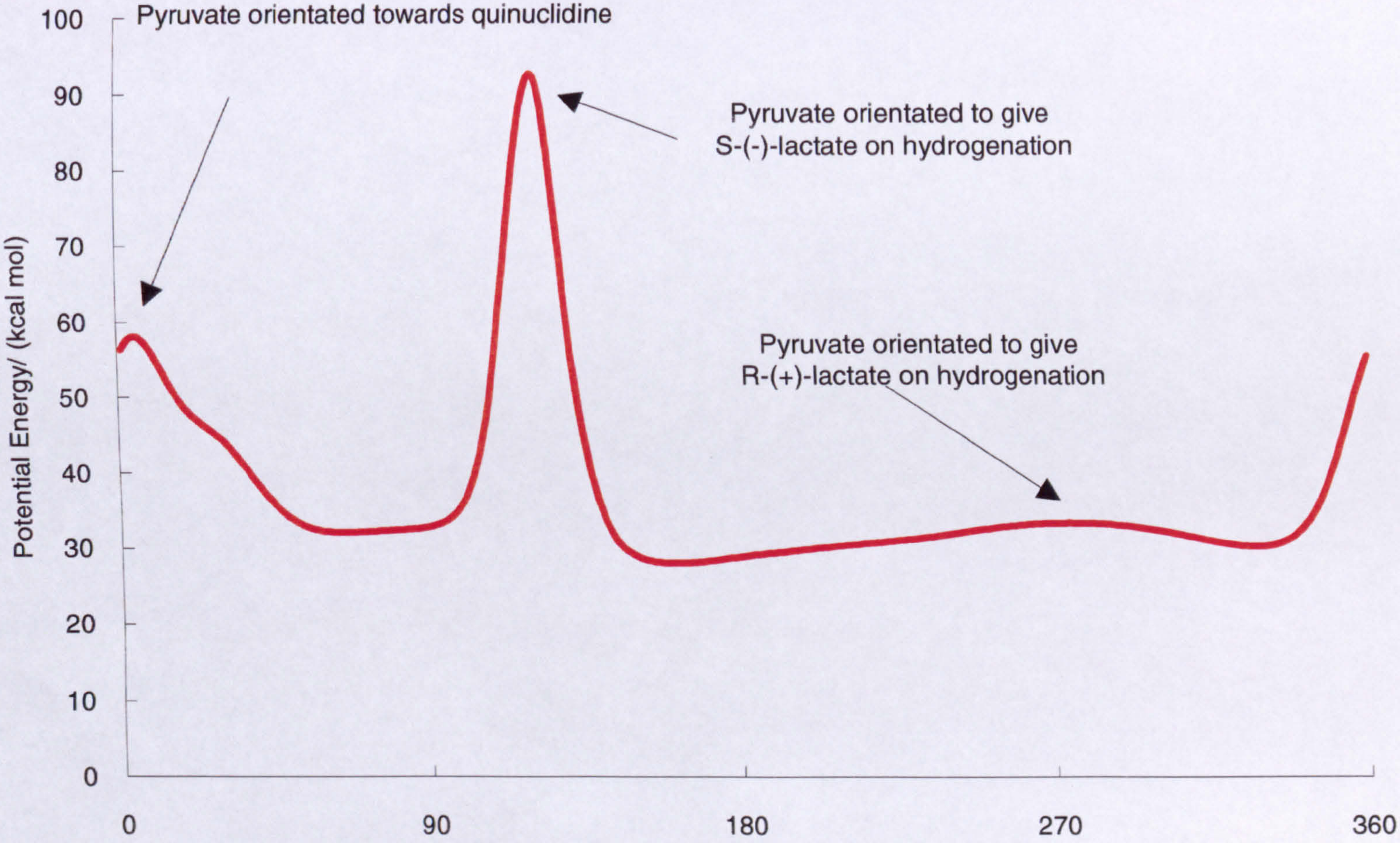

Figure 5.30
Effect of rotation of hhs of methyl pyruvate while maintainig H-bond to cinchonidine

workers[13] has suggested very strongly that the reaction mechanism involves a 1:1 interaction between pyruvate and alkaloid. The results of using a mixture of modifiers for the reaction, also presented in this thesis can be best interpreted in terms of a 1:1 interaction between pyruvate and alkaloid.

The important role of the nitrogen is also maintained in the mechanism, alkylation of which leads to a loss of activity and enantioselectivity in the reaction product[14]. The lack of activation and enantioselectivity of product exhibited by use of epiquinidine as modifier shows clearly the importance of the position of the location in space of the alicyclic nitrogen. If *conformation C†* is discounted, (as it probably does not exist) neither *A†* nor *B†* have the nitrogen in an equivalent position to that exhibited by either cinchonidine or cinchonine.

However, the model does have some limitations. It is not possible to take into account the effect of adsorption of the modifier on its conformation, nor does it take into account the influence of solvent in the system and morphology of the surface. However, it does provide (i) an interpretation of the high degree of enantiodifferentiation exhibited by the reaction, (ii) allows for the enhancement of reaction rate exhibited by the modified reaction, and (iii) follows the requirement for a 1:1 interaction of pyruvate and cinchonidine as suggested by the kinetics.

The model also indicates why quinine (or quinidine) produces product with lower enantioselectivity (see section 3.2). Figure 5.31 shows the adsorption of pyruvate and quinine exactly the same locations as used in figure 5.27 for pyruvate and cinchonidine. As can be seen, the pyruvate is slightly more hindered in its approach to the quinine molecule in a manner that would produce R-(+)-product. The adsorption of pyruvate in a manner to form S-(-)-product (not shown) is completely hindered. However the proximity of the pyruvate to the alkaloid could be relaxed slightly (but still maintaining the carbonyl groups over the Pt atoms) and a less hindered adsorption would result. This

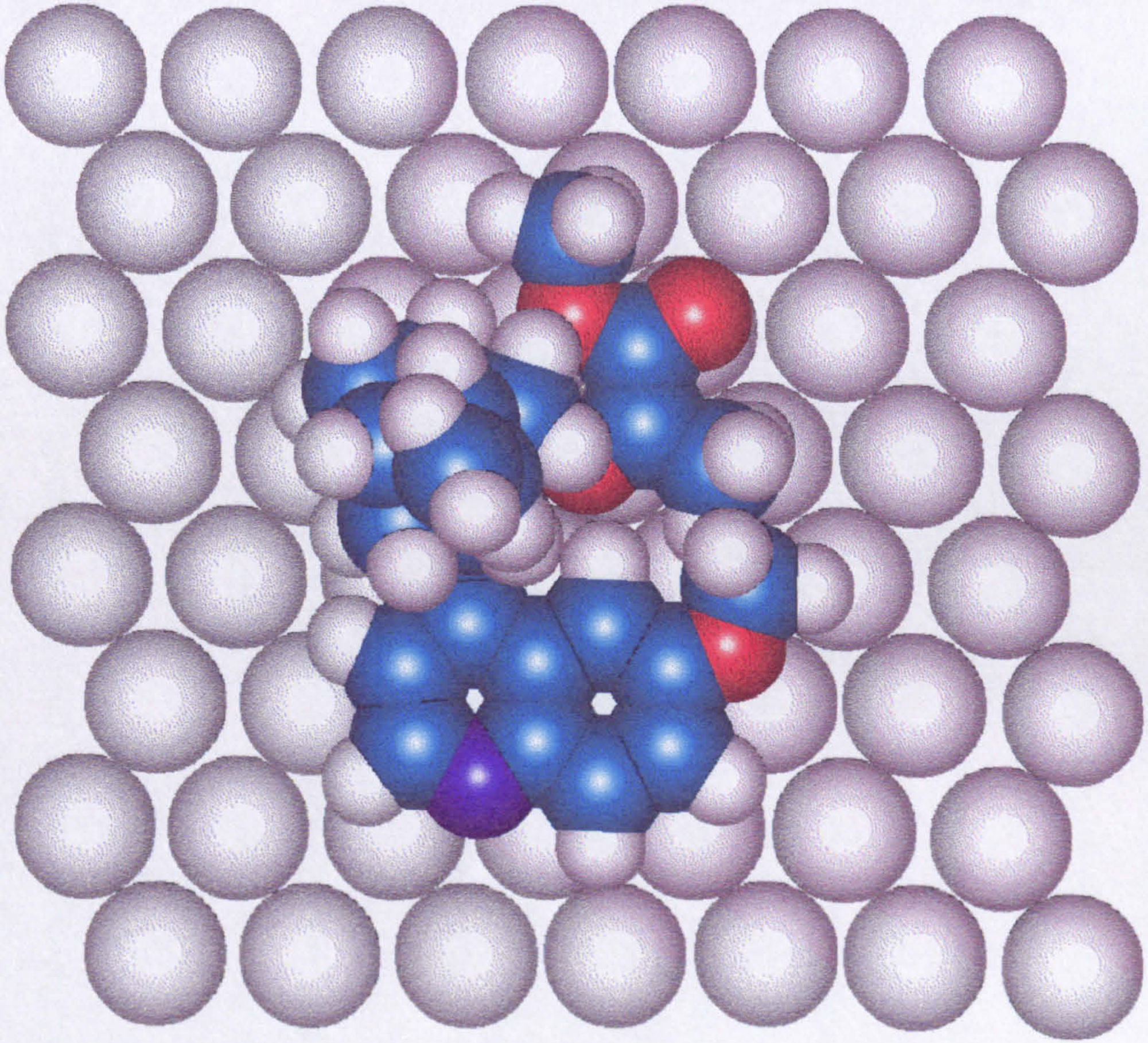

Figure 5.31
1:1 Interaction of Quinine and Methyl Pyruvate giving R-(+)-Methyl Lactate upon Hydrogenation

slightly increased steric hinderance suggested by the molecular modelling may interpret why the enantioselectivities observed by quinine or quinidine are reduced.

5.1.7 Other Models

During the writing of this thesis, two further models to interpret the enantioselectivity were proposed. The first model by Augustine *et al.* proposed that enantioselectivity was a result of two different modes of adsorption of the modifier at two specific different sites on a Pt crystallite[15]. Two different types of complexes, undergoing a 1:1 interaction of the modifier with the pyruvate were also proposed. Representations are reproduced from reference 16 in figure 5.32. One complex was formed with the modifier adsorbed flat on the Pt surface through the aromatic ring at sites adjacent to a corner atom. The pyruvate molecule which was not apparently adsorbed on the Pt formed an adduct with the modifier which was stabilised by hydrogen bonding between the C9-OH and the ester oxygen. As hydrogen was only available from one side of the pyruvate, enantioselectivity in favour of S-(-)-lactate formation resulted, but no rate acceleration was expected. The latter phenomenon had been observed, under *their* conditions at low concentrations of modifier.

R-(+)-lactate formation was achieved by the modifier adsorbing through the quinoline nitrogen, with the ring perpendicular to the surface at a site adjacent to a Pt adatom. A cinchonidine-pyruvate adduct was formed. This consisted of a six-membered ring formed by nucleophilic attraction between the quinuclidine-N and the keto carbon, and the oxygen at C_9-OH and the ester oxygen. The formation of this species accounted for the observed rate acceleration. The pyruvate molecule was co-adsorbed with hydrogen on the Pt adatom, presenting only one enantioface to the cinchonidine molecule and Pt adatom. This accounted for the observed enantioselectivity. The model has been critically reviewed by the author elsewhere[16].

The second model, proposed by Schwalm *et al.*[17] is similar enough to support the findings presented in this thesis. The model assumes that the cinchonidine molecule is protonated at the quinuclidine-N and that hydrogen bonding to the oxygen of the keto carbonyl exists. When this complex was minimised in energy by molecular mechanics calculations, it was found that the structure could easily adsorb in a manner which would give R-(+)-lactate product on hydrogenation. A second minimum energy complex, of slightly higher energy which would give S-(-)-lacate on hydrogenation could not easily adsorb on a flat Pt metal surface. These two complexes, superimposed on a Pt surface are reproduced from reference 17 in figure 5.33.

The structure of the complex expected to give R-(+)-lactate on hydrogenation, resembles that presented in figure 5.27. However, the Pt surface was not used as a reference point in calculations of Schwalm *et al.*, and therefore the carbonyl groups of the pyruvate are not clearly situated above adjacent Pt atoms. The Pt atoms would be expected to modify the nature of this complex. The same is true of the (energetically less feasible) complex calculated to exist to give S-(-)-lactate on hydrogenation. If the Pt atoms *were* allowed to influence the structure of the complex, it would reasonably be expected to resemble that presented in figure 5.28.

The major difference between the models is in the consideration of where the first hydrogen atom is added, to the quinuclidine-N or to the pyruvate molecule. Although it has been observed by NMR that the quinuclidine-N can be protonated by treatment with trifluoroacetic acid[18], quite how this could occur in a solvent such as toluene for example, is unclear. However, there is also no evidence for or against the existence of the half-hydrogenated state of the reaction intermediate required in the model presented in this thesis.

The other difference between the models is the assumption as to whether the pyruvate approaches a pre-adsorbed cinchonidine molecule, or whether a complex between the two forms first in solution and is subsequently adsorbed and hydrogenated.

There is again, no direct evidence for or against these two possibilities. These differences are therefore left as an open question.

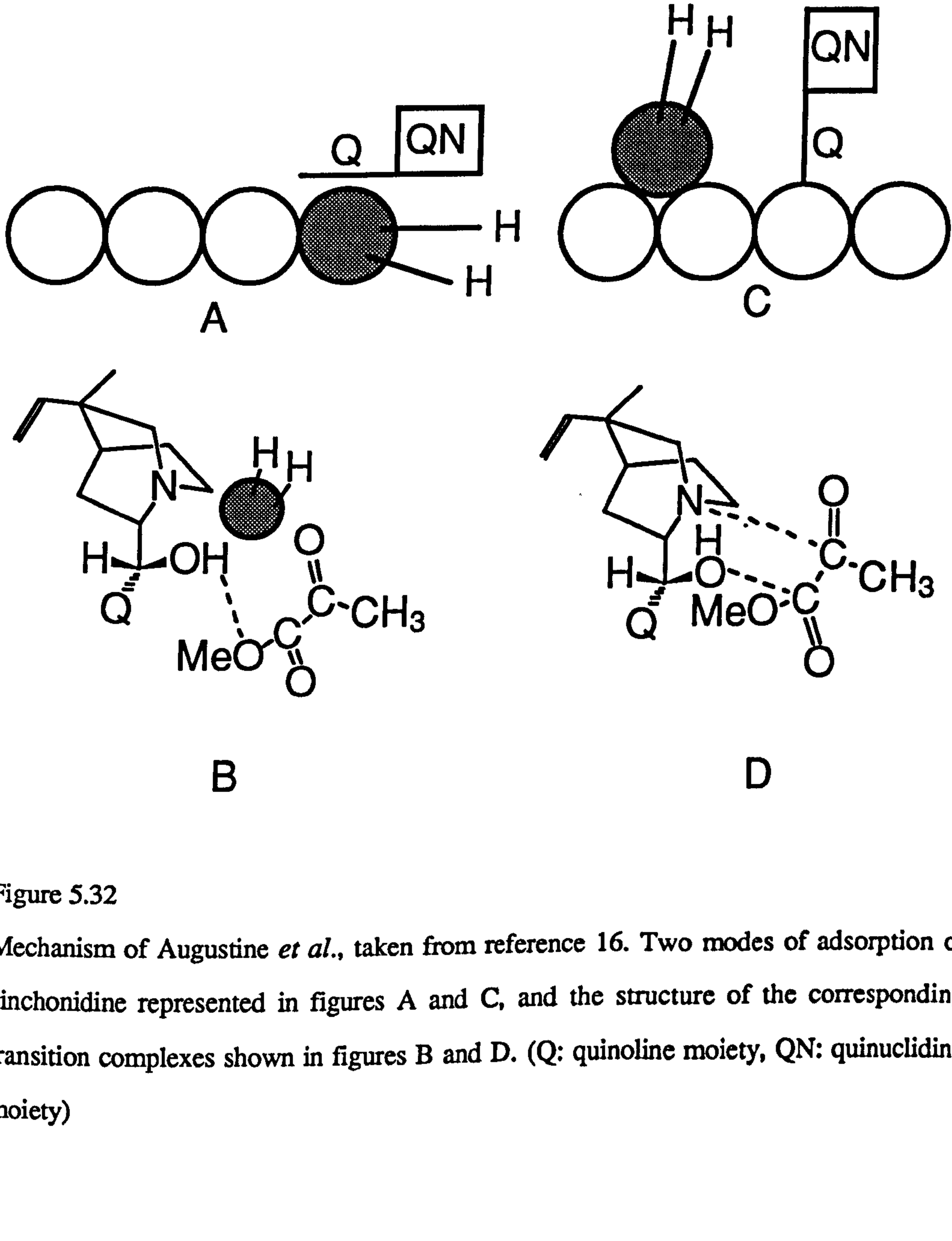

Figure 5.32

Mechanism of Augustine *et al.*, taken from reference 16. Two modes of adsorption of cinchonidine represented in figures A and C, and the structure of the corresponding transition complexes shown in figures B and D. (Q: quinoline moiety, QN: quinuclidine moiety)

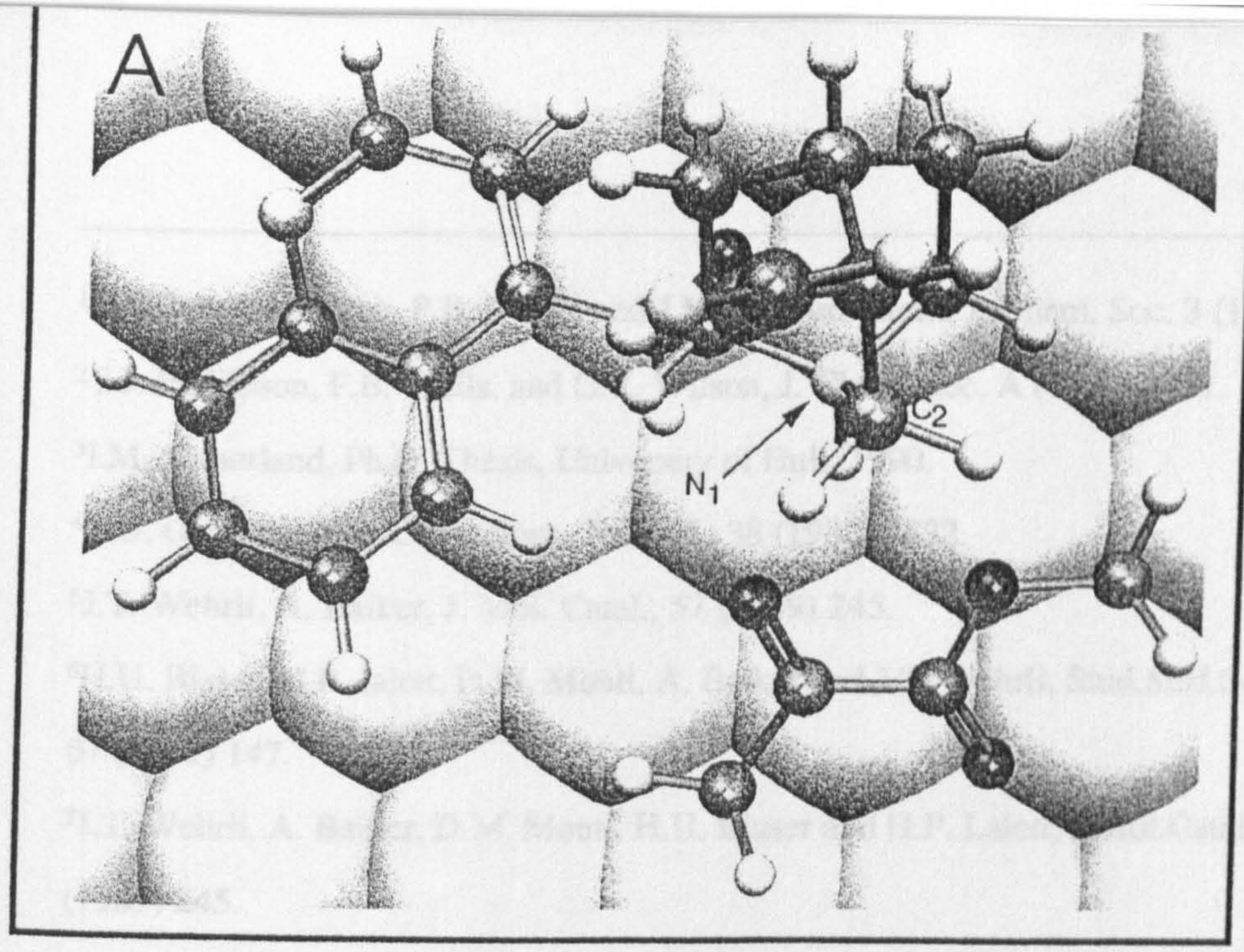

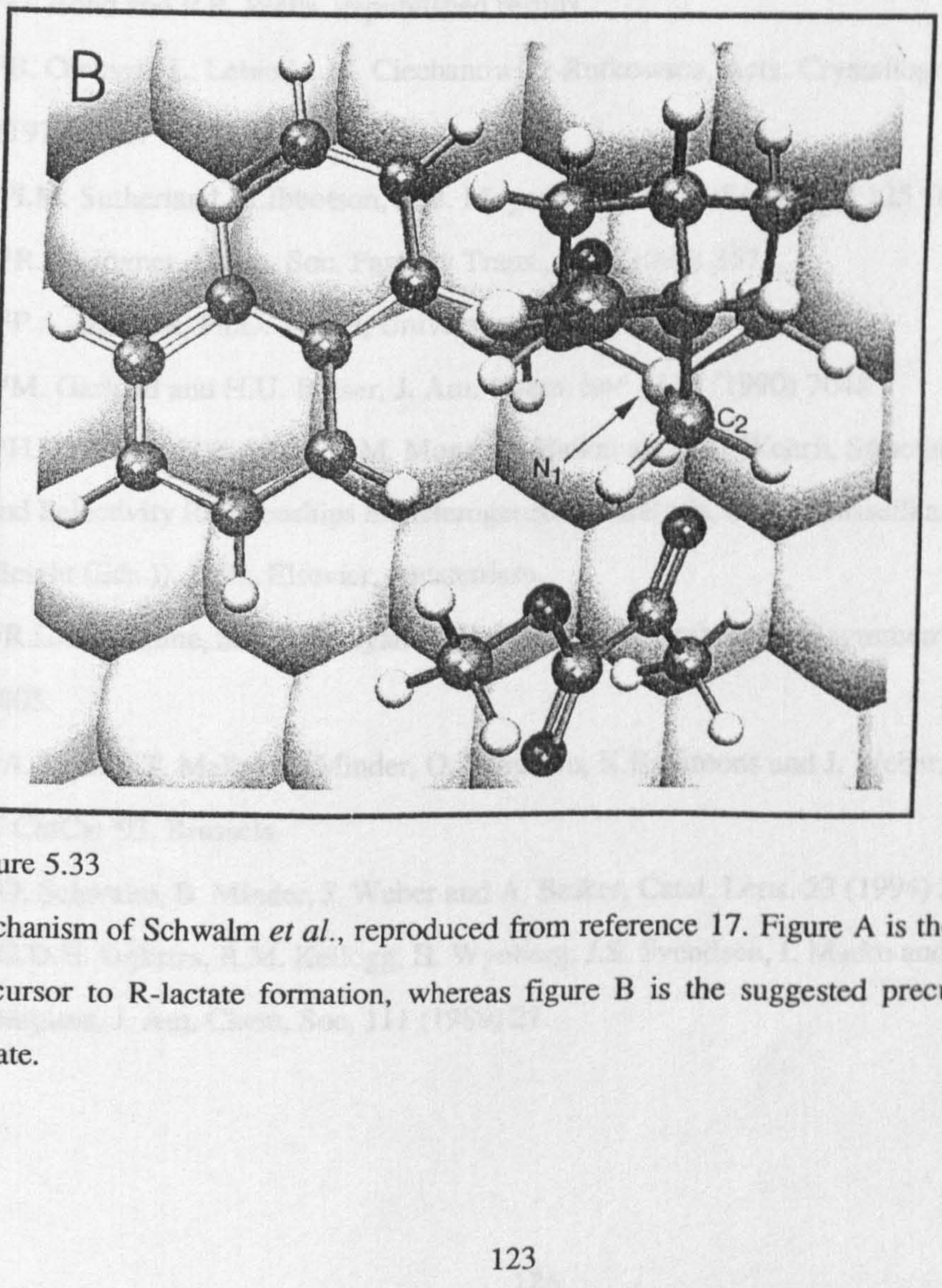

Figure 5.33

Mechanism of Schwalm *et al.*, reproduced from reference 17. Figure A is the suggested precursor to R-lactate formation, whereas figure B is the suggested precursor to S-lactate.

[1]G.C Bond, G.Webb, P.B. Wells, and J.M. Winterbottom, J. Chem. Soc. 3 (1965) 3218.

[2] J.J. Phillipson, P.B. Wells, and G.R. Wilson, J. Chem. Soc. A (1969) 1351.

[3]I.M. Sutherland, Ph.D. Thesis, University of Hull, 1990.

[4] R.J. Oleksyn, Acta.Crystallogr., Sect. B., 38 (1982) 1832.

[5]J.T. Wehrli, A. Baiker, J. Mol. Catal., 57 (1989) 245.

[6]H.U. Blaser, H.P. Jalett, D.M. Monti, A. Baiker and J.T. Wehrli, Stud.Surf.Sci.Catal. 67 (1991) 147.

[7]J.T. Wehrli, A. Baiker, D.M. Monti, H.U. Blaser and H.P. Lalett, J.Mol.Catal., 57 (1989) 245.

[8]G. Bond and P.B. Wells, unpublished results.

[9]B. Oleksyn, L. Lebioda, M. Ciechanowicz-Rutkowsca, Acta. Crystallogr., Sect. B 35 (1979) 440.

[10]I.M. Sutherland, A.Ibbotson, R.B. Moyes and P.B. Wells, J.Catal 125 (1990) 77.

[11]R.W. Joyner, Chem. Soc. Faraday Trans., I 76 (1980) 357.

[12]P.A. Meheux, Ph.D. Thesis, University of Hull, 1991.

[13]M. Garland and H.U. Blaser, J. Am. Chem. Soc., 112 (1990) 7048.

[14]H.U. Blaser, H.P. Jalett, D.M. Monti, A. Baiker and J.T. Wehrli, Structure-Activity and Selectivity Relationships in Heterogeneous Catalysis, (R.K. Grasselli and A.W. Sleight (Eds.)), 1991, Elsevier, Amsterdam.

[15]R.L. Augustine, S.K. Tanielyan and L.K. Doyle, Tetrahedron: Asymmetry., 4 (1993) 1803.

[16]A. Baiker, T. Mallat, B. Minder, O. Schwalm, K.E. Simons and J. Weber, proceedings of ChiCat '93, Brussels.

[17]O. Schwalm, B. Minder, J. Weber and A. Baiker, Catal. Letts. 23 (1994) 271.

[18]G.D.H. Dijkstra, R.M. Kellogg, H. Wynberg, J.S. Svendsen, I. Marko and K.B. Sharpless, J. Am. Chem. Soc, 111 (1989) 21.